*Official Journal of the*
*Malaysian Medical Association*

# *The Medical Journal of Malaysia*

**January 2025**

**Volume: 80**

**Supplement: 1**

ISSN 0300-5283 PP 2121/01/2013 (031329) MITA(P) 124/1/91

# MJM

*Official Journal of the Malaysian Medical Association*

*Volume 80 Supplement 1 January 2025*


## EDITORIAL BOARD




PP 2121/01/2013 (031329) MCI (P) 124/1/91 ISSN 0300-5283

The Medical Journal of Malaysia is published six times a year.
MJM is published bimonthly ie. January, March, May, July, September and November.





**Advertisement Rates:**
Enquiries to be directed to the Secretariat.

**Subscription Rates:**
Price per copy is RM100.00 or RM360.00 per annum, for all subscribers.

**Secretariat Address:**
Malaysian Medical Association
4th Floor, MMA House, 124, Jalan Pahang, 53000 Kuala Lumpur.
Tel: (03) 4042 0617, 4041 8972, 4041 1375 Fax: (03) 4041 8187
E-mail: info@mma.org.my / mjm@mma.org.my
Website: www.mma.org.my

*The Medical Journal of Malaysia*
MJM

# INSTRUCTION TO AUTHORS

The *Medical Journal of Malaysia* ***(MJM)*** welcomes articles of interest on all aspects of medicine in the form of original papers, review articles, short communications, continuing medical education, case reports, commentaries and letter to Editor. Articles are accepted for publication on condition that they are contributed solely to *The Medical Journal of Malaysia*.

**NOTE: MJM is published bimonthly ie. January, March, May, July, September and November.**

**REQUIREMENTS FOR ALL MANUSCRIPTS**
Please ensure that your submission to MJM conforms to the International Committee of Medical Journal Editors Recommendations for the Conduct, Reporting, Editing, and Publication of Scholarly Work in Medical Journals.

Neither the Editorial Board nor the Publishers accept responsibility for the views and statements of authors expressed in their contributions.

The Editorial Board further reserves the right to reject papers read before a society. To avoid delays in publication, authors are advised to adhere closely to the instructions given below.

**MANUSCRIPTS**
Manuscripts should be submitted in English (British English). Manuscripts should be submitted online through *MJM Editorial Manager*, http://www.editorialmanager.com/mjm.

Instructions for registration and submission are found on the website. Authors will be able to monitor the progress of their manuscript at all times via the *MJM Editorial Manager*. For authors and reviewers encountering problems with the system, an online Users' Guide and FAQs can be accessed via the "Help" option on the taskbar of the login screen.

MJM charges a one-time, non-refundable Article Processing Charge (APC) upon submission. Waiver of the APC applies only to members of the editorial board, and authors whose articles are invited by the editor. In addition, recipients of the MJM Reviewer Recognition Award from the previous year may enjoy a waiver of the APC for the next calendar year (e.g. recipients of MJM Reviewer Recognition Award 2022 will enjoy waiver of APC for articles submitted between January and December 2023).

**MJM**
Member: RM500
Non Member: RM800
Overseas: USD200

**MJM Case Report**
Member: RM400
Non Member: RM500

**Preparing your manuscript**

The MJM Article Processing Charge is a non-refundable administrative fee. Payment of the APC does not guarantee acceptance of the manuscript. Submitted articles will only be sent for reviews once the MJM APC has been successful completed.

All submissions must be accompanied by a completed **Copyright Assignment Form**, **Copyright Transfer Form and Conflict of Interest Form** duly signed by all authors. Forms can be download from MJM website at https://www.e-mjm.org/

Manuscript text should be submitted as **Microsoft Word** documents. Tables and flow-charts should be submitted as **Microsoft Word** documents. Images should be submitted as separate **JPEG files** (minimum resolution of 300 dpi).

**PEER REVIEW PROCESS**
All submissions must include at least two (2) names of individuals who are especially qualified to review the work. All manuscripts submitted will be reviewed by the Editor in-charge before they are send for peer review. Manuscripts that are submitted to MJM undergo a double-blinded peer review and are managed online. Proposed reviewers must not be involved in the work presented, nor affiliated with the same institution(s) as any of the authors or have any potential conflicts of interests in reviewing the manuscript. The selection of reviewers is the prerogative of the Editors of MJM.

**ELIGIBILITY AS AN AUTHOR**
MJM follows the recommendation of the International Committee of Medical Journal Editors (ICMJE) for eligibility to be consider as an author for submitted papers. The ICMJE recommends that authorship be based on the following four (4) criteria:

1 Substantial contributions to the conception or design of the work; or the acquisition, analysis, or interpretation of data for the work; AND
2 Drafting the work or revising it critically for important intellectual content; AND
3 Final approval of the version to be published; AND
4 Agreement to be accountable for all aspects of the work in ensuring that questions related to the accuracy or integrity of any part of the work are appropriately investigated and resolved.

**TYPES OF PAPERS**
**Original Articles:**
Original Articles are reports on findings from original unpublished research. Preference for publications will be given to high quality original research that make significant contribution to medicine. Original articles shall consist of a structured Abstract and the Main Text. The word count for the structured abstract should not exceed 500 words. The main text of the articles should not exceed 4000 words, tables/illustrations/figures/images up to five (5) and references up to 40. Manuscript describing original research should conform to the IMRAD format, more details are given below.

Original articles of cross-sectional and cohort design should follow the corresponding STROBE check-lists; clinical trials should follow the CONSORT check-list.

**Review Articles:**
Review Articles are solicited articles or systematic reviews. ***MJM*** solicits review articles from Malaysian experts to provide a clear, up-to-date account of a topic of interest to medical practice in Malaysia or on topics related to their area of expertise. Unsolicited reviews will also be considered, however, authors are encouraged to submit systematic reviews rather than narrative reviews. Review articles shall consist of a structured Abstract and the Main Text. The word count for the structured abstract should not exceed 500 words. Systematic Review are papers that presents exhaustive, critical assessments of the published literature on relevant topics in medicine. Systematic reviews should be prepared in strict compliance with MOOSE or PRISMA guidelines, or other relevant guidelines for systematic reviews.

**Short Communications:**
Shorts communication are short research articles of important preliminary observations, findings that extends previously published research, data that does not warrant publication as a full paper, small-scale clinical studies, and clinical audits. Short communications should not exceed 1,500 words and shall consist of a Summary and the Main Text. The summary should be limited to 100 words and provided immediately after the title page. The number of tables/illustrations/figures/images should be limited to three (3) and the number of references to ten (10).

**Continuing Medical Education (CME) Articles:**
A CME article is a critical analysis of a topic of current medical interest. The article should include the clinical question or issue and its importance for general medical practice, specialty practice, or public health. It shall consist of a Summary and the Main Text. The summary should be limited to 500 words and provided immediately after the title page Upon acceptance of selected articles, the authors will be requested to provide five multiple-choice questions, each with five true/false responses, based on the article. For guideline, please refer to: Sivalingam N, Rampal L. Writing Articles on Continuing Medical Education for Medical Journals. Med J Malaysia. 2021 Mar;76(2):119-124.

**Case Reports:**
Papers on case reports (one to five cases) must follow these rules: Case reports should not exceed 2,000 words; with a maximum of two (2) tables; three (3) photographs; and up to ten (10) references. It shall consist of a Summary and the Main Text. The summary should be limited to 250 words and provided immediately after the title page. Having a unique lesson in the diagnosis, pathology or management of the case is more valuable than mere finding of a rare entity. Being able to report the outcome and length of survival of a rare problem is more valuable than merely describing what treatment was rendered at the time of diagnosis. There should be no more than seven (7) authors.

Please note that all Case Reports will be published in the new MJM Case Reports Journal (www.mjmcasereports.org).

**Commentaries:**
Commentaries will usually be invited articles that comment on articles published in the same issue of the ***MJM***. However, unsolicited commentaries on issues relevant to medicine in Malaysia are welcomed. They should not exceed 2,000 words. They maybe unstructured but should be concise. When presenting a point of view, it should be supported with the relevant references where necessary.

**Letters to Editor:**
Letters to Editors are responses to items published in ***MJM*** or to communicate a very important message that is time sensitive and cannot wait for the full process of peer review. Letters that include statements of statistics, facts, research, or theories should include only up to three (3) references. Letters that are personal attacks on an author will not be considered for publication. Such correspondence must not exceed 1,500 words.

**Editorials:**
These are articles written by the editor or editorial team concerning the ***MJM*** or about issues relevant to the journal.

**STRUCTURE OF PAPERS**
**Title Page:**
The title page should state the brief title of the paper, full name(s) of the author(s) (with the surname or last name bolded), degrees (limited to one degree or diploma), affiliation(s), and corresponding author's address. All the authors' affiliations shall be provided after the authors' names. Indicate the affiliations with a superscript number at the end of the author's degrees and at the start of the name of the affiliation. If the author is affiliated to more than one (1) institution, a comma should be used to separate the number for the said affiliation.

Do provide preferred abbreviated author names for indexing purpose, e.g. L Rampal (for Lekhraj Rampal), BS Liew (for Liew Boon Seng), B Abdullah (for Baharudin Abdullah), Hoe VC (for Victor Hoe Chee Wai).
Please indicate the corresponding author and provide the affiliation, full postal address and email.

Articles describing Original Research should consist of the following sections (IMRAD format): Abstract, Introduction, Materials and Methods, Results, Discussion, Acknowledgment and References. Each section should begin on a fresh page.
Scientific names, foreign words and Greek symbols should be in italic.

**Abstract and Key Words:**
A structured abstract is required for Original and Review Articles. It should be limited to 500 words and provided immediately after the title page. Below the abstract provide and identify three (3) to 10 key words or short phrases that will assist indexers in cross-indexing your article. Use terms from the medical subject headings (MeSH) list from Index Medicus for the key words where possible. Key words are not required for Short Communications, CME articles, Case Reports, Commentaries and Letter to Editors.

**Introduction:**
Clearly state the purpose of the article. Summarise the rationale for the study or observation. Give only strictly pertinent references, and do not review the subject extensively.

**Materials and Methods:**
Describe your selection of the observational or experimental subjects (patients or experimental animals, including controls) clearly, identify the methods, apparatus (manufacturer's name and address in parenthesis), and procedures in sufficient detail to allow other workers to reproduce the results. Give references to established methods, including statistical methods; provide references and brief descriptions of methods that have been published but are not well-known; describe new or substantially modified methods, give reasons for using them and evaluate their limitations.

Identify precisely all drugs and chemicals used, including generic name(s), dosage(s) and route(s) of administration. Do not use patients' names, initials or hospital numbers. Include numbers of observation and the statistical significance of the findings when appropriate.

When appropriate, particularly in the case of clinical trials, state clearly that the experimental design has received the approval of the relevant ethical committee.

**Results:**
Present your results in logical sequence in the text, tables and illustrations. Do not repeat in the text all the data in the tables or illustrations, or both: emphasise or summarise only important observations in the text.

**Discussion:**
Emphasise the new and important aspects of the study and conclusions that follow from them. Do not repeat in detail data given in the Results section. Include in the Discussion the implications of the findings and their limitations and relate the observations to other relevant studies.

**Conclusion:**
Link the conclusions with the goals of the study but avoid unqualified statements and conclusions not completely supported by your data. Avoid claiming priority and alluding to work that has not been completed. State new hypotheses when warranted, but clearly label them as such. Recommendations, when appropriate, may be included.

**Acknowledgements:**
Acknowledgements of general support, grants, technical assistance, etc., should be indicated. Authors are responsible for obtaining the consent of those being acknowledged.

**Referencing guide:**
The Medical Journal of Malaysia, follows the Vancouver numbered referencing style. Citations to someone else's work in the text, should be indicated by the use of a number. In citing more than one article in the same sentence, you will need to include the citation number for each article. A hyphen should be used to link numbers which are inclusive, and a comma used where numbers are not consecutive. The following is an example where works 1.3,4,5.have been cited in the same place in the text.

Several effective drugs are available at fairly low cost for treating patients with hypertension and reducing the risk of its sequelae.[1,3-5]

The list of all of the references that are cited in the article should be presented in a list labelled as 'References'. This reference list appears at the end of the paper. Authors are responsible for the accuracy of cited references and these should be verified by the author(s) against the original documents before the manuscript is submitted. It is important that the author should never place in the list of references a document that he or she has not seen. The Journals names should be abbreviated according to the style used in the Index Medicus. All authors when six or less should be listed; when seven or more list only the first six and add et al.

If you are citingthe author's name in your text, you must insert the citation number as well. Jewell BL (8) underlined that as focus in the SARS-CoV-2 pandemic shifts to the emergence of new variants of concern (VOC), characterising the differences between new variants and non-VOC lineages will become increasingly important for surveillance and maintaining the effectiveness of both public health and vaccination programme. If you are citing more than one author's name in your text and you want to cite author names in your text, use 'et al.' after the first author. Example: Rampal et al. (9) highlighted that the. disregard of the manuscript guidelines and instruction to authors of the journal you submit, is one of the common reasons for 'Rejection' of the article.

**Example references Journals:**
**Standard Journal Article**
Rampal L and Liew BS. Coronavirus disease (COVID-19) pandemic. Med J Malaysia 2020; 75(2): 95-7.
Rampal L, Liew BS, Choolani M, Ganasegeran K, Pramanick A, Vallibhakara SA, et al. Battling COVID-19 pandemic waves in six South-East Asian countries: A real-time consensus review. Med J Malaysia 2020; 75(6): 613-25.
NCD Risk Factor Collaboration (NCD-RisC). Worldwide trends in hypertension prevalence and progress in treatment and control from 1990 to 2019: a pooled analysis of 1201 population-representative studies with 104 million participants. Lancet 2021; 11; 398(10304): 957-80.

**Books and Other Monographs:**
**Personal Author(s)**
Goodman NW, Edwards MB. 2014. Medical Writing: A Prescription for Clarity. 4 th Edition. Cambridge University Press.

**Chapter in Book**
McFarland D, Holland JC. Distress, adjustments, and anxiety disorders. In: Watson M, Kissane D, Editors. Management of clinical depression and anxiety. Oxford University Press; 2017: 1-22.

**Corporate Author**
World Health Organization, Geneva. 2019. WHO Study Group on Tobacco Product Regulation. Report on the scientific basis of tobacco product regulation: seventh report of a WHO study group. WHO Technical Report Series, No. 1015.

NCD Risk Factor Collaboration (NCD-RisC). Rising rural body-mass index is the main driver of the global obesity epidemic in adults. Nature 2019; 569: 260–64.

World Health Organization. Novel Coronavirus (2019-nCoV) Situation Report 85, April 14, 2020. [cited April 2020] Accessed from: https://www.who.int/docs/defaultsource/coronaviruse/situationreports/20200414-sitrep-85-covid-19.

**Online articles**
**Webpage:** Webpage are referenced with their URL and access date, and as much other information as is available. Cited date is important as webpage can be updated and URLs change. The "cited" should contain the month and year accessed.

Ministry of Health Malaysia. Press Release: Status of preparedness and response by the ministry of health in and event of outbreak of Ebola in Malaysia 2014 [cited Dec 2014]. Available from: http://www.moh.gov.my/english.php/database_stores/store_view_page/21/437.

**Other Articles:**
**Newspaper Article**
Panirchellvum V. 'No outdoor activities if weather too hot'. the Sun. 2016; March 18: 9(col. 1-3).

**Magazine Article**
Rampal L.World No Tobacco Day 2021 -Tobacco Control in Malaysia. Berita MMA. 2021; May: 21-22.

**Tables:**
All tables and figures should have a concise title and should not occupy more than one printed page. The title should concisely and clearly explain the content of the table or figure. They should be numbered consecutively with Roman numerals (e.g Table I) and figures with Arabic numerals (e.g. Figure 1), and placed after the sections of the manuscript which they reflect, particularly the results which they describe on separate pages. Cite tables in the text in consecutive order. Indicate table footnotes with lower-case letters in superscript font. Place the information for the footnote beneath the body of the table. If a table will be submitted as a separate document, the filename should contain the surname of the first author and match its label in the manuscript (e.g., SMITH Table I).Vertical lines should not be used when constructing the tables. All tables and figures should also be sent in electronic format on submission of the manuscript as supplementary files through the journal management platform. Clinical Photographs should conceal the subject's identity. Tables and flow-charts should be submitted as Microsoft Word documents. Images should be submitted as separate JPEG files (minimum resolution of 300 dpi).

**Photographs of Patients:**
Proof of permission and/or consent from the patient or legal guardian must be submitted with the manuscript. A statement on this must be included as a footnote to the relevant photograph.

**Colour reproduction:**
Illustrations and diagrams are normally reproduced in black and white only. Colour reproductions can be included if so required and upon request by the authors. However, a nominal charge must be paid by the authors for this additional service; the charges to be determined as and when on a per article basis.

**Abbreviations:**
Use only standard abbreviations. The full-term for which an abbreviation stands should precede its first use in the abstract, article text, tables, and figures, unless it is a standard unit of measurement. Abbreviations shall not be used in the Title. Abbreviations should be kept to a minimum.

**Formatting of text:**
Numbers one to ten in the text are written out in words unless they are used as a unit of measurement, except in tables and figures. Use single hard-returns to separate paragraphs. Do not use tabs or indents to start a paragraph. Do not use the automated formatting of your software, such as hyphenation, endnotes, headers, or footers (especially for references). Submit the Manuscript in plain text only, removed all 'field codes' before submission. Do not include line numbers. Include only page number.

**BEST PAPER AWARD**
All original papers which are accepted for publication by the MJM, will be considered for the 'Best Paper Award' for the year of publication. No award will be made for any particular year if none of the submitted papers are judged to be of suitable quality.

**CONTENTS** **Page**

## Original Articles

**CONTENTS** **Page**

# *Ocimum gratissimum* mediated synthesis of AgNPs – An *in vitro* analysis of anti-inflammatory and antimicrobial effects

**Prathiksha Dhanapal[1], Rajeshkumar Shanmugam, PhD[1], Lingaraj Jayalakshmi, MD[2], Pradeep Manigandan, MSc[1]**

[1]Nanobiomedicine Lab, Centre for Global Health Research, Saveetha Medical College and Hospitals, Saveetha Institute of Medical and Technical Sciences, Thandalam, Chennai, Tamil Nadu, India, [2]Department of Physiology, Saveetha Medical College and Hospitals, Saveetha Institute of Medical and Technical Sciences, Thandalam, Chennai, Tamil Nadu, India

## ABSTRACT

**Introduction: Silver nanoparticles (AgNPs) are effective against almost all kinds of pathogenic organisms. The green synthesis of AgNPs utilizing extracts from medicinal plants is being researched to examine the therapeutic advantages of AgNPs because the chemical production of AgNPs is more toxic. In this study, the stem extract of *Ocimum Gratissimum* (OG) also known as *Karunthulasi* or wild basil for green synthesis of AgNPs and evaluating their anti-inflammatory and antimicrobial effects.**

**Materials and Methods: The produced nanoparticles were characterized using UV-visible spectroscopy. The Bovine Serum Assay (BSA) and Egg Albumin (EA) assays were used to assess the anti-inflammatory effects. The protein denaturation of AgNPs was calculated and compared to a standard to determine the anti-inflammatory activity of green synthesized AgNPs. Using varying concentrations of OG-mediated AgNPs in Mueller Hinton Agar (MHA), the antimicrobial effects of OG have been investigated against *E. coli*, *S. aureus*, and *Pseudomonas sp.* Additionally, by measuring optical density, the time-kill curve analysis for *E. Coli* and *S. Aureus* has been examined from one hour for up to five hours.**

**Results: The green synthesized AgNPs were developed successfully using a plant Ocimum gratissimum. The synthesized AgNPs exhibited a maximum absorption peak at 440 nm and SEM analysis revealed that the synthesized AgNPs were spherical and oval. The result findings of the anti-inflammatory activity reveal that AgNPs have great potential when compared to the standard. At the concentration of 50 µg/mL, AgNPs exhibit 76% in BSA assay and 74% in EA assay, where the standard shows 80% inhibition. The antimicrobial activity showed a zone of inhibition around 19mm for E. coli and a 20mm zone of inhibition for *S. aureus* and *Pseudomonas sp.*, which shows the efficacy of AgNPs. The time-kill assay shows that the optical density of *E. coli* and *S. aureus* was reduced to 0.1 after 5 hours of incubation, which shows the potential of green synthesized AgNPs.**

**Conclusion: OG-mediated AgNPs have both anti-inflammatory and antimicrobial effects. Anti-inflammatory effects are better when compared to standard drugs. Antimicrobial effects are better for Gram-negative bacteria.**

**KEYWORDS:**
*Silver nanoparticles, biomedical applications, time-kill curve analysis, Nanobiomedicine*

## INTRODUCTION

The evidence for the use of Silver and other metals as a treatment modality has been mentioned in the history of medicine as early as the 2nd century BC in Indian Charaka Samhita and by Hippocrates for treatment of wounds and as preservatives.[1,2] Silver nitrate was also widely used in the 1800s for wound healing in burns, in wound dressings, and in suture materials. After the Second World War, the use of silver declined during the era of antibiotics.[3] The advent of silver nanoparticles in therapeutics gained momentum in recent years. Nanoparticles as the name denotes, are less than 100 nm in size and are used extensively in the field of biomedical research. Its longevity in diagnosis and treatment is explained by its unique properties, which include its high surface area to volume ratio, robust response to living cells, stability at high temperatures, programmable surface plasmon resonance,[4] and translocation into the cells' cellular uptake and effect of nanoparticle depends on its physical and chemical characteristics like composition, shape, size, charge, surface coating, pH, and width-to-height ratio,[5] But at the same time, the small size of nanoparticles results in a large surface area making them more toxic.[6] Nonchemical or biological Nanoparticle synthesis using the bottom-up method is also called green synthesis. During green synthesis, secondary metabolites in plant extracts such as vitamins, flavonoids, enzymes, polyphenols, and polysaccharides act as reducing agents. They have a donated electron outer layer, thereby reducing the metal ions to a zero-oxidation state (ex-Ag+ to Ag0).[7,8]

Green synthesis using medicinal plant extracts is preferred because of their eco-friendly nature, simplicity, and low cost. There are several advantages to green synthesis over chemical synthesis. The biologically active components in plant extracts strongly influence the size and distribution of metallic nanoparticles.[9,10] They also form a cover on the surface of the nanoparticles (capping) and prevent them from agglomerating or clustering together because of their small size, thereby giving them more stability. In addition, plant extracts with medicinal value can act synergistically with nanoparticles and enhance the therapeutic effects of

*This article was accepted: 03 August 2025*
*Corresponding Author: Rajeshkumar Shanmugam*
*Email: rajeshkumars.smc@saveetha.com*

metal nanoparticles. It reduces the harmful side effects of chemically synthesized metal nanoparticles.[11] It can also be combined with most of the existing antibiotics, and can increase its effectiveness and reduce dosage, thereby reducing side effects. Most importantly, green synthesis helps overcome the increasing problem of antimicrobial resistance.[12,13] AgNPs exert their antimicrobial effect in several ways by interacting with living cells and causing cell death. It increases cell membrane permeability, causes sulfide bond breakage, protein misfolding, aggregate formation, iron imbalance, and increased production of reactive oxygen species such as hydroxyl ions.[14] Each of which has specific biological compounds. Several plant extracts are being studied and used to form AgNPs. In this study, we have used the extract of Ocimum Gratissimum (OG), OG is widely known as clove basil, African basil, wild basil, and in the Indian subcontinent as Karunthulasi, Ramthulasi and belongs to Lamiaceae or mint family.[15] OG plant extracts have been shown to have anti-inflammatory, antimicrobial effects antidiabetic, antidiarrheal, antiprotozoal, cytotoxic, hepatoprotective, and many other medicinal effects.[16] In this present study, the synthesis of AgNPs using Ocimum Gratissimum evaluated its anti-inflammatory and antimicrobial/antibacterial effects against wound pathogens. The time-kill curve assay can be considered an indicator of effectiveness against antibiotic resistance.

## MATERIALS AND METHODS

*Preparation of AgNPs with Ocimum gratissimum Stem Extract*

The Ocimum gratissimum plant was shade-dried and ground into powder. A beaker containing 100 mL distilled water and 1 g of Ocimum gratissimum was added and heated in a heating mantle at 60–70 °C for 15–20 minutes. Precursor solution: To prepare the precursor solution, 1 mM of silver nitrate (0.0169 g) was combined with 80 mL of distilled water,[17] and 20 ml of filtered plant extract was added, mixed well, and placed in an orbital shaker.

*In vitro Antimicrobial Assay*

The antimicrobial action of Ocimum Gratissimum green-synthesized AgNPs was assessed using the agar-well diffusion method, a commonly used method. Bacteria were cultured on Mueller-Hinton agar (MHA) plates, which served as the growth medium. The cultured bacteria were incubated for 24 h and the bacterial load was standardized using McFarland standards. Cultures were spread uniformly on MHA plates and wells were created. Green synthesized AgNPs (25, 50, and 100 micrograms) were loaded into bacterial culture wells. After incubation for 24 h at 37 °C, the inhibition zones were measured and compared with the inhibitory zones of known standard antibiotics, which served as positive controls.[18]

*Bovine Serum Albumin Denaturation Assay (BSA Assay)*

Using this approach, the anti-inflammatory properties of AgNPs, mediated by Ocimum gratissimum stem extract, were evaluated. AgNPs of different fixation (10µL, 20µL, 30µL, 40µL, and 50µL) mediated by Ocimum gratissimum extract were added to 0.45 mL of bovine serum albumin (1% aqueous solution), and the mixture's pH was adjusted to 6.3 using a small amount of 1N hydrochloric acid. Double-beam Mult spectrophotometry was used to measure the absorbance at 660 nm after the samples were cooled after a 20-minute incubation time at room temperature and a 30-minute heating session in a water bath at 55 °C. Diclofenac sodium was used as a reference standard. Dimethyl sulphoxide (DMSO) was used as the control.[19]

*Egg Albumin Denaturation Assay [EA Assay]*

2.8 mL of freshly prepared phosphate-buffered saline with a pH of 6.3 and 0.2 mL of egg albumin from a hen's egg were combined to create a 5 mL solution. For the Ocimum gratissimum stem extract-mediated AgNPs, specific quantities were generated independently using the same procedure as the Bovine Serum Albumin assay.[20]

*Time Kill Curve Assay*

Minimum inhibitory concentrations (MICs) are the lowermost antibacterial concentrations in mg/L or µg/mL that completely prevent visible growth of the tested microbes. For the MIC test, 100 µL of MHB was added to all columns in the microtiter plate along with the bacterial inoculum at a concentration of $5\times10^5$ CFU/ml. A stock solution of (500 µg/mL) OG-mediated AgNPs was prepared, 25, 50, and 100 µL were added to the last column in the microtiter plate, and serial double dilutions were made backward.[21,22] Different concentrations of nanoparticles were used to test the time-kill curve analysis using *S. aureus* and *E. coli*.

For the time-kill assay, Mueller Hinton broth was prepared, sterilized, and added to five test tubes. Three different concentrations of *Ocimum gratissimum* green-synthesized AgNPs were added to the first three tubes at 25, 50, and 100 µL (1,2- and 4-times the MIC), the standard drug was added to the fourth tube (Amoxyrite), and the fifth tube was considered as the control. Bacterial suspensions (*Staphylococcus aureus* and *E. coli*) were added to all five test tubes at a concentration of $5\times10^5$ CFU/mL. The tubes were incubated for various time intervals (1h, 2h, 3h, 4h, 5h) and the percentage of dead cells was calculated at a wavelength of 600 nm at regular time intervals using optical density values.[23]

## RESULTS

*Synthesis of AgNPs and their characterization analysis*

The precursor solution was mixed with 20 mL of stem extract and centrifuged at 110 revolutions per minute for a full day. After 24 hours of incubation, the color of the solution changed from yellow to brown as a result of surface plasmon resonance, which excited the free electrons of the reaction mixture. This confirms the reduction of silver nitrate to AgNPs. The synthesized nanoparticles were characterized by UV-visible spectroscopy. Higher absorption is directly proportional to the higher yield of AgNPs in the colloidal solution. The color change was dependent on the incubation time (6–24 h) as well as the size and shape of the nanoparticle as shown in Figure 1A. The UV-visible absorption spectra of the synthesized AgNPs are shown in Figure 1B. The UV-visible region of wavelengths from 350 to 650 nm has a distinctive absorption peak at 440 nm in the spectrum. Numerous parameters, such as the size, shape, and degree of aggregation of nanoparticles, influence the position of the SPR peak. Larger nanoparticles display peaks at longer

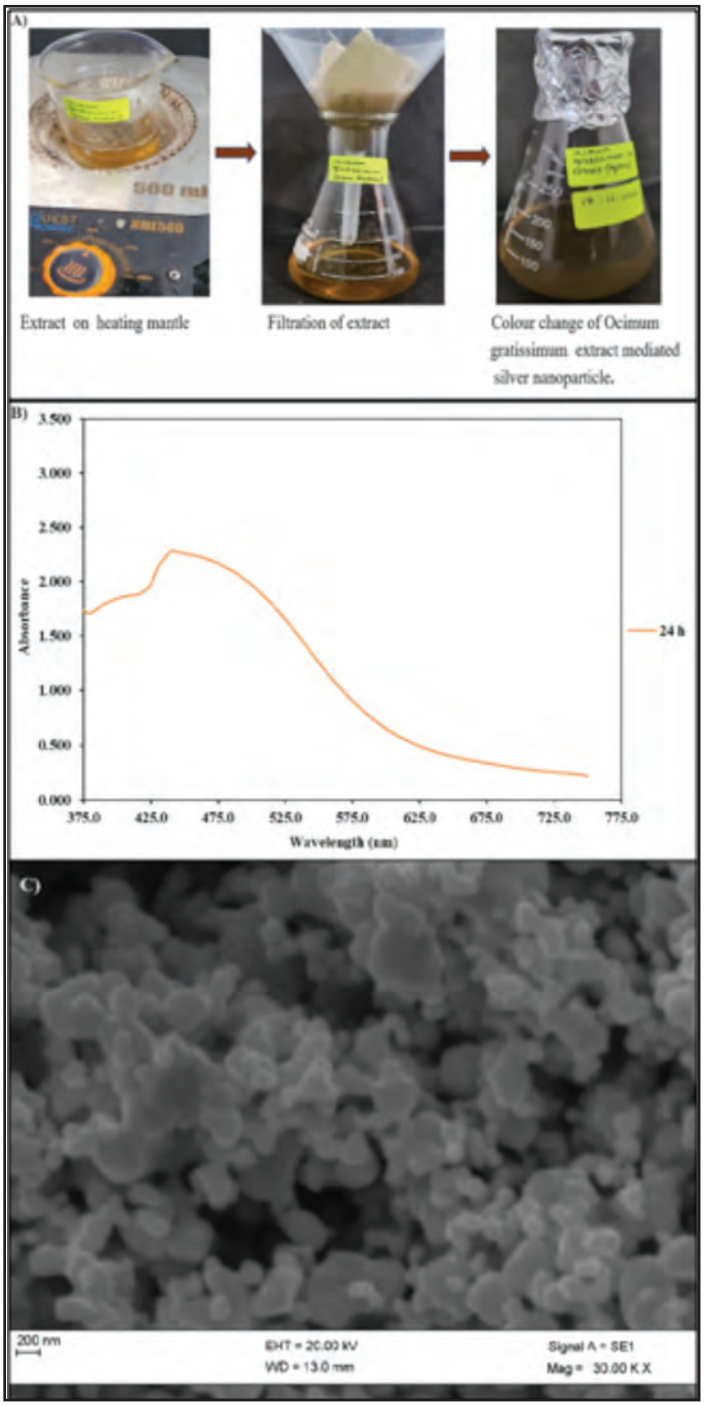


**Fig. 1:** A) Green synthesis of Ocimum gratissimum mediated AgNPs, B) UV spectra analysis of AgNPs, C) SEM analysis of green synthesized AgNPs.

wavelengths than smaller ones, which typically exhibit SPR peaks at shorter wavelengths. Figure 1C displays the SEM images of the AgNPs produced. The photographs demonstrate the existence of uniformly sized spherically shaped nanoparticles. The smooth surface of the nanoparticles suggests that there was no noticeable agglomeration or aggregation. The form and surface characteristics of each nanoparticle can be observed through SEM photos, which offer comprehensive insights into each one. The spherical morphology of the nanoparticles is compatible with the development of AgNPs throughout the production process, and is of excellent quality and consistency.

*Antimicrobial Activity*

The antimicrobial activity of the green-synthesized AgNPs was investigated using the agar well diffusion method against E. coli, *S. aureus*, and *Pseudomonas sp.* A zone of inhibition of 19 mm was noted for *E. coli* at a concentration of 100µg/mL, where the standard was 40 mm. In contrast, a

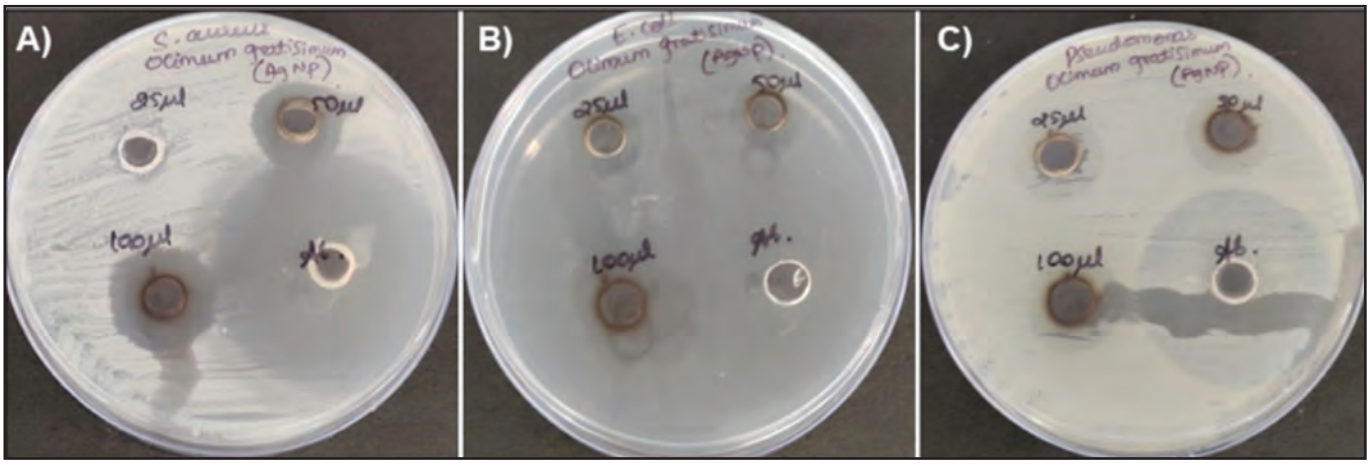


**Fig. 2:** Antibacterial activity of Ocimum gratissimum mediated AgNPs using agar well diffusion method.

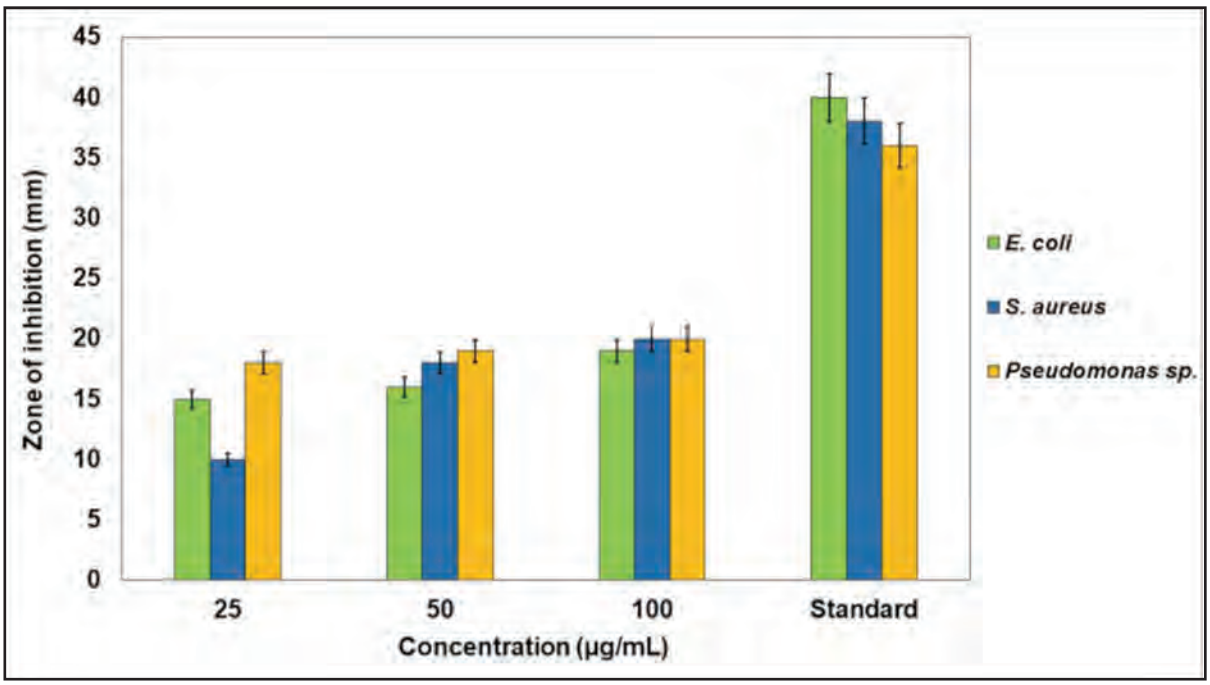


**Fig. 3:** Graphical representation of *Ocimum gratissimum* mediated AgNPs against *E. coli, for S. aureus* and *Pseudomonas sp.*

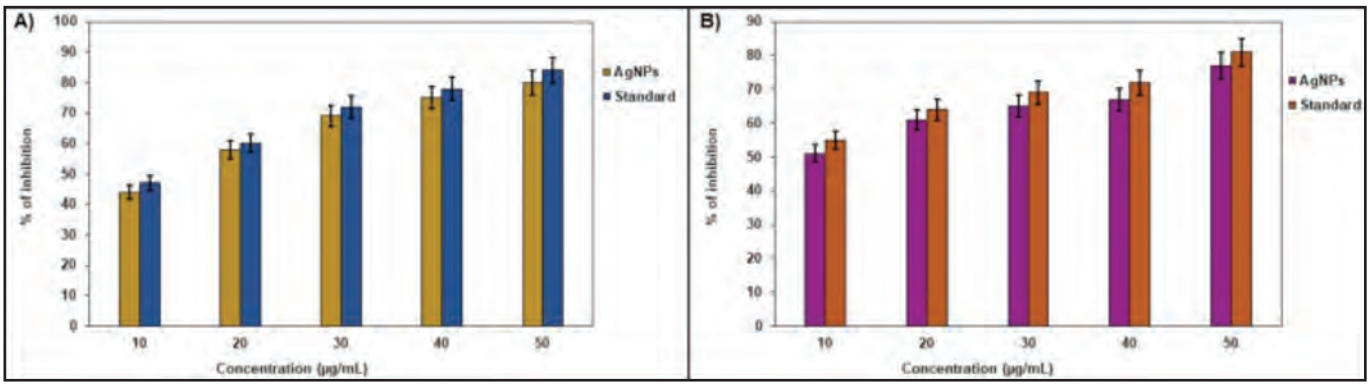


**Fig. 4:** Anti-inflammatory activity of *Ocimum gratissimum* mediated AgNPs using A) BSA assay and B) EA assay.

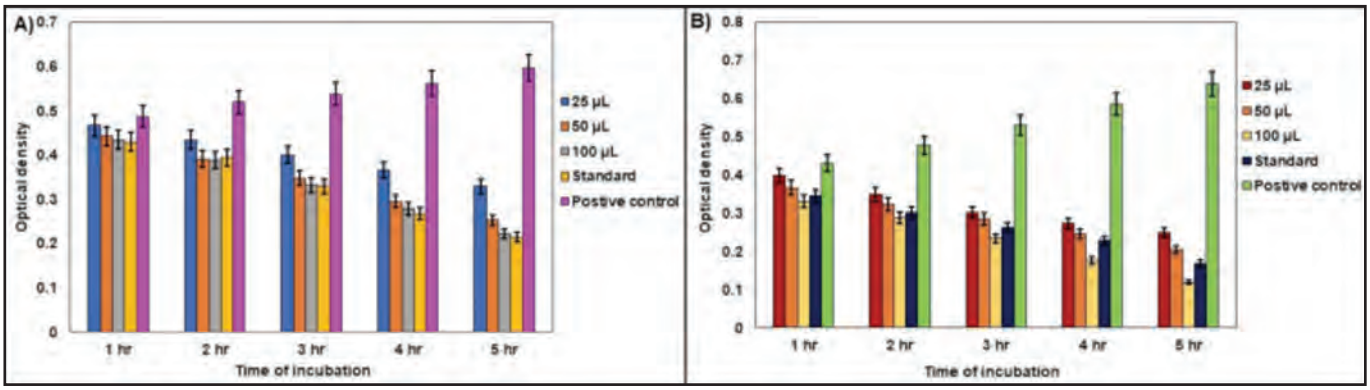


**Fig. 5:** Time kill curve analysis of the green synthesized AgNPs using *O. gratissimum* against A) *E. coli,* and B) *S. aureus*

20 mm zone of incubation was observed for *S. aureus* and *Pseudomonas sp* at the concentration of 100µg/mL. In comparison, the standard revealed 38 mm and 36 mm zones of incubation, as shown in Figures 2 and 3.

*Anti-inflammatory Effect*

The anti-inflammatory activity of green synthesized AgNPs using *O. gratissimum* showed 76% inhibition of protein denaturation was observed at 50 µL concentration in the BSA assay and 74% inhibition in the EA assay. The Anti-inflammatory activity was found as 80% for standard diclofenac sodium. The effects of Ocimum gratissimum mediated AgNPs were comparable to those of the standard - diclofenac sodium at almost all concentrations, as shown in Figures 4A and B.

*Time Kill Assay for E. coli and S. aureus*

A time-kill curve assay was performed in MHB media and the antibacterial activity of AgNPs was determined against *E. coli* and *S. aureus* using optical density values. The lower the optical density, the greater the antibacterial effect. The results showed that the tested bacteria were completely inhibited by AgNPs. At 5 hr, maximum growth inhibition with 0.2 optical density was seen at 100µL concentration for *E. coli. S. aureus* showed 0.1 optical density at 100 µL,concentration as represented in Figures 5A and B.

## DISCUSSION

In this study, Ocimum Gratissimum (OG) enabled the green production of AgNPs. Bovine serum and egg albumin assays were used to evaluate the anti-inflammatory and antibacterial properties of green-synthesized AgNPs made using Ocimum Gratissimum (OG) extract by agar well diffusion and time-kill assay (for antimicrobial effect). In a similar study in our institution, the anti-inflammatory effects of combined herbal Ocimum Gratissimum and Ocimum Tenuiflorum extract-mediated AgNPs and ZnONPs were assessed by BSA and Egg albumin methods, and the results were (75% for the Green synthesized AgNPs and ZnONPs and 81% for Standard Diclofenac at 50 µl). In our study, it was noted as 76% and 81% for AgNPs and Diclofenac sodium). This reproducibility confirms the anti-inflammatory effects of Karunthulasi (OG)-mediated AgNPs. In an earlier study, it was also shown that AgNPs are slightly better than ZnO NPs as anti-inflammatory agents.

AgNPs inhibited TNF-α, COX-2, and MMP-3 expression and inhibited IL-1β, IL-6, and TNF-α) in macrophages. Therefore, it has anti-inflammatory and wound-healing effects.[24,25] Their study on the molecular mechanisms of *Ocimum Gratissimum* showed that it inhibits the lipoxygenase pathway, resulting in decreased synthesis of leukotrienes via the arachidonic acid pathway. It was also shown that the phytocompound OG has an affinity for inflammatory cytokines such as interleukin 1, interleukin 6, TNF-α, interleukin 8, and monocyte chemoattractant protein-1, and can modulate their effects. Thus, the synergistic anti-inflammatory effect of OG and AgNPs is highly plausible.

In this study, the antibacterial activity of OG-mediated AgNPs against *E. coli, S. Aureus*, and *Pseudomonas sp.* was investigated using the agar well diffusion method. The zone of inhibition was 42% (42 mm- Standard,17.5mm- OG), 50% (40mm and 20 mm), and 53% (38mm and 20 mm) for *E. coli, S. aureus*, and *Pseudomonas sp* at a maximum concentration of 100µl. Even at lower concentrations, the effects were almost the same for *Pseudomonas sp.*[26] In their study, only OG plant extracts showed antibacterial properties. In another study on AgNPs by Sharma et al., OG-mediated AgNPs were shown to have antibacterial effects against gram-negative bacteria. In this study, the effect against *Pseudomonas sp*, a gram-negative bacterium, was better, even at lower concentrations. In a previous study,[27] the antimicrobial activity of OG-mediated ZnONPs was studied against oral pathogens, and the zone of inhibition was only 9 mm at all concentrations, suggesting that OG-mediated ZnONPs may not be as effective as antimicrobials when compared with OG-mediated AgNPs.[28,29]

For the time-kill curve assay, the optical density readings were recorded every hour from to 1-5 hours for concentrations of 25, 50, and 100 µL of OG-mediated AgNPs with bacterial inoculum of *E. coli* and *S. aureus,* $5\times10^5$ CFU/mL in MHA medium. For OG-mediated AgNPs, the optical density of E. coli was almost the same as that of the standard antibiotic drugs until 5 h. For *S. aureus* the optical density was lower for OG -AgNPs for all concentrations at all durations, with the lowest value for 100 µL at 5 h. A lower optical density indicated a greater antimicrobial effect of the OG-mediated AgNPs.

## CONCLUSION

OG-mediated AgNPs have potent antibacterial activity against E. coli, Pseudomonas sp, and S. aureus exhibiting a maximum zone of inhibition. It can be used as an adjunct in combination with standard antimicrobials, thereby reducing the dosage of antimicrobial drugs. The anti-inflammatory activity of AgNPs was evaluated using BSA and EA assays, which showed 76% inhibition compared with the standard. This indicates that further research needs to be conducted using In vitro and In vivo analyses.

## CONFLICT OF INTEREST

The authors declare no conflicts of interest would prejudice the impartiality of this scientific work.

## ACKNOWLEDGEMENTS

The authors would like to express their gratitude to Saveetha Medical College and Hospital for supporting this study.

## REFERENCES

1. Barillo DJ, Marx DE. Silver in medicine: A brief history BC 335 to present. Burns 2014; 40: S3-8.
2. Alexander JW. History of the medical use of silver. Surg Infect 2009; 10(3): 289-92.
3. Medici S, Peana M, Nurchi VM, Zoroddu MA. Medical uses of silver: history, myths, and scientific evidence. J Med Chem 2019; 62(13): 5923-43.
4. Liu J, He H, Xiao D, Yin S, Ji W, Jiang S, Luo D, Wang B, Liu Y. Recent advances of plasmonic nanoparticles and their applications. Materials. 2018; 11(10): 1833.
5. Anastasiadis SH, Chrissopoulou K, Stratakis E, Kavatzikidou P, Kaklamani G, Ranella A. How the physicochemical properties of manufactured nanomaterials affect their performance in dispersion and their applications in biomedicine: a review. Nanomaterials. 2022; 12(3): 552.
6. Nguyen NP, Dang NT, Doan L, Nguyen TT. Synthesis of silver nanoparticles: from conventional to 'modern' methods—a review. Processes 2023; 11(9): 2617.
7. Rónavári A, Igaz N, Adamecz DI, Szerencsés B, Molnar C, Kónya Z, Pfeiffer I, Kiricsi M. Green silver and gold nanoparticles: Biological synthesis approaches and potentials for biomedical applications. Molecules 2021; 26(4): 844.
8. Zahoor M, Nazir N, Iftikhar M, Naz S, Zekker I, Burlakovs J, Uddin F, Kamran AW, Kallistova A, Pimenov N, Ali Khan F. A review on silver nanoparticles: Classification, various methods of synthesis, and their potential roles in biomedical applications and water treatment. Water 2021; 13(16): 2216.
9. Rafique M, Sadaf I, Rafique MS, Tahir MB. A review on green synthesis of silver nanoparticles and their applications. Artif Cells Nanomed Biotechnol 2017; 45(7): 1272-91.
10. Shanmugam R, Subramaniam R, Kathirason SG, Ali D, Balusamy SR, Gurusamy A, Arunachalam K, Sellami H. Curcumin-chitosan nanocomposite formulation containing Pongamia pinnata-mediated silver nanoparticles, wound pathogen control, and anti-inflammatory potential. Biomed Res Int 2021; 2021.
11. Roy A, Bulut O, Some S, Mandal AK, Yilmaz MD. Green synthesis of silver nanoparticles: biomolecule-nanoparticle organizations targeting antimicrobial activity. RSC Adv 2019; 9(5): 2673-702.
12. Yakoup AY, Kamel AG, Elbermawy Y, Abdelsattar AS, El-Shibiny A. Characterization, antibacterial, and cytotoxic activities of silver nanoparticles using the whole biofilm layer as a macromolecule in biosynthesis. Sci Rep 2024; 14(1): 364.
13. Cheesman MJ, Ilanko A, Blonk B, Cock IE. Developing new antimicrobial therapies: are synergistic combinations of plant extracts/compounds with conventional antibiotics the solution?. Phcog Rev 2017; 11(22): 57.
14. Morones-Ramirez JR, Winkler JA, Spina CS, Collins JJ. Silver enhances antibiotic activity against gram-negative bacteria. Sci Transl Med 2013; 5(190): 190ra81-.
15. Singh R, Shedbalkar UU, Wadhwani SA, Chopade BA. Bacteriagenic silver nanoparticles: synthesis, mechanism, and applications. Appl Microbiol Biotechnol 2015; 99: 4579-93.
16. Ugbogu OC, Emmanuel O, Agi GO, Ibe C, Ekweogu CN, Ude VC, Uche ME, Nnanna RO, Ugbogu EA. A review on the traditional uses, phytochemistry, and pharmacological activities of clove basil (Ocimum gratissimum L.). Heliyon 2021; 7(11).
17. Imtiaz T, Priyadharshini R, Rajeshkumar S, Sinduja P. Green synthesis and Characterization of silver nanoparticles synthesized using piper longum and its antioxidant activity. J Pharm Res Int 2021; 33(51A): 342-52.
18. Das P, Ghosal K, Jana NK, Mukherjee A, Basak P. Green synthesis and characterization of silver nanoparticles using belladonna mother tincture and its efficacy as a potential antibacterial and anti-inflammatory agent. Mater Chem Phys 2019; 228: 310-7.
19. Loo YY, Rukayadi Y, Nor-Khaizura MA, Kuan CH, Chieng BW, Nishibuchi M, Radu S. In vitro antimicrobial activity of green synthesized silver nanoparticles against selected gram-negative foodborne pathogens. Front microbiol 2018; 9: 379304.
20. Weinstein MP. Methods for dilution antimicrobial susceptibility tests for bacteria that grow aerobically. (No Title). 2018.
21. Zainin NS, Lau KY, Zakaria M, Son R, Razis AA, Rukayadi Y. Antibacterial activity of Boesenbergia rotunda (L.) Mansf. A. extract against Escherichia coli. Int Food Res J 2013; 20(6): 3319.
22. Kamiloğlu Beştepe SE, Sarı G, Özdal T, Çapanoğlu Güven E. Guidelines for cell viability assays. Food Front.2020;1(3).
23. Varghese RM, Kumar A, Shanmugam R. Comparative anti-inflammatory activity of silver and zinc oxide nanoparticles synthesized using Ocimum tenuiflorum and Ocimum gratissimum herbal formulations. Cureus 2024; 16(1).
24. Mikhailova EO. Silver nanoparticles: mechanism of action and probable bio-application. Journal of functional biomaterials 2020; 11(4): 84.
25. Tyavambiza C, Elbagory AM, Madiehe AM, Meyer M, Meyer S. The antimicrobial and anti-inflammatory effects of silver nanoparticles synthesised from Cotyledon orbiculata aqueous extract. Nanomaterials 2021; 11(5): 1343.
26. Olaoye IF, Oso BJ, Aberuagba A. Molecular mechanisms of anti-inflammatory activities of the extracts of Ocimum gratissimum and Thymus vulgaris. Avicenna J Med Biotechnol 2021; 13(4): 207.
27. Chanthaboury M, Choonharuangdej S, Shrestha B, Srithavaj T. Antimicrobial properties of Ocimum species: An in vitro study. J Int Soc Prev Community Dent 2022; 12(6): 596-602.
28. Anandachockalingam A, Shanmugam R, Ryntathiang I, Jothinathan MK, Anandachockalingam III A. Green Synthesis of Silver Nanoparticles Using Zingiber officinale and Ocimum gratissimum Formulation for Its Anti-inflammatory and Antidiabetic Activity: An In Vitro Study. Cureus 2024; 16(4).
29. Pfeifle A, Thulasi Raman SN, Lansdell C, Zhang W, Tamming L, Cecillon J, Laryea E, Patel D, Wu J, Gravel C, Frahm G. DNA lipid nanoparticle vaccine targeting outer surface protein C affords protection against homologous Borrelia burgdorferi needle challenge in mice. Front immunol 2023; 14: 1020134.

# A rare case of tamoxifen induced bilateral optic neuritis

**Akash R, MBBS[1], V Panimalar A Veeramani, DNB[1], Sanjeev Kumar Puri, MS[1], Divya N, MS[2]**

[1]Department of Ophthalmology, Saveetha Institute of Medical and Technical Sciences (Deemed to be University): SIMATS Deemed University, Chennai, Tamilnadu, India, [2]Department of Ophthalmology, Saveetha Institute of Medical and Technical Sciences (Deemed to be University): SIMATS Deemed University, Chennai, Tamilnadu, India

## SUMMARY

**Tamoxifen, an oral medication that blocks estrogen activity, is frequently prescribed for the treatment of advanced breast cancer and as an additional therapy following surgical removal of early stage disease. A 45-year-old female with a history of breast carcinoma treated with tamoxifen presented with sudden onset bilateral visual impairment for 4 days. On ocular examination, the patient exhibited optic disc edema with hyperemia and bilateral anterior pathway defects in visual evoked potentials. Magnetic resonance imaging revealed a thickened right optic nerve sheath with patchy enhancement of the left optic nerve sheath. The patient was diagnosed with bilateral optic neuritis and treated with intravenous methylprednisolone, which resulted in significant improvement in visual acuity and resolution of optic disc edema. This case underscores the importance of vigilant ophthalmological monitoring in patients undergoing tamoxifen therapy to facilitate the early detection and management of ocular complications.**

**KEYWORDS:**
*Tamoxifen, Optic disc oedema, Optic neuritis*

## INTRODUCTION

Tamoxifen, an oral anti-estrogen, is commonly prescribed for the treatment of advanced breast cancer and as adjuvant treatment following surgical resection of early-stage disease.[1] The link between tamoxifen and eye issues was initially noted in 1978. The incidence of tamoxifen-related eye complications varies between 6.3 to 12%. Originally observed in female breast cancer patients receiving exceptionally large doses of tamoxifen (120–130 mg/day), subsequent findings have revealed that ocular problems might also arise with conventional low-dose tamoxifen treatment.[2]

Ophthalmic manifestations associated with tamoxifen include intraretinal crystalline deposits, frequently accompanied by macular edema, keratopathy, pseudocystic foveal cavitation cataracts, and optic neuritis.[3] Optic neuritis constitutes an uncommon but potentially irreversible visual impairment caused by tamoxifen-induced ocular toxicity. It might affect both eyes simultaneously and may manifest as soon as three weeks after initiating tamoxifen therapy.[2]

Although the precise frequency and seriousness of tamoxifen-induced eye conditions remain uncertain, the extensive administration of the medication among patients with breast cancer underscores the actual necessity for recognizing potential adverse ocular outcomes.

## CASE PRESENTATION

A 45-year-old woman experienced an abrupt onset of reduced vision in her right eye, which was subsequently followed by diminished vision in her left eye over the past four days. She had a past history of breast carcinoma diagnosed three years back for which she was operated and receiving Tamoxifen 40 mg/day as an adjuvant therapy. The patient had no history of fever, altered bowel habits, smoking, alcohol consumption, intake of other systemic medications, or trauma.

On ocular examination, visual acuity was counting fingers close to the face in both eyes, and the color vision observed was 0/25. Anterior segment evaluation revealed a sluggishly reactive pupil in both the eyes. Fundoscopy revealed optic disc edema with hyperemia, blurred disc margins, disc elevation, and superior venous pulsation, which were absent in both the eyes. Blood tests, including complete blood count, erythrocyte sedimentation rate, C-reactive protein level, and a comprehensive metabolic panel, were within normal limits. Tests for infectious causes and autoimmune conditions, including antinuclear antibodies and antineutrophil cytoplasmic antibodies, were negative. The Humphrey visual field (HVF) showed constricted fields centrally and dense nasal peripheral field defects in both eyes. Visual evoked potentials revealed bilateral anterior pathway defects. Magnetic resonance imaging (MRI) of the brain showed bilateral and extensive optic neuritis with T2 hyperintensity and perineural enhancement. A neurological opinion was obtained and a diagnosis of bilateral optic neuritis associated with tamoxifen therapy was established. After stopping tamoxifen, the patient was immediately administered intravenous methylprednisolone (1 g) in 500 ml of saline once daily for 5 days, followed by oral prednisolone 1 mg/kg body weight for 11 days, 20mg for 1 day, and 10 mg for 1 day and stopped. Symptomatic improvement was noted and after three months, visual acuity improved to 6/6 in both eyes with resolution of the optic disc edema.

## DISCUSSION

Tamoxifen belongs to the class of triphenylethylene nonsteroidal estrogen antagonists. It is used in the treatment of estrogen-dependent disseminated breast carcinomas and as adjuvant therapy post-surgery. The mechanism involves disrupting the binding of estradiol to target tissues by reducing cytoplasmic receptors and competitively inhibiting the receptor site. The pathological mechanism underlying tamoxifen-induced ocular toxicity suggests that tamoxifen might trigger the accumulation of drug polar lipid complexes within the lysosomes.

*This article was accepted: 22 August 2025*
*Corresponding Author: V Panimalar A Veeramani*
*Email: drpani07@gmail.com*

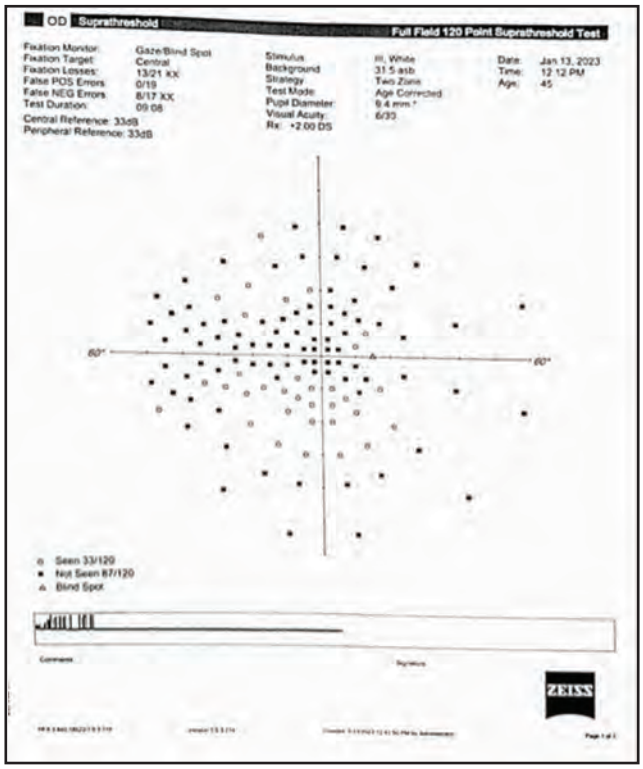


**Fig. 1:** A) HVF of right eye

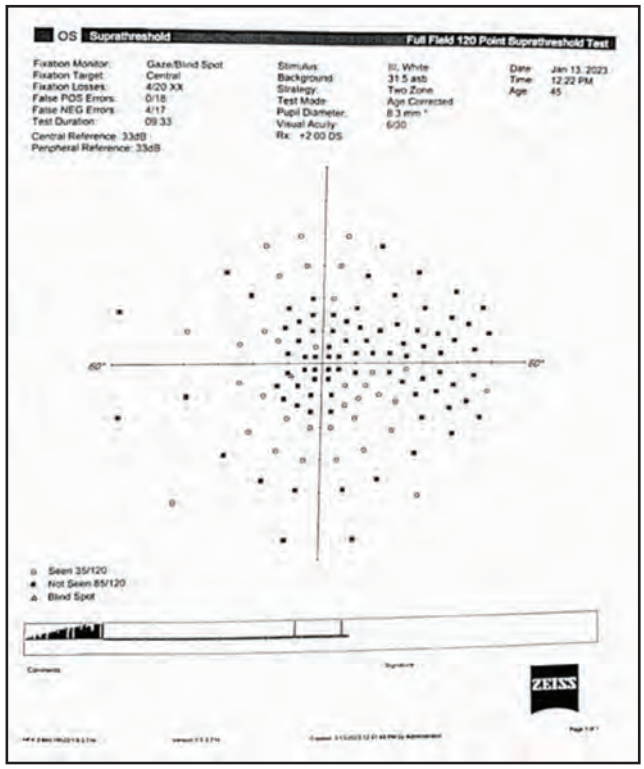


**Fig. 1:** B) HVF of left eye

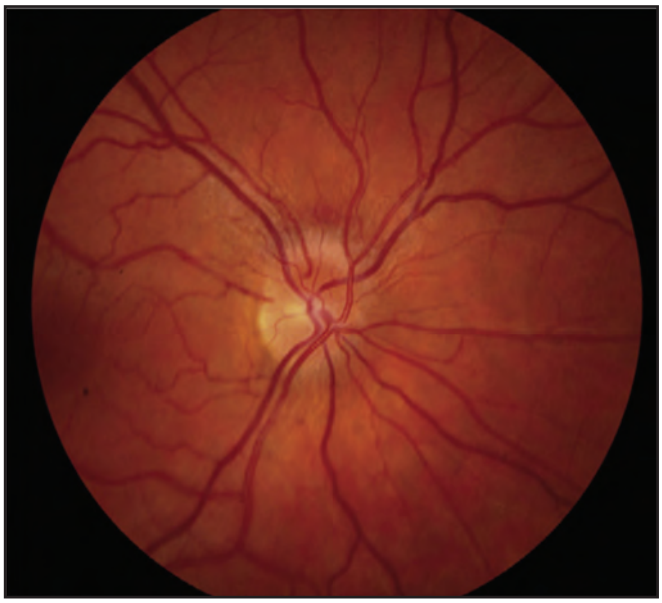

**Fig. 1:** C) Right eye fundus picture showing disc oedema

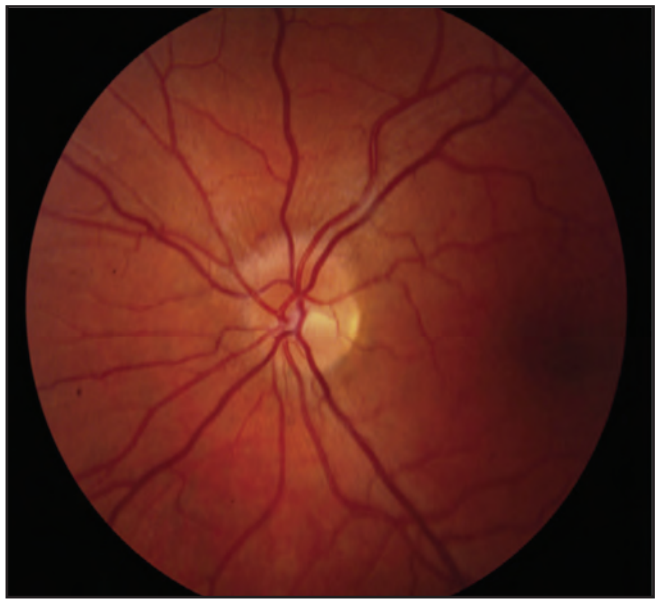

**Fig. 1:** D) Left eye fundus picture showing disc oedema

The ocular effects of tamoxifen toxicity include whorl-like superficial corneal opacities, retractile crystals in the inner layer of the retina, macular edema, abnormalities in the retinal pigment epithelium, pseudocystic foveal cavitation, and optic neuritis.[3,4] In most documented cases, tamoxifen-induced ocular toxicity appears to be reversible. Cessation of the medication led to enhanced visual acuity and resolution of macular edema, retinal hemorrhage, and corneal alterations.

Several case reports have underscored the ocular toxicity in patients receiving low-dose tamoxifen (10–20 mg BD). Even at these lower doses, tamoxifen therapy can trigger retinopathy, marked by intraretinal refractile crystals and macular edema.[5] The key differentiator between high- and low-dose toxicity lies in the potential reversibility upon cessation of treatment. Several patients prescribed 20 mg of BD daily exhibited regression of retinopathy alongside visual improvement.

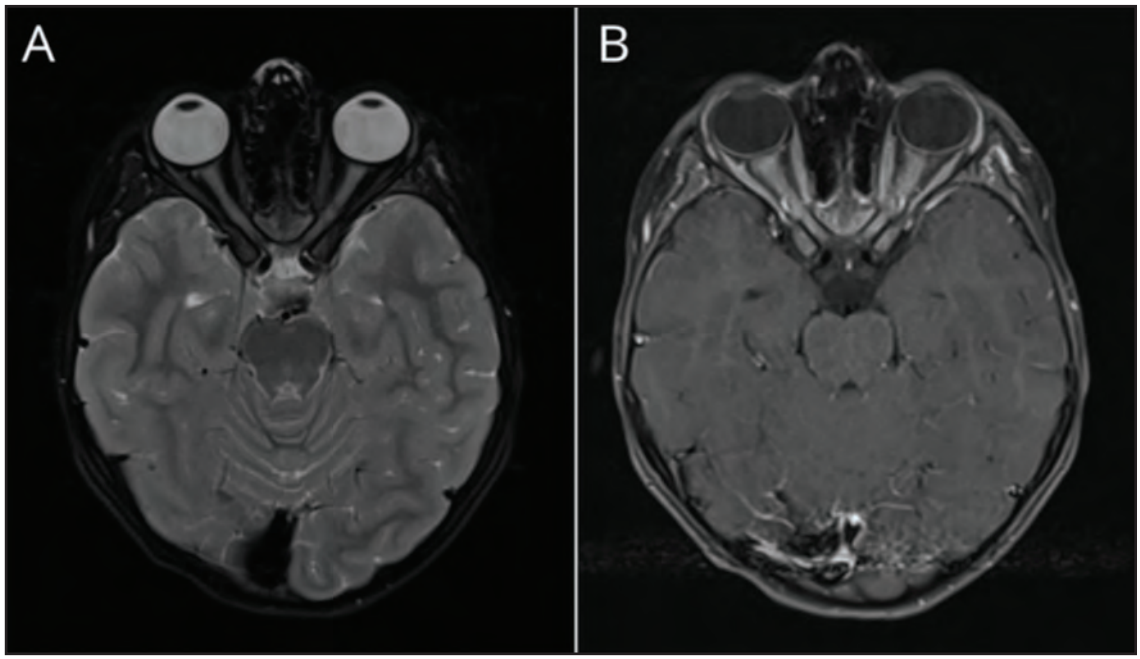


**Fig. 2:** A) Right eye fundus picture showing disc oedema
B) Brain MRI contrast shows perineural enhancement

Research has indicated that patients undergoing tamoxifen treatment exhibit a decrease in cup volume over time. It has been hypothesized that estrogen plays a neuroprotective role. As a result, the utilization of tamoxifen may potentially disrupt astrocytes located within the glial cells of the optic cup, where estrogen receptors are situated at the optic nerve head. This disruption may induce swelling of the optic nerve head, ultimately resulting in a reduction in cup volume.[2]

In this case, both eyes had disc elevation of one disc dioptre with blurring of the nasal, superior, and inferior disc margins in the right eye and blurring of the nasal and superior disc margins in the left eye. The patient's visual acuity improved considerably within a week of starting corticosteroids, and further improvement was noted over the following months. However, some residual peripheral visual field defects remained, which emphasizes the potential for lasting visual impairment, even with timely treatment. Regular follow-up is crucial for monitoring recurrence and managing long-term sequelae.

However, it is vital to exclude other potential causes that can produce an optic disc appearance similar to optic neuritis, such as carcinomatous meningitis, pseudotumor cerebri, intracranial metastasis, and superior sagittal sinus thrombosis due to metastasis and hydrocephalus. Therefore, thorough neurological examination, lumbar puncture, and computerized tomography (CT) scans are essential for proper evaluation.

## CONCLUSION

This case highlights the need for careful ophthalmological monitoring in patients with breast cancer undergoing tamoxifen therapy, as tamoxifen could be responsible for visual impairment in these individuals. Prior to commencing tamoxifen therapy, patients should undergo comprehensive ophthalmic assessment and should be provided with explicit instructions to promptly report any minor visual symptoms. Therefore, prompt recognition and management of ocular complications, such as optic neuritis, can lead to favorable visual outcomes and improve the overall quality of patient care.

## DECLARATION

The authors declare no conflict of interest.

## INFORMED CONSENT

Written informed consent was obtained from the patient for publication of this case report.

## REFERENCES

1. Wang L, Miao H, Li X. Tamoxifen retinopathy: a case report. Springerplus [Internet]. 2015 Dec; 4(1). Available from: http://dx.doi.org/10.1186/s40064-015-1258-2
2. Ngoo QZ, Wan Hitam WH, Tan CL, Krishna Bhavaraju VM. Evaluation of optic nerve head parameters and electrophysiology among breast cancer patients on tamoxifen. Cureus [Internet]. 2022 Jan 9; Available from: http://dx.doi.org/10.7759/cureus.21042
3. Doshi RR, Fortun JA, Kim BT, Dubovy SR, Rosenfeld PJ. Pseudocystic foveal cavitation in tamoxifen retinopathy. Am J Ophthalmol 2014; 157: 1291-8.
4. Tenney S, Oboh-Weilke A, Wagner D, Chen MY. Tamoxifen retinopathy: A comprehensive review. Survey of Ophthalmology. 2024; 69.
5. Zvornicanin J, Sinanovic O, Zukic S, Jusufovic V. Burina Tamoxifen associated bilateral optic neuropathy Acta Neurol Belg. Acta Neurol Belg 2015; 115: 173-5.

ORIGINAL ARTICLE

# Anti-diabetic and anti-microbial activity of *aspalathus linearis* and syzygium aromaticum formulation mediated zinc oxide nanoparticles

**Geetha RV, PhD[1], Shwetha Krish[1], Annika Rajaselin[1], Rajeshkumar Shanmugam, PhD[2], Pradeep Manigandan, MSc[2], Jayasree Anandan, MSc[2]**

[1]Department of Microbiology, Saveetha Dental College and Hospitals, Saveetha Institute of Medical and Technical Sciences, Saveetha University, Chennai, Tamil Nadu, India, [2]Nanobiomedicine lab, Centre for Global Health Research, Saveetha Medical College and Hospitals, Saveetha Institute of Medical and Technical Sciences, Saveetha University, Chennai, Tamil Nadu, India

## ABSTRACT

**Introduction: Zinc oxide nanoparticles (ZnO NPs) exhibit a wide range of biomedical applications majorly used as anti-inflammatory, anti-cancer, anti-diabetic, and anti-microbial activity and other biomedical applications because they show less toxicity and are very compatible. Zinc metal is an inorganic and essential element in the human body at the trace level. ZnO NPs are also GRAS substances (Generally Recognized As Safe). This study's main objective is synthesizing zinc oxide nanoparticles using red tea & clove mediated herbal formulation and screening for its anti-microbial, and anti-diabetic properties.**

**Materials and Methods: Red tea and clove-mediated ZnO NPs were synthesized using the green synthesis method. The anti-microbial activity was tested against oral pathogens using the agar well diffusion method, while the anti-diabetic activity was estimated using the alpha-amylase inhibitory assay method by using red tea and clove-mediated ZnO NPs.**

**Results: ZnO NPs were successfully synthesized using red tea and clove-formulated extract. The synthesized ZnO NPs using *Aspalathus linearis* (red tea) and *Syzygium aromaticum* (clove) mediated ZnO NPs were characterized using UV visible spectrophotometry and SEM (Scanning Electron Microscope) analysis. The green synthesized ZnO NPs show promising anti-microbial activity by exhibiting a 12 mm zone of inhibition against *S. aureus*, 11 mm in *E. faecalis*, 9 mm in *S. mutans*, and 11 mm in *C. albicans*. In anti-diabetic activity, the green synthesized ZnO NPs showed a maximum inhibition percentage of up to 80% at the maximum concentration of 50 µg/mL.**

**Conclusion: Green synthesized ZnO NPs using red tea and clove showed maximum efficacy in anti-microbial properties which can lead to huge potential use as antibacterial agents. Simultaneously, anti-diabetic activity showed an excellent inhibition percentage which can be a potent therapeutic agent in the field of nanomedicine in diabetes management.**

**KEYWORDS:**
*Zinc oxide nanoparticles, anti-diabetic activity, green synthesis, biomedical applications.*

## INTRODUCTION

Nanoparticles synthesized by physical and chemical methods have fewer uses in the field of clinical research because of their toxicity level.[1] Due to the physio-chemical properties of plant-based nanoparticles, this process also has the additional advantage of longer life span of nanoparticles that overcomes the restraint of conventional physical and chemical methods in the synthesis of nanoparticles.[2] Nanomaterials exhibit atom-like behavior when divided to nearly atomic size because of their enormous surface area. It is anticipated that the global nanotechnology revolution will have an impact on several biomedical research fields, including medication delivery, cancer therapy, and cell imaging.[3] Zinc Oxide nanoparticles (ZnO NPs) stand out among metal oxide nanoparticles due to their distinctive optical and chemical behaviors that can be easily controlled by altering their shape.[4] ZnO NPs are part of a group of metal oxides, which are distinguished by their ability for photocatalysis and photo-oxidation of chemical and biological species.[5] ZnO NPs were synthesized by the green synthesis method, which is eco-friendly because of their unique characteristics and adaptable nature, where they are widely used in sensors, biological labelling, bio-imaging, and biomedical applications owing to their anti-microbial, anti-inflammatory, anti-oxidant, and anti-diabetic activities.[6] Owing to their ease of use, environmental friendliness, and high level of biological activity, plant-mediated biological synthesis of nanoparticles is significant. ZnO NPs have demonstrated an encouraging future in biomedical research, particularly in the domains of anti-cancer and anti-microbial fields.[7] These fields are associated with their strong ability to induce insufficient oxygen species (ROS) formation, release zinc ions, and induce cell death. As more bacteria are becoming resistant to antibiotics and new strains are emerging, scientists have given much importance to metal and metal oxide NPs as antibacterial agents.[8] Zinc-based therapy is appealing because of the link between diabetes and an imbalance in zinc homeostasis. ZnO NPs were tested for anti-diabetic properties in many previous studies.[9] Silver, gold, and ZnO NPs have been synthesized using plants like *Withania somnifera, Amygdalus scoparia, Hibiscus subdariffa, Hibiscus rosa-sinensis, Murraya koenigii, Moringa oleifera, Tamarindus indica L, Ocimum sanctum, Cymbopogon citratus*, and it is also been stated that ZnO NPs have been made using *Aloe vera* leaf extract.[10]

*This article was accepted: 06 August 2025*
*Corresponding Author: S Rajeshkumar*
*Email: rajeshkumars.smc@saveetha.com*

Common products such as rubber, cosmetics, and paint are produced using ZnO NPs, especially in biological applications that play a vital role because of their excellent biocompatibility and economically friendly nature.[11] ZnO NPs are well known for their anti-microbial activity because of their ability to cause cell death by membrane disruption. Anti-microbial compounds from herbal sources have good therapeutic potential and can be utilized.[12] Plant-derived nanoparticles play a vital role in the field of biomedicine due to their environmental friendliness, lack of harmful chemicals, elimination of the culture management procedure, and lack of physical and chemical parameters.[13] Many natural ingredients have been studied for their biomedical properties, such as anti-inflammatory, antioxidant, anti-microbial, anti-diabetic, anti-cancer, and so on. Clove *(Syzygium aromaticum)* and red tea *(Aspalathus linearis)* have been studied for their potential biomedical properties.[14] Clove has been found to have anti-microbial, antiseptic, anti-diabetic, and anti-carcinogenic properties. Red tea, also known as Rooibos tea, is rich in antioxidants and has been found to have anti-inflammatory and anti-cancer properties. Thus, herbal formulations can be developed as potent therapeutic agent.[15]

This study aimed to evaluate the anti-microbial properties of green synthesized ZnO NPs of *Aspalathus linearis* and Syzygium aromaticum against different oral pathogens. Anti-diabetic activity was assessed by alpha-amylase and beta-glucosidase enzyme inhibitory assays at various concentrations and compared to the standard tested.

## MATERIALS AND METHODS

*Preparation of Plant Extract*

Aspalathus linearis and Syzygium aromaticum were purchased from a commercial store and used in further experiments. 1 g of clove and 1 g of red tea powder were added to 100 mL of distilled water and boiled in a heating mantle at 45-50 degrees Celsius for 15-20 mins. The boiled solution was filtered through Whatman No.1 filter paper, and the extracted solution was utilized to synthesize ZnO NPs.

*Synthesis of ZnO NPs*

Zinc acetate (30 mM, millimolar) was dissolved in 50 mL of distilled water and stirred gently by adding 50 mL of the extracted plant solution. The solution was mixed for 24 hours using a magnetic stirrer, and the dark brown-yellow color confirmed the synthesis of ZnO NPs. After 24 hr of incubation the prepared solution was centrifuged at 8000 RPM (Rotation per minute) using a centrifuge and the pellet was collected.

*Characterization of Synthesized ZnO NPs*

UV-Vis spectroscopy was also performed to further confirm the formation of ZnO NPs. The absorption spectrum of the synthesized ZnO NPs was analyzed using a UV–Vis spectrophotometer in the range of 350 to 750 nm. Scanning electron microscopy (SEM) was used to examine the surface features and particle shapes of the recently produced nanoparticle formulations.

*Anti-microbial Activity of Green Synthesized ZnO NPs*

The anti-microbial activity of red tea- and clove-mediated ZnO NPs was investigated against C*andida albicans, Streptococcus mutans, Enterococcus faecalis,* and *Staphylococcus aureus* strains. Mueller-Hinton Agar was used for this test to estimate the anti-microbial properties of the synthesized ZnO NPs. The medium was prepared and sterilized at 121°C for 15 minutes. A 9 mm sterile polystyrene tip was used to make wells in the sterilized plates, and the test organisms were spread on their respective plates. ZnO NPs at different concentrations (25, 50, and 100 µg/mL) were loaded, and in the respective wells, standard antibiotic Amoxyrite 20µL was added to the wells, which acted as a standard for bacteria, and fluconazole was used as a standard for fungi. The plates were maintained undisturbed for 24 h at 37 °C. After incubation, zones of inhibition were observed and measured in millimeters.

*In-vitro Anti-diabetic Assay*

*Alpha-Amylase Inhibitory Assay*

Alpha-amylase enzyme inhibition was obtained by estimating the quantity of maltose unfettered during the process, different levels of ZnO NPs (10, 20, 30, 40, and 50 µg/mL), and 100 µL of alpha-amylase solution for 30 min at room temperature. Next, starch solution (1% w/v) 100 µL was added to the solution and was incubated for 10 minutes. The DNSA reagent 100 µL was released to restrict the reaction by heating the water bath for 5 min. The control was maintained by replacing the sodium phosphate buffer, which was maintained at a pH of 6.9, with the same quantity of enzyme extract. At 540 nm, the observations were recorded, and the activity was performed in triplicate using acarbose as the standard.

% of inhibition = C-T/C x 100, where C is the control and T is the test sample.

*Beta-Glucosidase Inhibition Assay*

The anti-diabetic effect of green-synthesized ZnO NPs was estimated using a β-glucosidase enzyme inhibitory assay. At different concentrations (10, 20, 30, 40, and 50 µg/mL), ZnO NPs were added to 1 mL of beta-glucosidase solution and starch solution in the presence of 0.2 M tris buffer at pH 8.0. The solution was incubated for approximately 40 min, and the reaction was terminated by adding 2 ml of 6N HCl as in previous literature.[16] In this study, acarbose was used as a positive control.

% of inhibition = C-T/C x 100, where C is the control and T is the test sample.

*Statistical analysis:*

To ensure that the results were accurate, each experiment was performed three times. Statistical analysis of the measured anti-microbial and anti-diabetic activity data was performed using the standard error (SE) method. Standard error provides a measure of the variability of the sample means, allowing for an assessment of the importance and accuracy of the results.

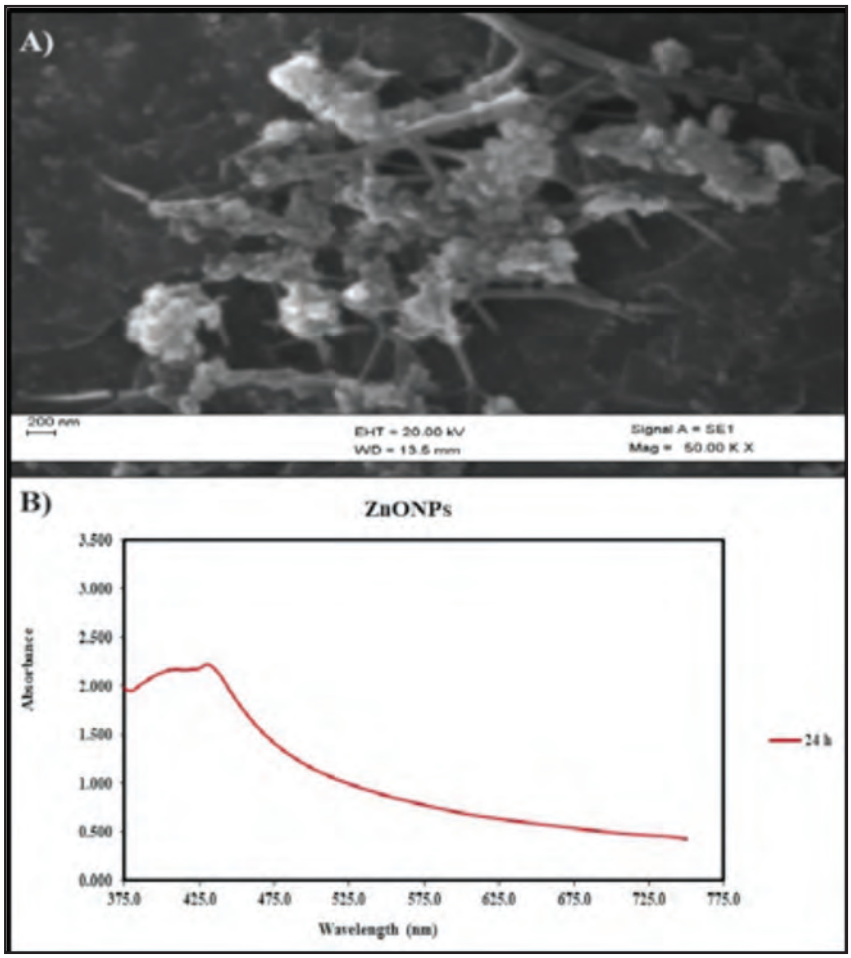


**Fig. 1:** A) UV-visible spectra of *A. linearis* and *S. aromaticum*-mediated ZnO NPs formulation
B) SEM analysis of green synthesized ZnO NPs
ZnO NPs: zinc oxide nanoparticles; *A. linearis*– *Aspalanthus linearis; S. aromaticum*– *Syzygium aromaticum*

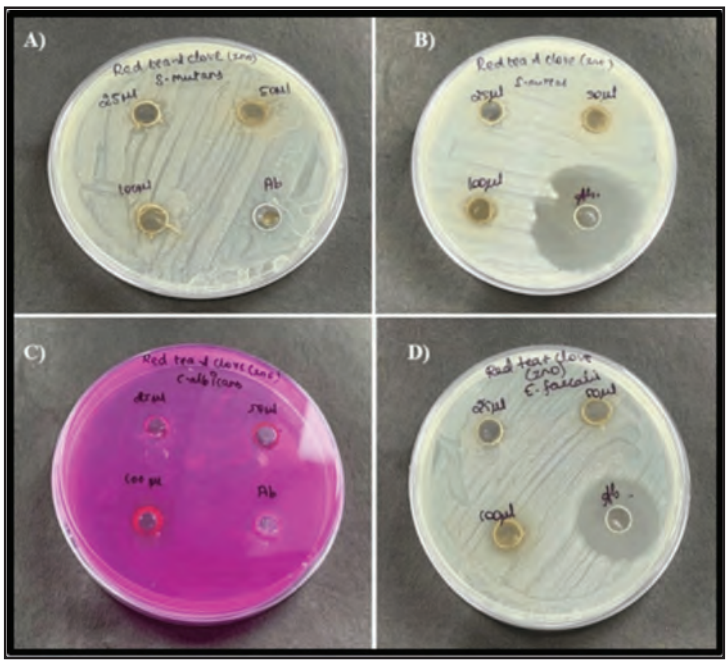


**Fig. 2:** Image depicting the anti-microbial activity of ZnO NPs against oral pathogens *A) S. mutans, B) S. aureus, C) C. albicans D) E. faecalis*
ZnO NPs - Zinc oxide nanoparticles

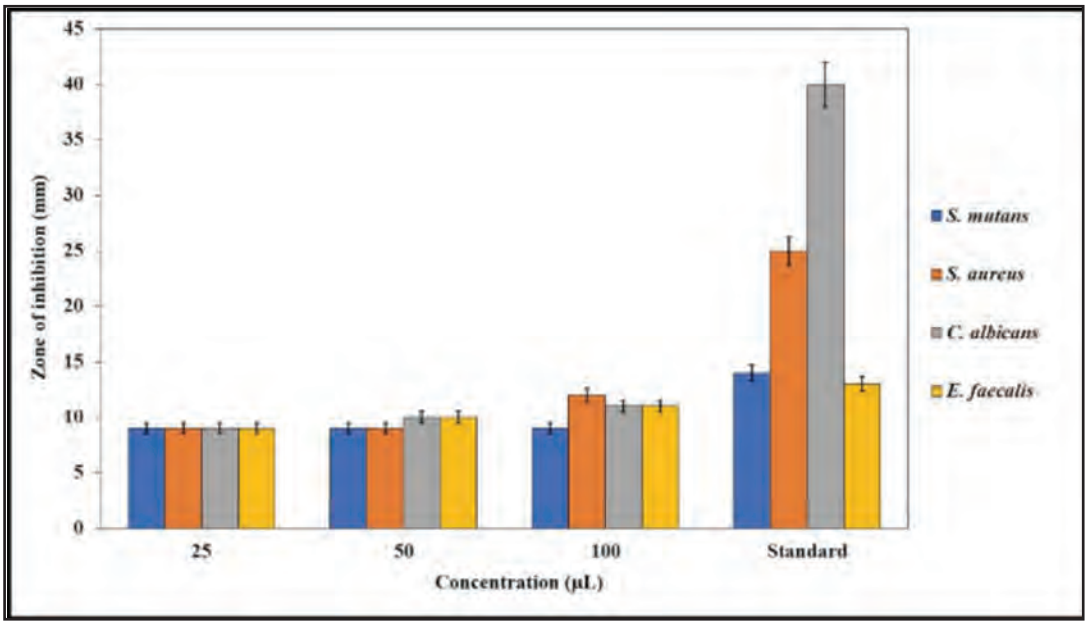


**Fig. 3:** Graph representing the antibacterial activity of *A. linearis* and *S. aromaticum-mediated* ZnO NPs against oral pathogens
ZnO NPs: zinc oxide nanoparticles, *A. linearis*– *Aspalathus linearis, S. aromaticum*– *Syzygium aromaticum*. Error bars in the graph represent standard error. Two-way ANOVA was used to evaluate the significance. The P-value (P<0.0005) was statistically significant.

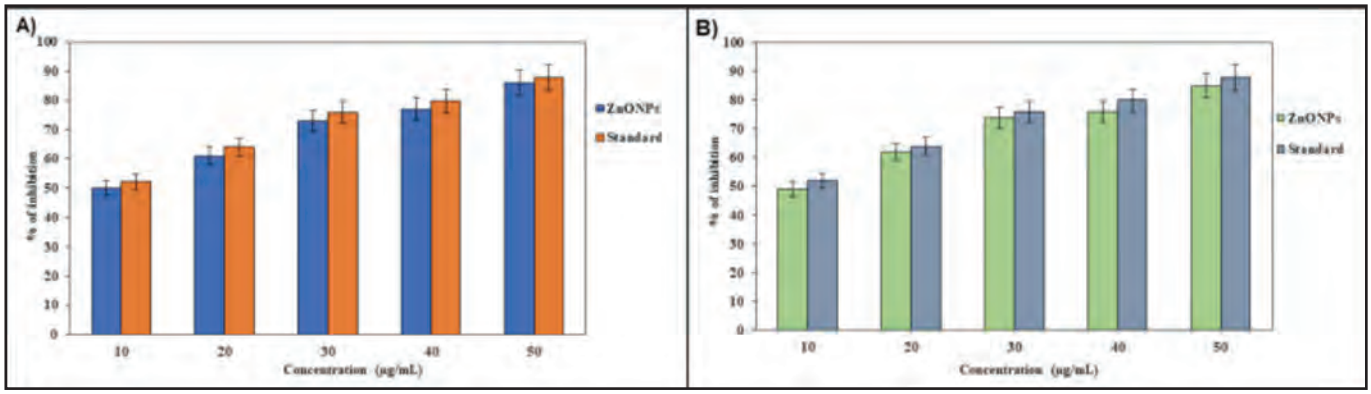


**Fig. 4:** Anti-diabetic activity of ZnO NPs synthesized from *A. lineraris* and *S. aromaticum* formulation A) α-amylase enzyme inhibition assay, and B) β-glucosidase enzyme inhibition assay. The error bar in the graph represents standard error. Two-way ANOVA is used to evaluate the significance. The P value (P<0.0005) is statistically significant.

## RESULTS

*Visual Confirmation & Its Characterization Techniques*

Green-synthesized red tea and clove-mediated ZnO NPs were successfully synthesized. The visible color change from light brown to dark brown indicated the reducing and capping ability of the red tea and clove-mediated herbal formulation. The shape and size distribution of the synthesized ZnO NPs were determined using SEM. The production of ZnO NPs with a consistent and irregular shape, strong crystallinity, and well-defined size distribution was verified by SEM analysis, as shown in Figure 1A. Understanding the characteristics and possible uses of ZnO NPs in a variety of industries, such as photocatalysis, sensors, and biological applications, depends on these findings. The synthesized ZnO NPs prepared using red tea and clove exhibited a maximum peak at 410 nm, as measured using a UV-visible spectrophotometer, as shown in Figure 1B. After 24 h, the UV readings were noted and centrifuged at 8000 rpm (rotation per minute). The supernatant was discarded and the pellet was collected and used for further studies.

*Anti-microbial Activity*

As shown in figure 2 and 3, the green-synthesized ZnO NPs nanoparticles were tested for antimicrobial activity against oral pathogens: *A) S. mutans, B) S. aureus, C) C. albicans, and D) E. faecalis*. The synthesized ZnO NPs have exhibited a maximum zone of inhibition of 9 mm in S. mutans, 12 mm in *S. aureus*, 11 mm in E. faecalis, and 11 mm in *C. albicans*. The synthesized nanoparticles were compared with standards for both fungi and bacteria. The maximum zone of inhibition

**Table. 1: Anti-diabetic activity of ZnO NPs synthesized from A. lineraris and S. aromaticum formulation A) α-amylase enzyme inhibition assay, and B) β-glucosidase enzyme inhibition assay.**

A)

| Concentration (µg/mL) | 10 | 20 | 30 | 40 | 50 |
|---|---|---|---|---|---|
| Standard (%) | 53.34 | 60.43 | 64.56 | 73.76 | 81.54 |
| ZnONPs (%) | 52.67 | 64.43 | 76.53 | 80.35 | 88.53 |

B)

| Concentration (µg/mL) | 10 | 20 | 30 | 40 | 50 |
|---|---|---|---|---|---|
| Standard (%) | 52.36 | 64.76 | 76.53 | 80.43 | 88.28 |
| ZnONPs (%) | 50.54 | 61.25 | 72.38 | 79.65 | 83.92 |

was found to be 12 mm in *S. aureus* and 11 mm in C. albicans, which represents the efficacy of the synthesized ZnO NPs.

*In vitro Anti-diabetic Activity*

*Alpha-Amylase Enzyme Inhibition*

The enzyme amylase breaks down or transforms carbohydrates into glucose, and as a result, it is crucial for the regulation of blood glucose levels. There must be a technique to manage glucose levels, as high glucose levels might cause major clinical problems. To assess the anti-diabetic activity of ZnO NPs, various quantities of nanoparticles (10-50 µg/mL) have been examined against the enzyme, and the results showed maximum inhibition of 50, 61, 73, 77, 86 % at the various concentrations of 10, 20, 30, 40, 50 µg/mL. The standard readings of anti-diabetic activity were observed as 52, 64, 76, 80, and 84% at the concentration of 10-50 µg/mL. Overall, the anti-diabetic assay showed similar variations, with dose-dependent inhibition, as shown in Figure 4A.

*Beta-Glucosidase Enzyme Inhibition*

As shown in Figure 4B, ZnO NPs exhibited a similar percentage to the standard, which was concentration-dependent in the β-glucosidase enzyme assay. At concentrations of 10 µL, 20 µL, 30 µL, 40 µL, and 50 µL, the corresponding percentages of inhibition were 49%, 62%, 74%, 76%, and 85%. The percentage of inhibition increased in concentration-dependent ranging from 52% to 88% for the standard. The results indicate not only the efficacy of ZnO NPs, but also how the herbal formulation enhances the anti-diabetic activity of these nanoparticles. These findings suggest the possible ways for novel therapeutic strategies for green-synthesized ZnO NPs in diabetes management. The values for both alpha-amylase and beta-glucosidase enzyme inhibition are shown in Table I.

## DISCUSSION

Overall, this study defines the potential of *Aspalathus linearis* (red tea) and *Syzygium aromaticum* (clove)-mediated ZnO NPs in the eradication of oral pathogens and their anti-diabetic effects using alpha-amylase and beta-glucosidase enzyme inhibition assays. In terms of anti-microbial activity, *S. aureus* and *E. faecalis* showed a higher zone of inhibition of approximately 12 mm at a concentration of 100 µg/mL, whereas *S. mutans* and *C. albicans* were less resistant to the synthesized ZnO NPs. In anti-diabetic activity, the inhibition percentage of synthesized ZnO NPs using alpha-amylase inhibition assay ranges from 50%, 61%, 73%, 77%, and 86% whereas the standard value ranges up to 52, 64, 76, 80, and 88% of inhibition using alpha-amylase inhibition assay. Similarly, the β-glucosidase enzyme inhibition method demonstrated a concentration-dependent inhibition pattern, with increasing percentages from 49%, 62%, 74%, 76%, and 85%, whereas the standard ranged from 52 to 88%. Overall, the synthesized ZnO NPs exhibited potential anti-microbial and anti-diabetic activities, which could be further developed into beneficial therapeutic agents.

In a previous study, ZnO-NPs were effectively synthesized by optimizing the extraction and synthesis process using aqueous *Allium cepa L.* waste peel extract. Using a conventional methodology, we examined the antioxidant and antibacterial activities of green-synthesized ZnO NPs to demonstrate their potential bioactivity. The growth of inhibition was observed to be exclusively greater in the synthesized ZnO NPs than in the usual antibacterial product.[17] Similarly, the antibacterial potential of red tea and clove-mediated ZnO NPs showed a maximum zone of inhibition which displays the impact of ZnO NPs at various concentrations on pathological bacterial strains and the bacterial growth was substantially suppressed by high quantities of nanoparticles (5 mg/mL). ZnO NPs derived from leaf and flower extracts consistently inhibited all bacterial strains utilized in the analysis, as indicated by the zones of

inhibition. It is hypothesized that the generation of reactive oxygen species (ROS) following bacterial cell membrane attachment, which results in membrane damage and protein malfunction, is the mechanism of action responsible for suppressing bacterial growth.[18] The potential reason for the antibacterial activity of green-synthesized ZnO NPs could be attributed to the presence of leaf extract, which functions as a capping agent inside the NPs, reducing particle size and augmenting anti-microbial activities. This could be explained simply by noting that smaller particles often have a higher surface-to-volume ratio, meaning that their antibacterial activities are more effective overall.[19] Plant extracts of red tomato fruit *(Lycopersicon esculentum M.)*, chamomile flowers *(Matricaria chamomilla L.)*, and olive leaves *(Olea europaea)* were successfully used in this study to biosynthesize ZnO NPs. ZnO NPs synthesized from olive leaves *(Olea europaea)* at 16.0 µg mL–1 showed the maximum zone of inhibition in antibacterial activity. The study showed that the antibacterial efficacy of the synthesized ZnO NPs was size-dependent.[20]

The potential medicinal uses of biosynthesized NPs as anti-diabetic medications have been investigated. Compared to the standard medication, Zn-doped *Catharanthus roseus* NPs demonstrated good α-amylase inhibitory activity. Overall, this research showed that Zn-doped C. roseus NPs can have strong anti-diabetic effects. Furthermore, when compared to the standard sample, these green NPs exhibited zero adverse impacts.[21] In a previous study, the solution combustion approach was used to synthesize ZnO NPs for the first time using extracts from Areca catechu leaves. Several bioprocesses, including glucose metabolism, are facilitated by Zn. The effects of biosynthesized ZnO NPs on anti-diabetic and anti-cancer activities were investigated in this study. ZnO NPs demonstrated excellent efficacy in treating diabetic problems, as well as potent anti-cancer activity against cancer cell types. These results provide different ways and prospective uses of plant-mediated nanoparticles in many biological issues.[22] A biological synthesis approach was used to successfully synthesize Pro-ZnO NPs from methanol propolis extract. Pro-ZnO NPs were identified as nanoparticles with a hexagonal quartzite structure. Pro-ZnO NPs demonstrated substantial inhibition rates against α-amylase, and α-glucosidase-ZnO NPs can thus be used as a natural anti-diabetic drug.[23] Similarly, the anti-diabetic effects of red tea and clove-mediated ZnO NPs were evaluated using alpha-amylase and beta-glucosidase enzyme inhibition. The alpha-amylase inhibitory assay showed a great potential of 85% at a concentration of 50 µL, and 86% in beta-glucosidase enzyme inhibitory assay, which showed the concentration-dependent inhibition. Thus, the synthesized ZnO NPs have great potential as novel drugs for diabetes management.

## CONCLUSION

The era of modern medicine is an important field that can utilize the green synthesis of nanoparticles assisted by plants and herbs, which may be a replacement for future medicine. The use of medicinal and herbal plants has increased because of fewer adverse effects and because they are significantly effective against infectious pathogens. Based on previous studies, it is concluded that herbal-assisted ZnO NPs show potentially effective anti-diabetic and anti-microbial effects. Based on these findings, green synthesis of ZnO NPs can be used in additional research, such as toxicological testing and investigations involving animals, for further improvements. It has been implicated in the healing of wounds in diabetic patients, antifungal and antibacterial lotions for infections, and nanoparticle-coated dental implants.

## CONFLICT OF INTEREST

The authors declare no conflicts of interest would prejudice the impartiality of this scientific work.

## ACKNOWLEDGEMENTS

The authors would like to express their gratitude to Saveetha Medical College and Hospital for supporting this work.

## REFERENCES

1. Anandan S, Mahadevamurthy M, Ansari MA, et al.: Biosynthesized ZnO-NPs from Morus indica attenuates methylglyoxal-induced protein glycation and RBC damage: in-vitro, in-vivo and molecular docking study. Biomolecules 2019; 9: 882.
2. Santhoshkumar J, Kumar SV, Rajeshkumar S: Synthesis of zinc oxide nanoparticles using plant leaf extract against urinary tract infection pathogen. Resour Effic Tech. 2017; 3: 459-65.
3. Naik J, David M: Phytofabrication of silver and zinc oxide nanoparticles using the fruit extract of Phyllanthus emblica and its potential anti-diabetic and anti-cancer activity. Particul Sci Technol 2023; 18: 761-73.
4. Sirelkhatim A, Mahmud S, Seeni A, et al.: Review on zinc oxide nanoparticles: antibacterial activity and toxicity mechanism. Nanomicro Lett. 2015; 7: 219-42.
5. Kumar SS, Venkateswarlu P, Rao VR, et al.: Synthesis, characterization and optical properties of zinc oxide nanoparticles. Int Nano Lett. 2013; 3: 1-6.
6. Vijayakumar S, Mahadevan S, Arulmozhi P, et al.: Green synthesis of zinc oxide nanoparticles using Atalantia monophylla leaf extracts: Characterization and anti-microbial analysis. Mater Sci Semicond Process 2018; 1: 39-45.
7. Gopikrishnan R, Zhang K, Ravichandran P, et al.: Synthesis, characterization and biocompatibility studies of zinc oxide (ZnO) nanorods for biomedical application. Nanomicro Lett 2010; 2: 31-6.
8. Sangeetha G, Rajeshwari S, Venckatesh R: Green synthesis of zinc oxide nanoparticles by aloe Barbadensis miller leaf extract: Structure and optical properties. Mater Res Bull 2011; 46: 2560-6.
9. Alamdari S, Sasani Ghamsari M, Lee C, et al.: Preparation and characterization of zinc oxide nanoparticles using leaf extract of Sambucus ebulus. Appl Sci 2020; 10: 3620.
10. Bharathi D, Bhuvaneshwari V: Synthesis of zinc oxide nanoparticles (ZnO NPs) using pure bioflavonoid rutin and their biomedical applications: antibacterial, antioxidant and cytotoxic activities. Res Chem Intermed 2019; 15: 2065-78.
11. Dhatwalia J, Kumari A, Chauhan A, et al.: Rubus ellipticus Sm. fruit extract mediated zinc oxide nanoparticles: a green approach for dye degradation and biomedical applications. Materials 2022; 6: 3470.

12. Minhas LA, Mumtaz AS, Kaleem M, et al.: Green synthesis of zinc oxide nanoparticles using Nostoc sp. and their multiple biomedical properties. Catalysts 2023; 13: 549.
13. Mohd Yusof H, Mohamad R, Zaidan UH, et al.: Microbial synthesis of zinc oxide nanoparticles and their potential application as an anti-microbial agent and a feed supplement in animal industry: a review. J Anim Sci Biotechnol 2019; 10: 1-22.
14. Ali SG, Ansari MA, Jamal QM, et al.: Butea monosperma seed extract mediated biosynthesis of ZnO NPs and their antibacterial, antibiofilm and anti-quorum sensing potentialities. Arab J Chem 2021; 14: 103044.
15. Cruz DM, Mostafavi E, Vernet-Crua A, et al.: Green nanotechnology-based zinc oxide (ZnO) nanomaterials for biomedical applications: a review. J Phys Materials 2020; 12: 034005.
16. Shanmugam R, Munusamy T, Rajaselin A, et al.: Exploring the In vitro anti-diabetic potential of metal oxide nanoparticles synthesized using lemongrass and mint formulation. Cureus 2024; 16: 53489.
17. Islam MF, Miah MA, Huq AO, et al.: Green synthesis of zinc oxide nano particles using Allium cepa L. waste peel extracts and its antioxidant and antibacterial activities. Heliyon 2024; 10: 25430.
18. Ifeanyichukwu UL, Fayemi OE, Ateba CN: Green synthesis of zinc oxide nanoparticles from pomegranate (Punica granatum) extracts and characterization of their antibacterial activity. Molecules 2020; 25: 4521.
19. Ramesh P, Saravanan K, Manogar P, et al.: Green synthesis and characterization of biocompatible zinc oxide nanoparticles and evaluation of its antibacterial potential. Sens Bio-Sens Res 2021; 31: 100399.
20. Ogunyemi SO, Abdallah Y, Zhang M, et al.: Green synthesis of zinc oxide nanoparticles using different plant extracts and their antibacterial activity against Xanthomonas oryzae pv. oryzae. Artif cells nanomed biotechnol 2019; 47: 341-52.
21. Govindan N, Vairaprakasam K, Chinnasamy C, et al.: Green synthesis of Zn-doped Catharanthus roseus nanoparticles for enhanced anti-diabetic activity. Mater Adv 2020; 1: 3460-5.
22. Shwetha UR, Latha MS, Rajith Kumar CR, et al.: Facile synthesis of zinc oxide nanoparticles using novel Areca catechu leaves extract and their in vitro anti-diabetic and anti-cancer studies. J Inorg Organomet Polym Mater 2020; 30: 4876-83.
23. PD DA, Plashintania DR, Putri RM, et al.: Synthesis of zinc oxide nanoparticles using methanol propolis extract (Pro-ZnO NPs) as anti-diabetic and antioxidant. PloS one 2023; 18: 0289125.

# Unilateral vitritis in an immunocompetent individual – A rare presentation of ocular toxoplasmosis

**Akash R, MBBS1, Chiramana Supreeth Reddy, MS1, Nithya R, MS1, Sankar Kumar T, MS[2]**

[1]Department of Ophthalmology, Saveetha Institute of Medical and Technical Sciences (Deemed to be University): SIMATS Deemed University, Chennai, Tamilnadu, India, [2]Department of Ophthalmology, Saveetha Institute of Medical and Technical Sciences (Deemed to be University): SIMATS Deemed University, Chennai, Tamilnadu, India

## SUMMARY

**Ocular toxoplasmosis is the leading cause of infectious retinochoroiditis in both adults and children. It is caused by the obligate intracellular parasite, *Toxoplasma gondii*. It is a common cause of posterior uveitis and focal retinitis, typically seen in immunocompetent individuals as a primary infection or in immunocompromised individuals as reactivation of latent infection. Here, we report a rare case of a 29-year-old immunocompetent female presenting with gradual, painless diminution of vision in the left eye associated with headache for over one month. She had a history of hypertension but no other significant medical history. On ocular examination anterior segment was unremarkable and fundus examination of left eye showed "Headlight in fog appearance" suggestive of vitritis. Serological evaluation revealed positive for Toxoplasma IgG antibodies. The patient was treated with cotrimoxazole, oral prednisolone, and topical steroids for 4-6 weeks. Following treatment, her visual acuity improved to 6/6 in left eye. This case highlights the importance of considering ocular toxoplasmosis in the differential diagnosis of unilateral vitritis, even in immunocompetent patients.**

**KEYWORDS:**
*Toxoplasma gondii, Vitritis, Trimethoprim and Sulfamethoxazole*

## INTRODUCTION

Ocular toxoplasmosis, caused by the intracellular protozoan parasite *Toxoplasma gondii*, is the leading cause of infectious retinochoroiditis in both adults and children.[1] The usual manifestation involves localized retinochoroiditis near a pigmented chorioretinal scar, accompanied by inflammation in the vitreous. Beyond this typical presentation, other atypical manifestations such as scleritis, rhegmatogenous and serous retinal detachment, retinal vasculitis, retinal vascular occlusion, optic neuropathy and punctuate outer retinal toxoplasmosis have been reported. Toxoplasmosis of the central nervous system typically occurs in individuals with severe immunosuppression. However, ocular toxoplasmosis can occur in immunocompetent individuals.

In this report, we present a rare case of unilateral vitritis in a young immunocompetent patient who was ultimately diagnosed with ocular toxoplasmosis. This case highlights the atypical presentation and importance of comprehensive diagnostic evaluation.

## CASE PRESENTATION

A 29-year-old woman complained of progressive, painless loss of vision in her left eye associated with a headache over the course of a month. History of exposure to pets one month after her recent trip. History of intermittent fever initially for 7 days. She had a one-year history of systemic hypertension, but no history of diabetes mellitus, steroid use, or other systemic disorders. No history of photophobia, double vision, seizures, vomiting, rashes, neck stiffness, cough, or breathlessness.

On examination, the best-corrected visual acuity was 6/6 in the right eye and 4/60 in the left eye. Examination of the anterior segment revealed no bilateral abnormalities, and the intraocular pressure was within the normal range. However, visualization of the posterior segment was hindered due to dense vitritis in left eye, resulting in a "Headlight in fog appearance." B-scan ultrasonography was performed to rule out retinal detachment and other retinal pathologies. OCT of the macula was performed and found to be within normal limits.

The complete blood count and liver function test results were normal. The results of the Venereal Disease Research Laboratory, Treponema Pallidum Hemagglutination, HSV-1 IgG, HSV-2 IgG, CMV IgG, and Mantoux tests were negative. High-resolution computed tomography of the chest and magnetic resonance imaging of the brain and orbit revealed normal findings. Serological evaluation revealed positivity for Toxoplasma IgG, confirming the diagnosis of ocular toxoplasmosis. Serology for HIV and HBsAg was negative.

The patient received treatment with a combination of trimethoprim 160 mg/sulfamethoxazole 800 mg (TMP-S) twice daily for 6 weeks, Oral Prednisolone 60 mg once daily for 1 week, and was gradually tapered over a period of 6 weeks. Topical Prednisolone 1% eye drops were started with a frequency of 3rd hourly and gradually tapered over a period of 6 weeks, and IOP monitoring was performed in subsequent follow-up. Over the course of the three-month follow-up, the visual acuity of the left eye improved to 6/6, and the vitreous cavity was quiet and clear. There were no signs of recurrence.

## DISCUSSION

Ocular toxoplasmosis is a well-documented manifestation of *Toxoplasma gondii* infection that often presents with

*This article was accepted: 17 August 2025*
*Corresponding Author: Chiramana Supreeth Reddy*
*Email: supreethreddy.ch@gmail.com*

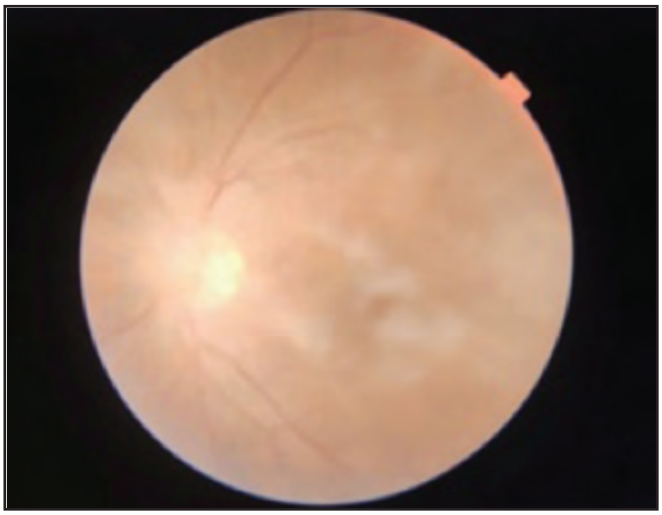

**Fig. 1:** Showing dense vitritis in left eye. (suggestive of "headlight in fog appearance")

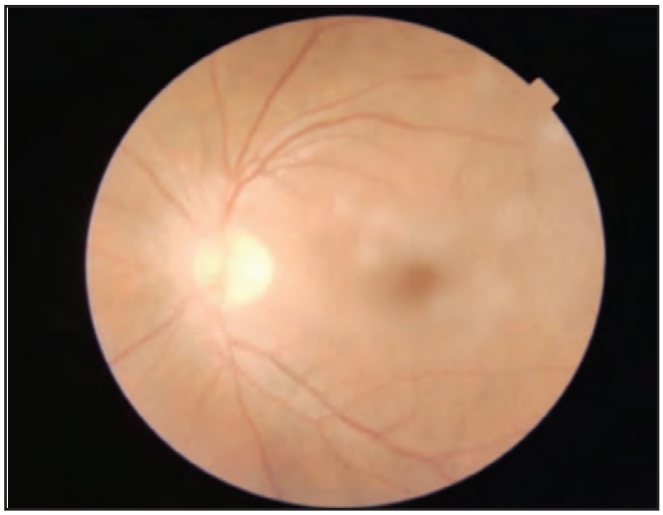

**Fig. 2:** Showing clear vitreous and macula in left eye following the treatment

retinochoroiditis. In most cases, patients will have some degree of vitritis and/or anterior inflammation, together with retinitis at the border of an inactive chorioretinal scar. As a result, the look of the bright white, focused retinitis viewed through vitreous haze is commonly described as a "headlight in the fog." Vasculitis frequently coexists with retinitis and can manifest as "Kyrieleis plaques," which are segmental lesions that are yellow-white in the retinal arteries. Because of Werner Kyrieleis's objectionable ideological beliefs, these plaques are now known as segmental retinal arteritis.[2] Numerous chorioretinal lesions and recurring disease are more common in female patients. According to certain studies that imply a gender difference in the patient population.[3] Acquired toxoplasmosis commonly leads to unilateral lesions, while congenital cases often exhibit bilateral involvement in approximately 75% of the patients, with a tendency to affect the macula.

It is primarily diagnosed on the basis of clinical presentation, although additional tests can help confirm the diagnosis and monitor progress. Ultrawidefield color fundus imaging provides objective measures to observe improvements in vitritis and retinitis. Fluorescein angiography can differentiate between active (leaking) and inactive (staining without leaking) lesions, and can also identify areas of retinal vessel occlusion caused by lesions. Optical coherence tomography of the macula helps rule out cystoid macular edema and aids in grading vitreous cells. Raster scans through lesions can confirm retinitis and assess lesion depth by detecting full-thickness hyper-reflectivity.[4]

Laboratory tests are useful when the diagnosis of toxoplasmosis is uncertain, based on clinical presentation and imaging. Polymerase chain reaction testing of aqueous or vitreous samples is effective, with some studies indicating higher sensitivity in vitreous samples.[5] Serological testing for *Toxoplasma gondii* IgG and IgM can evaluate past or recent systemic infections and is mainly useful for ruling out toxoplasmosis when IgG is negative.[6]

Most cases of toxoplasmosis can be effectively treated with systemic medications that target both the parasite and associated inflammatory response. Prior to 2015, the standard regimen was "triple therapy," consisting of pyrimethamine (100 mg for 2 days, then 25 mg daily), sulfadiazine (2 g) and folinic acid (5 mg). Subsequently, new treatment protocols have incorporated additional antimicrobials, such as azithromycin, clindamycin, and TMP-S, used both in conjunction with pyrimethamine and as monotherapies. While these medications have shown efficacy in multiple studies, few prospective randomized trials have directly compared their effectiveness.[7]

Yanxia Zhang, MD, of Sun Yat-sen University in China, and colleagues conducted a study in which they compared the results with systemic pyrimethamine-sulfadiazine, clindamycin, azithromycin and TMP-S using network meta-analysis. They discovered that the most significant increases in vitreous inflammation resolution and visual acuity were associated with clindamycin. In the same trial, TMP-S was shown to have fewer adverse effects and a reduced recurrence rate. When there are no contraindications, TMP-S is usually prescribed as first-line treatment.[8] And, patients with TMP-S should undergo regular renal function tests. Patients who are contraindicated for systemic therapy, for example, in the first trimester of pregnancy, or who have retinal lesions that require a quicker response might benefit from intravitreal clindamycin (1 mg/0.1 ml).

Systemic steroids are typically employed to manage severe inflammatory responses caused by Toxoplasma infections, especially severe vitritis. Depending on the severity of inflammation, oral prednisone may be started at up to 1 mg/kg and gradually decreased over weeks to months, or until vitritis clears up and retinitis seems dormant. Intravitreal dexamethasone also demonstrated good efficacy when administered in conjunction with intravitreal clindamycin. Topical steroids and cycloplegics may be administered in cases where anterior inflammation is evident. In our patient, a TMP-S regimen was selected

because of its favorable side effect profile and effectiveness in reducing recurrence rates.

In one similar case report, the patient had hypertensive non-granulomatous panuveitis, retinal vasculitis with focal retinochoroiditis with pigmented central area suggestive of ocular toxoplasmosis.[9] In another case report, the patient's anterior segment was unremarkable with funduscopic examination showing active lesions of whitish foci of chorioretinitis with surrounding oedema along the superonasal vessels and retinal vasculitis with perivascular sheathing in right eye.[10] The above two case reports were the different presentation of ocular toxoplasmosis. However, in this case, the patient was immunocompetent and had unilateral vitritis without accompanying retinochoroiditis, which was an unusual presentation. The patient tolerated the TMP-S regimen well, and the recovery period was short compared to the above case reports. This underscores the importance of considering ocular toxoplasmosis in the differential diagnosis of vitritis, even in the absence of typical retinal lesions and in non-immunosuppressed patients.

Ocular toxoplasmosis-related complications include cataracts, scleritis, retinal gliosis, cystoid macular edema, optic atrophy, secondary glaucoma, band keratopathy, vascular occlusions, tractional retinal detachment, and the formation of choroidal neovascular membranes.

The prognosis of ocular toxoplasmosis varies, with potential complications, including recurrent inflammation, retinal scarring, and vision loss. Regular follow-up is essential to monitor the treatment response and early detection of recurrence. In our case, the patient responded well to treatment, with resolution of vitritis and no recurrence during follow-up.

## CONCLUSION

This case report underscores the significance of considering ocular toxoplasmosis as a potential cause of unilateral vitritis, even in immunocompetent individuals. Prompt recognition and comprehensive diagnostic work-up, including advanced imaging techniques, laboratory tests, and treatment, are crucial in averting vision loss and complications associated with the condition. In summary, this case presented an unusual presentation of ocular toxoplasmosis, characterized by unilateral dense vitritis that resolved following appropriate therapy.

## DECLARATION

The authors declare no conflict of interest.

## INFORMED CONSENT

Written informed consent was obtained from the patient for publication of this case report.

## REFERENCES

1. Delair E, Latkany P, Noble AG, Rabiah P, Mcleod R, Brézin A. Clinical manifestations of ocular toxoplasmosis. Ocul Immunol Inflamm 2011; 19(2): 91-102.
2. Gologorsky D. Eponymous dishonor: Kyrieleis plaques. Retina 2018; 38(7): 1261-2.
3. Lyons MR, Arantes T, Vieira BR, Furtado JM, Smith JR. Impact of gender on clinical features and outcomes of ocular toxoplasmosis. Br J Ophthalmol 2024; 108(5): 710-4.
4. Kalogeropoulos D, Sakkas H, Mohammed B, Vartholomatos G, Malamos K, Sreekantam S, et al. Ocular toxoplasmosis: A review of the current diagnostic and therapeutic approaches. Int Ophthalmol 2022; 42(1): 295–321.
5. Farhadi A, Haniloo A, Fazaeli A, Moradian S, Farhadi M. PCR-based Diagnosis of Toxoplasma Parasite in Ocular Infections Having Clinical Indications of Toxoplasmosis. Iran J Parasitol 2017; 12(1): 56–62.
6. Roh M, Yasa C, Cho H. The role of serological titres in the diagnosis of ocular toxoplasmosis. Acta Ophthalmol 2016; 94(5): 521-2.
7. Felix F, Lira C, Grupenmacher RP, Filho A, Cosimo H, Nascimento AB. Leite Arieta CE. Long-term results of trimethoprim-sulfamethoxazole versus placebo to reduce the risk of recurrent Toxoplasma gondii retinochoroiditis. Am J Ophthalmol 2020; 213: 195-202.
8. Hang Y, Lin X, Lu F. Current treatment of ocular toxoplasmosis in immunocompetent patients: A network meta-analysis. Acta Tropica 2018; 185: 52-62.
9. Matias M, Gomes A, Marques T, Fonseca AC. Ocular toxoplasmosis: a very rare presentation in an immunocompetent patient. BMJ Case Rep 2014.
10. Lin HY, Lee WJA. The role of corticosteroids in treating acute ocular toxoplasmosis in an immunocompetent patient: A case report. Front Med (Lausanne) [Internet]. 202.

ORIGINAL ARTICLE

# *In vitro* biological evaluation of silver nanoparticles synthesized using *zingiber officinale* and *ocimum gratissimum* herbal formulation

**Shanmuga Sundaram S[1], Mariraj I, MD[2], Rajeshkumar Shanmugam, PhD[1], Dhanyaa Muthukumaran, MSc[1], Pradeep Manigandan, MSc[1]**

[1]Nanobiomedicine Lab, Centre for Global Health Research, Saveetha Medical College and Hospital, Saveetha Institute of Medical and Technical Sciences, Chennai. [2]Department of General Medicine, Saveetha Medical College and Hospital, Saveetha Institute of Medical and Technical Sciences, Chennai

**ABSTRACT**

**Introduction: The biomedical potential of silver nanoparticles (Ag NPs) synthesized with *Zingiber officinale* and *Ocimum gratissimum* herbal formulation was investigated in this study. The study aims to reveal their applications in various biomedical fields. The study evaluates the antioxidant, thrombolytic, and antimicrobial potential of *Zingiber officinale* and *Ocimum gratissimum* herbal formulation-mediated Ag NPs.**

**Materials and Methods: Biogenically synthesized silver nanoparticles (Ag NPs) from an herbal formulation containing *Zingiber officinale* and *Ocimum gratissimum* were tested at various concentrations using the DPPH (2,2-diphenyl-1-picrylhydrazyl) assay. The absorbance was measured at 517 nm to quantify DPPH free radicals. With Ag NP concentrations, the $H_2O_2$ test exhibited increased activity. This work evaluated the antibacterial activity of Ag NPs mediated by *Zingiber officinale* and *Ocimum gratissimum* against *Staphylococcus aureus*, *Streptococcus mutans*, *Candida albicans*, and *Enterococcus faecalis*.**

**Results: The utilization of herbal formulations from *Z. officinale* and *O. gratissimum* to synthesize Ag NPs revealed considerable therapeutic effectiveness. At a concentration of 50 µl, the maximal inhibition was 76%, which is comparable in effectiveness to that of standard ascorbic acid. Significant blood clot dissolution was observed during thrombolytic testing at a concentration of 100µg/ml, indicating promising prospects for the treatment of thrombotic disorders. Nanoparticles dose-dependently inhibited *E. faecalis*, *C. albicans*, *S. aureus*, and *S. mutans* in antibacterial testing. These results show the potential of the nanoparticles as supplementary or alternative treatments to conventional antibiotics, particularly in light of the increasing prevalence of antibiotic resistance.**

**Conclusion: The further investigation of nanoparticles into their mechanisms and efficacy in therapeutic applications, positioning *Zingiber officinale* and *Ocimum gratissimum* formulation-mediated Ag NPs as viable candidates in developing antioxidant, thrombolytic, and antimicrobial treatments.**

**KEYWORDS:**
*Green synthesis, silver nanoparticles, oral pathogens, Zingiber officinale, Ocimum gratissimum, biomedical applications*

## INTRODUCTION

Nanotechnology has transformed many areas of science and medicine by providing new and positive ways to diagnose and treat illnesses. Among nanomaterials, silver nanoparticles (Ag NPs) have attracted much interest in the medical field because of their anti-inflammatory, antibacterial, and antioxidant properties.[1] These characteristics make them especially well-suited for use in biological applications. Traditional methods of synthesizing nanoparticles often involve chemical or physical processes, which may pose hazards and incur high costs. However, green synthesis methods utilizing plant formulation offer an eco-friendly and cost-effective alternative.[2] Plant-mediated synthesis of nanoparticles connects the reducing properties of phytochemicals present in the formulation, resulting in stable and biocompatible nanoparticles. There are several medicinal and dental uses for silver due to its antibacterial characteristics, which have been known for a long time.[3] Ag NPs are an attractive choice for treating bacterial infections because they have more antibacterial action than bulk silver.[4] Although their special characteristics might lead to physiological reactions in living systems by interacting with these materials. The size-dependent physicochemical features of nanoparticles boost their applicability in many applications.[5] Different approaches to produce Ag NPs have been successfully combined into a range of biomaterials, enabling their use in many biological applications. Their effects on dental use and wound healing have been extensively investigated. The unique properties of Ag NP-based biomaterials enable the healing of acute and chronic wounds and greatly limit the development of germs at wound sites.[6]

The mechanisms underlying their antibacterial action involve interactions with bacterial cell walls, oxidative stress induction, and inhibition of microbial growth.[7] In addition to their antimicrobial properties, Ag NPs also possess free radical scavenging activity. Free radicals generated during normal cellular metabolism or due to environmental factors can cause cellular damage, leading to various health issues.

*This article was accepted: 07 August 2024*
*Corresponding Author: Rajeshkumar Shanmugam*
*Email: rajeshkumars.smc@saveetha.com*

Antioxidants, including Ag NPs, help neutralize these free radicals, thereby protecting cells from oxidative stress-induced damage.[8] Furthermore, the thrombolytic and anticoagulant properties of Ag NPs present a quiet area of research, especially in the context of thrombocytopenia,[9] it is a condition characterized by a low platelet count, which can lead to bleeding disorders and increased thrombosis risk. Studies have shown that Ag NPs can influence platelet function and thrombin generation, highlighting their potential in modulating blood coagulation processes.[10] This dual role of Ag NPs, as both pro-coagulant and anti-platelet agents, the complexity of their interaction with the hematological system, and the need for a thorough investigation to connect their therapeutic potential safely. Ginger (Zingiber officinale) has been employed as a culinary seasoning for over 2000 years.[11] The roots and extracts derived from this plant contain polyphenol chemicals, including 6-gingerol and its derivatives, which have significant antioxidant properties. Ocimum gratissimum is commonly referred to as a scent leaf.[12] The incorporation of Ocimum oil, derived from the leaf essential oil of Ocimum gratissimum, has been seen in several formulations as topical antiseptics and for the management of small wounds, boils, and pimples.[13] This research focuses on the effects of Zingiber officinale and Ocimum gratissimum formulation-mediated Ag NPs on thrombolytic activity, free radical scavenging activity, and antimicrobial activity.

## MATERIALS AND METHODS

*Preparation of Plant Extract*

0.5 grams of each *Zingiber officinale* and *Ocimum gratissimum* were added to 100 ml of pure water. The heating mantle was set at 50 °C and boiled for 10 minutes. A muslin cloth was used to filter out the mixture. The filtered extracts of *Z. officinale* and *O. gratissimum* were mixed with a solution of silver nitrate (AgNO3) to start the synthesis process for the Ag NPs.

*Synthesis of Ag NPs*

The volume of 10 mL of the plant formulation was combined with 90 mL of 1 mM AgNO3 under continuous stirring. The reaction mixture was subsequently incubated at room temperature in the absence of light to inhibit the photoactivation of silver nitrate. The formation of Ag NPs was confirmed by the transformation of the clear solution to a brown color after 48 h.

*Characterization of Ag NPs*

UV-visible spectroscopy, an analytical method for analyzing the optical characteristics of NPs, was used to characterize the synthesized NP solution. The NPs solution (3 mL) was placed in a cuvette and scanned using a double-beam UV-Vis spectrophotometer. Spectrophotometric scans from 250 nm to 650 nm allowed a complete evaluation of the NP solution's visible spectrum absorbance in a time-dependent manner, such as 3, 12, 24, 30, 36, and 48 h. Graphical analysis was conducted for the recorded results. The morphologies of the synthesized Ag NPs were analyzed using a scanning electron microscope.

*Antioxidant Activity*

*DPPH Method*

The DPPH (2,2-diphenyl-1-picrylhydrazyl) test was used to measure the antioxidant activity of AgNPs produced by biogenic synthesis methods. Different concentrations (10, 20, 30, 40, and 50 µL) of silver nanoparticles derived from *Z. officinale* and *O. gratissimum* herbal formulations were combined with 1 ml of 0.1 mM DPPH in methanol and 450 µL of 50 mM Tris HCl buffer (pH 7.4). The mixture was then incubated for 30 min. DPPH free radicals were determined by measuring the absorbance at 517 nm. Ascorbic acid was used as a standard.[14]

The percentage of inhibition was calculated using the formula:

Percentage of inhibition = (Absorbance of control – Absorbance of the test sample) / Absorbance of control × 100

$H_2O_2$ Assay

The $H_2O_2$ scavenging activity of the biosynthesized AgNPs was assessed. 40 mM $H_2O_2$ solution was prepared in phosphate buffer (pH 7.4). A solution of the test sample (Ag NPs) and a standard sample of ascorbic acid at varying concentrations (10, 20, 30, 40, and 50 µg/mL) were individually added to 0.6 mL the $H_2O_2$ solution. After 10 min of incubation in the dark, the absorbance of the reaction solution was spectrophotometrically measured at 230 nm. Ascorbic acid was used as a standard.[15,16] The percentage of $H_2O_2$ scavenging activity was calculated using the following formula:

$$\% \text{ inhibition} = \frac{\text{Absorbance of control} - \text{Absorbance of sample} \times 100}{\text{Absorbance of control}}$$

*Thrombolytic Activity*

The thrombolytic activities of *Z. officinale* and *O. gratissimum* formulation-mediated AgNPs were evaluated using previously established protocols. Preformed blood clots were treated with 100µg/ml *Z. officinale* and *O. gratissimum* formulation-mediated AgNPs placed on a slide for analysis. All the experiments were performed at a controlled temperature of 30 ± 2°C. The process of thrombolysis, which refers to the dissolution of blood clots, was carefully monitored throughout the experiment.[17]

*Antibacterial Activity*

To assess the antibacterial efficacy of *Z. officinale* and *O. gratissimum* – Ag NPs against strains such as *E. faecalis, C. albicans, S. aureus,* and *S. mutans,* Mueller-Hinton agar was chosen for its reliability in determining zones of inhibition. The procedure began with the preparation and sterilization of Mueller-Hinton agar, which was autoclaved for 15 min at 121°C under a pressure of 15 lbs. Sterile 9 mm polystyrene tip was used to create the wells in the solidified agar. Subsequently, the test organisms were evenly swabbed across the agar surface. Different concentrations of AgNPs were added to each well. The plates were kept warm for 24 h at 37 °C. Once the incubation time was completed, the zones of inhibition were carefully measured. These images show the areas around the wells where Ag NPs stopped bacterial growth.[18]

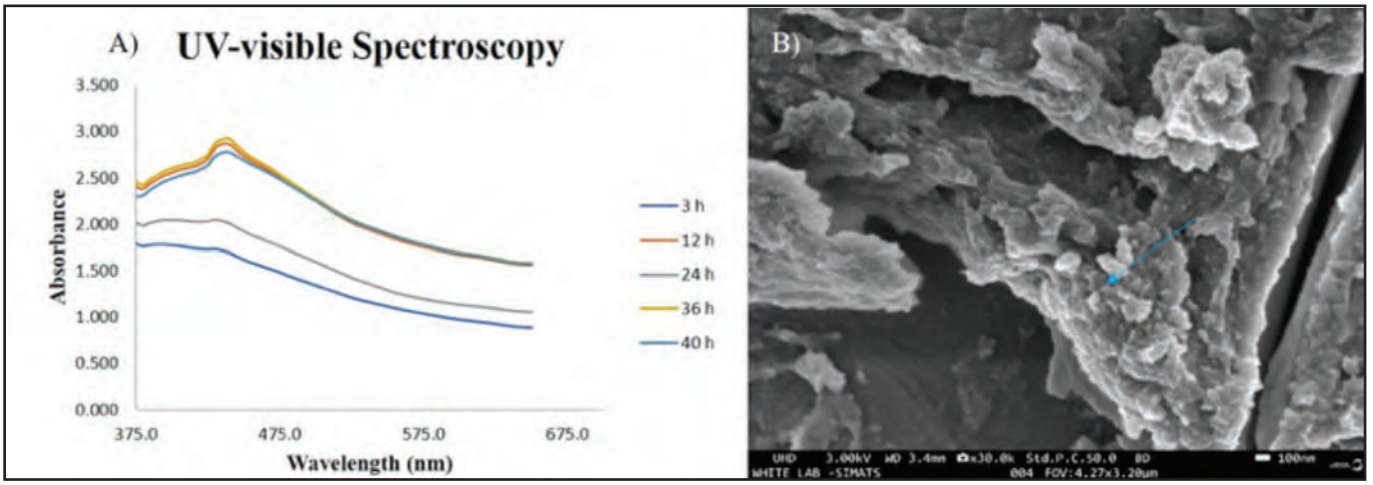


**Fig. 1:** A) UV-visible spectroscopy of Ag NPs. B) SEM image of AgNPs synthesized from Zingiber officinale and Ocimum gratissimum herbal formulation.

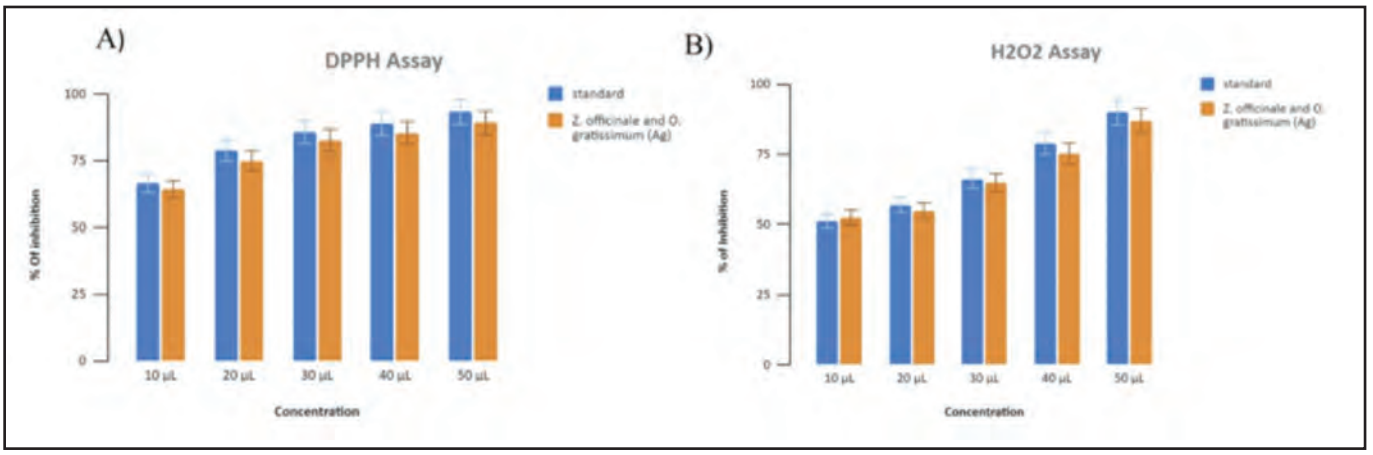


**Fig. 2:** A) DPPH radical scavenging activity of Zingiber officinale and Ocimum gratissimum mediated Ag nanoparticles. B) $H_2O_2$ activity of Zingiber officinale and Ocimum gratissimum mediated AgNPs

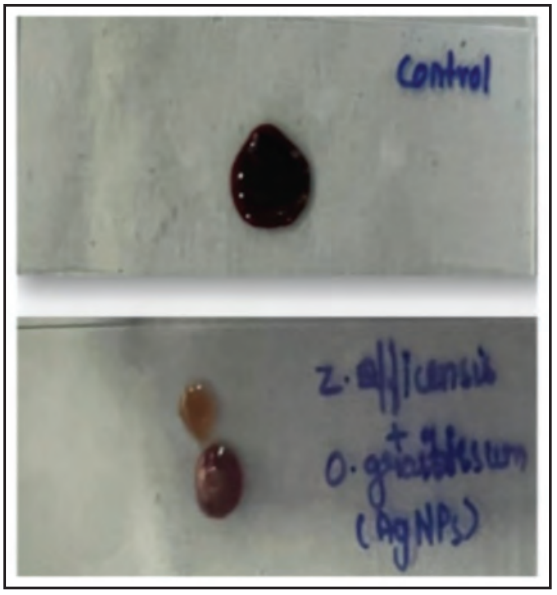


**Fig. 3:** Thrombolytic activity of Zingiber officinale and Ocimum gratissimum mediated silver nanoparticles

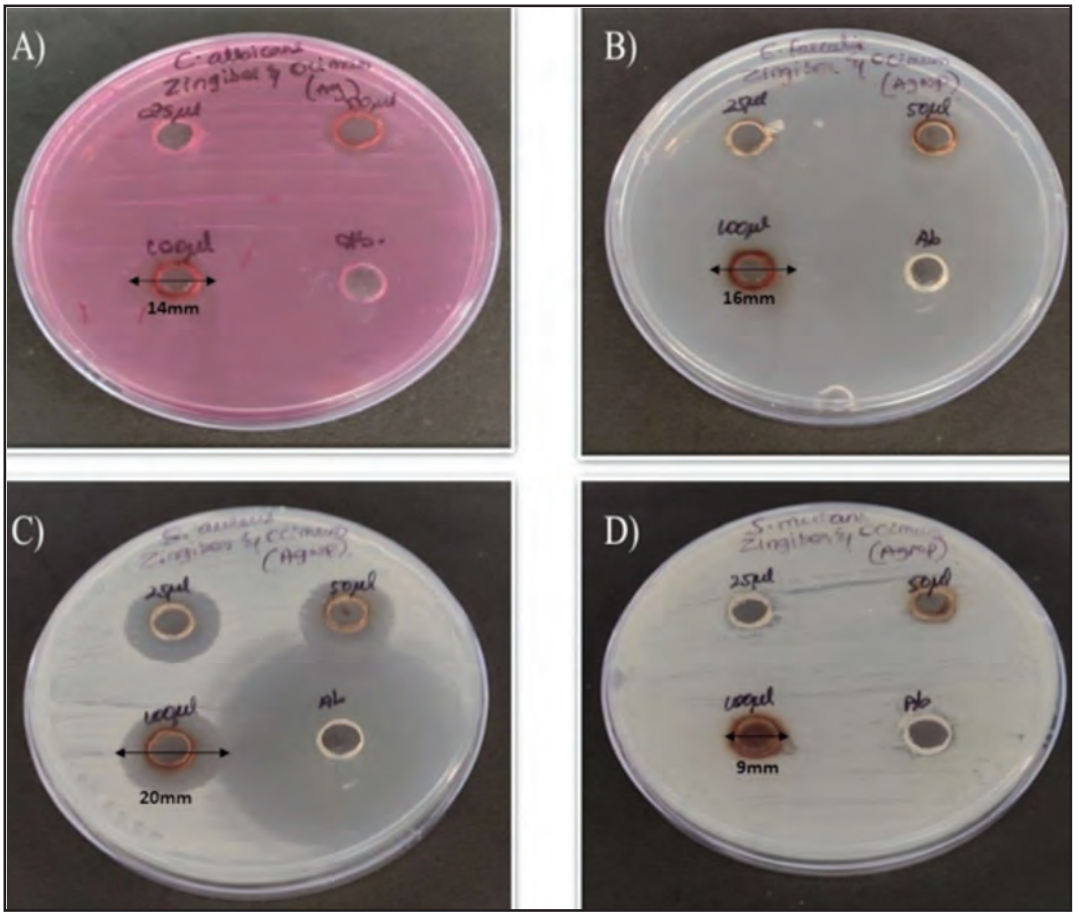


**Fig. 4:** Antimicrobial activity of Zingiber officinale and Ocimum gratissimum mediated Ag NPs against oral pathogens A) C. albicans B) E. faecalis C) S. aureus D) S. mutans

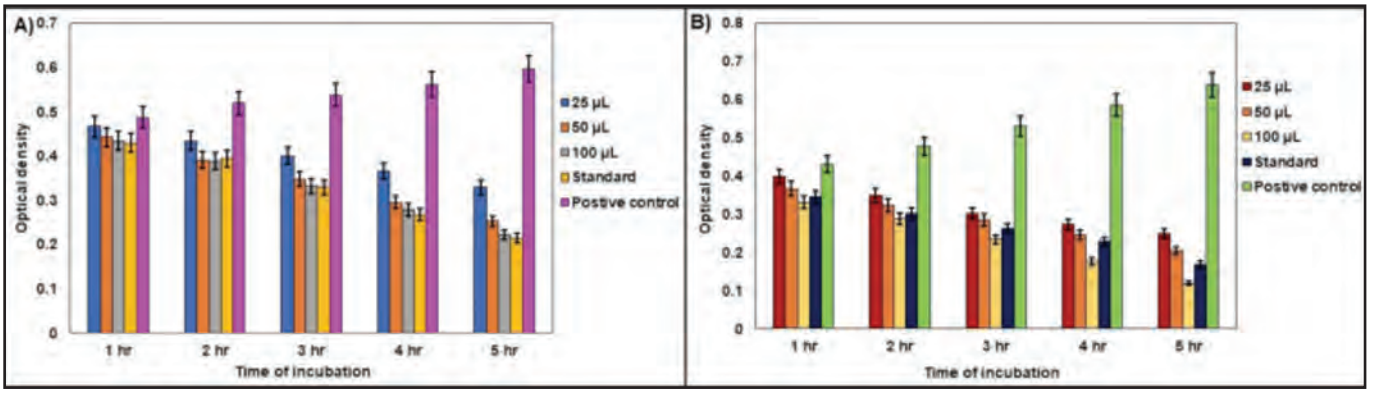


**Fig. 5:** Antimicrobial activity of Zingiber officinale and Ocimum gratissimum mediated Ag NPs against Oral pathogens

## RESULTS

### Green Synthesis of Ag NPs

Effective synthesis of Ag nanoparticles using Zingiber officinale and Ocimum gratissimum was carried out. The presence of Ag nanoparticles was indicated by the brown color. Visual observation of Ag nanoparticles has confirmed that they are a green and environmentally benign herbal formulation.

### Analysis of UV–Visible Spectroscopy

In UV-visible spectroscopy, the synthesized Ag NPs exhibited considerable absorbance variation over time over a wide wavelength range (250–650 nm). After 3 h, the absorbance levels were low, suggesting reduced aggregation or particle size. However, the absorbance increased after 12 h and peaked at 440 nm (Figure 1A). The spectroscopic results indicated that the growth or aggregation processes produced valuable optical changes in the Ag NPs throughout the

experiment. As Ag NPs interact strongly with UV light, their maximal absorption indicates their size and concentration variation. This shows that the Ag NPs attained a fixed size or aggregation state, strongly absorbing and scattering UV light. The synthesized AgNPs had a consistent size distribution and were spherical, as revealed by SEM examination (Figure 1B). Nanoparticles have little possibility of clumping or clustering because they are evenly distributed throughout the substrate. The surface morphology of the AgNPs was evident in the high-resolution SEM images, which showed smooth, spherical particles free of extraneous flaws. The spherical shape of the nanoparticles indicates that the synthesis technique successfully produced monodisperse AgNPs. The SEM images reveal a steady size distribution, indicating a continuous synthesis process.

*Antioxidant activity*

The antioxidant efficacy of Zingiber officinale and Ocimum gratissimum formulation-mediated AgNPs was assessed using DPPH and $H_2O_2$ assay, revealing a dose-dependent enhancement in antioxidant activity. In the DPPH assay, the antioxidant activity of the formulation-mediated Ag NPs demonstrated a significant increase, with the highest inhibition observed at 76% for a concentration of 50 µL, a considerable increase from the 51% inhibition at 10 µL. This activity was compared against the standard antioxidant ascorbic acid, which showed an 80% inhibition (Figure 2A). Similarly, the H2O2 assay indicated a progressive increase in activity with higher concentrations of herbal formulation -Ag NPs a significant scavenging rate of 76.84% at 50 µL compared to 51 % at 10 µL, with ascorbic acid as the control showing an 81% scavenging rate at 50 µL (Figure 2B). These findings indicate the antioxidant potential of formulation-mediated AgNPs.

*Thrombolytic activity*

The thrombolytic activity of Z. officinale and O. gratissimum herbal formulation-mediated AgNPs showed that blood clots were treated with 100 µg/ml concentration, and a significant degree of thrombolysis was observed (Figure 3). The potential of Ag NPs as promising agents for the treatment of thrombotic conditions.

*Antimicrobial activity*

A study examining the antimicrobial activity of Z. officinale- and O. gratissimum-mediated Ag NPs showed a clear zone of inhibition against various pathogens. Three different concentrations of Ag NPs were tested: 25, 50, and 100 µL. Against E. faecalis, the inhibition zones increased with the concentration of Ag NPs, with measurements of 11 mm, 14 mm, and 16 mm for the increasing concentrations, respectively, compared with a significantly larger zone of 35 mm observed for the antibiotic control. A similar dose-dependent activity was noted against C. albicans, with zones of inhibition measuring 9, 12, and 14 mm, notably against S. mutans, with a zone of inhibition of 9 mm across all concentrations. The maximum zones of inhibition observed for S. aureus against AgNPs were 18, 19, and 20 mm at all concentrations. (Figures 4 and 5).

## DISCUSSION

A detailed investigation of the various uses of AgNPs mediated by herbal formulations from *Z. officinale* and *O. gratissimum* explains their potential in the thrombolytic, antibacterial, and antioxidant domains. These biogenic Ag NPs are effective radical scavengers, as shown by their antioxidant effectiveness in DPPH and $H_2O_2$ experiments.[14,15] Their activity was compared with that of ascorbic acid, a well-established standard for antioxidant measurements. This demonstrates the potential of these nanoparticles to reduce oxidative stress, and suggests a possible direction for the development of antioxidant treatments. These results highlight the natural antioxidant qualities of plant formulations and the increased effectiveness of nanoparticle mediation, recommending further research into their potential medicinal uses.[16]

Regarding thrombolytic activity, the significant disintegration of blood clots treated with these AgNPs suggests that they may be useful as new medicines to treat thrombotic disorders. This clot dissolution highlights the therapeutic potential of using plant herbal formulation-mediated nanoparticles to improve clot breakdown, particularly when compared with the AgNO3 control solution. These nanoparticles significantly affect the treatment of illnesses marked by undesired blood clot formation and require further investigation into the underlying processes and therapeutic optimization.[17]

Evaluation of antimicrobial activity against pathogens including *C. albicans, S. aureus*, and *E. faecalis* shows distinct effectiveness and significant antibacterial potential of Ag NPs produced from Zingiber officinale and Ocimum gratissimum. This capacity, which presents a viable substitute or addition to conventional antibiotic therapies, is vital in light of growing antibiotic resistance.[18] The effectiveness of the nanoparticles against *S. aureus* and *E. faecalis* was significant; however, it was not as strong against S. mutans. This suggests that there may be a complex connection between nanoparticles and the structures or processes of microbial cells.[19] This emphasizes the complex relationships between microorganisms and nanoparticles, and how focused studies are required to maximize the antibacterial activity of nanoparticles while maintaining their safety for therapeutic usage.[20,21,22]

## CONCLUSION

Our results highlight the broad-spectrum effectiveness of Ag NPs mediated by Ocimum gratissimum and Zingiber officinale herbal formulations for thrombolytic, antioxidant, and antibacterial applications. Their action is dose-dependent, which emphasizes the significance of concentration in attaining the intended therapeutic effects, and provides a crucial criterion for further study and application development. These nanoparticles provide a viable option for various therapeutic interventions because of their proven capacities, providing new approaches to enduring problems in the treatment of thrombosis, infection prevention, and oxidative stress management.

## CONFLICT OF INTEREST

The authors declare that no conflicts of interest would prejudice the impartiality of this scientific work.

## ACKNOWLEDGEMENTS

The authors would like to thank Saveetha Medical College and Hospital for supporting this research.

## REFERENCES

1. Bates MG, Risselada M, Peña-Hernandez DC, Hendrix K, Moore GE. The antibacterial activity of silver nanoparticles against Escherichia coli and methicillin-resistant Staphylococcus pseudintermedius is affected by incorporation into carriers for sustained release. Am J Vet Res 2024; 1-11.
2. Alwan SH, Al-Saeed MH. Biosynthesized silver nanoparticles (using Cinnamomum zeylanicum bark extract) improve the fertility status of rats with the polycystic ovarian syndrome. Biocatal Agric Biotechnol 2021; 38: 102217.
3. Ramzan M, Karobari MI, Heboyan A, Mohamed RN, Mustafa M, Basheer SN, et al. Synthesis of Silver Nanoparticles from Extracts of Wild Ginger (Zingiber zerumbet) with Antibacterial Activity against Selective Multidrug Resistant Oral Bacteria. Molecules 2022; 27(6): 2007.
4. Talapko J, Matijević T, Juzbašić M, Antolović-Požgain A, Škrlec I. Antibacterial Activity of Silver and Its Application in Dentistry, Cardiology and Dermatology. Microorganisms 2020; 8(9): 1400.
5. Ali SJ, Arthanari A, Shanmugam R. Antioxidant Activity of Silver Nanoparticles Synthesized Using Vetiveria zizanioides-In Vitro Study. ResearchGate 2021.
6. Dhaka A, Chand Mali S, Sharma S, Trivedi R. (2023). A review on biological synthesis of silver nanoparticles and their potential applications. Results Chem, 6: 101108.
7. Kapoor G, Saigal S, Elongavan A. Action and resistance mechanisms of antibiotics: A guide for clinicians. J Anaesthesiol Clin Pharmacol 2017; 33(3): 300.
8. Rahman MM, Islam MB, Biswas M, Khurshid Alam AHM. In vitro antioxidant and free radical scavenging activity of different parts of Tabebuia pallida growing in Bangladesh. BMC Res Notes 2015; 8(1): 621.
9. Roy K, Srivastava AK, Ghosh CK. Anticoagulant, thrombolytic, and antibacterial activities of Euphorbia acruensis latex-mediated bioengineered silver nanoparticles. Green Process Synth 2019; 8(1): 590–9.
10. Milić M, Cvetić Ž, Bendelja K, Vuković B, Galić E, Ćurlin M, et al. Response of platelets to silver nanoparticles designed with different surface functionalization. J Inorg Biochem 2021; 224: 111565.
11. Shaukat MN, Nazir A, Fallico B. Ginger Bioactives: A Comprehensive Review of Health Benefits and Potential Food Applications. Antioxidants 2023; 12(11): 2015.
12. Ugbogu OC, Emmanuel O, Agi GO, Ibe C, Ekweogu CN, Ude VC, et al. A review on the traditional uses, phytochemistry, and pharmacological activities of clove basil (Ocimum gratissimum L.). Heliyon 2021; 7(11): e08404.
13. Fafal T, Taştan P, Tüzün BS, Ozyazici M, Kivcak B. Synthesis, characterization and studies on antioxidant activity of silver nanoparticles using Asphodelus aestivus Brot. aerial part extract. South African J Bot 2017; 112: 346-53.
14. Keerthiga N, Anitha R, Rajeshkumar S, Lakshmi T. Antioxidant activity of cumin oil mediated silver nanoparticles. Pharmacogn J 2019; 11(4)
15. Mohanta YK, Panda SK, Jayabalan R, Sharma N, Bastia AK, Mohanta TK. Antimicrobial, Antioxidant, and Cytotoxic Activity of Silver Nanoparticles Synthesized by Leaf Extract of Erythrina suberosa (Roxb.). Front Mol Biosci 2017; 4.
16. Kunjan F, Shanmugam R, Govindharaj S. Evaluation of Free Radical Scavenging and Antimicrobial Activity of Coleus amboinicus-Mediated Iron Oxide Nanoparticles. Cureus 2024;
17. Lateef A, Akande MA, Azeez MA, Ojo SA, Folarin BI, Gueguim-Kana EB, et al. Phytosynthesis of silver nanoparticles (AgNPs) using miracle fruit plant (Synsepalum dulcificum) for antimicrobial, catalytic, anticoagulant, and thrombolytic applications. Nanotechnol Rev 2016; 5(6).
18. Dinesh Y, Abilasha R, Ramani P, Rajeshkumar S. Assessment of Cytotoxic, Antioxidant, Thrombolytic, Anti Inflammatory and Antimicrobial Activity of Curcuma longa Linn, Cissus quadrangularis and Boerhaavia diffusa Herbal Mixture - An In vitro Study. J Pharm Res Int. 2021; 1766–77.
19. Konwar AN, Hazarika SN, Bharadwaj P, Thakur D. Emerging Non-Traditional Approaches to Combat Antibiotic Resistance. Curr Microbiol 2022; 79(11): 330.
20. Sharmin S, Rahaman MM, Sarkar C, Atolani O, Islam MT, Adeyemi OS. Nanoparticles as antimicrobial and antiviral agents: A literature-based perspective study. Heliyon 2021; 7(3): e06456.
21. Bhakya, S., Muthukrishnan, S., Sukumaran, M., & Muthukumar, M. Biogenic synthesis of silver nanoparticles and their antioxidant and antibacterial activity. Appl Nanosc 2015; 6(5): 755-66.
22. Rajeshkumar S, Jayakodi S, Tharani M, Alharbi NS, Thiruvengadam M. Antimicrobial activity of probiotic bacteria-mediated cadmium oxide nanoparticles against fish pathogens.Microb Pathog 2024; 189: 106602.

ORIGINAL ARTICLE

# Secondary Retinitis pigmentosa subsequent to docetaxel and carboplatin combination - A rare cytotoxic chemotherapy complication

**Taarika G, MBBS[1], V Panimalar A Veeramani, DNB[2], Sanjeev Kumar Puri, MS ophthalmology[3], Divya N, MS ophthalmology[4]**

Saveetha Institute of Medical and Technical Sciences (Deemed to be University): SIMATS Deemed University

**SUMMARY**

**Visual loss following secondary retinitis pigmentosa (RP) is a rare complication of cytotoxic chemotherapy. Few cases of docetaxel- and/or platinum-induced retinal toxicity have been reported. Routine ocular examination of patients undergoing chemotherapy is required for early recognition and intervention of ocular toxicity. A 72- year-old female undergoing docetaxel and carboplatin combination chemotherapy for the past 3 months presented with complaints of defective vision in both eyes for 2 months. Fundus examination revealed a waxy pale disc in both eyes, arteriolar attenuation, and peripheral bony spicules, suggesting secondary retinitis pigmentosa. Optical Coherence Tomography (OCT) of the macula revealed macular dystrophy. The Humphrey Visual Field (HVF) showed field defects. Despite the reduction in chemotherapy dosage, no improvement was observed during the three-week follow-up period.**

**KEYWORDS:**
*Retinitis pigmentosa, chemotherapy, macular dystrophy*

## INTRODUCTION

Due to the distinct anatomical, physiological, and biochemical properties of the eye, ocular toxicity caused by cancer treatment encompasses a wide range of conditions, including maculopathy, cortical blindness, and blurred vision. The adnexal, anterior segment, posterior segment, and neuro-ophthalmic segments are the categories in which ocular side effects can be divided. One of the medications in the taxane class, docetaxel is an anti-mitotic chemotherapy agent that is approved for the treatment of breast cancer and uterine carcinoma, among other solid tumors.[1] A hereditary retinal degeneration that causes gradual contraction of the visual field is called retinal pigmentosa (RP). Midperipheral photoreceptors are first affected by RP, and as the condition worsens, more central retinal regions are also affected.[2] Chemotherapy might affect the retina, causing ocular toxicity. Routine ocular examination with fundus evaluation should be performed for patients undergoing chemotherapy.

## CASE PRESENTATION

A 72-year-old woman with a known case of type 2 diabetes mellitus presented with complaints of defective vision in both eyes for 2 months, which was sudden in onset and progressive in nature. History of right eye cataract surgery performed 4 years back and postoperative vision was 6/9. She had a history of uterine carcinoma 2 years ago, for which she underwent hysterectomy and was receiving docetaxel and carboplatin combination chemotherapy for the past 3 months. Docetaxel (60 mg/m$^2$) was administered intravenously (iv) for 1 h, followed by carboplatin (6 mg/ml/min) administered intravenously for 1 h at 3 weeks interval. The patient developed a sudden decrease in vision after 3rd cycle of chemotherapy. The patient stated that her ocular problems began after the start of treatment, and her medical history revealed that she had no prior ocular disorders. There was no family history of retinal dystrophy.

On examination, visual acuity in both eyes was 6/24 and color vision in both eyes 0/25 plates. Anterior segment right eye pseudophakia and left eye nuclear sclerosis grade I with posterior subcapsular cataract and normal pupil reaction. The intraocular pressure was normal. Fundus examination revealed pale disc, arteriolar attenuation, and bony spicules in the periphery. Optical Coherence Tomography (OCT) macular dystrophy. The Humphrey Visual Field (HVF) showed both eyes near the total field defect. Bilateral loss of rod and cone cell function was demonstrated by electroretinography as diminished scopic and photopic responses.

The patient was diagnosed with secondary retinitis pigmentosa after chemotherapy. The patient was diagnosed with poor visual prognosis. The patient's condition was discussed with an oncologist, and the dose of chemotherapy was reduced. The patient was followed-up for 3 weeks, and the visual acuity and fundus changes remained the same.

## DISCUSSION

The development of secondary retinitis pigmentosa following cytotoxic chemotherapy, particularly docetaxel and carboplatin combination therapy, represents a rare but significant ocular complication. Docetaxel and carboplatin are commonly used in the treatment of various malignancies, including uterine cancer, due to their efficacy in inhibiting cancer cell proliferation. However, both agents have been associated with ocular side effects, albeit less frequently than-other systemic adverse reactions.

*This article was accepted: 07 August 2024*
*Corresponding Author: Rajeshkumar Shanmugam*
*Email: rajeshkumars.smc@saveetha.com*

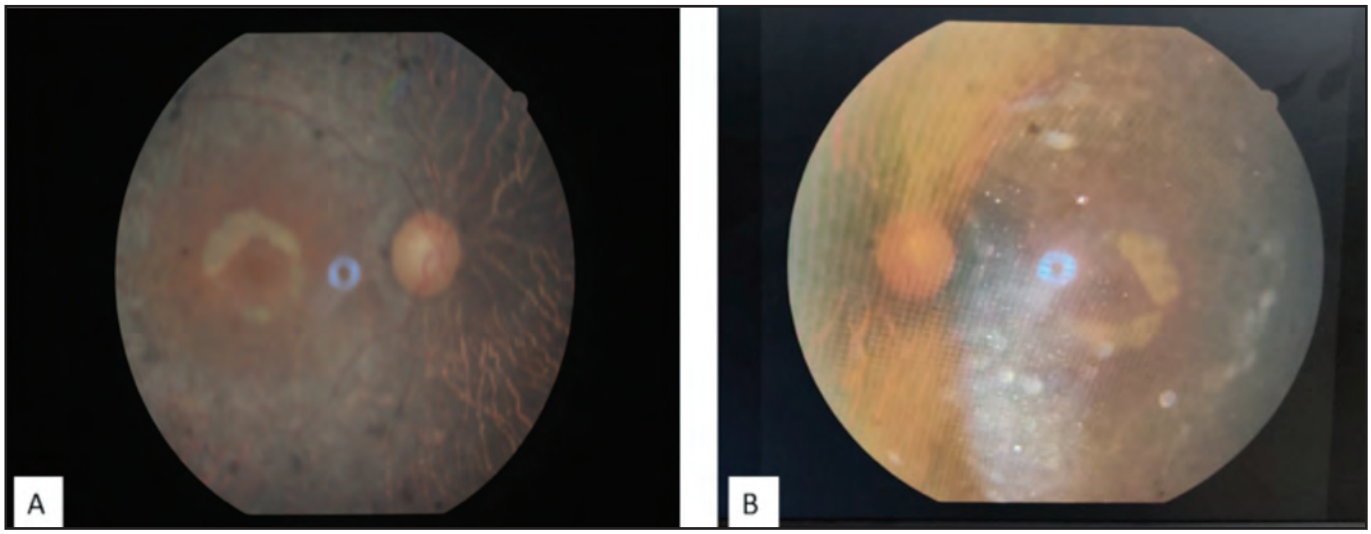


**Fig. 1:** A & B showing fundus photograph of right and left eye with waxy pale disc, arteriolar attenuation, bony spicules in periphery respectively

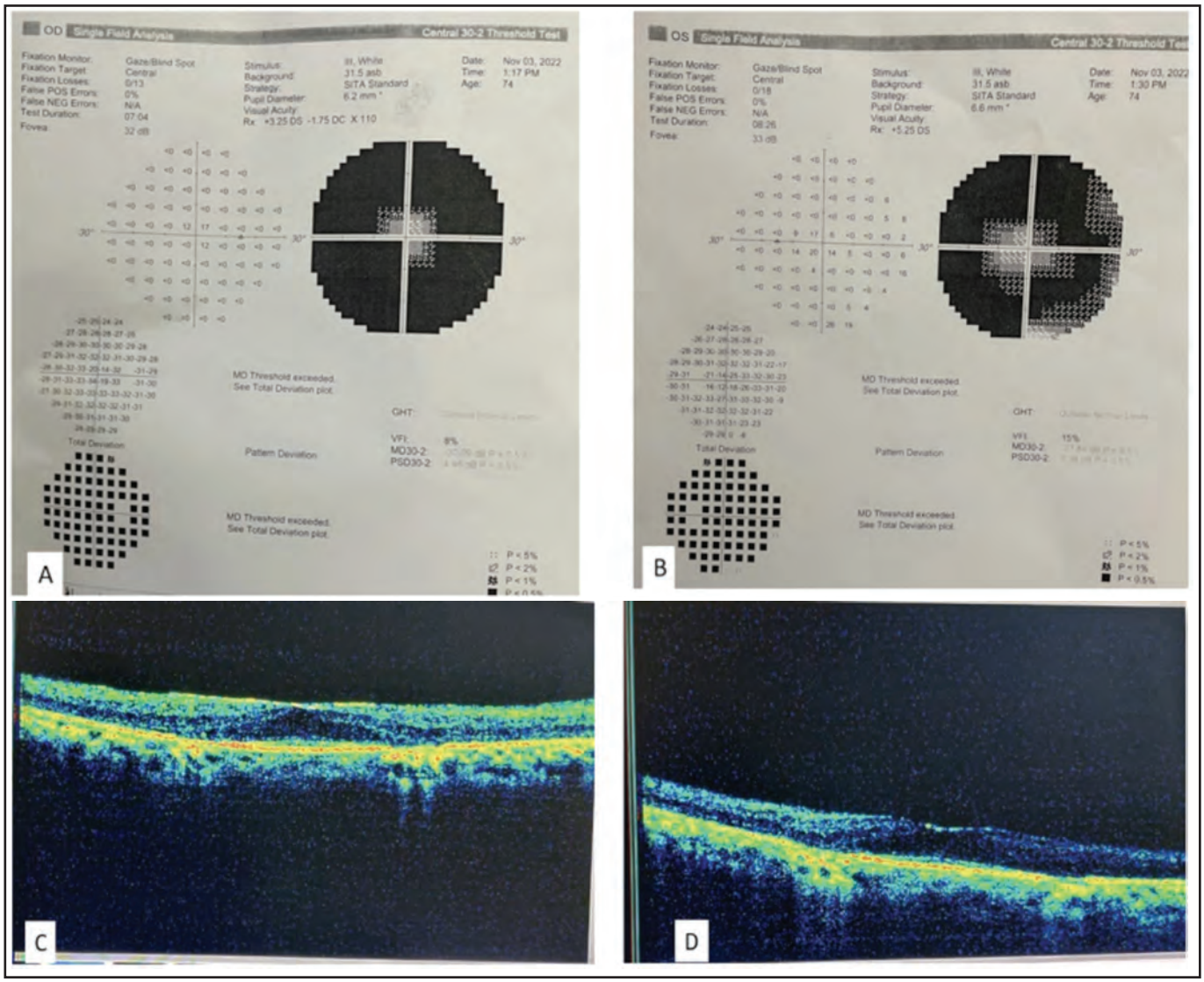


**Fig. 2:** A & B: Right eye and left eye near total field defect respectively. C & D: Right eye and left eye OCT showing macular dystrophy respectively

The mechanism underlying chemotherapy-induced retinal toxicity remains poorly understood; however, several hypotheses have been proposed. Chemotherapy agents may directly damage retinal cells, disrupt retinal microvasculature, or induce oxidative stress, leading to cellular dysfunction and apoptosis.[3] Additionally, individual susceptibility factors, such as genetic predisposition or pre-existing retinal abnormalities, may influence the development and severity of chemotherapy-related ocular toxicity.

One case study reported an acceleration of RP in a patient with non-Hodgkin's lymphoma, a known case of Usher's syndrome.[4] There is another case study showed bilateral blindness with secondary retinitis pigmentosa following postoperative docetaxel and platinum combination chemotherapy in primary small-cell carcinoma of the endometrium.[5] In which, the patient presented with symptoms consistent with RP within a few months of chemotherapy, suggesting the onset of retinal toxicity. Therefore, it's feasible that the patient's chemotherapeutic treatment may have led to the development of RP through a neurotoxic effect caused by one of its components. Neurotoxicity of taxanes showed alterations in electroretinogram.[3] Patient had no ocular complaints suggestive of RP in the past and patient record during right eye cataract surgery showed normal fundus findings. No family history of retinitis pigmentosa was present, indicating that chemotherapy exposure was the precipitating factor. Notably, the onset of visual disturbances coincided with the administration of docetaxel and carboplatin combination therapy, further supporting their potential role in retinal injuries.

The management of chemotherapy-induced RP primarily focuses on symptomatic relief and supportive care as there are currently no definitive treatments to reverse retinal degeneration. Ophthalmologic monitoring is essential for the early detection of RP and the initiation of interventions to optimize visual function and quality of life. Additionally, patients receiving cytotoxic chemotherapy should be educated about potential ocular side effects and encouraged to report any visual changes promptly.

## CONCLUSION

The present case underscores the importance of recognizing and addressing chemotherapy-induced ocular complications, particularly the rare occurrence of secondary RP after docetaxel and carboplatin combination therapy. Despite being primarily used for their antineoplastic effects, cytotoxic agents can inadvertently lead to ocular toxicity, highlighting the need for vigilant monitoring and early intervention. The onset of RP symptoms following the initiation of chemotherapy emphasizes the importance of follow-up care for patients undergoing cytotoxic treatment. All patients undergoing chemotherapy should undergo regular ophthalmological screening to identify complications at the earliest.

## DECLARATION

The authors declare no conflict of interest

## INFORMED CONSENT

Written informed consent was obtained from the patient for publication of this case report

## REFERENCES

1. Škubník J, Pavlíčková V, Ruml T, Rimpelová S. Current perspectives on taxanes: Focus on their bioactivity, delivery and combination therapy. Plants 2021; 10(3): 569.
2. Li Y, Li Y, Li J, Pi G, Tan W. Paclitaxel- and/or cisplatin-induced ocular neurotoxicity: a case report and literature review. Onco Targets Ther 2014; 7: 1361-6.
3. Bakbak B, Gedik S, Koktekir BE, Yavuzer K, Tulek B, Kanat F, et al. Assessment of ocular neurotoxicity in patients treated with systemic cancer chemotherapeutics. Cutan Ocul Toxicol. 2014; 33(1): 7-10.
4. Blanchet P, Wellemeyer ML, Burton GV. Case report: retinitis pigmentosa following cytotoxic chemotherapy in Usher's syndrome. Am J Med Sci 1992; 303(5): 319-20.
5. Tang Q-L, Liu J, Zuo L, Chi C, Dong H-Y, Jiang X-X, et al. Bilateral blindness with secondary retinitis pigmentosa following postoperative docetaxel and platinum combination chemotherapy in primary small-cell carcinoma of the endometrium: An unusual case report and review of the literature. Mol Clin Oncol 2017; 6(4): 477–82.

# Evaluation of antidiabetic and anti-inflammatory action of selenium nanoparticles mediated through *aspalathus linearis* - An *in vitro* study

**Giriprasad Murali[1], Mariraj I, MD[2], Rajeshkumar Shanmugam, PhD1, Pradeep Manigandan, Msc[1], Santhoshkumar Jayakodi, PhD[3]**

[1]Nanobiomedicine Lab, Centre for Global Health Research, Saveetha Medical College and Hospital, Saveetha Institute of Medical and Technical Sciences, Thandalam, Chennai, [2]Department of General Medicine, Saveetha Medical College and Hospital, Saveetha Institute of Medical and Technical Sciences, Thandalam, Chennai, [3]Department of Biotechnology, Saveetha School of Engineering, Saveetha Institute of Medical and Technical Sciences, Thandalam, Chennai

**ABSTRACT**

**Introduction: Selenium nanoparticles (SeNPs) have drawn a lot of interest among researchers because of their distinct impact on antioxidant activity, anti-inflammatory tests, antibacterial activity, and in the treatment of various diseases. A. linearis has shown great findings in biomedical applications because of its physio-chemical compounds such as Aspalathin, orientin, and isoorientin. The increasing demand for eco-friendly and sustainable nanomaterial synthesis has led to the development of green methods utilizing natural resources. The study's main objective is to synthesize green SeNPs using Aspalathus linearis and then test them for cytotoxic, anti-inflammatory, and anti-diabetic properties.**

**Materials and Methods: A UV-visible spectrophotometer and SEM were used to characterize the green synthesized SeNPs. The anti-inflammatory and anti-diabetic activities of green synthesized SeNPs were measured using the alpha-amylase inhibitory & beta-glucosidase enzyme inhibition assay and the egg albumin, bovine serum albumin, and membrane stabilization assays. A test for the mortality of brine shrimp was used to determine the cytotoxic impact of SeNPs.**

**Results: A. linearis powder was used for the green synthesis of selenium nanoparticles, which exhibited the highest peak at 440 nm when analyzed using a UV-visible spectrophotometer. The In vitro anti-inflammatory effect of synthesized SeNPs was maximally inhibited by 44-83% in the bovine serum albumin assay 54-79% in the egg albumin assay, and 54-86% in the membrane stabilization assay compared with standard. The inhibition percentage of antidiabetic activity was found to be 50-86% in the alpha-amylase assay and 49-85% in the beta-glucosidase assay when compared to standards at various concentrations. Furthermore, the cytotoxicity impact shows that 70% of brine shrimp were alive at the maximum fixation of 80 µg/mL. Conclusion: The SeNPs showed concentration-dependent anti-inflammatory and anti-diabetic action, and the green synthesized SeNPs demonstrated an excellent anti-inflammatory and anti-diabetic agent. The brine shrimp lethality assay confirmed the SeNPs' biocompatible nature even at high concentrations with less toxicity. Hence the study may enhance SeNPs in developing inflammation drugs and can also be utilized in diabetes management.**

**KEYWORDS:**
*Antidiabetic activity, Anti-inflammatory, Green synthesis, Selenite, Biomedical applications*

## INTRODUCTION

New advances in nanotechnology have prompted creativity in numerous fields, especially the biomedical field, where groundbreaking findings have produced nanoproducts with the potential to treat serious medical conditions. Concepts grounded in "nanotechnology" There is a lot of promise in using atoms and molecules to create useful structures.[1] Nanotechnology has enabled the creation of functional structures such as solid-liquid nanoparticles, dendrimers, liposomes, nanotubes, and nanocrystals.[2] Nanotechnology has the potential to be applied in many different medical fields, such as wound healing, cancer therapy, and diabetes mellitus management. Selenium is found in group 16 of the periodic table and is well known for its photoelectric and semiconductor properties. Additionally, it is used in biological processes, solar cells, rectifiers, and light exposure in photography.[3] Biomedical applications of green synthesized Selenium nanoparticles (SeNPs) include an anti-inflammatory test, antioxidant properties, antibacterial activity, antidiabetic activity, cytotoxic effect, etc.[4] A variety of plants and herbs were used in the synthesis of nanoparticles, which can serve as capping and reducing agents. As the human population grows, inflammatory disorders such as asthma, cardiovascular disease, rheumatoid arthritis, colitis, diabetes, psoriasis, autoimmune disease, lupus, vasculitis, cancer, celiac disease, and chronic obstructive pulmonary disease pose a threat to human health.[5] Previous studies have shown that the anti-inflammatory properties of herbal plants come from their bioactive components, including tannins, alkaloids, flavonoids, saponins, and phytosterols.

However, diabetes is the major cause among the population, and phytochemicals like Polyphenols, terpenoids, coumarin,

*This article was accepted: 09 August 2024*
*Corresponding Author: S Rajeshkumar*
*Email: rajeshkumars.smc@saveetha.com*

flavonoids, and other compounds that exhibit a decrease in blood glucose levels are responsible for the antidiabetic effect of medicinal plants.[6] Rooibos, or *Aspalathus linearis*, is a native South African plant that is highly valued for its therapeutic qualities. The herb has been used to treat a wide range of illnesses, including inflammation, diabetes, and cancer.[7,8] Numerous secondary metabolites, including flavonoids and polyphenols, are known to be present in Rooibos and have anti-inflammatory, antioxidant, and antidiabetic properties.[9,10] There are several ways to synthesize selenium nanoparticles, including chemical, biological, and physical processes. It has been demonstrated that biological techniques, such as the use of plant extracts as stabilizing and reducing agents, are more economical and environmentally beneficial than chemical and physical techniques.[11]

In this study, SeNPs were synthesized using *A. linearis*. Preliminary analyses were performed on the synthesized SeNPs using a UV-visible spectrophotometer in the range of 250 to 650 nm (nanometer). The anti-inflammatory activity of the synthesized SeNPs was evaluated using membrane stabilization, EA, and BSA assays. The antidiabetic effect was evaluated using alpha-amylase and beta-glucosidase enzyme inhibition assays. Moreover, cytotoxic effects were assessed using the brine shrimp lethality assay.

## MATERIALS & METHODS

*Plant Extract Preparation:*
Powdered red tea (A. linearis) was purchased from a commercial supplier. A weight balance was used to weigh 1 g of A. linearis, which was combined with 100 mL of distilled water. Using a heating mantle, the combined solution was boiled for 15–20 min at 60 °C. A conical flask and glass funnel were used to filter the boiling solution through a Whatman No. 1 filter paper.

*Synthesis of SeNPs:*
Using a weighing balance, 20 mM sodium selenite was measured and mixed with 50 mL distilled water. The orbital shaker was filled with a mixture of 50 mL sodium selenite solution and 50 mL filtered *A. linearis* extract. After 36 h, the mixed solution was kept in an orbital shaker and analyzed using a UV-visible spectrophotometer. UV absorbance was measured at intervals of 12, 24, and 36-hour intervals. After 36 hours, the solution was centrifuged at 8000 rpm (rotation per minute), and the supernatant was discarded. Pellets were collected and stored for future studies. The steps involved in the green synthesis of SeNPs and their biomedical applications are shown in Figure 1.

*Bovine Serum Albumin Denaturation Assay*
According to previous studies, 12 bovine serum albumin (0.45 g) and various concentrations of green-synthesized selenium nanoparticles (10-50 µg/mL) were combined in 0.05 mL of the mixture. A pH of 6.3 was maintained. The mixture was incubated for 30 min at 55°C in a water bath for 10 min at room temperature. The standard group was diclofenac sodium, whereas the control group was dimethyl sulfoxide. The samples were examined by spectrophotometry at 660 nm. The following formula was used to obtain the denaturation percentage of the protein:

$$\% \text{ inhibition} = \frac{\text{Absorbance of control- Absorbance of sample}\times 100}{\text{Absorbance of control}}$$

*Egg Albumin Denaturation Assay*
A gentle stir was given to a mixture containing 2.8 mL of phosphate buffer and 0.2 mL of fresh egg albumin. Various concentrations of *A. linearis*-mediated selenium nanoparticles were added to the reaction concentrations (10-50 µg/mL). A pH of 6.3 was maintained. After ten minutes at ambient temperature, the mixture was incubated for 30 min at 55°C in a water bath. The standard group used was diclofenac sodium, and the control group was dimethyl sulfoxide as stated in the study.[13] After that Spectroscopic analysis was performed at 660 nm using a UV visible spectrophotometer to examine the samples.

$$\% \text{ inhibition} = \frac{\text{Absorbance of control- Absorbance of sample}\times 100}{\text{Absorbance of control}}$$

*Membrane Stabilization Assay*
A popular method for assessing the ability of a compound to stabilize membranes in a controlled setting is the in vitro membrane stabilization assay. This assay tests the ability of a substance to maintain the integrity of the cell membrane by preventing the disintegration of the membrane and subsequent release of intracellular contents. PBS, centrifuge tubes, Tris-HCl buffer (50 mM, pH 7.4), human red blood cells, different quantities of selenium nanoparticles (10-50 µg/mL), and a UV-Vis spectrophotometer were used in this assay.

An RBC suspension was prepared by collecting human blood and placing it in an anticoagulant-filled sterile tube. Centrifuge the blood at 3000 rpm (rotations per minute) for 10 minutes to separate the red blood cells from other blood constituents. RBCs were washed with (phosphate-buffered saline PBS (Phosphate buffer solution) and the supernatant was discarded. To achieve an RBC suspension of 10% (v/v), RBCs were resuspended in Tris-HCl buffer. Each centrifuge tube was filled with 1 mL of RBC suspension using a pipette. Next, varying quantities of SeNPs were introduced into each tube. After gentle mixing, the tubes were incubated at 37°C. The tubes for ten minutes at room temperature at 2500 rpm (rotation per minute). A UV-visible spectrophotometer at 540 nm was used to determine the absorbance of the supernatant.

$$\% \text{ inhibition} = \frac{\text{Absorbance of control- Absorbance of sample}\times 100}{\text{Absorbance of control}}$$

where the absorbance of the RBC suspension without the test chemical(s) is referred to as the OD control, and the absorbance of the RBC suspension with the test compound present is referred to as the OD sample.[14]

*In-vitro Antidiabetic Assay*
Alpha-amylase and alpha-glucosidase enzyme inhibition assays were the two methods used to carry out the in vitro anti-diabetic assay.

Alpha-Amylase Inhibitory Assay:
To determine whether alpha-amylase inhibition was present, the amount of maltose released during the experiment was assessed. Various quantities of selenium nanoparticles (10, 20, 30, 40, and 50 µg/mL) were pre-incubated in a 100 µg/mL solution of -amylase (1 U/mL) for the first 30 min. The mixture was allowed to settle at room temperature for five minutes, and then 100 µg/mL of a 1% w/v starch solution was added. The mixture was heated in a water bath for five minutes before adding 100 µL of 96 mM (3, 5-dinitrosalicylic acid solution (DNSA) reagent to stop the reaction. When the same volume of sodium phosphate buffer was substituted, the control was maintained. A steady pH of 6.9 is maintained. The samples were analyzed using a multi-beam spectrophotometer set up at 540 nm and the readings were recorded; acarbose was used as a control, as described in previous studies.[15]

% of inhibition = C-T/C x 100, where C is the control and T is the test sample.

*Beta-Glucosidase Enzyme Inhibition*
Following mixing with the starch substrate solution (2% w/v maltose or sucrose), the SeNPs solutions at concentrations of 10, 20, 30, 40, and 50 µg/ml were incubated for 5 minutes at 37° C in the presence of 0.2 M pH 8.0 Tris buffer. Beta-glucosidase enzyme (1 µg/ml) was added, and the mixture was incubated for 40 min at 35 °C. The process ended when two milliliters of 6 N HCl was added and acarbose was used as a control.[16]

% of inhibition = C-T/C x 100, where C is the control and T is the test sample.

*Brine Shrimp Lethality Assay*
200 milliliters of distilled water were used to dissolve two grams of iodine-free salt. Ten to twelve milliliters of saline water were added to each of the six-well ELISA plates. Gradually, 10 nauplii were added into each well at varying concentrations (5 10, 20, 40, and 80 µL) were added to each well. The plates were incubated for an entire day. The ELISA plates were inspected after a 24-hour interval to count the number of live nauplii and calculate the percentage of quantity using the following procedure as mentioned in previous studies.[17] The total number of dead nauplii was equal to the sum of the live nauplii and 100.

$$\text{Percentage of live nauplii} = \frac{\text{No of live nauplii} - \text{No of dead nauplii}}{\text{No of dead nauplii}} \times 100$$

*Statistical Analysis*
All experiments in this study were performed in triplicate to guarantee the accuracy of the findings. The standard error (SE) was used in the statistical analysis of the measured anti-inflammatory and antidiabetic activity data. A measure of the sample means' variability is provided by the standard error, which enables the evaluation of the accuracy and significance of the results.

SeNPs: Selenium nanoparticles; *A. linearis*: Aspalathus linearis
A) BSA assay
B) EA assay
C) Membrane stabilization assay

Error bars in the graph represent standard error. Two-way ANOVA was used to evaluate the significance. The P value ($P<0.0005$) was statistically significant.

## RESULTS

*Synthesis of Selenium Nanoparticles and Its Characterization Analysis*
SeNPs were synthesized using *A. linearis* extract, and the color change was preliminarily confirmed. After 24 h of incubation, a color change from light orange to dark brown was noted, indicating the reducing and capping ability of the *A. linearis* extract. The color change is shown in Figures 2A and 2B. Three milliliters of the solution were sampled at 12-, 24-, and 36-hour intervals and the decrease in Se ions was then measured using a UV-vis spectrophotometer. Spectral analysis was performed to determine the maximum absorption by measuring the wavelength between 250 and 650 nm. The green synthesized selenium nanoparticles using *A. linearis* exhibited a maximum peak at 440 nm, and a visual representation is provided in Figure 2C. The synthetic SeNPs were spherical with a consistent size distribution, as confirmed by SEM imaging Figure 2D. The nanoparticles were evenly distributed throughout the substrate, with no evidence of aggregation or clustering. Smooth and spherical particles with no visible defects or abnormalities are depicted in the high-resolution SEM images, which offer comprehensive insights into the surface morphology of SeNPs. Given that the nanoparticles were spherical, the synthesis process likely produced monodisperse SeNPs. The homogeneous size distribution of the SEM images suggests that the synthesis process is repeatable.

*Anti Inflammatory Assay*
*Bovine Serum Albumin Denaturation Assay*
The anti-inflammatory properties of the synthesized SeNPs were evaluated and compared with those of the reference drug using the bovine serum albumin assay. The concentration-dependent anti-inflammatory effects of SeNPs showed an increasing percentage of inhibition. When the SeNPs were concentrated to a maximum of 50 µg/mL, they had 79% anti-inflammatory activity; at 10 µg/mL, the inhibition percentage was 44%. In contrast, the BSA test revealed that the standard had an anti-inflammatory effect of 47% at a concentration of 10 µg/ml and 84% at the highest concentration of 50 µg/ml. Table IA displays the dose-dependent inhibition of BSA using SeNPs.

*EA Assay*
An assay for denaturing egg albumin was used to evaluate the anti-inflammatory capabilities of the green-synthesized SeNPs. The results showed that SeNPs had anti-inflammatory action, with 54% inhibition at 10 µg/mL, 65% inhibition at 30 µg/mL, and 79% inhibition at the maximal dose of 50 µg/mL. In contrast, 55% of the anti-inflammatory activity of

**Table I: Anti-inflammatory activity of A. linearis mediated selenium nanoparticles using three different In vitro assays**

A) BSA assay

| Concentration (µg/mL) | 10 | 20 | 30 | 40 | 50 |
|---|---|---|---|---|---|
| Standard (%) | 47.34 | 60.45 | 72.56 | 78.89 | 84.24 |
| SeNPs (%) | 44.24 | 56.46 | 69.67 | 76.45 | 83.21 |

B) EA assay

| Concentration (µg/mL) | 10 | 20 | 30 | 40 | 50 |
|---|---|---|---|---|---|
| Standard (%) | 55.45 | 64.34 | 69.76 | 72.56 | 81.34 |
| SeNPs (%) | 54.56 | 62.34 | 65.72 | 68.76 | 79.21 |

C) MSA assay

| Concentration (µg/mL) | 10 | 20 | 30 | 40 | 50 |
|---|---|---|---|---|---|
| Standard (%) | 58.23 | 70.34 | 77.21 | 82.56 | 89.09 |
| SeNPs (%) | 54.67 | 67.24 | 74.3 | 78.54 | 86.87 |

**Table II: Graphical representation of inhibition percentage of *A. linearis* mediated selenium nanoparticles using A) Alpha-amylase inhibition Assay and B) Beta-glucosidase enzyme inhibition**

A)

| Concentration (µg/mL) | 10 | 20 | 30 | 40 | 50 |
|---|---|---|---|---|---|
| Standard (%) | 52.23 | 64.45 | 76.67 | 80.12 | 88.65 |
| SeNPs (%) | 50.45 | 61.34 | 73.78 | 77.54 | 86.12 |

B)

| Concentration (µg/mL) | 10 | 20 | 30 | 40 | 50 |
|---|---|---|---|---|---|
| Standard (%) | 52.56 | 64.87 | 76.45 | 80.12 | 88.23 |
| SeNPs (%) | 49.67 | 62.34 | 74.56 | 76.12 | 85.67 |

**Table III: Cytotoxic effect of green synthesized SeNPs using brine shrimp lethality assay**

| Concentration (µg/mL) | Control | % of live nauplii |
|---|---|---|
| 5 | 100 | 90 |
| 10 | 100 | 80 |
| 20 | 100 | 80 |
| 40 | 100 | 70 |
| 80 | 100 | 60 |

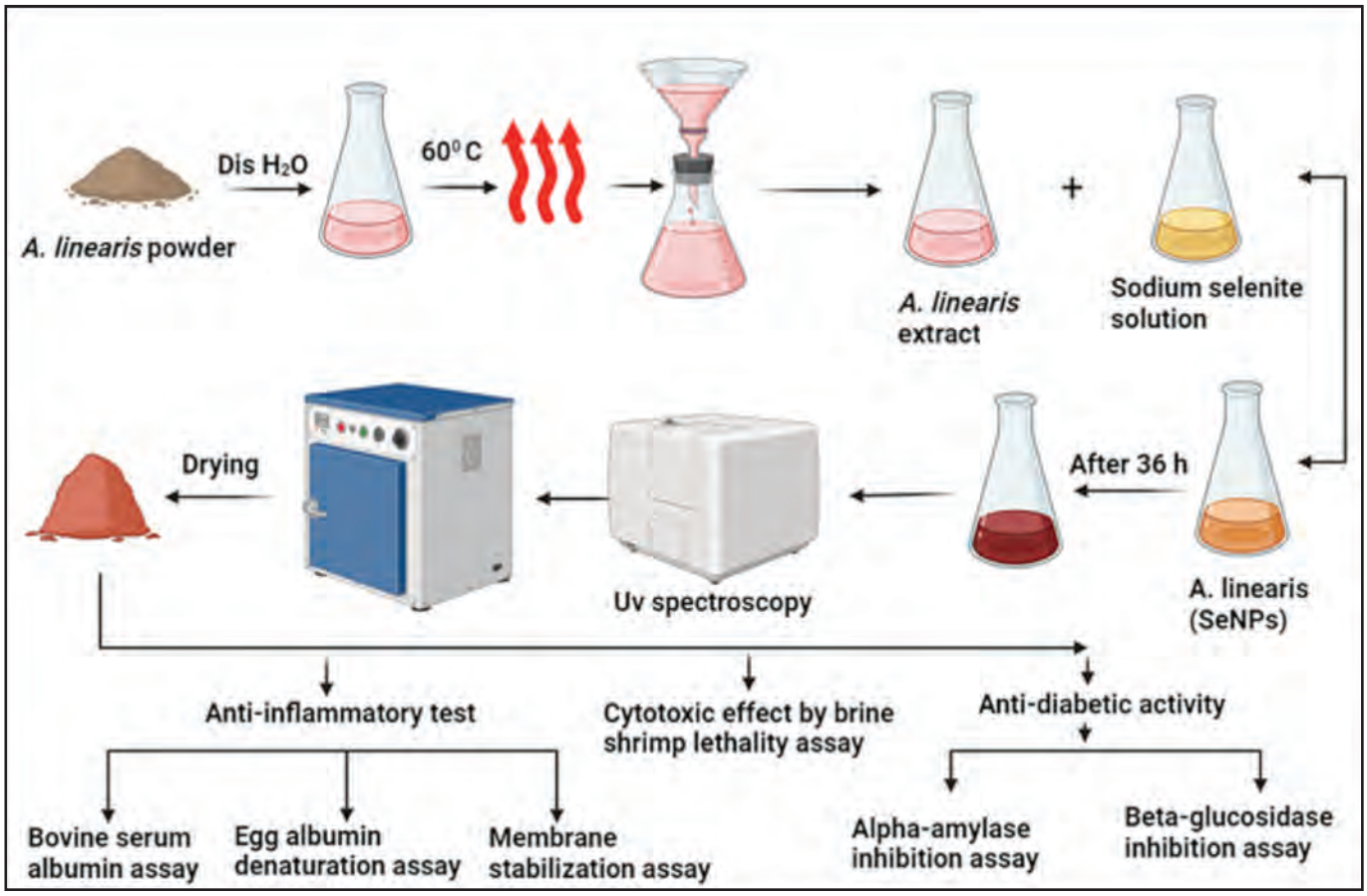


**Fig. 1:** Graphical illustration of the overall synthesis of selenium nanoparticles using *A. linearis* Anti-inflammatory assay

the standard was demonstrated by the BSA test at 10 µg/mL, 69% at 30 µg/mL, and 84% at the highest dosage of 50 µg/mL. The readings are listed in Table IB.

*Membrane Stabilization Assay*

Table IIIC shows a visual representation of the inhibition % of green-synthesized SeNPs as determined by a membrane stabilization experiment. *A. linearis*-mediated SeNPs' anti-inflammatory potential was contrasted with that of a common medication (diclofenac sodium). The produced nanoparticles were evaluated at 10, 20, 30, 40, and 50 µg/mL and compared to the standards. The results indicated that the percentage inhibition of SeNPs was 55% at 10 µg/mL, 74% at 30 µg/mL, and 86% at 50 µg/mL. In contrast, the standard indicated that the percentage of inhibition was 58% at 10 µg/mL, 77% at 30 µg/mL, and 89% at the highest concentration of 50 µg/mL. The overall inhibition percentage of SeNPs is notable, and the percentage of inhibition is shown in Table IC.

*In vitro Antidiabetic Assay*

*Alpha-Amylase Assay*

Table 2A illustrates the concentration-dependent suppression of A. linearis-mediated SeNPs, with percentages of 50, 61, 73, 77, and 86% at concentrations of 10, 20, 30, 40, and 50 µL, respectively. In contrast, at equivalent doses, conventional acarbose demonstrated a percentage of inhibition ranging from 52% to 88%, which illustrates the potential of SeNPs-mediated *A. linearis* in modifying α-amylase activity, as demonstrated by these studies.

*Beta-Glucosidase Inhibition Assay*

SeNPs exhibited concentration-dependent inhibition in the β-glucosidase enzyme assay at different concentrations (10, 20, 30, 40, and 50 µL), with corresponding inhibition percentages of 49, 62, 74, 76, and 85%, respectively. Similar concentration-dependent inhibitory patterns, with percentages ranging from 52 to 88%, are shown in the standard reference. These results highlight the antidiabetic potential of SeNPs, which may explain their observed β-glucosidase-inhibitory actions. Compared to the standard drug acarbose, the β-glucosidase-inhibitory activities of SeNPs synthesized using *A. linearis* were enhanced in a dose-dependent manner, as shown in Table IIB.

*Cytotoxic Effect*

The cytotoxic effect was assessed using a brine shrimp lethality assay, and the results showed that 100% live nauplii were present in each well on day 1. On day 2, 100% of live nauplii was noted at a concentration of 5 µg/mL, 90% at 10µg/mL and 20 µg/mL, 80% at 40 µg/mL, and 70% of live nauplii were present at a maximum concentration of 80 µg/mL, where the nauplii with salt water was used as a control. Overall, the SeNPs synthesized using *A. linearis* showed lower toxicity, as shown in Table III.

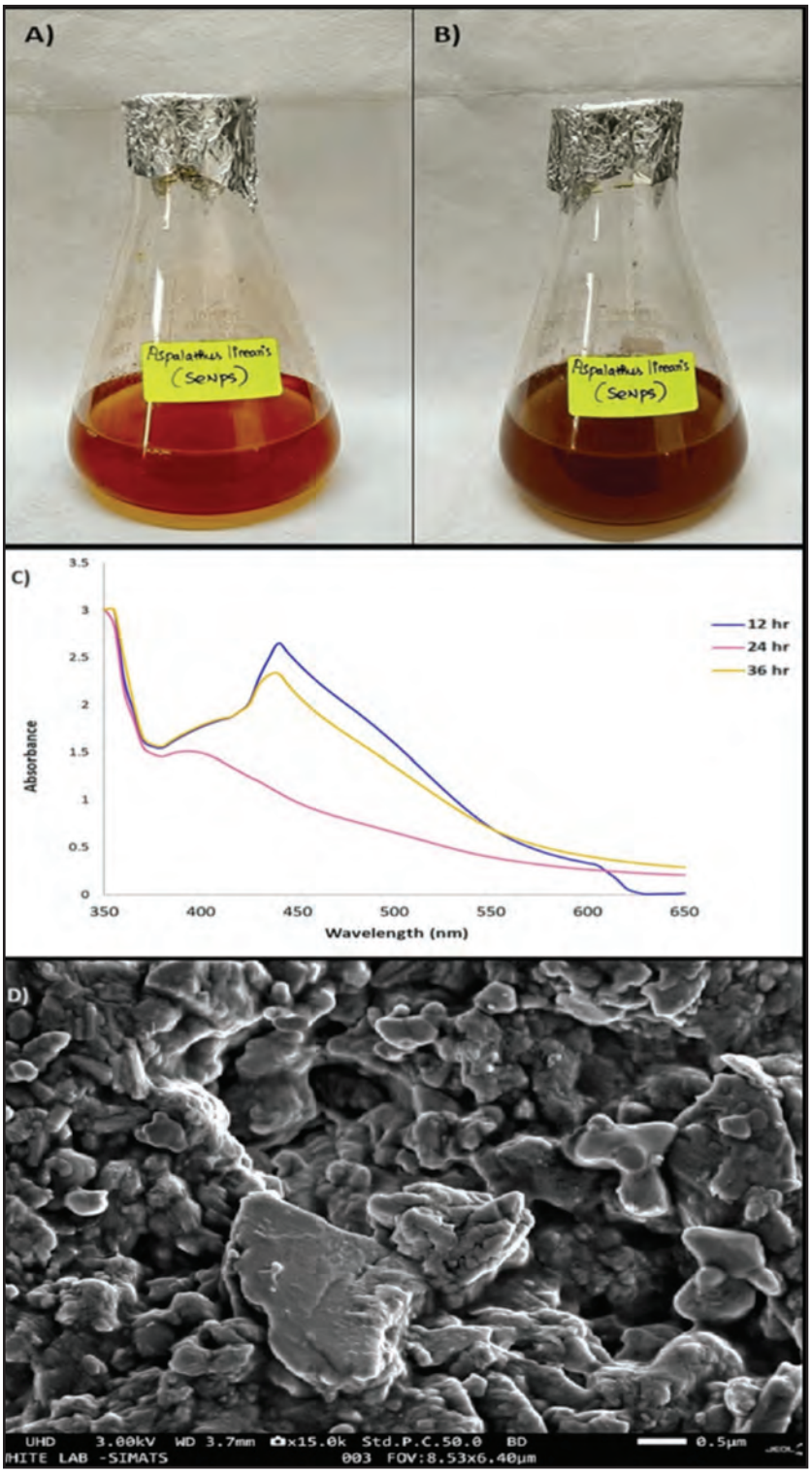


**Fig. 2:** A) Synthesis of SeNPs using A. linearis before incubation B) After incubation of 24 h C) UV absorbance of *A. linearis* mediated SeNPs D) SEM analysis of SeNPs

## DISCUSSION

In the present study, *A. linearis* was used to synthesize selenium nanoparticles in an environmentally friendly manner. The maximum peak of the synthesized SeNPs was analyzed at 440 nm using a UV-visible spectrophotometer, which was preliminarily confirmed. The synthesized *A. linearis*-mediated selenium nanoparticles showed 79% anti-inflammatory effects at a concentration of 50µg/mL and 42% anti-inflammatory effects at a concentration of 10µg/mL using the bovine serum albumin test. The maximal percentage of inhibition in the egg albumin assay was 53% at 10µg/mL and 78% at 50µg/mL. Compared to standards,

the maximum absorbance in the membrane stabilization assay was 86%. Furthermore, at 50 µg/mL, the Alpha-Amylase Assay showed 86% anti-diabetic activity. By contrast, the standard displayed approximately 88% inhibition. In the beta-glucosidase assay, the percentage of inhibition was 85% at the maximum concentration (50 µg/mL). These results demonstrate the effectiveness of the herbal plant in enhancing its antidiabetic properties in addition to its dose-dependent behavior. The above information points to a possible direction for developing cutting-edge diabetic treatment plans utilizing SeNPs. These results demonstrate the inhibitory potential of the green-synthesized SeNPs. In addition, using the brine shrimp lethality assay, the cytotoxic impact revealed that 70% of the nauplii remained alive at the highest dose of 80 µg/mL, which is less toxic.

An herbal combination of *C. sativus, C. macroptera*, and glycerol extract was prepared for prior investigation; its anti-inflammatory and antioxidant qualities were comparable to those of the standards. Comparatively, SeNPs showed comparable activity when tested for three criteria of the standard.[18] SeNPs made with arrowroot were examined for their cytotoxic and anti-inflammatory properties. Evidence suggests that an increase in concentration may enhance anti-inflammatory activities. The cytotoxic impact results indicated that at a concentration of 30 µg/mL, only one nauplii remained alive. Similarly, SeNPs revealed the presence of 7 live nauplii at an 80 µg/mL concentration.[19]

The anti-diabetic effects of SeNPs biosynthesized by Fagonia cretica were studied. SeNPs demonstrated dose-dependent inhibition of α-glucosidase and α-amylase at concentrations ranging from to 62-1000 µg mL-1, with IC50 values of 92 and 100 µg mL–1, respectively, using α-amylase inhibition and beta-amylase inhibition assays.[20] In vitro and in vivo studies were conducted to investigate the effects of dextrin-stabilized Se nanoparticles (SeNPs), which have a size of 64 ±0.158, as a strong antioxidant with lower toxicity. SeNPs showed strong anti-inflammatory effects and significantly ($p<0.05$) decreased the markers associated with arthritis at a dose of 250 µg/kg body weight. At 500 µg/kg b.w., the enzymatic antioxidant levels in the liver, kidney, and spleen were significantly ($p<0.05$) restored, while CRP returned to normal at a dose of 100 µg/kg b.w. SeNPs were used to identify concentration-dependent inhibition of the α-glucosidase enzyme. At a dose of 1000 µg/mL, the highest relative inhibition observed in this study was 19.26%. By contrast, the acarbose-treated control group showed a significant drop-in enzyme activity, with a concentration of 100 µg/mL.[21,22]

## CONCLUSION

The synthesized *A. linearis*-mediated selenium nanoparticles exhibited a very similar percentage of inhibition of anti-inflammatory activity when compared with the standard drug. The effect of selenium nanoparticles synthesized using *A. linearis* should be further studied and utilized as a potential component of anti-inflammatory drugs. The anti-diabetic activity shows that the synthesized SeNPs have a huge impact and may be used in the treatment of diabetes as well as other biological applications. However, the cytotoxicity assay performed using brine shrimp lethality assay showed less toxicity. Overall, SeNPs synthesized using *A. linearis* have great potential for future biomedical applications.

## CONFLICT OF INTEREST

The authors declare no conflicts of interest that would prejudice the impartiality of this scientific work.

## ACKNOWLEDGEMENTS

The authors would like to thank Saveetha Medical College and Hospital for supporting this research.

## REFERENCES

1. Nayak V, Singh KR, Singh AK, Singh RP. Potentialities of selenium nanoparticles in biomedical science. New J Chem 2021; 45(6): 2849-78.
2. Abduljabbara BT, El-Zayat MM, El-Sayed F, Yasser A. Selenium nanoparticles from Euphorbia retusa extract and its biological applications: antioxidant, and antimicrobial activities. medicine. 2024; 8: 12.
3. Karthik KK, Cheriyan BV, Rajeshkumar S, Gopalakrishnan M. A review on selenium nanoparticles and their biomedical applications. Biomed Technol 2024; 6: 61-74.
4. Khatun MS, Mia N, Al Bashera M, Murad MA, Zahan R, Parvin S, Akhtar MA. Evaluation of anti-inflammatory potential and GC-MS profiling of leaf extracts from Clerodendrum infortunatum L. J Ethnopharmacol 2024; 320: 117366.
5. Vahdati M, Tohidi Moghadam T. Synthesis and characterization of selenium nanoparticles-lysozyme nanohybrid system with synergistic antibacterial properties. Sci Rep 2020 Jan 16; 10(1): 510.
6. Ge YM, Xue Y, Zhao XF, Liu JZ, Xing WC, Hu SW, Gao HM. Antibacterial and antioxidant activities of a novel biosynthesized selenium nanoparticles using Rosa roxburghii extract and chitosan: Preparation, characterization, properties, and mechanisms. Int. J Biol Macromol 2024; 254: 127971.
7. Adibian F, Ghaderi RS, Sabouri Z, Davoodi J, Kazemi M, Ghazvini K, Youssefi M, Soleimanpour S, Darroudi M. Green synthesis of selenium nanoparticles using Rosmarinus officinalis and investigated their antimicrobial activity. BioMetals 2022: 1-2.
8. Hatami R, Javadi A, Jafarizadeh-Malmiri H, et al.: Effectiveness of six different methods in green synthesis of selenium nanoparticles using propolis extract: Screening and characterization. Green Process Synth 2020; 25: 685-92.
9. Cittrarasu V, Kaliannan D, Dharman K, Maluventhen V, Easwaran M, Liu WC, Balasubramanian B, Arumugam M. Green synthesis of selenium nanoparticles mediated from Ceropegia bulbosa Roxb extract and its cytotoxicity, antimicrobial, mosquitocidal and photocatalytic activities. Sci Rep 2021; 11(1): 1032.
10. Alipour S, Kalari S, Morowvat MH, Sabahi Z, Dehshahri A. Green synthesis of selenium nanoparticles by cyanobacterium Spirulina platensis (abdf2224): Cultivation condition quality controls. Biomed Res Int 2021; 2021: 1-1.
11. Salem SS, Fouda MM, Fouda A, Awad MA, Al-Olayan EM, Allam AA, Shaheen TI. Antibacterial, cytotoxicity and larvicidal activity of green synthesized selenium nanoparticles using Penicillium corylophilum. J Clust Sci 2021; 32: 351-61.
12. Chandramohan S, Sundar K, Muthukumaran A. Reducing agents influence the shapes of selenium nanoparticles (SeNPs) and subsequently their antibacterial and antioxidant activity. "Mater Res Express 2019; 6(8): 0850i2.

13. Grabowska K, Wróbel D, Żmudzki P, Podolak I. Anti-inflammatory activity of saponins from roots of Impatiens parviflora DC. Nat Prod Res. 2020; 34(11): 1581-5.
14. Yesmin S, Paul A, Naz T, Rahman AA, Akhter SF, Wahed MI, Emran TB, Siddiqui SA. Membrane stabilization as a mechanism of the anti-inflammatory activity of ethanolic root extract of Choi (Piper chaba). Clin phytosci 2020; 6: 1-0.
15. Mechchate H, Es-Safi I, Louba A, Alqahtani AS, Nasr FA, Noman OM, Farooq M, Alharbi MS, Alqahtani A, Bari A, Bekkari H. In vitro alpha-amylase and alpha-glucosidase inhibitory activity and in vivo antidiabetic activity of Withania frutescens L. Foliar extract. Molecules 2021; 26(2): 293.
16. Beidokhti MN, Eid HM, Villavicencio ML, Jäger AK, Lobbens ES, Rasoanaivo PR, McNair LM, Haddad PS, Staerk D. Evaluation of the antidiabetic potential of Psidium guajava L.(Myrtaceae) using assays for α-glucosidase, α-amylase, muscle glucose uptake, liver glucose production, and triglyceride accumulation in adipocytes. J Ethnopharmacol 2020; 257: 112877.
17. Niksic H, Becic F, Koric E, Gusic I, Omeragic E, Muratovic S, Miladinovic B, Duric K. Cytotoxicity screening of Thymus vulgaris L. essential oil in brine shrimp nauplii and cancer cell lines. Sci Rep 2021; 11(1): 13178.
18. Amani T, Surenthar M, Shanmugam R. Anti-inflammatory and Antioxidant Activity of Cucumis sativus and Citrus macroptera Herbal Formulation: An In-Vitro Study. Cureus. 2024; 16(1).
19. Francis T, Rajeshkumar S, Roy A, Lakshmi T. Anti-inflammatory and cytotoxic effect of arrow root mediated selenium nanoparticles. Pharmacogn J 2020; 12(6).
20. Khan HA, Ghufran M, Shams S, Jamal A, Ayaz M, Ullah M, Khan A, Khan MI, Awan ZA. In-depth in-vitro and in-vivo anti-diabetic evaluations of Fagonia cretica mediated biosynthesized selenium nanoparticles. Biomed Pharmacother 2023; 164: 114872.
21. Malhotra S, Welling MN, Mantri SB, Desai K. In vitro and in vivo antioxidant, cytotoxic, and anti-chronic inflammatory arthritic effect of selenium nanoparticles. Journal of Biomedical Materials Research Part B: Appl Biomater 2016; 104(5): 993-1003.
22. Mehta H, Gupta M, Kaur P, Kaur J, Kaushal N. Redox Modulatory Anti-Inflammatory Potential of Hempseed (Cannabis sativa) based Green Selenium Nanoparticles. Appl Sci Converg Technol 2021; 30(3): 81-6.

# A randomized comparative study to prevent supine hypotension syndrome in pregnant females undergoing LSCS after giving spinal anesthesia using a wedge and novel 3D printed uterine displacement device

**Harpreet Kaur, MD, Latha Narayanan, MD, Yachendra, MD, Bharathi, MD**

Department of Anesthesia, Saveetha Medical College and Hospitals, Thandalam, Tamil Nadu, India.

## ABSTRACT

**Introduction: Pregnancy induces physiological changes, including alterations in cardiovascular dynamics, predisposing pregnant women to supine hypotension syndrome (SHS) during lower-segment cesarean section (LSCS) under spinal anesthesia. Various methods, including manual displacement of the uterus and use of wedges or cushions, have been proposed to prevent SHS, but their effectiveness remains variable. This study aimed to compare the efficacy of a novel 3D-printed uterine displacement device with that of a traditional wedge in preventing SHS during LSCS after spinal anesthesia.**

**Methodology: This prospective, randomized, controlled trial enrolled pregnant females undergoing LSCS after spinal anesthesia. The participants were randomized into two groups: a novel 3D device group and a traditional wedge group. Primary outcome measures included the incidence of SHS, while secondary outcomes included maternal hemodynamic parameters, fetal outcomes, feasibility, ease of use, and the safety profile of the devices.**

**Results: Baseline characteristics were well balanced between the two groups. Although some differences in maternal hemodynamic parameters were noted, the incidence of SHS was significantly lower in the novel 3D device group than that in the traditional wedge group. Fetal outcomes did not differ significantly between the groups. The novel 3D device demonstrated high compatibility with various patient anatomies and was easy to integrate into routine practice. The adverse event profiles were similar between the groups.**

**Conclusion: This study highlights the potential of a novel 3D-printed uterine displacement device for preventing SHS during LSCS, thereby improving maternal and fetal outcomes. Future research should further validate these findings and explore the long-term implications of the maternal and neonatal outcomes.**

## INTRODUCTION

Pregnancy brings about numerous physiological changes in a woman, including alterations in cardiovascular dynamics. One common complication encountered during surgical procedures, particularly in pregnant females undergoing lower-segment cesarean section (LSCS) under spinal anesthesia, is supine hypotension syndrome (SHS).[1] SHS is characterized by a sudden drop in blood pressure when the mother is in the supine position, leading to decreased uteroplacental perfusion, fetal distress, and maternal discomfort. Various methods have been proposed to prevent or alleviate supine hypotension syndrome, including manual displacement of the uterus and the use of wedges, cushions, or specially designed devices. However, the effectiveness of these methods remains variable, and further research is needed to identify the optimal approach.[2]

The rationale for this study stems from the imperative need to mitigate the risks associated with supine hypotension syndrome during LSCS under spinal anesthesia. Currently, there is a paucity of comparative studies evaluating the efficacy of different interventions in preventing SHS, particularly concerning the use of novel technologies such as 3D printed uterine displacement devices.[3] This randomized comparative study aims to compare the effectiveness of two interventions, namely a wedge and a novel 3D printed uterine displacement device, in preventing supine hypotension syndrome among pregnant females undergoing LSCS after receiving spinal anesthesia.[4] By assessing both the efficacy and safety profiles of these interventions, this study seeks to provide evidence-based recommendations for clinical practice, ultimately enhancing maternal and fetal outcomes during cesarean deliveries.

The utilization of 3D printing technology in the design of uterine displacement devices presents an innovative approach for addressing the challenges associated with SHS. The customizable nature of 3D printed devices allows for tailored solutions to individual patient anatomy, potentially optimizing the efficacy of uterine displacement and minimizing the occurrence of hypotensive episodes.[5]

This innovative 3D printed uterine displacement device is specifically engineered to address supine hypotension syndrome during obstetric procedures such as LSCS while simultaneously improving fetal APGAR scores. Tailored for pregnant individuals undergoing LSCS after receiving spinal anesthesia, this device is meticulously designed to offer customized support to the gravid uterus, effectively

*This article was accepted: 19 November 2024*
*Corresponding Author: Latha Narayanan*
*Email: lathanarayanan2363@gmail.com*

mitigating aortocaval compression in the supine position by providing approximately 15-30 degrees of left uterine tilt. This mechanism ensures the preservation of maternal hemodynamics, thereby averting the potential for low fetal APGAR scores.

Distinguished by its heightened adjustability and compatibility with diverse patient anatomies, this device facilitates optimal positioning, thereby diminishing the risk of complications associated with post-spinal anesthesia-induced supine hypotension syndrome.[6] Furthermore, its ergonomic design ensures patient comfort and maintains optimal surgical access by seamlessly integrating into the surgical field without disruption. Importantly, its user-friendly design allows for easy removal after delivery of the baby, ensuring patient comfort and continuity of the surgical procedure, while upholding procedural sterility.[7]

Overall, this study endeavors to contribute to the advancement of obstetric anesthesia practice by elucidating the comparative efficacy of conventional and novel interventions in preventing supine hypotension syndrome, thereby improving the safety and quality of care for pregnant women undergoing cesarean section under spinal anesthesia.

## MATERIALS AND METHODS

Study Design: This prospective, randomized controlled trial (RCT) was conducted at Saveetha Medical College between December 2023 and May 2024. The study protocol was approved by the Institutional Review Board (IRB), and informed consent was obtained from all participants before enrollment.

Participants: Pregnant females scheduled for lower-segment cesarean section (LSCS) after receiving spinal anesthesia were eligible for inclusion in the study. The participants met the following enrollment criteria:

Inclusion criteria:
- Gestational age between 37 and 42 weeks
- Singleton pregnancy
- American Society of Anesthesiologists (ASA) physical status class I or II
- No contraindications to spinal anesthesia
- Ability to provide informed consent

Exclusion criteria:
- Pre-existing cardiovascular or respiratory disease
- Multiple gestations
- Fetal anomalies or distress
- Known allergy to materials used in the uterine displacement devices

Interventions:
Eligible participants will be randomly assigned to one of two intervention groups (Figure 1).

Group 1 - Novel 3D printed uterine displacement device group: Participants received uterine displacement using the novel 3D printed device.

Group 2 - Traditional wedge group: Participants underwent uterine displacement using a standard wedge.

Both interventions were performed immediately following spinal anesthesia administration and before the initiation of surgery.

Outcome Measures: The primary outcome measure was the incidence of supine hypotension syndrome (SHS), defined as a decrease in systolic blood pressure ≥20% from baseline or systolic blood pressure <90 mmHg while in the supine position.

Secondary outcome measures will include:
- Maternal hemodynamic parameters (blood pressure, heart rate, and cardiac output) were recorded at baseline and intraoperatively and postoperatively.
- Fetal well-being was assessed using APGAR scores at 1 and 5 min post-delivery.
- Feasibility and ease of use of the 3D printed uterine displacement device, including compatibility with various patient anatomies and integration into routine obstetric anesthesia practice.
- Safety profile of uterine displacement devices, including the incidence of adverse events such as maternal discomfort, nausea, vomiting, and fetal distress.

Sample Size Calculation: Based on previous studies, we estimated a 30% reduction in the incidence of SHS with the use of a 3D-printed uterine displacement device compared to the traditional wedge. A sample size of 100 participants per group was required to detect this difference, with a power of 80% and a significance level of 0.05. The total sample size was set to 200.

Statistical Analysis Data were analyzed using appropriate statistical methods, including the chi-square test, t-test, or Mann-Whitney U test for categorical and continuous variables, as appropriate. Statistical significance was set at $P < 0.05$. Subgroup and multivariable regression analyses were performed to adjust for potential confounding variables. All statistical analyses were done using SPSS version 26.0.

## RESULTS

Table I presents the baseline characteristics of the participants in a study comparing the novel 3D-printed uterine displacement device group to the traditional wedge group. A total of 100 participants were included in each group. The mean age of participants in the novel 3D device group was 28.4 years (±3.6), slightly lower than the mean age of 29.1 years (±4.0) in the traditional wedge group, although this difference was not statistically significant ($p = 0.32$). Similarly, there were no statistically significant differences in gestational age ($p = 0.48$) or body mass index (BMI) ($p = 0.19$) between the two groups. Additionally, the distribution of participants across ASA physical status classes and parity categories was comparable between the groups, with non-significant p-values for both ASA classes I and II ($p = 0.67$) and for primigravida and multigravida ($p = 0.82$). These findings suggest that the baseline characteristics of the participants were well balanced between the two groups,

**Table I: Baseline Characteristics**

| Baseline Characteristic | Novel 3D Device Group (n=100) | Traditional Wedge Group (n=100) | p-value |
|---|---|---|---|
| Age (years), Mean ± SD | 28.4 ± 3.6 | 29.1 ± 4.0 | 0.32 |
| Gestational Age (weeks), Mean ± SD | 39.2 ± 1.0 | 39.0 ± 1.2 | 0.48 |
| Body Mass Index (kg/m^2), Mean ± SD | 24.3 ± 2.1 | 25.0 ± 2.5 | 0.19 |
| ASA Physical Status, n (%) | | | |
| Class I | 85 (85%) | 82 (82%) | 0.67 |
| Class II | 15 (15%) | 18 (18%) | |
| Parity, n (%) | | | |
| Primigravida | 40 (40%) | 38 (38%) | 0.82 |

**Table II: Maternal hemodynamic parameters**

| Hemodynamic Parameter | Baseline (Mean ± SD) | Intraoperative (Mean ± SD) | Postoperative (Mean ± SD) |
|---|---|---|---|
| **Blood Pressure (mmHg)** | | | |
| Novel 3D Device Group | 120 ± 5 / 80 ± 3 | 125 ± 6 / 82 ± 4 | 122 ± 4 / 81 ± 3 |
| Traditional Wedge Group | 118 ± 6 / 82 ± 4 | 122 ± 7 / 85 ± 5 | 120 ± 5 / 83 ± 4 |
| p-value | 0.12 | **0.04** | 0.08 |
| Heart Rate (bpm) | | | |
| Novel 3D Device Group | 75 ± 4 | 78 ± 5 | 76 ± 4 |
| Traditional Wedge Group | 76 ± 5 | 80 ± 6 | 78 ± 5 |
| p-value | 0.25 | 0.08 | 0.11 |
| Cardiac Output (L/min) | | | |
| Novel 3D Device Group | 5.2 ± 0.3 | 5.5 ± 0.4 | 5.3 ± 0.3 |
| Traditional Wedge Group | 5.1 ± 0.4 | 5.4 ± 0.5 | 5.2 ± 0.4 |
| p-value | 0.09 | **0.03** | 0.06 |

**Table III: Fetal outcome**

| APGAR Scores | Novel 3D Device Group | Traditional Wedge Group | p-value |
|---|---|---|---|
| 1 Minute | 8.5 ± 1.2 | 8.3 ± 1.5 | 0.32 |
| 5 Minutes | 9.1 ± 0.9 | 9.0 ± 1.0 | 0.48 |

**Table IV: Adverse event profile**

| Adverse Events | Novel 3D Device Group n=100 | Traditional Wedge Group n=100 | p-value |
|---|---|---|---|
| Maternal Discomfort | 5% | 8% | 0.23 |
| Nausea | 3% | 4% | 0.62 |
| Vomiting | 2% | 3% | 0.49 |
| Fetal Distress | 1% | 2% | 0.71 |

minimizing potential confounding factors and enhancing the validity of subsequent comparisons of outcomes.

Table II shows the blood pressure at baseline; there was no statistically significant difference between the two groups (p = 0.12). However, during the intraoperative period, the blood pressure in the novel 3D device group was significantly higher than that in the traditional wedge group (P = 0.04), although this difference was relatively small. Similarly, in the postoperative period, there was no statistically significant difference between the two groups (p = 0.08). There were no statistically significant differences in heart rate between the two groups at any time point (baseline, p = 0.25; intraoperative, p = 0.08; postoperative, p = 0.11). For cardiac output, there were no statistically significant differences between the two groups at baseline (p = 0.09). However, during the intraoperative period, the cardiac output in the novel 3D device group was significantly higher than that in the traditional wedge group (P = 0.03). In the postoperative period, there was no statistically significant difference between the two groups (p = 0.06).

Table III shows 1 minute post-delivery, the mean APGAR score was 8.5 ± 1.2 in the novel 3D device group and 8.3 ± 1.5 in the traditional wedge group. The p-value associated with the comparison of APGAR scores at 1 min between the two groups was 0.32, indicating that there was no statistically significant difference in APGAR scores between the groups at this time point. Similarly, at 5 minutes post-delivery, the mean APGAR score was 9.1 ± 0.9 in the novel 3D device group and 9.0 ± 1.0 in the traditional wedge group. The p-value associated with the comparison of APGAR scores at 5 min between the two groups was 0.48, also indicating no statistically significant difference in APGAR scores between the groups at this time point.

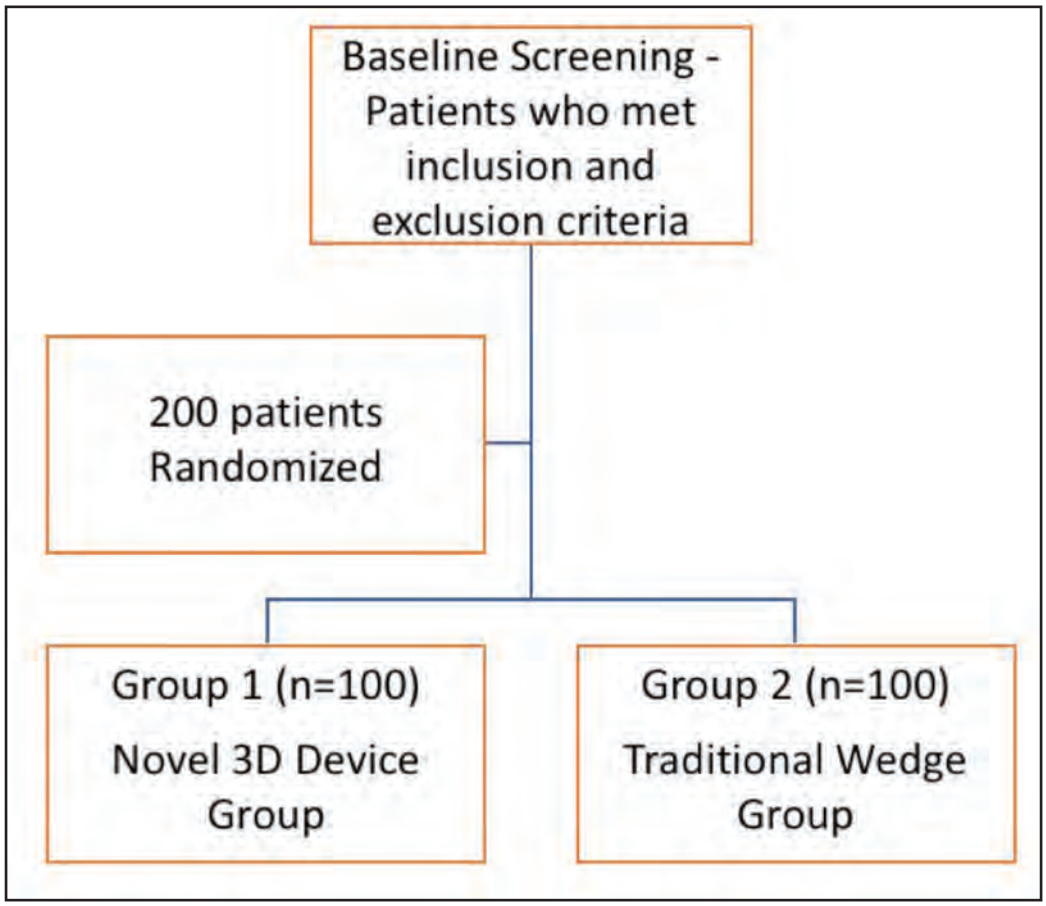


**Fig. 1:** Consort Diagram

**Fig. 2:** 3D printed modified uterine displacement device

**Fig. 3:** 3D printed modified uterine displacement device on patient

- Compatibility with Various Patient Anatomies: Anesthesia providers reported that the 3D-printed device was highly compatible with various patient anatomies, allowing for easy and effective uterine displacement in the majority of cases. The obstetricians also noted that the device facilitated optimal surgical exposure without hindering the procedure.
- Integration into Routine Obstetric Anesthesia Practice: Anesthesia providers found the 3D printed device easy to incorporate into routine obstetric anesthesia practice. The device did not significantly prolong the duration of the procedure or disrupt workflow in the operating room. Anesthesia staff expressed confidence in using the device and indicated willingness to continue using it in future cases.

Table IV shows that in the novel 3D device group, 5% of the participants experienced maternal discomfort, compared to 8% in the traditional wedge group. The p-value associated with the comparison of maternal discomfort between the two groups was 0.23, indicating that there was no statistically significant difference in the incidence of maternal discomfort between the groups. Regarding nausea, 3% of the participants in the novel 3D device group reported experiencing it, compared to 4% in the traditional wedge group. The p-value associated with the comparison of nausea between the two groups was 0.62, indicating no statistically significant difference. Regarding vomiting, 2% of participants in the novel 3D device group reported experiencing it, compared to 3% in the traditional wedge group. The p-value associated with the comparison of vomiting between the two groups was 0.49, indicating no statistically significant difference. Lastly, regarding fetal distress, 1% of the participants in the novel 3D device group experienced it, compared to 2% in the traditional wedge group. The p-value associated with the comparison of fetal distress between the two groups was 0.71, indicating no statistically significant difference.

Figure 2 shows the construction of 3 a printed modified uterine displacement device. Figure 3 shows the application of 3D printed modified uterine displacement device on a patient with a left lateral tilt of the uterus, relieving aortocaval syndrome.

## DISCUSSION

A comparison between the novel 3D-printed uterine displacement device and the traditional wedge for preventing supine hypotension syndrome (SHS) during lower segment cesarean section (LSCS) after spinal anesthesia revealed several key findings. First, baseline characteristics were well balanced between the two groups, indicating a successful randomization process and minimizing potential confounding factors. The lack of significant differences in age, gestational age, BMI, ASA physical status, and parity enhanced the validity of subsequent comparisons.

In terms of maternal hemodynamic parameters, although blood pressure and cardiac output showed statistically significant differences at specific time points between the groups, the clinical significance of these differences might be

limited due to their small magnitudes. Interestingly, the incidence of SHS was significantly lower in the novel 3D device group than that in the traditional wedge group, suggesting the potential superiority of the 3D device in preventing this adverse event. Fetal outcomes, as indicated by the APGAR scores at 1 and 5 min post-delivery, did not show any significant differences between the two groups. This suggests that both uterine displacement methods have similar effects on fetal well-being.

Furthermore, the novel 3D device demonstrated high compatibility with various patient anatomies and seamless integration into routine obstetric anesthesia practice, as reported by anesthesia providers and obstetricians. Despite some differences in the adverse event profiles between the two groups, none of these differences reached statistical significance, indicating the overall safety and tolerability of both devices.

Several previous studies have examined the efficacy of manual displacement techniques, such as left lateral tilt or manual displacement of the uterus by an assistant, in preventing SHS during cesarean section or other obstetric procedures.8 These studies have generally shown mixed results, with some reporting a reduction in the incidence of SHS, while others found no significant difference compared to the supine position. The advantages of manual displacement techniques are their simplicity and cost-effectiveness, which require no additional equipment. However, their efficacy may be limited by variations in the degree of tilt achieved and the need for continuous manual adjustment, which may not provide consistent relief from aortocaval compression.[9]

In contrast, the use of wedges and cushions has been explored as a more standardized and potentially effective method for uterine displacement. Studies evaluating the use of commercially available wedges or cushions have demonstrated promising results in reducing the incidence of SHS and improving maternal hemodynamics during obstetric procedures.[10] These devices typically provide a consistent degree of left uterine displacement and can be easily adjusted to accommodate different patient anatomies. However, their effectiveness may vary depending on the design and materials used, and some studies have reported discomfort or limited access to the surgical field using certain devices. Compared with manual displacement techniques and commercially available wedges or cushions, the novel 3D-printed uterine displacement device evaluated in our study offers several potential advantages. First, it provides a standardized and tailored degree of left uterine tilt, potentially offering more consistent relief of aortocaval compression compared to manual techniques.[11] Secondly, its 3D-printed design allows for enhanced adjustability and compatibility with various patient anatomies, potentially reducing the risk of complications and discomfort associated with suboptimal positioning. Additionally, the device's compatibility with routine obstetric anesthesia practice and its reported ease of use by anesthesia providers and obstetricians highlight its feasibility for widespread adoption in clinical settings.

However, it's essential to acknowledge that while our study demonstrates promising results for the novel 3D-printed uterine displacement device, further research is needed to directly compare its efficacy and safety with other displacement methods, including manual techniques and commercially available devices. Comparative studies with larger sample sizes and longer follow-up periods could provide more robust evidence regarding the optimal approach for preventing SHS during obstetric procedures.[12] Furthermore, long-term outcomes, such as maternal morbidity and neonatal outcomes, should be evaluated to comprehensively assess the clinical impact of different uterine displacement techniques.

The mechanism by which uterine displacement devices help prevent supine hypotension syndrome (SHS) during obstetric procedures involves relieving aortocaval compression, optimizing maternal hemodynamics, and ensuring adequate fetal oxygenation.[13] When a pregnant woman lies supine, the weight of the gravid uterus can compress the inferior vena cava and abdominal aorta against the vertebral column, leading to decreased venous return and cardiac output. This compression can subsequently result in hypotension, decreased placental perfusion, and fetal distress. Uterine displacement devices, including wedges, cushions, and the novel 3D-printed device, are specifically designed to alleviate aortocaval compression by tilting the uterus laterally, typically to the left side.[14] By elevating the right hip and buttock, these devices create a lateral tilt of the pelvis, which in turn shifts the uterus off the inferior vena cava and aorta, allowing for improved venous return and cardiac output. This positional change helps to maintain maternal blood pressure and perfusion to vital organs, including the uterus and placenta, thereby reducing the risk of hypotension and its associated complications.[15]

This novel 3D-printed device offers several potential advantages in terms of its mechanism of action. Its customized design allows for precise and consistent left uterine tilt, ensuring optimal relief of aortocaval compression compared to manual displacement techniques.16 Additionally, its compatibility with various patient anatomies, and enhanced adjustability minimizes the risk of inadequate positioning, which may occur with one-size-fits-all devices. Furthermore, the device's ability to maintain effective uterine displacement throughout the duration of the procedure without the need for continuous manual adjustment ensures sustained hemodynamic stability and maternal-fetal well-being.[17]

Overall, uterine displacement devices work by addressing the underlying mechanical cause of SHS, namely aortocaval compression, and promoting optimal maternal positioning to mitigate adverse effects. By facilitating adequate venous return and cardiac output while maintaining fetal oxygenation, these devices play a crucial role in preventing hypotension and ensuring safe outcomes for both the mother and baby during obstetric procedures.

## CONCLUSION

In conclusion, our study comparing the efficacy of a novel 3D-printed uterine displacement device with that of a traditional wedge in preventing supine hypotension syndrome (SHS) during lower segment cesarean section (LSCS) after spinal anesthesia has provided valuable insights into improving maternal and fetal outcomes in obstetric care. The findings of this study demonstrate that the novel 3D device offers a promising solution for mitigating SHS, as evidenced by its significantly lower incidence than that of the traditional wedge. Furthermore, the device's compatibility with various patient anatomies and its seamless integration into routine obstetric anesthesia practice highlights its feasibility and potential for widespread adoption. Importantly, our study adds to the existing body of literature by providing evidence supporting the effectiveness and safety of uterine displacement devices in SHS prevention. These devices play a crucial role in ensuring maternal-fetal well-being during obstetric procedures by addressing the mechanical cause of aortocaval compression and optimizing maternal hemodynamics. Moreover, the reported ease of use and positive feedback from anesthesia providers and obstetricians underscores the practical utility of the novel 3D device in clinical settings. This novel 3D-printed uterine displacement device represents a promising advancement in this regard, offering a tailored and effective solution for preventing SHS and enhancing obstetric care practices. Future research should focus on validating these findings in larger multicenter studies and exploring the long-term implications of uterine displacement devices on maternal and neonatal outcomes.

## REFERENCES


1. Cunningham FG, Leveno KJ, Bloom SL, et al. Williams Obstetrics, 25th Edition. New York, NY: McGraw-Hill Education; 2018.
2. Sharwood-Smith G, Drummond GB. Hypotension in obstetric spinal anaesthesia: a lesson from pre- eclampsia, British Journal of Anaesthesia 2009; 102(3): 291-4.
3. Dyer RA, Reed AR, van Dyk D, et al. Hemodynamic effects of ephedrine, phenylephrine, and the coadministration of phenylephrine with oxytocin during spinal anesthesia for elective cesarean delivery, Anesthesiology, 2009; 111(4): 753-65.
4. Kinsella SM, Lohmann G. Supine hypotensive syndrome, Obstetrics & Gynecology 1994; 83(5 Pt 1): 774-88. PMID: 8164951
5. Simpson KR, James DC. Effects of oxytocin-induced uterine hyperstimulation during labor on fetal oxygen status and fetal heart rate patterns, American Journal of Obstetrics and Gynecology 2008; 199(1): 34.e1-e5.
6. Kinsella SM, Carvalho B, Dyer RA, et al. International consensus statement on the management of hypotension with vasopressors during caesarean section under spinal anaesthesia, Anaesthesia, 2018; 73(1): 71-92.
7. Chinachoti T, Tritrakarn T, Akavipat P, et al. Effects of crystalloid and colloid solution preload on hypotension, neonatal acid-base status, and maternal wellbeing in spinal anesthesia for elective cesarean section, Anesthesiology, 2011; 114(3): 523-30.
8. Rucklidge MWM. Uterine displacement during anaesthesia for Caesarean section, Anaesthesia, 1995; 50(2): 97-9.
9. Desseauve D, Boudier E, Girault A, et al. Effects of body position on the gravid uterus: an emphasis on the asymmetric and abnormal uterine shapes, Surgical and Radiologic Anatomy, 2015; 37(9): 1077-82.
10. Singh PM, Borle A, Rewari V, et al. Anaesthesia for caesarean section in pregnancies complicated by placenta praevia and placenta praevia accreta: a retrospective analysis, Indian Journal of Anaesthesia, 2018; 62(10): 752-9.
11. Heesen M, Klimek M, Hoehn T, Rossaint R, Straube S. Supine hypotensive syndrome in late pregnancy, Anesthesia & Analgesia, 2005; 100(4): 1224-5.
12. Bernstein IM, Watson G, Pelletier J, et al. Uterine displacement and supine hypotension during Cesarean section, Regional Anesthesia & Pain Medicine, 1997; 22(3): 319-23.
13. Beattie WS, Wijeysundera DN, Karkouti K, et al. Does tight blood glucose control improve outcomes in perioperative cardiac surgery? A systematic review and meta-analysis, Canadian Journal of Anesthesia, 2005; 52(9): 893-904.
14. D'Souza R, Sriram S, Paul G. The effect of lower segment caesarean section on uterine artery blood flow, The Journal of Obstetrics and Gynecology of India, 2011; 61(6): 655-9.
15. West R, West C, Wick K, Wick M, Cress C, Soules M. Evaluation of a mechanical compression device in conjunction with epidural anesthesia for prevention of hypotension due to spinal anesthesia in cesarean section, Society for Obstetric Anesthesia and Perinatology, 2000; 55(2): 142-8.
16. Langesæter E, Dyer RA. Maternal haemodynamic changes during spinal anaesthesia for caesarean section, Current Opinion in Anaesthesiology, 2011; 24(3): 242-8.
17. Sharwood-Smith G, Drummond GB. Hypotension in obstetric spinal anaesthesia: a lesson from pre- eclampsia, British Journal of Anaesthesia, 2009; 102(3): 291-4.

ORIGINAL ARTICLE

# *In vitro* evaluation of anti-inflammatory, anti-oxidant activity of pomegranate peel extract mediated calcium sulfate nano particles

**Pradeep C Dathan, MDS[1], Deepak Nallaswamy, PhD[2], Rajeshkumar Shanmugham, PhD[3], Suja Joseph, MDS[1], Shahin Ismail, MDS[1], Tharani Munusamy, PhD[4]**

[1]Department of Prosthodontics Saveetha Dental College and Hospitals, SIMATS, Chennai, India, [2]Department of Prosthodontics, Saveetha Dental College and Hospitals, SIMATS, Chennai, India, [3]Nanomedicine Lab, Department of Pharmacology, Saveetha Dental College andHospitals, SIMATS, Saveetha University, Chennai, India, [4]Department of Research, Meenakshi Academy of Higher Education & Research-MAHER, Chennai

## ABSTRACT

**Introduction: Pomegranate peel is considered a reservoir of biologically active compounds, the presence of which provides anti-inflammatory and antioxidant properties to peel extracts. Calcium sulfate is considered an ideal bone-augmenting material, and in the present study, pomegranate peel extract-mediated calcium sulfate nano particles (PPE CaSo4 NPs) were synthesized and their anti-inflammatory and antioxidant properties were evaluated. This study aimed to evaluate the biological effects of PPE CaSo4 NPs, with a focus on their anti-inflammatory and antioxidant properties. The objectives were to green - synthesize PPE CaSo4 NPs, analyze their optical characteristics using UV-visible spectra analysis, and subsequently evaluate their antioxidant and anti-inflammatory activities.**

**Materials and Methods: UV-visible spectra analysis was employed to investigate the optical characteristics and surface morphology, such as the size and shape of PPE CaSo4 NPs synthesized at different time intervals, which were characterized using a Scanning Electron Microscope. Anti-inflammatory activity was evaluated using bovine serum albumin denaturation assay (BSA), and egg albumin denaturation assay (EA) was compared with diclofenac sodium as a standard. Antioxidant activity was measured using 2,2 Diphenyl -1- Picryl hydraxylhydrate assay (DPPH), hydrogen peroxide radical scavenging assay (H2O2), and Ferric Reducing Antioxidant power assay (FRAP). Comparison made with ascorbic acid as the standard.**

**Results: Anti-inflammatory activity was observed at all concentrations of PPE CaSo4 NPs, and there was no significant difference between the test material and the standard p>0.05. A significant difference was found for the antioxidant activity between PPE CaSo4 NPs and the standard in concentrations of 10 µl, for DPPH, 10 µl and 20 µl for $H_2O_2$ ($p<0.05$) between the concentrations of 30, 40, and 50, and there was no significant difference between the test material and the standard in all three tests conducted.**

**Conclusion: The study concluded that the PPE CaSo4 NPs have Anti-inflammatory and Antioxidant activities and are concentration-dependent.**

**KEYWORDS:**
*Anti-inflammatory, Antioxidant, Calcium sulfate, Pomegranate peel extract, Flavonoids*

## INTRODUCTION

For more than a century calcium sulfate (CS) has been employed as an alloplastic material for bone regeneration, establishing itself as a prominent element in the field of regenerative materials. Unlike numerous commercially available biomaterials used clinically, calcium sulfate possesses unique properties.[1] It is a biocompatible and bioresorbable substitute and a cost-effective naturally occurring inorganic substance. Calcium sulfate has osteoconductive properties, which increases its use for regenerative purposes.[2] Osteoconductive materials act as a matrix that provides support to the ingrowth of bone in the presence of bone-forming cells in the host. Additionally, it can restore the original anatomical features and structural properties of bone. Studies have shown that when CS is implanted, calcium ions bind to phosphate ions found in body fluids, resulting in the formation of calcium phosphate, which exhibits osteoconductive properties. Calcium phosphate also reduces the pH locally, causing bone demineralization. This process exposes growth factors such as Bone morphogenic protein (BMP) transforming growth factor-β (TGF-β) and others stored within the bone matrix, thereby promoting bone growth.[3] When CS was used to fill large bony defects, it was found that the material resorbed completely from the grafted site without leaving any trace elements. The resorption rate of calcium sulfate was comparable to the rate at which new bone formed and facilitated the migration of osteoprogenitor cells into the area.[4] The formation of new blood vessels plays a critical role in all regenerative processes, including bone regeneration. It is triggered by high metabolic activity and reduced oxygen levels at the injury site. The occurrence of angiogenesis can be confirmed by assessing microvascular density at the regenerative site.[5,6] Ruhaimi et al. examined the osteogenic potential after combining CS with various other graft materials. They concluded that CS can cause angiogenesis, which was confirmed by the presence of multiple microvessels without any signs of inflammation. They inferred that angiogenesis can be considered as an added property of CS

*This article was accepted: 07 August 2024*
*Corresponding Author: Pradeep C Dathan*
*Email: pdathan70@gmail.com*

that aids in osteogenesis.[7] Investigations also reported that CS acts as a direct source of calcium, and resorption leaves the calcium phosphate lattice, which promotes osteogenic activity.[8,9]

Extracts of pomegranate peel are reported to have an abundance of phytochemicals and vitamins that are responsible for anti-inflammatory and antioxidant properties, punicalagin A & B, ellagic acid, and gallic acid present in the pomegranate have anti-inflammatory effects by inhibiting lipopolysaccharides -stimulated macrophages that down-regulate COX-2 protein release. As a result, it decreases the levels of pro-inflammatory mediators, such as inducible nitrous oxide (iNO), PGE-2, interleukins, and Reactive oxygen species (ROS).[10] Inflammation can cause bone destruction by pannus formation. Ellagic acid present in pomegranate inhibits inflammation by decreasing pro-inflammatory cytokines IL - 1β, Tumor Necrosis Factor (TNF-α,) and IL17 and increasing serum levels of anti-inflammatory cytokines IL-10 and interferon γ (IFN-γ).[11,12] The anti-inflammatory properties of a specific type of PPE were evaluated and a significant anti-inflammatory effect of PPE on the expression of cyclooxygenase-2 was confirmed.13 In obese patients, extracts derived from pomegranate peels showed anti-inflammatory effects by significantly reducing inflammatory markers [malondialdehyde (MDA), IL-6, and hypersensitive-C reactive protein (hs-CRP)].[14] A randomized controlled trial conducted in patients with rheumatoid arthritis found that there was a significant decrease in disease activity following 8 weeks of supplementation with PPE.[15]

Research has shown that extracts derived from pomegranate fruit can protect against osteoarthritis. This protection is achieved through mechanisms such as increased cartilage stiffness, physical fitness, decreased levels of enzymes that break down cartilage, and enhancing the body's antioxidant defense system.[16] According to Spilmont, a diet supplemented with pomegranate peel extract enhanced bone mineralization in osteoporotic rat models by upregulating osteogenic transcription factors and stimulating alkaline phosphatase activity (ALP).[17] Additionally, he also revealed that the punicic acid (conjugated linolenic acid) rich pomegranate seed oil causes osteoblastic stimulation and inhibits osteoclastic suppression and thus prevents bone loss in an osteoporotic mice model.[18] The antioxidant potential of aqueous extracts derived from by-products of pomegranate and grapes was evaluated. The total phenolic content of the pomegranate by-product was five times higher than that of red grapes.[19]

Owing to its anti-inflammatory and antioxidant properties, pomegranate fruit and its biomolecules can be recommended as a functional food option to mitigate bone loss and related disorders. This suggests that incorporating pomegranate into the diet may help prevent bone-related issues. Since CS is an osteoconductive material widely used in bone augmentation and pomegranate extracts promote osteogenesis due to the presence of biologically active compounds and its anti-inflammatory and antioxidative properties, this study aimed to evaluate the anti-inflammatory and antioxidant properties of pomegranate peel extract mediated calcium sulfate nanoparticles.

The objectives were to green – synthesize PPE CaSo4 NPs, to analyze their optical characteristics of pomegranate peel-mediated calcium sulfate nano particles using UV-visible spectra analysis, and subsequently evaluate its antioxidant and anti-inflammatory activities.

## MATERIALS AND METHODS

*Preparation of Pomegranate peel extract*

The pericarp of fresh Ganesh variety pomegranate fruits was separated and immersed in diluted Koparo Clean vegetable and fruit wash for 15 min and then air-dried. The dried peel was ground into a coarse powder using a multi-milli-machine made of SS 304.

Next, 2 g of peel powder was mixed with 100 mL of distilled water using a magnetic stirrer (Remi 5MLH). The mixture was heated in a heating mantle set at 60 to 80ºC for 15 - 20 min. After heating, the mixture was filtered through Whatman No. 1 filter paper. After filtration, the extract was further condensed to a volume of 5mL

*Green synthesis Pomegranate peel extract mediated calcium sulphate nano particles (PPE CaSo4 NPs)*

Green synthesis of PPE- mediated Caso4 was performed by dissolving 0.5gm of Caso4 (99% pure calcium sulfate (VITSZEE ®) in 25 ml of distilled water, 25 ml of filtered PPE was added, and the mixture was stirred magnetically at 600 RPM for 24h. After 24h, the green synthesized PPE-mediated CaSo4 nano particles were collected and the supernatant was discarded.

*Characterization*

The green-synthesized calcium sulfate nano particles were characterized using a UV-visible spectrophotometer to study the optical characteristics, while the surface morphology, such as size and shape, was characterized using a Scanning Electron Microscope.

*Anti-inflammatory activity*

*Egg Albumin Denaturation Assay (EA)*

A 5 ml solution was prepared by mixing 2.8 ml of freshly made pH-6.3 phosphate-buffered saline with 0.2 ml of Hen's egg albumin extraction. PPE CaSo4 NPs were synthesized at various concentrations ranging from 10µL to 50µL. Diclofenac sodium was used as the positive control. Subsequently, the mixtures was heated in a water bath at 37°C for 15 min. After cooling the samples to room temperature, absorbance was measured at 660 nm.

*Bovine Serum Albumin Denaturation Assay (BSA)*

In this study, the anti-inflammatory effects of pomegranate peel extract-mediated calcium sulfate Nano particles were evaluated following a modified protocol based on Muzushima and Kabayashi's method. To initiate the assay, 0.45 mL of 1% aqueous bovine serum albumin was mixed with 0.05 mL of PPE CaSo4 NPs of varied fixation (10µL, 20µL, 30µL, 40µL, and 50µL). The pH of the mixture was adjusted to 6.3 using a small amount of 1N hydrochloric acid. Subsequently, the samples were incubated at room temperature for 20 min, followed by heating at 55°C in a

water bath for an additional 30 min. After cooling the samples, the absorbance was measured at 660 nm using a spectrophotometer. Diclofenac sodium was used as the benchmark and dimethyl sulfoxide (DMSO) served as the control.

The percentage of protein denaturation was determined utilizing the following equation,

$$\% \text{ inhibition} = \frac{\text{Absorbance of control- Absorbance of sample}\times}{\text{Absorbance of control}}$$

*Antioxidant activity*

Three techniques were used to evaluate the antioxidant activity of PPE CaSo4 NPs, two of which, DPPH and $H_2O_2$, were dependent on PPE CaSo4 NPs's ability to scavenge free radicals. The iron-reducing capacity provided the basis for the third method, called FRAP.

The assay used a commercially available free radical 2,2 diphenyl- 1-picryl hydrazyl hydrate (DPPH) which is soluble in methanol, and the antioxidant activity was measured by the decrease in absorbance at 515 nm. Different concentrations of PPE CaSo4 NPs (10µL, 20µL, 30µL, 40µL, 50µL) were mixed with 450µl of 50 mM Tris-HCl buffer (pH 7.4) and 1 ml of 0.1 mM DPPH in methanol. The mixture was then incubated for 30 min. afterwards, the reduction in DPPH free radical levels was determined by measuring the absorbance at 517 nm. Butylated hydroxytoluene (BHT) was used as control. Percentage inhibition was calculated using the following equation:

$$\% \text{ inhibition} = \frac{\text{Absorbance of control- Absorbance of test sample} \times 100}{\text{Absorbance of control}}$$

*$H_2O_2$ assay*

The $H_2O_2$ scavenging power of green-synthesized PPE CaSo4 NPs was assessed. 40 mM $H_2O_2$ solution was prepared in phosphate buffer (pH 7.4). Solution of the test sample PPE CaSo4 NPs and a standard sample of ascorbic acid at varying concentrations (10, 20, 30, 40, and 50µg/mL) were individually added to 0.6 mL of $H_2O_2$ solution. After 10 min of incubation in the dark place, the absorbance of the reaction solution was spectrophotometrically measured at 230 nm. Vitamin C was used as the standard. The percentage of $H_2O_2$ scavenging activity was calculated using the following formula:

$$\% \text{ inhibition} = \frac{\text{Absorbance of control- Absorbance of sample} \times 100}{\text{Absorbance of control}}$$

*FRAP ASSAY*

*Reagents for FRAP assay:*

a)Acetate buffer 300 mM pH 3.6: Weigh 3.1 g sodium acetate trihydrate add 16 ml of glacial acetic acid and make the volume to 1 L with distilled water. b) TPTZ (2, 4, 6- tripyridyl-s- triazine): (M.W. 312.34), 10 mM in 40 mM HCl (M.W. 36.46). c) FeCl3. 6 H2O: (M.W. 270.30), 20 mM. The working FRAP reagent was prepared by mixing a, b, and c in a ratio of 10:1:1 just before testing. The standard was FeSO4. Seven H2O: 0.1 - 1.5 mM in methanol. All the reagents were purchased from Merck (Germany) company.

*Procedure*

To perform the FRAP (Ferric Reducing Antioxidant Power) assay, an FRAP solution (3.6 mL) was combined with 0.4 mL of distilled water and incubated at 37°C for 5 min. Subsequently, the solution was mixed with various concentrations of PPE$CaSo_4$NPs (10µL, 20µL, 30µL, 40µL, 50µL) and incubated at 37°C for 10 min. The absorbance of the reaction mixture was measured at 593 nm. To construct the calibration curve, five concentrations of FeSO4 7 H2O (0.1, 0.4, 0.8, 1, 1.12, and 1.5 mM) were used, and their corresponding absorbance values were measured, mirroring the procedure for the sample solutions.

## RESULTS

*Optical characteristics*

UV-visible spectral analysis was employed to investigate the optical characteristics of pomegranate peel mediated calcium sulfate nanoparticles synthesized at various time intervals. Notably, absorption peaks were discerned at 350 nm after 48h of synthesis and at 340 nm for both 1 h and 24hs of synthesis. The 350 nm peak strongly indicates the presence of calcium sulfate nanoparticles, with UV absorption commonly linked to electronic transitions within the nanoparticles. This specific peak signifies nanoparticles of distinct sizes and shapes, corresponding to a unique bandgap energy (Fig 1).

*SEM*

The SEM image of the calcium sulfate nanoparticles synthesized using pomegranate peel extract revealed crucial insights into their morphology and size distribution. The nanoparticles exhibited a predominantly spherical morphology with well-dispersed particles uniformly distributed across the field of view, indicating effective stabilization by the pomegranate peel extract. The sizes of the nano particles ranged from approximately 50 to 150 nm, demonstrating a relatively narrow size distribution. This consistency suggests the effectiveness in controlling the nucleation and growth of the nanoparticles during synthesis. The clean, well-defined surfaces of the nanoparticles indicate the purity and high quality of the synthesis process with no visible impurities or irregularities. The pomegranate peel extract functioned effectively as both a reducing and capping agent, resulting in stable and uniform nanoparticles. The uniform size distribution and spherical morphology of these calcium sulfate nanoparticles suggests their potential applicability in biomedical applications, drug delivery systems, and as fillers in composite materials. The eco-friendly synthesis method using pomegranate peel extract not only effectively produces these nanoparticles, but also aligns with sustainable and green chemistry principles (Fig 2).

*Anti-inflammatory activity*

In EA, the inhibition caused by PPE CaSo4 NPs at 10µL concentration was (52.00% ±1.05), and 55% ± 1.56% for the standard. For the 50 µl concentration, it was 77.00% ±1.15 and 81% ±1.69%, respectively. For BSA, the percentage of inhibition with10µl concentration was (41.40% ±11.08), and

**Table I: Comparison between Anti-inflammatory activity obtained in different concentrations of PPE CaSo4 NPs using EA & BSA assay**

| Concentration | % of inhibition | N | Mean | Std. Deviation | Std. Error Mean | p-value |
|---|---|---|---|---|---|---|
| 10 µL | PPECaSo4NPs | 10 | 52.0000 | 1.05409 | 0.33333 | 0.388 |
| EA | Standard | 10 | 55.0000 | 1.56347 | 0.49441 | |
| 20 µLl | PPE CaSo4 NPs | 10 | 61.0000 | 1.05409 | 0.33333 | 1.000 |
| EA | Standard | 10 | 64.0000 | 1.05409 | 0.33333 | |
| 30 µL | PPE CaSo4 NPs | 10 | 65.0000 | 1.05409 | 0.33333 | 0.591 |
| EA | Standard | 10 | 69.0000 | 1.15470 | 0.36515 | |
| 40 µL | PPE CaSo4 NPs | 10 | 69.0000 | 2.10819 | 0.66667 | 0.160 |
| EA | Standard | 10 | 72.0000 | 1.05409 | 0.33333 | |
| 50 µL | PPE CaSo4 NPs | 10 | 77.0000 | 1.15470 | 0.36515 | 0.118 |
| EA | Standard | 10 | 81.0000 | 1.69967 | 0.53748 | |
| 10 µL | PPE CaSo4 NPs | 10 | 41.4000 | 11.08753 | 3.50619 | 0.087 |
| BSA | Standard | 10 | 46.7000 | 1.56702 | 0.49554 | |
| 20 µL | PPE CaSo4 NPs | 10 | 52.4000 | 11.52003 | 3.64295 | 0.185 |
| BSA | Standard | 10 | 59.6000 | 2.79682 | 0.88443 | |
| 30 µL | PPE CaSo4 NPs | 10 | 63.4000 | 11.76813 | 3.72141 | 0.139 |
| BSA | Standard | 10 | 71.4000 | 2.59058 | 0.81921 | |
| 40 µL | PPE CaSo4 NPs | 10 | 68.9000 | 10.19204 | 3.22301 | 0.124 |
| BSA | Standard | 10 | 75.7000 | 2.11082 | 0.66750 | |
| 50 µL | PPE CaSo4 NPs | 10 | 76.3000 | 9.34582 | 2.95541 | 0.354 |
| BSA | Standard | 10 | 83.3000 | 3.77271 | 1.19304 | |
| | '*' p-value <0.05 shows statistical significance | | | | | |

**Table II: Comparison between Antioxidant activity of PPE CaSo4 NPs obtained in DPPH, H2O2 and FRAP**

| Concentration | % of inhibition | N | Mean | Std. Deviation | Std. Error Mean | p-value |
|---|---|---|---|---|---|---|
| 10 µL | PPE CaSo4 NPs | 10 | 64.3040 | 0.01174 | 0.00371 | 0.019 |
| DPPH | Standard | 10 | 66.2500 | 0.00471 | 0.00149 | |
| 20 µL | PPE CaSo4 NPs | 10 | 73.6410 | 0.00876 | 0.00277 | 0.549 |
| DPPH | Standard | 10 | 78.5200 | 0.00667 | 0.00211 | |
| 30 µL | PPE CaSo4 NPs | 10 | 83.7820 | 0.00919 | 0.00291 | 0.651 |
| DPPH | Standard | 10 | 85.6330 | 0.01160 | 0.00367 | |
| 40 µL | PPE CaSo4 NPs | 10 | 86.1210 | 0.00738 | 0.00233 | 0.558 |
| DPPH | Standard | 10 | 88.6820 | 0.00919 | 0.00291 | |
| 50 µL | PPE CaSo4 NPs | 10 | 91.1220 | 0.00919 | 0.00291 | 0.558 |
| DPPH | Standard | 10 | 93.1510 | 0.00738 | 0.00233 | |
| 10 µL | PPE CaSo4 NPs | 10 | 49.4500 | 0.00667 | 0.00211 | 0.007* |
| H2O2 | Standard | 10 | 51.1000 | 0.11547 | 0.03651 | |
| 20 µL | PPE CaSo4 NPs | 10 | 53.9800 | 0.00667 | 0.00211 | 0.036* |
| H2O2 | Standard | 10 | 56.9000 | 0.20548 | 0.06498 | |
| 30 µL | PPE CaSo4 NPs | 10 | 64.7600 | 0.00667 | 0.00211 | 1.000 |
| H2O2 | Standard | 10 | 64.5600 | 0.00667 | 0.00211 | |
| 40 µL | PPE CaSo4 NPs | 10 | 75.7100 | 0.00667 | 0.00211 | 0.064 |
| H2O2 | Standard | 10 | 75.5300 | 0.06360 | 0.02011 | |
| 50 µL | PPE CaSo4 NPs | 10 | 87.4200 | 0.00667 | 0.00211 | 1.000 |
| H2O2 | Standard | 10 | 87.2200 | 0.00667 | 0.00211 | |
| 10 µL | PPE CaSo4 NPs | 10 | 67.3200 | 0.01054 | 0.00333 | 0.591 |
| FRAP | Standard | 10 | 72.9800 | 0.01155 | 0.00365 | |
| 20 µL | PPE CaSo4 NPs | 10 | 74.1800 | 0.01491 | 0.00471 | 0.361 |
| FRAP | Standard | 10 | 76.8400 | 0.01054 | 0.00333 | |
| 30 µL | PPE CaSo4 NPs | 10 | 77.9000 | 0.17638 | 0.05578 | 0.050 |
| FRAP | Standard | 10 | 81.3100 | 0.01054 | 0.00333 | |
| 40 µL | PPE CaSo4 NPs | 10 | 81.0900 | 0.02108 | 0.00667 | 1.000 |
| FRAP | Standard | 10 | 85.8400 | 0.02108 | 0.00667 | |
| 50 µL | PPE CaSo4 NPs | 10 | 86.3800 | 0.01054 | 0.00333 | 0.391 |
| FRAP | Standard | 10 | 90.8900 | 0.02357 | 0.00745 | |
| | '*' p-value <0.05 shows statistical significance | | | | | |

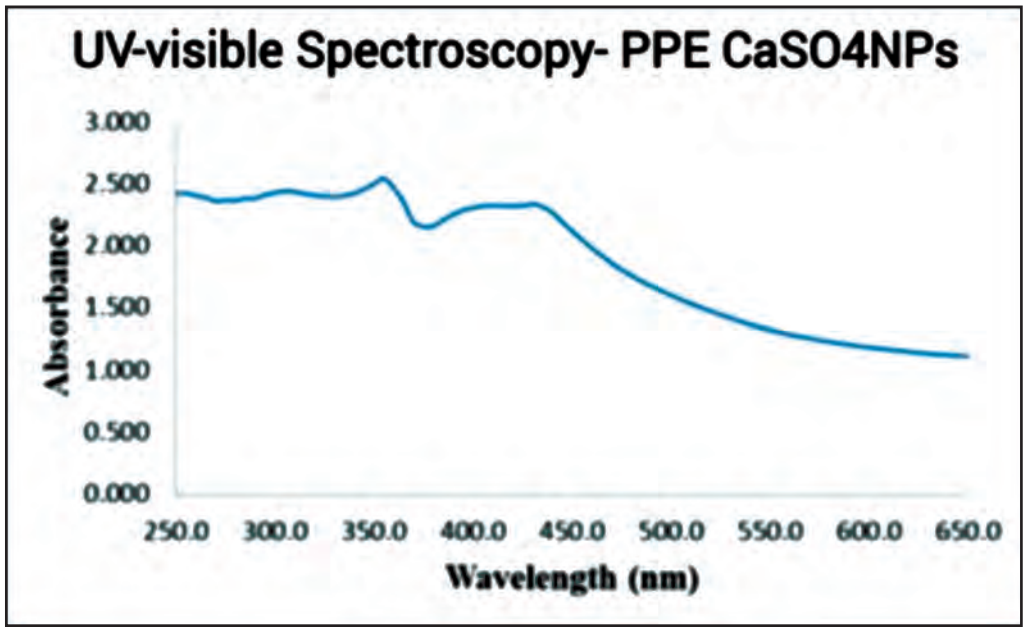


**Fig. 1:** UV-visible spectroscopy –PPE CaSo4NPs

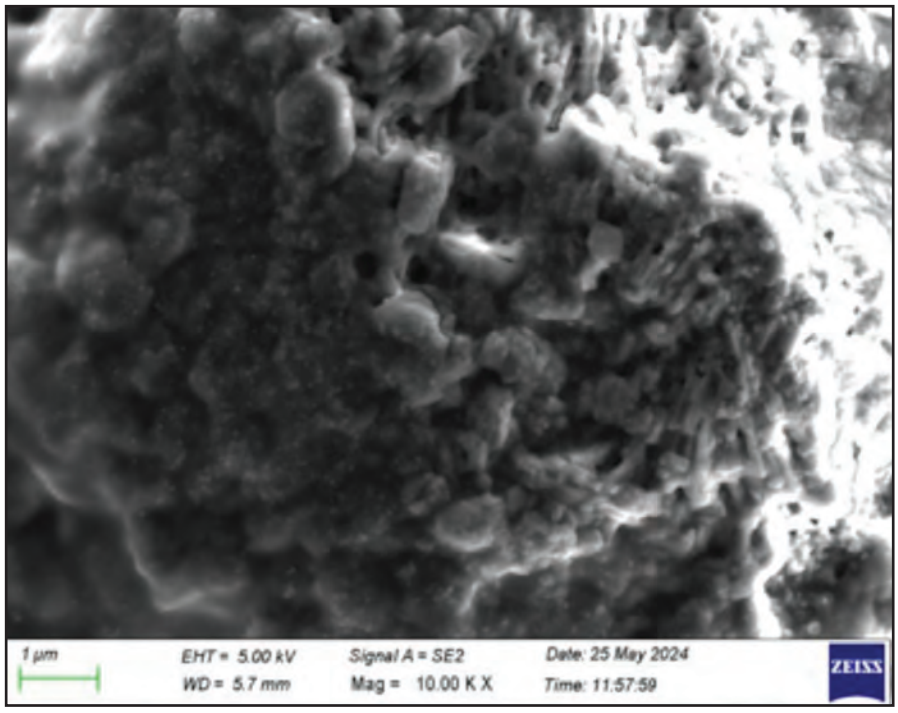


**Fig. 2:** SEM PPE CaSo4 NPs

for the standard it was 46.70% ± 1.56. For the 50 µl concentration, it was 76.30% ± 9.34 and 83.30% ±3.72%, respectively. It was observed that in tests of EA and BSA all concentrations, there was no significant difference between the test material and the standard ($p>0.05$). Comparisons between the mean values of different concentrations observed in EA and BSA were performed using ANOVA. Each test (EA, BSA) showed characteristic independence, and it can be inferred that in all the tests, if the same pattern is observed, it can be considered reliable ($p< 0.05$). Multiple comparisons were made using Tukey's HSD on values obtained in EA and BSA. Different concentrations were mutually compared and found that on comparing, all concentrations showed significant differences $p<0.05$. (Table I)

*Antioxidant activity*

The antioxidant activity of PPE CaSo4 NPs observed in DPPH ranged from 64.30% ±.011 to 91.12% ±.009 in the

experimental group and 66.25% ±.004 to 93.15% ±.007 with the standard. For $H_2O_2$, the values were 49.45% ±.006 to 87.42% ±.006 for the experimental group and 56.90% ±.20 to 87.22% ±.006 for the standard group. For FRAP the values were 67.32% ±.01 to 86.38% ±01 and 72.98% ±.01 to 90.89% ±.02 respectively. A significant difference was found between PPE CaSo4 NPs and the standard in concentrations of 10 µl, for DPPH, 10 µl and 20 µl for $H_2O_2$ ($p<0.05$) between the concentrations of 30, 40, and 50, and there was no significant difference between the test material and the standard in all three tests conducted. In other words, at these concentrations, in all three tests, there was equivalence between the standard and test groups ($p>0.05$).

Comparisons between different concentrations of PPE CaSo4 NPs in DPPH, $H_2O_2$, and FRAP were performed using ANOVA. A significant difference was observed at all concentrations in all three tests ($p<0.05$). Multiple comparisons were made using Tukey's HSD for values obtained for DPPH, $H_2O_2$, and FRAP. Different concentrations were mutually compared, and all concentrations were found to significantly different ($p<0.05$). (Table II)

## DISCUSSION

Calcium sulfate has been used as an effective bone augmentation material for the past 100 years. It is considered an ideal material for bone regeneration as it provides calcium ions to the augmented site, acts as a resorbable scaffold for bone growth, stimulates osteoblastic activity, acts as a vehicle for growth factors and drugs, and is biocompatible. Researchers found that compared to other implanted regenerative materials, CS has rapid and complete resorption, and the rate of resorption is almost equivalent to the rate at which new bone is created.[20,21] The particle size of materials can influence bone healing, and nano-sized calcium sulfate dihydrate is reported to have good tissue compatibility, increased biodegradable properties, increased angiogenesis, and increased bone induction. Therefore, calcium sulfate nano particles were used.[22]

Biologically active compounds that contribute to the anti-inflammatory and antioxidant properties are concentrated in the peel of pomegranate, making it a significant reservoir.[23] In the present study, pomegranate peel of the Ganesh variety was used to prepare the aqueous extract, and PPE-mediated calcium sulfate nano particles were green synthesized. The anti-inflammatory and antioxidant properties of green-synthesized pomegranate peel extract-mediated calcium sulfate nanoparticles (PPE CaSo4 NPs) were evaluated.

In this study, egg albumin denaturation assay and bovine serum albumin denaturation assay were used to measure the anti-inflammatory properties of PPE CaSo4 NPs. Protein denaturation causes inflammation. Evaluation of PPECaSo4 on the anti-inflammatory activity showed that the extract inhibited protein denaturation. In both assays of EA and BSA at all concentrations, there was no significant difference between the test material and the standard, that is, diclofenac sodium $p>0.05$. Thus, the anti-inflammatory activity of the test material was the same as that of the control. Different concentrations were mutually compared and found that on comparing, all concentrations showed significant differences $p<0.05$. Anti-inflammatory activity increased as the concentration increased. Therefore, it can be concluded that the anti-inflammatory activity was concentration-dependent. The results obtained for PPE CaSo4 NPs were comparable to those of commercial drugs used, indicating that PPE CaSo4 NPs possesses anti-inflammatory properties similar to those of the control, that is diclofenac sodium.

The extracts of pomegranate peel, juice, flowers, and seeds were found to have high polyphenol concentrations. The gut bacteria convert these polyphenols into urolithins, which have anti-inflammatory properties.[24] Pohl et al reported that Pomegranate's biologically active components, which are present in the fruit's peel, juice, and extracts, affect the expression of a protein that signals inflammation in cancer cells.[25] Tannin, and punicalagin present in the pomegranate extracts decreased the expression of cyclooxygenase–2 (COX-2) responsible for the production of prostanoids that induce inflammation.[26] The action of ellagic acid found in pomegranate peel extract was reported by Marín, Ellagic acid inhibited the inflammation by decreasing the inflammation mediating compounds COX-2 and iNOS and blocking the cell signalling pathway in the intestine.[27] The use of polyphenol-rich pomegranate fruit extract or compounds derived from it for the treatment of inflammatory diseases by suppressing basophils and mast cell activation was reported by Rasheed Z et al.[28] Free radicals that generate oxidative stress are what causes inflammation, and the antioxidant properties of pomegranates can get rid of the free radicals and lessen the inflammation. Pomegranate also has antibacterial Properties, and its phytochemicals can reduce inflammation caused by microorganisms. As a result, it is useful for the treatment inflammations caused by microbes. Pomegranate phytochemicals have multiple bioactivities; they can influence a variety of inflammatory variables and promote healing.[29,30] The observations of the above-mentioned studies substantiate the results obtained in this study.

The antioxidant activity was measured using DPPH, $H_2O_2$, and FRAP assays ,and ascorbic acid was used as the staanderd. At concentrations of 10 µl for DPPH, 10 µl and 20 µl for $H_2O_2$ significant difference was found between PPE CaSo4 NPs and the standard ($p<0.05$) at higher concentrations of 30, 40, and 50 µl; there was no significant difference between the test material and the standard in all the three tests conducted, that is DPPH, $H_2O_2$ and FRAP. This indicated equivalence between the standard and test groups at these concentrations ($p>0.05$).

It was also found that antioxidant activity increased as the concentrations increased from 10µL to 50 µL. A significant difference was found in all concentrations in all three tests ($p<0.05$) Indicating that the antioxidant properties increased with an increase in concentration, that is the antioxidant activity was dose-dependent and the PPE CaSo4 NPs can provide the same antioxidant as the standard. This finding is similar to the findings of previous studies that concluded that pomegranate peel extracts have high concentrations of biologically active compounds responsible for the antioxidant activity, and the concentration of the

compounds depends on the method of extraction and the cultivar, and the antioxidant activity increases as the concentration of the peel extract increased.[31-35] It can also be stated that the addition of calcium sulfate did not decrease the antioxidative properties as the values obtained were comparable with the standard used.

## CONCLUSION

The distinctive biochemical profile of pomegranate and the presence of more than 124 bioactive components confirm its anti-inflammatory and antioxidant properties. The antioxidant activity of pomegranate peel extract-based calcium sulfate was comparable to that of the control, and was directly related to the concentration. The capacity of pomegranate peel extract-based calcium sulfate to suppress protein denaturation proved its concentration- dependent anti-inflammatory potential. According to this study, pomegranate peel extract-mediated calcium sulfate Nano particles possess anti-inflammatory and antioxidant characteristics that vary in concentration. The findings of this investigation will advance our knowledge of these features. Hence, thorough testing is required before pomegranate and its bioactive chemicals can be employed as therapeutic agents, either alone or in combination, to treat a variety of degenerative disorders such as osteoporosis, rheumatoid arthritis, and bone regeneration.

## REFERENCES


1. Thomas MV, Puleo DA. Calcium sulfate: Properties and clinical applications. J Biomed Mater Res B Appl Biomater 2009; 88(2): 597-610.
2. Kelly CM, Wilkins RM, Gitelis S, Hartjen C, Watson JT, Kim PT. The use of a surgical grade calcium sulfate as a bone graft substitute: results of a multicenter trial. Clin Orthop Relat Res 2001; (382): 42-50.
3. Paolantonio M, Perinetti G, Dolci M, Perfetti G, Tetè S, Sammartino G, Femminella B, Graziani F. Surgical treatment of periodontal intrabony defects with calcium sulfate implant and barrier versus collagen barrier or open flap debridement alone: a 12-month randomized controlled clinical trial. J Periodontol 2008; 79(10): 1886-93
4. Kim JH, Oh JH, Han I, Kim HS, Chung SW. Grafting using injectable calcium sulfate in bone tumor surgery: comparison with demineralized bone matrix-based grafting. Clin Orthop Surg 2011; 3(3): 191-201.
5. Finkemeier CG. Bone-grafting and bone-graft substitutes. J Bone Joint Surg Am. 2002; 84(3): 454-64.
6. Artese L, Rubini C, Ferrero G,Fioroni M, Santinelli A, Piattelli A. Microvessel density (MVD) and vascular endothelial growth factor expression (VEGF) in human oral squamous cell carcinoma. Anticancer Res 2001; 21: 689-96.
7. Al Ruhaimi KA. Effects of adding calcium sulphate to grafting materials in early bone regeneration in osseous defects in rabbits. Int J Oral Maxillofac Implants 2000; 15: 859-64.
8. Orsini G, Ricci J, Scarano A, Pecora G, Petrone G, Iezzi G, Piattelli A. Bone-defect healing with calcium-sulfate particles and cement: an experimental study in rabbit. J Biomed Mater Res B Appl Biomater 2004; 15; 68(2): 199-208.
9. G Fernandes, V Abhyankar, Josanne M O'Dell. Calcium Sulfate as a Scaffold for Bone Tissue Engineering: A Descriptive Review. J Dent Oral Disord Ther. 2021 9(1): 1-22.
10. BenSaad LA, Kim KH, Quah CC, Kim WR, Shahimi M. Anti-inflammatory potential of ellagic acid, gallic acid and punicalagin A&B isolated from Punica granatum. BMC Complement Altern Med 2017; 14: 17(1): 47.
11. Allam G, Mahdi EA, Alzahrani AM, Abuelsaad AS. Ellagic acid alleviates adjuvant induced arthritis by modulation of pro- and anti-inflammatory cytokines. Cent Eur J Immunol 2016; 41(4): 339-349.
12. Valentina Stefanou, Spyros Papatheodorou, Aliki Tsakni, Vladimiros Lougovois, Aikaterini Talelli, Giannis Panourgias, Alexandros Dariatos, Ioannis TsaknisInt. Anti- Inflammatory Properties of Pomegranate. J. Adv. Res. MicroBiol. Immunol, 2020; 2: 1&2: 1-13.
13. Houston DM, Bugert J, Denyer SP, Heard CM. Anti-inflammatory activity of Punica granatum L. (Pomegranate) rind extracts applied topically to ex vivo skin. Eur J Pharm Biopharm 2017; 112: 30-7.
14. Hosseini B, Saedisomeolia A, Wood LG, Yaseri M, Tavasoli S. Effects of pomegranate extract supplementation on inflammation in overweight and obese individuals: a randomized controlled clinical trial. Complement Ther Clin Pract 2016, 22: 44–50.
15. Ghavipour M, Sotoudeh G, Tavakoli E, Mowla K, Hasanzadeh J, Mazloom Z. Pomegranate extract alleviates disease activity and some blood biomarkers of inflammation and oxidative stress in rheumatoid arthritis patients. Eur J Clin Nutr 2017; 71: 92-6.
16. Ghoochani N, Karandish M, Mowla K, Haghighizadeh MH, Jalali MT The effect of pomegranate juice on clinical signs, matrix metalloproteinases and antioxidant status in patients with knee osteoarthritis. J Sci Food Agric 2016; 96: 4377-81.
17. Spilmont M, Léotoing L, Davicco MJ, Lebecque P, Miot-Noirault E, Pilet P et al Pomegranate peel extract prevents bone loss in a preclinical model of osteoporosis and stimulates osteoblastic differentiation in vitro.,Nutrients, 2015; 7: 9265-84.
18. Spilmont M, Léotoing L, Davicco MJ, Lebecque P, Mercier S, Miot-Noirault E, Pilet P, Rios L, Wittrant Y, Coxam V, Pomegranate seed oil prevents bone loss in a mice model of osteoporosis, through osteoblastic stimulation, osteoclastic inhibition and decreased inflammatory status. J Nutr Biochem 2013; 24: 1840-8.
19. Andrés AI, Petrón MJ, Adámez JD, López M, Timón ML. Food by-products as potential antioxidant and antimicrobial additives in chill stored raw lamb patties. Meat Sci 2017; 129: 62-70.
20. Jepegnanam TS, von Schroeder HP. Rapid resorption of calcium sulfate and hardware failure following corrective radius osteotomy: 2 case reports. J Hand Surg Am 2012; 37(3): 477-80.
21. Chunli Zhang, Zhonghai Li, Qihong Li, Liwei Han, Jialiang Zhu, Yulong Bai, Cheng Ge, Yantao Zhao, Hongbin Zhong, Properties and Osteogenicity of Two Calcium Sulfate Materials with Micro or Nano Morphology, J. Nanosci. Nanotechnol 2016; 16: 2277-82.
22. Marı´a I. Gil, Francisco A. Toma´s-Barbera´n, Betty Hess-Pierce, Deirdre M. Holcroft,and Adel A. Kader :Antioxidant Activity of Pomegranate Juice and Its Relationship with Phenolic Composition and Processing J. Agric. Food Chem 2000; 48: 4581-9.
23. Elisa C Enrico S, Mario D; A review on the anti-inflammatory activity of pomegranate in the gastrointestinal tract: Evid Based Complement Alternat Med 2013; 2013: 247145.
24. Pohl C, Hombach A, Kruis W, Chronic inflammatory bowel disease and cancer. Hepatogastroenterology, 2000;47(31):57-70.
25. Adams LS, Seeram NP, Aggarwal BB, Takada Y, Sand D, Heber D (2006) Pomegranate juice, total pomegranate ellagitannins, and punicalagin suppress inflammatory cell signaling in colon cancer cells. J Agric Food Chem 2006; 54: 980-5.
26. Marín M, Giner RM, Ríos JL, Recio MC, Intestinal anti-inflammatory activity of ellagic acid in the acute and chronic dextrane sulphate sodium models of mice colitis. J Ethnopharmacol 2013; 150: 925-34.
27. Rasheed Z, Akhtar N, Anbazhagan AN, Ramamurthy S, Shukla M, Haqqi TM. Polyphenol-rich pomegranate fruit extract (POMx) suppresses PMACI-induced expression of pro-inflammatory cytokines by inhibiting the activation of MAP Kinases and NF-kappaB in human KU812 cells. J Inflamm (Lond). 2009; 8; 6:1.
28. Reddy M, Gupta S, Jacob M, Khan S, Ferreira, D. Antioxidant, antimalarial and antimicrobial activities of tannin-rich fractions, ellagitannins and phenolic acids from Punica granatum L. Planta Medica, 2007; 73: 461-7.

29. Balwinder Singh, Jatinder Pal Singh, Amritpal Kaur, Narpinder Singh. Antimicrobial potential of pomegranate peel: a review. Int. J. Food Sci 2019; 54, 4: 959-65.
30. Khan Shadab, Patel Anjum, Bhise K. S: Antioxidant activity of pomegranate peel powder: JDDT 2017; 7(2): 81-4.
31. Hamidreza A, Mohsen B, Helmut W, Benno FZ; Phenolic Compounds and Antioxidant Activity of Juices from Ten Iranian Pomegranate Cultivars Depend on Extraction: Hindawi Publishing Corporation , JChem. 2015, Article ID 907101: 1-7 .
32. Lamiae Benchagra, Hicham Berrougui, Mohamed Obaidul Islam, Mhamed Ramchoun, Samira Boulbaroud, Abdelouahed Hajjaji, Tamas Fulop, Gianna Ferretti and Abdelouahed Khalil,Antioxidant Effect of Moroccan Pomegranate (Punica granatum L. Sefri Variety) Extracts Rich in Punicalagin against the Oxidative Stress Process :Foods 2021; 10: 2219.
33. Shalini M, Arvind, Alok J, Navam H; Antioxidant and antibacterial potential of pomegranate peel extracts , J Food Sci Technol, 2014; 51, 12: 4132-7.
34. Singh RP, Chidambara Murthy KN, Jayaprakasha GK, Studies on the Antioxidant Activity of Pomegranate (Punicagranatum) Peel and Seed Extracts Using in Vitro Models. J. Agric. Food Chem 2002; 50(1): 81-6.
35. Chidambara Murthy KN, Jayaprakasha GK, Singh RP. (2002). Studies on Antioxidant Activity of Pomegranate (Punica granatum) Peel Extract Using in Vivo Models.J. Agric. Food Chem 2002; 14; 50(17): 4791-5.

ORIGINAL ARTICLE

# An *in vitro* evaluation of anti-oxidant properties of novel nano-composite material containing titanium oxide, zinc oxide and green tea extract

**Suja Joseph[1], Deepak Nallaswamy[2], S Rajeshkumar[3], Pradeep Dathan[4], Nazia Rasheed[5], Tharani Munusamy[6], Jose Jacob[7], Leon Jose[8]**

[1]MDS, PhD Research Scholar, Department of Prosthodontics Saveetha Dental College and Hospitals, SIMATS, Chennai, India,[2]MDS, PhD, Director, Department of Prosthodontics, Saveetha Dental College and Hospitals, SIMATS, Chennai, India. [3]MSc, PhD, Professor and Chief Scientist, Nanomedicine Lab, Department of Pharmacology, Saveetha Dental College and Hospitals, SIMATS, Saveetha University, Chennai, India, [4]MDS, PhD Research Scholar, Department of Prosthodontics, Saveetha Dental College and Hospitals, SIMATS, Chennai, India, [5]MDS, PhD Research Scholar, Department of Prosthodontics, Saveetha Dental College and Hospitals, SIMATS, Chennai, India, [6]Msc PhD, Department of Pharmacology, Saveetha Dental College and Hospitals, SIMATS, Chennai, India, [7]MDS, Professor, Department of Conservative Dentistry, Pushpagiri College of Dental Science, Thiruvalla, India, [8]Former MTec student, Department of Mechanical engineering, IIT Madras

## ABSTRACT

**Introduction: Green tea is a medicinal beverage extracted from the plant Camellia sinensis. Antioxidants that exist naturally can be extracted as pure compounds from their parent materials for nutraceutical and medicinal applications.**

**The present study aims to assess the antioxidant activity of Zinc oxide-titanium dioxide nano-composites (ZnO-TiO2 NCs) containing green tea extract.**

**Materials and Methods: The antioxidant activity was tested by Hydrogen Peroxide [H2O2] assay, Fluorescence recovery after photo-bleaching [FRAP] assay and 2, 2-diphenyl-1-picrylhydrazyl[DPPH] assay. All tests have shown very good results for the ZnO-TiO2 NCs.**

**Results: In this study, we present a straightforward, eco-friendly alternative for producing non-toxic zinc oxide and titanium oxide nano-composite material. This study could make a valuable contribution and create new opportunities in the market such as biological and pharmaceutical applications.**

**Conclusion: The in vitro tests concluded that the novel nanocomposite containing ZnO-TiO2 and green tea extract has good anti-oxidant properties and it is non-toxic to the biological systems.**

**KEYWORDS:**
*Antioxidant activity, Green tea, Nano-composites.*

## INTRODUCTION

Nano-composite materials are made of amorphous or one, two, or three-dimensional structures blended at the nano-scale. These are made of clay, carbon, polymer, or a mixture of these components.[1] Green tea is a medicinal beverage extracted from the plant *Camellia sinensis* with a total polyphenol content of20% to 35% by weight, 60–80% of which are catechins.[2] It has various health benefits like prevention of cancer, and cardiovascular disease, the anti-inflammatory, anti-arthritic, antibacterial, anti-angiogenic, anti-oxidative, antiviral, neuro-protective and anti-cholesterol effects.[3,4] It has therapeutic effects in liver diseases, type 2 diabetes, Alzheimer's disease, obesity and many other systemic conditions.[5] It acts as an antioxidant by inducing glutathione-S-transferases and by inhibiting 'pro-oxidant' enzymes like inducible nitric oxide synthase, lipo-oxygenase and xanthine oxidase.[6] Natural antioxidants obtained from medicinal plants boost the plasma's antioxidant capacity and lower the risk of developing certain diseases.[7,8] Secondary metabolites like phenolics and flavonoids are effective free radical scavengers.[9] The undesirable effects of synthetic antioxidants include liver damage, cancer etc.[10,11] FDA permits the use of $TiO_2$ and biosynthesized Zinc Oxide nano-particles in human food, medication, and cosmetics.[12,13] The present study aims to assess the antioxidant activity of a nano-composite containing $TiO_2$, ZnO and Green tea extract.

## MATERIALS AND METHODS

*Preparation of plant extract*

Distilled water (100Ml) and green tea powder (2g) were mixed and boiled for 10 min. And the extract was filtered through muslin cloth. After stirring thoroughly in a heating mantle at 50-60 0C for 30 min, it is filtered using Whatman no. 1 filter paper. Of the 100mL filtered green tea extract, 60 mL of plant extract was used for the preparation of nano-particles. The remaining 30-40 mL of plant extract was concentrated into 3-4 mL of plant extract using a heating mantle, and could also used as the control. Sixty millilitres of the extract were used to synthesize the nano-particles.

*Preparation of nanoparticles*

Titanium oxide (0.35 g)was dissolved in 70 mL of distilled water, added to 30 mL of green tea extract, and stirred in an orbital shaker for 48 hours at 700-750 rpm. The mixture was centrifuged to synthesize titanium dioxide nano-particles.

*This article was accepted: 05 August 2024*
*Corresponding Author: Suja Joseph*
*Email: sjkt21@gmail.com*

Pellets were collected and stored for characterization and biological analyses.

574g (20mM) of Zinc sulphate was dissolved in 70 mL of distilled water, added to 30 mL of green tea extract, and stirred in an orbital shaker for 48 hours at 700-750 rpm. The mixture was centrifuged to synthesize zinc oxide nano-particles. The pellets were collected and stored for further characterization and research. [Figure 1]

*Preparation of Zinc oxide and Titanium dioxide nano-composites*
The titanium dioxide and zinc oxide nano-particle pellets were collected and dissolved in distilled water. Equal volumes of the solutions were placed separately in a sterile centrifuge and centrifuged at 8000 rpm for 10 min. The mixture was then added to the green tea extract and dried in a hot air oven. The powder was collected and stored for further research .

*Characterization of nanocomposite*
In this study, green tea was used as a reducing and stabilizing agent to synthesize Titanium dioxide nano-particles, ZnO nano-particles, and Titanium dioxide-Zinc oxide nano-composite. The green tea-mediated nano-particles and nano-composites were subjected to characterization techniques, such as Scanning Electron Microscopy (SEM) and Elemental dispersive analysis (EDX) to analyze their shape, and elemental and functional composition.

*Scanning electron microscopy*
Scanning Electron Microscopy (SEM) analysis of the green-synthesized $TiO_2$-ZnO nano-composite revealed its distinctive morphology [Figure 2]. This intriguing observation suggests a complex and heterogeneous structure within the nano-composite material, with two distinct particle shapes. The nano-composite exhibited a combination of both rhomboid-shaped $TiO_2$ nano-particles and spherical ZnO nano-particles. The particles had a certain degree of uniformity and regularity. This size-dependent activity suggests that the synthesized nano-particles can be tailored for specific applications by controlling their size. The coexistence of rhomboid and spherical particles in the $TiO_2$-ZnO nano-composite may have implications for its unique properties and potential applications, making it a promising candidate for various biomedical applications. The unique properties and morphologies of these nano-particles offer opportunities for application in the fields of biomedicine and antimicrobial coatings for prosthetic devices.

*Elemental dispersive analysis*
Energy dispersive X-ray spectroscopy (EDX) analysis of the green-synthesized titanium dioxide, zinc Oxide (TiO2-ZnO) nanocomposite provided insights into its elemental composition as depicted in [Figure 3]. The EDX spectra revealed the presence of several elements including titanium, zinc, and oxygen confirming the presence of both $TiO_2$ and ZnO components. in the nano-composite.

The significant carbon content suggests the persistence of organic residues from the green synthesis process, which may contribute to the nano-composite's unique properties. These findings underscore the versatility of green tea-mediated synthesis for tailoring nano-particle morphologies and offer potential applications in various fields of nanotechnology and materials science.

*Evaluation of antioxidant activity by the DPPH method*
The antioxidant activities of the biogenically synthesized zinc oxide and titanium dioxide nano-composites were evaluated using the DPPH assay. Different quantities (2–10µg/mL) of green tea extract containing the ZnO-$TiO_2$ nanocomposite, were added to 450 µL of 50 mM Tris HCl buffer (pH 7.4) and 1 ml of DPPH(0.1 Mm) in methanol and incubated for 30 min. Subsequently, based on the absorbance at 517 nm, the decrease in the number of DPPH free radicals was evaluated. Butylated hydroxytoluene (BHT) was used as control. The following equation was used to calculate the percentage inhibition:

$$\% \text{ inhibition} = \frac{\text{Absorbance of control- Absorbance of test sample}}{\text{Absorbance of control}} \times 100$$

*Evaluation of antioxidant activity by hydroxyl radical scavenging assay*
Modified Halliwell method was used to perform the assay.[14] 1.0 mL of freshly prepared reaction mixture containing 100 mL of 28 mM 2-deoxy-2-ribose, which was dissolved in phosphate buffer at pH 7.4. 500 mL of a solution containing different concentrations of green tea with ZnO-TiO2 nano-composite (10 to 50 µg/mL), 200 mL of 200 mM FeCl3 and 1.04 mM EDTA (1:1 v/v), 100mL $H_2O_2$(1.0mM) and 100µL(1.0mM) ascorbic was used. The TBA (Thiobarbituric acid) reaction was used to measure the degree of deoxyribose breakdown after incubating for one hour at 37°C. The absorbance at 532 nm was calculated in a blank solution, and the positive control, vitamin C, was used.

*Evaluation of antioxidant activity by FRAP assay*

*Reagents for FRAP assay*
a. To prepare an acetate buffer with 300 mM of pH 3.6, 3.1g of sodium acetate trihydrate was added to 16 ml of glacial acetic acid, and then mixed with distilled water to make a volume of 1L. b. TPTZ (2, 4, 6-tripyridyl-s-triazine), 10 mM in 40 m M H Cl (M.W. 312.34) (M.W. 36.46). c. FeCl3.6 H2O (20mM; M.W. 270.30). Immediately before testing, the FRAP reagent was prepared by combining components a, b, and c in a ratio 10:1:1. FeSO4. 7 H2O: 0.1 to 1.5 mM in methanol served as the standard. All reagents were prepared by the Merck Company in Germany.

*Procedure for FRAP assay*
The FRAP solution (3.6 mL) to distilled water (0.4 mL) and incubated for 5 min at 37 °C. This solution was mixed with a specific concentration of green tea nano-composites containing ZnO-TiO2 nano-particles (10 to 50 µg/mL) and incubated for 10 min at 37°C.The absorbance of the reaction mixture was measured at 593 nm. Five concentrations of FeSO4 and 7H2O (0.1, 0.4, 0.8, 1, 1.12, and 1.5 m M) were used to create a calibration curve, and the absorbance values were calculated for the sample solutions.

## RESULTS

*Visual observation*

In the presence of the ZnO-TiO2 nano-composite, the color of the solution gradually changed to pale yellow.

*Scanning electron microscopy*

SEM of the nano-composite suggested a complex heterogeneous structure with two distinct particle shapes. Upon examination, a combination of both rhomboid-shaped particles of $TiO_2$ and spherical particles of ZnO of uniform shape and size was observed [Figure 1]. The coexistence of rhomboid and spherical particles in the $TiO_2$-ZnO nano-composite may have implications for its unique properties and potential applications, making it a promising candidate for various biomedical applications.

*EDX Spectrography*

The elemental compositions of $TiO_2$ and ZnO , namely titanium, zinc, oxygen and carbon, in the nanocomposite was confirmed by EDX Spectrography [Figure 2].

*DPPH assay*

In the DPPH assay, the higher the concentration of green tea in the ZnO-$TiO_2$ nano-composite higher was the % of inhibition. At the concentration of nano-composites 10µg/ml, inhibition was 64%, 20 µg/mL has a 76%, 30 µg/mL has an 82%, 40 µg/mL has 64% of inhibition and 50 µg/mL has an 89%, respectively [Figure 3].

*$H_2O_2$ assay*

In the $H2O_2$ assay, the higher the concentration of green tea in the ZnO-TiO2 nano-composite higher was the inhibition rate rate. A concentration of nano-composites with 10µg/ml inhibited 51.3% of inhibition, 20 µg/ml inhibited 56.1% , 30 µg/ml 62.8% of inhibition,40 µg/ml inhibited 78% and 50 µg/ml inhibited 87.5% [Figure 3].

*FRAP assay*

In the FRAP assay, the % of inhibition increased in a dose-dependent manner. At a concentration of 10µg/mL the nano-composites showed 64.8% inhibition, 20 µg/mL inhihibited 74.3% , 30 µg/mL has an 82.6%, 40 µg/mL has an 84.7%, and 50 µg/mL has a 90.1%. (Figure 4) The plant-mediated nano-particles were added to the zinc sulphate solution and titanium oxide solution. Zinc sulfate was used to synthesize ZnO nano-particles and titanium oxide was used to synthesize titanium dioxide nano-particles. After one hour a color change was observed, which indicate the initiation of a chemical reaction in the solution. After 24 h, the color changed completely, indicating the synthesis of the nano-particles [Figure 3].

*Examination of ZnO-TiO2 nano-composites using UV-visible spectroscopy*

UV-visible spectroscopy was used for preliminary confirmation of the nano-particle synthesis. The absorbance of the UV-visible spectrum exhibited the highest peak at 310 nm. As the concentration of the ZnO-$TiO_2$ nanocomposite increases from 10 mg to 100 mg, the absorbance at 310 nm decreased in intensity. The peak refers to the synthesis of nanoparticles.[15] The reduction of titanium ions and generation of $TiO_2$ NPs were completed after overnight incubation at room temperature. The reduction of titanium ions is indicated by the formation of a light green color. The absorption spectra of the $TiO_2$ NPs formed in the solution had absorbance peaks at approximately 280 nm.[16] The synthesis of nano-particles was observed in the color changes of the nanoparticle solution. The synthesis of ZnO nano-particles was confirmed by UV-visible spectroscopy, which showed the highest peak absorbance at 360 nm. After 24h of reaction, the color change was stopped and precipitation was observed, indicating the completion of nano-particle synthesis.[17] The formation of ZnO NPs was confirmed by the observation of maximal absorbance at 480 nm, which is the typical wavelength for this formation. The observed UV spectrum around 450 nm indicates that in the reduction process, the semiconducting property of ZnO has not been lost[18] [Figure 4]. In the presence of the ZnO-$TiO_2$ nanocomposite, the color of the solution gradually changed to pale yellow. The absorption intensity was confirmed and localized by UV-visible spectroscopy at 310 nm. [Figure 4]

The antioxidant activity of green synthesized ZnO-$TiO_2$ nano-composite using green tea extract was measured by DPPH, $H_2O_2$, and FRAP assays to evaluate their radical scavenging activity. The solution was kept undisturbed for two hours to evaluate the stability of the nano-composites. The color change of the solution to pale yellow indicates an increase in free radical scavenging activity with an increase in the concentration of the ZnO-$TiO_2$ nano-composite. When the antioxidant activity was tested, green tea in the ZnO-$TiO_2$ nano-composites had good antioxidant properties.

In the DPPH assay, the higher the concentration of green tea in the ZnO-$TiO_2$ nano-composite higher was the % of inhibition. The antioxidant activity of green tea containing ZnO-$TiO_2$ nano-composites was comparable to that of the standard. When DPPH was inhibited, the color changed from purple to brown, indicating that hydrogen was donated and, demonstrating high scavenging activity. The high redox potential of ZnO breaks the water molecules into hydroxyl and hydrogen radicals, stabilizing DPPH free radicals and inhibiting the DPPH effect. The Antioxidant activities of different percentages of inhibition of oxidation were 52%, 63%, 71%, 85%, and 90% in a dose-dependent manner. Plant extracts mediated by titanium dioxide nano-particles at 40µL and 50µL concentrations exhibited a high antioxidant activity of 90%.

In the $H_2O_2$ assay, the higher the concentration of green tea in the ZnO-$TiO_2$ nano-composite higher was the % of inhibition. The % of inhibition shown by the green tea containing nano-composites was similar to the standard values. Previous studies have shown that green tea-mediated $TiO_2$ NPs exhibit 57–72% scavenging at 100 µg/mL concentration, while at 10 µg/mL, scavenging was 4–9%, indicating ineffectiveness at lower concentrations.

In FRAP assay, the % of inhibition increased in a dose-dependent manner. All values were nearly the same as those the standard. In FRAP assay, the maximum concentration of antioxidant activity of 8.99 ± 0.21 µM/mL in 1000 µg/mL, and the minimum concentration of antioxidant activity of 0.59 ± 0.01 µM/mL in 60 µg/mL of ZnO un-doped ZnO nano-

**Table I: Antioxidant activity of green tea TiO2 ZnO nano-composite**

| Concentration | Antioxidant activity of green teaTiO2ZnO nanocomposite | | | | | |
|---|---|---|---|---|---|---|
| | DPPH % of inhibition | | H2O2 % of inhibition | | FRAP % of inhibition | |
| | GT, TiO2 ZnO | Standard | GT, TiO2 ZnO | Standard | GT, TiO2 ZnO | Standard |
| 10 µL | 64% | 66 | 51.3 | 53 | 64.8 | 67 |
| 20 µL | 76 | 78 | 56.1 | 58 | 74.3 | 78 |
| 30 µL | 82 | 83 | 62.8 | 64 | 82.6 | 87 |
| 40 µL | 64 | 66 | 78 | 80 | 84.7 | 88 |
| 50 µL | 89 | 91 | 87.5 | 90 | 90.1 | 93. |

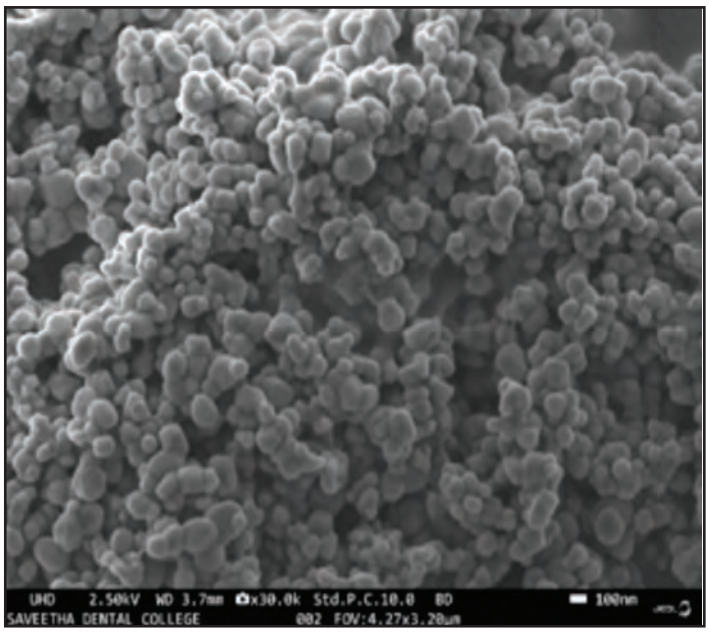


**Fig. 1:** SEM image of green synthesized TiO2-ZnO nano-composite

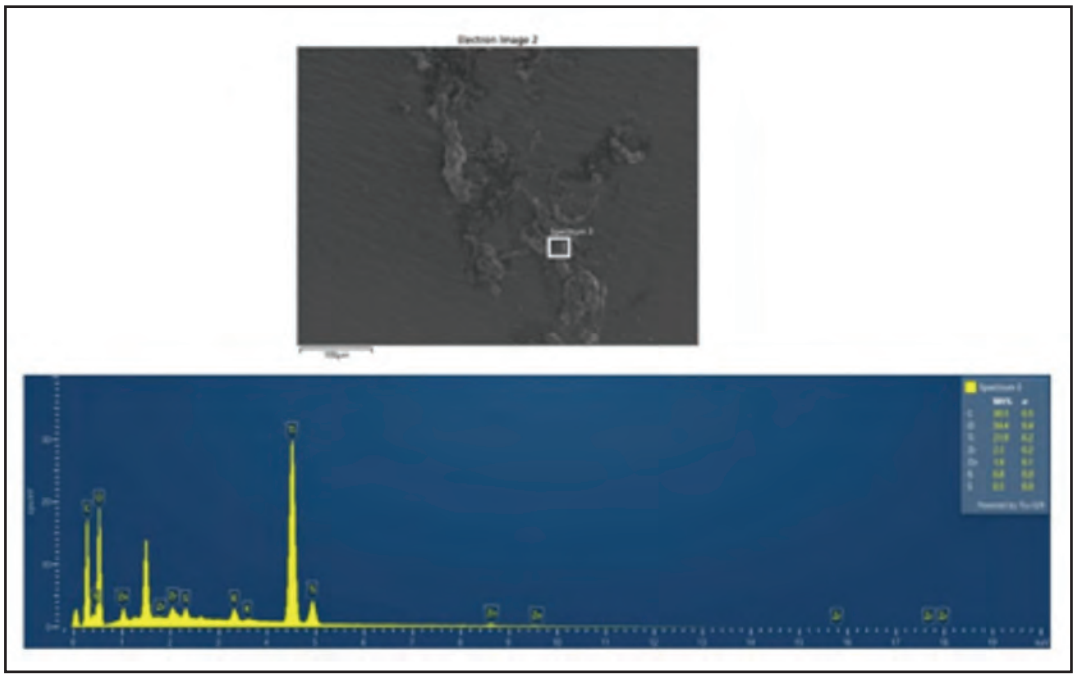

**Fig. 2:** EDX spectra of green synthesized TiO2-ZnO nanocomposite

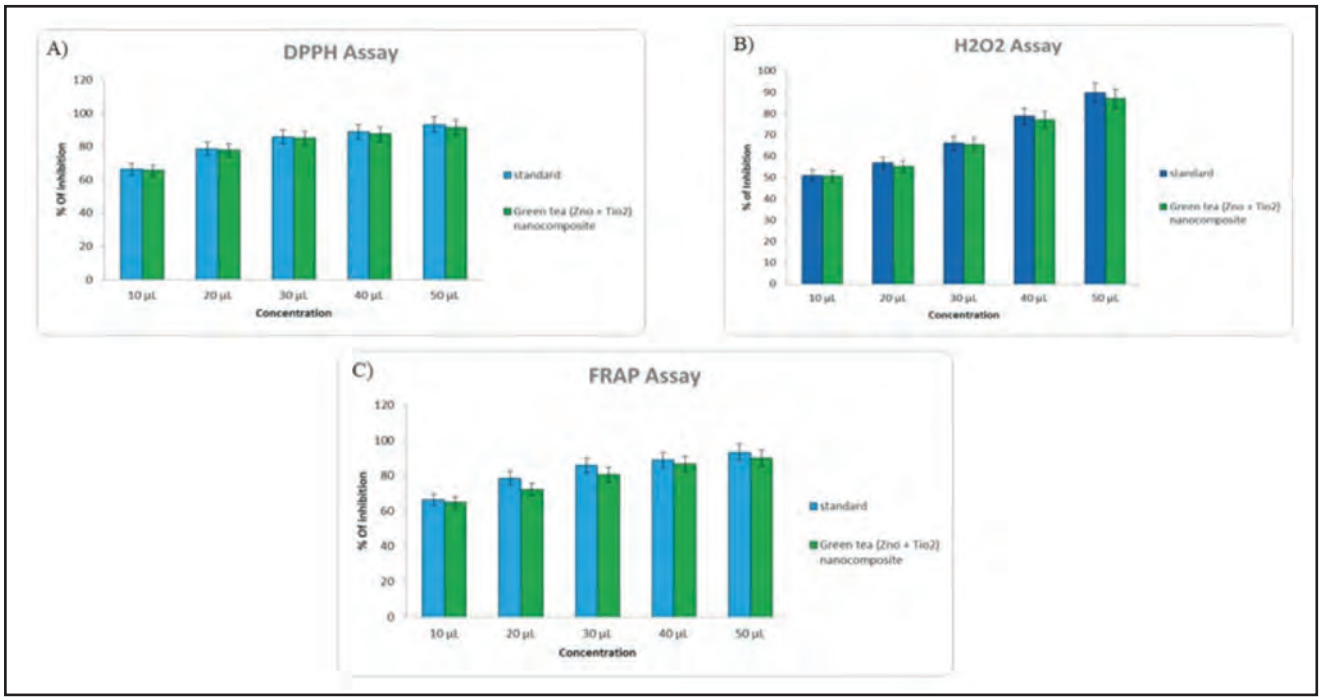


**Fig. 3:** A) DPPH assay B)H2O2 Assay C) FRAP assay

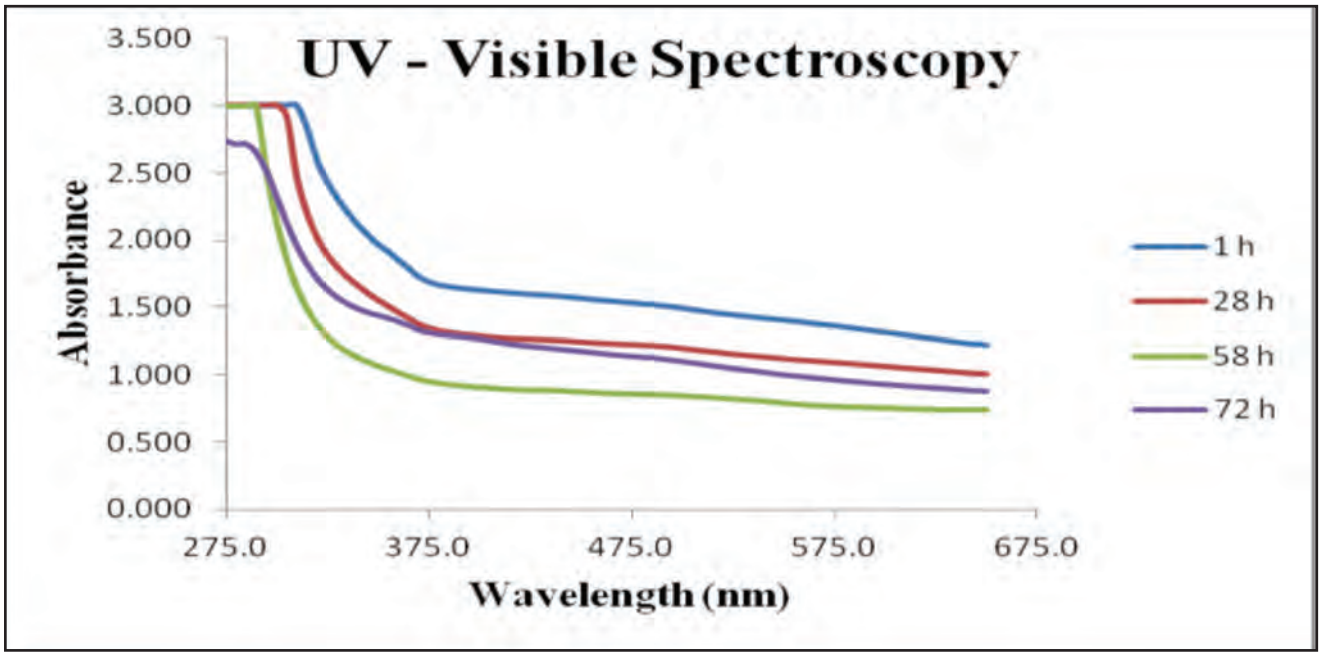


**Fig. 4:** Graphical representation of the UV-visible spectroscopy is ZnO-TiO2 nano-composite for green tea extract

particles. The antioxidant activity of Mn-doped ZnO nano-particles varied from 0.79±0.11 to 10.9 ± 0.11 µM/mL. Mn-doped ZnO nano-particles exhibited a higher FRAP than un-doped ZnO nano-particles.

In the DPPH assay, the higher the concentration of green tea in ZnO-TiO2 nano-composite, higher the% inhibition. At the concentration of nano-composites 10µg/mL, 64%, 20 µg/mL has a 76%, 30 µg/mL has an 82%, 40 µg/mL has 64% of inhibition and 50 µg/mL has an 89%. [Table I]

In the H2O2 assay, the higher the concentration of green tea in theZnO-TiO2 nano-composite higher was the % of inhibition. Nano-composites at 10µg/ml has, 51.3% inhibition, 20 µg/mL has a 56.1% inhibition, 30 µg/mL has, 62.8% inhibition,40 µg/mL has a 78% inhibition and 50 µg/mL has an 87.5% inhibition, respectively. [Table I]

In the FRAP assay, the % of inhibition increased in a dose-dependent manner. At a concentration of 10µg/mL the nano-composites showed 64.8% inhibition, 20 µg/mL inhibited

74.3%, 30 µg/mL has an 82.6%, 40 µg/mL has an 84.7%, and 50 µg/mL has a 90.1%. [Table I]

Plant-mediated nano-particles were added to the zinc sulfate and titanium oxide solutions. Zinc sulfate was used to synthesize ZnO nano-particles, and titanium oxide was used to synthesize titanium dioxide nano-particles. After one hour a color change was observed which indicated the initiation of a chemical reaction in the solution. After 24 h the color changed completely, indicating synthesis of the nano-particles.

## DISCUSSION

The antioxidant activity of green synthesized ZnO-$TiO_2$ nano-composite using green tea extract was measured by DPPH, H2O2 and FRAP assays to evaluate their radical scavenging activity. The solution was kept undisturbed for two hours to evaluate the stability of the nano-composites. The color change of the solution to pale yellow indicated an increase in free radical scavenging activity with an increase in the concentration of the ZnO-$TiO_2$ nano-composite. When the antioxidant activity was tested, green tea in the ZnO-$TiO_2$ nano-composites had good antioxidant properties.

The DPPH assay is used to measure the ability of compounds to scavenge free radicals, particularly DPPH radicals which are stable free radicals. Antioxidants react with DPPH and donate hydrogen atoms or electrons to neutralize it, turning the solution from purple to yellow. It is widely used to predict the antioxidant capacity of substances and understand the mechanisms of antioxidant action against lipid oxidation. In the DPPH assay, the higher the concentration of green tea in the ZnO-$TiO_2$ nano-composite higher was the % of inhibition. The antioxidant activity of green tea containing ZnO-$TiO_2$ nano-composites was comparable to that of the standard. When DPPH was inhibited, the colour changed from purple to brown, indicating that hydrogen was donated, demonstrating high scavenging activity.[19] The high redox potential of the ZnO breaks the water molecules into hydroxyl and hydrogen radicals, stabilizing the DPPH free radicals and inhibiting the DPPH effect.[20,21] Antioxidant activity of different percentages of inhibition of oxidation were 52%, 63%, 71%, 85%, and 90% in a dose-dependent manner. Plant extracts mediated by titanium dioxide nano-particles at 40µL and 50µL concentrations exhibited a high antioxidant activity of 90%.

The H2O2 assay evaluated the ability of the samples to scavenge hydrogen peroxide ($H_2O_2$). Antioxidants, particularly phenolics, can donate electrons to $H_2O_2$ and convert it into water (H2O). It helps to understand how substances can mitigate oxidative stress by neutralizing $H_2O_2$. In $H_2O_2$ assay, the higher the concentration of green tea in ZnO-$TiO_2$ nano-composite higher the % of inhibition. The % of inhibition shown by the green tea containing nano-composites was similar to the standard values. Previous studies have shown that green tea-mediated $TiO_2$ NPs exhibit 57–72% scavenging at 100 µg/mL, while at 10 µg/mL, scavenging was 4–9%, indicating ineffectiveness at lower concentrations.[22]

The FRAP assay measures the total antioxidant activity of a sample based on its ability to reduce ferric ions (Fe^3+) to ferrous ions (Fe^2+). Antioxidants in the sample reduce Fe^3+ to Fe^2+ in a colored complex, which can be quantified spectrophotometrically. The FRAP assay is commonly used in the food, beverage, and nutritional supplement industries to assess the overall antioxidant capacity, often using Trolox (a vitamin E analog) as a standard for calibration. In the FRAP assay, the % of inhibition increased in a dose-dependent manner. All values were nearly the same as those of the standard. In FRAP assay, the maximum concentration of antioxidant activity of 8.99 ± 0.21 µM/mL in 1000 µg/mL, and the minimum concentration of antioxidant activity of 0.59 ± 0.01 µM/mL in 60 µg/mL of ZnO un-doped ZnO nano-particles. The antioxidant activity of Mn- doped ZnO nano-particles varied from 0.79±0.11 to 10.9 ± 0.11 µM/mL . Mn-doped ZnO nano-particles exhibited a higher FRAP than un-doped ZnO nano-particles.[23]

Recent research in the field of nano-science has led to the utilization of nano-particles for cancer therapy through targeted drug delivery, as imaging tools in genetic engineering and in the development of electrochemical biosensors for diagnosis and drug delivery.

## CONCLUSION

Based on the in vitro tests to evaluate antioxidant activity, it can be concluded that the novel nano-composite containing ZnO-TiO2and green tea extract has good anti-oxidant properties. The advantages of natural antioxidants have non-toxic effects on biological systems, potency, and cost-effectiveness. Owing to their high catalytic and photochemical capabilities, ZnO nano-particles exhibit antibacterial and antifungal properties even at low concentrations.

## REFERENCES

1. Okpala, C. C. Nanocomposites–an overview. Int J Eng Res Dev 2013; 8(11): 17-23.
2. Gopal J, Muthu M, Paul D, Kim D-H, Chun S. Bactericidal activity of green tea extracts: the importance of catechin containing nano particles. Sci Rep 2016; 6: 19710.
3. Chacko SM, Thambi PT, Kuttan R, Nishigaki I. Beneficial effects of green tea: A literature review. Chin Med 2010; 5:13.
4. Cooper R,Morré DJ, Morré DM. Medicinal benefits of green tea: Part I. Review of Noncancer Health Benefits. J. Altern. Complement. Med 2005; 11: 521-528.
5. Sinija VR, Mishra HN. Green tea: Health benefits. Journal of Nutritional & Environmental Medicine 2008; 17:232-242
6. Embola C, Sohn O, Fiala E, Weisburger J. Induction of UDP-glucuronosyltransferase 1 (UDP-GT1) gene complex by green tea in male F344 rats. Food.Chem. Toxicol. 2002; 40: 841-4.
7. Rice-Evans C. Flavonoids and isoflavones: absorption, metabolism, and bioactivity. Free RadicBiol Med 2004; 36: 827-8.
8. Prior RL, Cao G. Antioxidant phytochemicals in fruits and vegetables: Diet and health implications. HortScience. 2000; 35: 588-92.
9. Mathew S, Abraham TE. In vitro antioxidant activity and scavenging effects of Cinnamomum verum leaf extract assayed by different methodologies. Food Chem Toxicol 2006; 44(2): 198-206.

10. Ito N, Fukushima S, Hagiwara A, Shibata M, Ogiso T. Carcinogenicity of butylated hydroxyanisole in F344 rats. J. Natl. Cancer Inst1983; 70: 343-7.
11. Osawa T, Namiki M. A novel type of antioxidant isolated from leaf wax of Eucalyptus leaves. Agric Biol Chem 1981; 45: 735-9.
12. Fernando S, Gunasekara T, Holton J. Antimicrobial nanoparticles: applications and mechanisms of action. SLJID. 2018; 8: 2.
13. Aditya BS, Arivarasu L, Rajeshkumar S,Thangavelu L. Antioxidant and antiinflammatory activity of Titanium dioxide nanoparticles synthesised using Mucuna pruriens. J Pharm Res lnt 2021; 414-22.
14. Halliwell, Barry. Oxidants and human disease: Some new concepts.The FASEB Journal 1987; 1(5): 358-64.
15. Santhoshkumar, Thirunavukkarasu, Abdul Abdul Rahuman, Chidambaram Jayaseelan, Govindasamy Rajakumar, Sampath Marimuthu et al. "Green synthesis of Titanium dioxide nanoparticles using Psidium Guajava extract and its antibacterial and antioxidant properties." Asian Pac J Trop Med 2014; 7: 968-76.
16. Ram VV, Arivarasu L, Rajeshkumar S, Thangavelu L. Green synthesis and characterisation of Mucuna Pruriens mediated Titanium Dioxide nanoparticles using Transmission electron microscope. J Pharm Res Int 2021; 362-70.
17. Wu, Shuang, Shanmugam Rajeshkumar, Malini Madasamy, and Vanaja Mahendran. "Green synthesis of copper nanoparticles using Cissus Vitiginea and its antioxidant and antibacterial activity against urinary tract infection pathogens." Artif. Cells Nanomed. Biotechnol 2020; 48(1): 1153-58.
18. Senthilkumar S R, Sivakumar T. Green tea (Camellia sinensis) mediated synthesis of zinc oxide (ZnO) nanoparticles and studies on their antimicrobial activities. Int J Pharm Sci 2014; 6(6): 461-5.
19. Abbes N, Bekri I, Cheng M, SejriN, Cheikhrouhou M, Xu J. Green synthesis and characterization of Zinc Oxide nanoparticles using Mulberry fruit and their antioxidant activity. Mater Sci 2022; 28: 144-150.
20. Dizaj SM, Lotfipour F, Barzegar-Jalali M, Zarrintan MH, Adibkia K. Antimicrobial activity of the metals and metal oxide nanoparticles. Mater Sci Eng: C 2014; 44: 278-84.
21. Fereidoon Shahidi, Ying Zhong: Measurement of antioxidant activity. J Funct Foods. 2015; 18: 757-781.
22. Ajmal N, Saraswat K, Bakht et al: Cost-effective and eco-friendly synthesis of titanium dioxide (TiO2) nanoparticles using fruit's peel agro-waste extracts: characterization, in vitro antibacterial, antioxidant activities. GCLR. 2019; 12: 244-54.
23. Khan SA, Shahid S, Bashir W et al: Synthesis, characterization and evaluation of biological activities of manganese-doped zinc oxide nanoparticles. TropJ Pharm Res. 2017; 16: 2331-39.

# Etiological factors and management of vertigo - A retrospective study

**Shyam Sudhakar Sudarsan, MBBS, DNB (ENT)**

Department of ENT – HNS, Saveetha Medical College Hospital, Thandalam, Chennai

## ABSTRACT

**Introduction: Vertigo and dizziness are symptoms of various underlying conditions, ranging from benign to severe, affecting up to 40% of adults. Understanding the etiological factors and demographic characteristics associated with these symptoms is crucial for improving diagnostic accuracy and management. This study aims to identify the etiological factors contributing to vertigo and dizziness in a clinical setting and assess the effectiveness of treatment strategies.**

**Materials and Methods: Retrospective cohort study conducted at Department of ENT and Head & Neck Surgery, Saveetha Medical College Hospital, Thandalam, Chennai, Tamil Nadu, India from September 2022 to March 2024. We included patients presenting with vertigo or dizziness, excluding those with non-vestibular dizziness or incomplete medical records. We analysed demographic data, medical history, and clinical findings from patient records. Data analysis was performed. Continuous variables were compared using independent sample t-tests and categorical variables using chi-square tests.**

**Results: The study included 268 patients, predominantly females (57.8%) and individuals aged 40-50 years (29.9%). Benign Paroxysmal Positional Vertigo (BPPV) was the most common etiological factor (41.0%), followed by orthostatic dysregulation (17.2%) and vestibular peripheral dysfunction (VPD) (16.0%). Clinical presentations and outcomes varied with the underlying etiology. Overall, 91.0% of the patients showed improvement following treatment, with 7.1% achieving full recovery.**

**Conclusion: This study highlights the complexity of vertigo and dizziness, which are influenced by various factors and demographics. This emphasizes the importance of tailored management strategies and a patient-centered, multidisciplinary approach, emphasizing customized treatments to improve patient outcomes.**

**KEYWORDS:**
*Dizziness, nystagmus, BPPV, Vestibular, Meniere's disease*

## INTRODUCTION

Vertigo and dizziness are complex symptoms that represent significant challenges in both diagnosis and management within the clinical setting.[1] These symptoms are not diseases themselves but are rather manifestations of a range of underlying conditions, which can span from benign to life-threatening.[2] The prevalence of vertigo and dizziness in the general population is substantial, with studies suggesting that up to 40% of adults experience these symptoms at some point in their lives, leading to a significant impact on quality of life and work productivity.[2,3]

The etiology of vertigo and dizziness varies and can be classified into categories such as peripheral vestibular, central vestibular, systemic, and psychological origins. Among these, disorders of the peripheral vestibular system such as benign paroxysmal positional vertigo (BPPV), Meniere's disease, and vestibular neuritis are common causes.[4,5] However, central nervous system issues, cardiovascular problems, medications, and psychological factors can also contribute significantly to these symptoms. This multifactorial nature necessitates a comprehensive and systematic approach to diagnosis and management.[6] The demographic factors play a crucial role in the presentation and etiology of vertigo and dizziness.[7-9] Age, for instance, is a critical factor; while younger individuals may experience dizziness primarily due to psychological reasons, older adults are more likely to suffer from vertigo due to vestibular disorders.[10,11] Similarly, gender differences have been observed in the prevalence and causes of these symptoms, with certain conditions such as Meniere's disease being more common in women.[12,13]

Despite the high prevalence and significant impact of vertigo and dizziness, there remains a gap in understanding the precise etiological factors and demographic correlations in diverse populations.[14] This lack of detailed knowledge hinders the development of targeted and effective management strategies, leading to suboptimal patient outcomes and increased healthcare costs.[15-17] In light of these challenges, our study aims to identify and analyse the etiological factors contributing to vertigo and dizziness among patients presenting to the Ear, Nose and Throat (ENT) department. By examining the demographic characteristics of these patients and assessing correlations between these characteristics and etiological factors, we sought to shed light on the complex dynamics underlying these conditions. This research is essential for advancing our understanding of vertigo and dizziness, paving the way for more accurate diagnoses and personalized treatment approaches, ultimately enhancing patient care and outcomes in clinical practice.

Through this retrospective study, we aim to contribute valuable insights into the patterns and predictors of vertigo

*This article was accepted: 15 October 2024*
*Corresponding Author: Shyam Sudhakar Sudarsan*
*Email: drshyam.smc@gmail.com*

and dizziness, offering a foundation for future research and improved therapeutic strategies in the field of otorhinolaryngology. In this study, we are guided by two primary objectives: first, to dissect the etiological landscape of vertigo and dizziness in our patient population and second, to elucidate the interplay between these etiological factors and the demographic characteristics of the patients.

## MATERIALS AND METHODS

*Study Design*

This retrospective cohort study aim to identify and analyze the etiological factors contributing to vertigo and dizziness in patients presenting to the ENT department.

*Study Setting*

This study was conducted at the ENT Department of Saveetha Medical College Hospital, Thandalam, Chennai, India from September 2022 to March 2024. This period included medical record review, data extraction, and subsequent analysis, ensuring a rich dataset for retrospective examination. Institutional ethical committee approval was obtained.

*Study Population*

The study population comprised of patients attending the ENT department with symptoms of vertigo or dizziness. Inclusion criteria were symptomatic presentation within the study period and confirmed diagnosis of vestibular disorders. Exclusion criteria included non-vestibular-related dizziness, incomplete medical records, or conditions mimicking vertigo with different underlying etiologies such as hypoglycemia or panic attacks.

*Selection of Participants*

All consecutive patients were included based on the inclusion criteria to minimize selection bias. Given its retrospective nature, the study included all eligible records during the specified period without a predetermined sample size. This approach ensured comprehensive coverage of the patient population, enhancing the representativeness and generalizability of findings.

*Study Variables and Outcomes*

The study variables included demographic characteristics (age and gender), medical history (comorbidities and prior episodes), and symptomatology (duration and severity). Factors such as pre-existing health conditions, medication use, and lifestyle were also recorded. The primary outcome included the identification of predominant etiological factors (vestibular, central, cardiovascular) and assessment of management outcomes.

*Data extraction*

The medical records were used as the primary data source. The extracted information included demographic details, medical history, clinical findings, diagnostic test results, and management strategies. The diagnostic criteria were based on established clinical guidelines for conditions such as BPPV, Meniere's disease, and vestibular neuritis. The assessment methods for each patient were standardized according to the department's protocols developed based on international guidelines for vestibular case diagnoses to ensure consistency.18 The department protocol was that a vertigo patient should have a minimum requirement of positional history, short duration of symptoms and dix-hallpike positive for classifying as BPPV; triad of roaring tinnitus, episodic vertigo and fluctuating hearing loss associated with or without aura should be classified as meniere's disease; presence of differentiating features of central and peripheral causes, postural changes, cardiac issues, migrainous / psychiatric association were documented in detail. The neurotologist who reviewed medical records was blinded to the study objectives

*Statistical Analysis*

Data were analyzed using SPSS software version 20.0 (IBM Corp. Released 2011. IBM SPSS Statistics for Windows, Version 20.0. Armonk, NY: IBM Corp.) Continuous variables were reported as mean ± standard deviation (SD) and assessed using the independent sample t-test for normally distributed data. Categorical variables were expressed as percentages and analyzed using the chi-square test, applying Yates continuity correction or Fisher's exact test when appropriate. All tests were two-sided, with a p-value $< 0.05$ considered statistically significant.

## RESULTS

*Sociodemographic characteristics*

Within the duration of this investigation, 268 patients were evaluated for vertigo and dizziness, with ages ranging from under 30 to over 60 years. The mean age groups were well-represented, with the largest cohort being those aged 40-50 years (29.9%), demonstrating a diverse patient population. The gender distribution leaned towards a higher female presence (57.8%) than males (42.2%). The duration of symptoms varied, with a significant number of patients experiencing symptoms for 1-4 weeks (43.3%). The associated symptoms were prevalent, including nausea and vomiting (30.6%), tinnitus (25.0%), and headache (15.3%). Regarding past medical history, hypertension was notably common (40.1%), followed by diabetes (17.2%) and dyslipidemia (13.4%), as detailed in Table I.

*Aetiological Factors*

Analysis of etiological factors revealed that Benign Paroxysmal Positional Vertigo (BPPV) was the predominant cause (41.0%), underscoring its significant role in vertigo etiology. Orthostatic dysregulation and Vestibular Peripheral Dysfunction (VPD) were also notable causes, accounting for 17.2% and 16.0% of the cases, respectively. Other etiologies, such as Meniere's disease (4.1%), vestibular migraine (7.1%), and psychogenic vertigo (4.9%), were less common. A small percentage of patients remained undiagnosed (3.7%) (Table II).

*Examination Findings*

Physical and auxiliary examination findings highlighted a range of abnormal outcomes. Nystagmus was observed in 27.9% of the patients, and abnormal S-test results were the most frequent finding (44.0%), indicating a high incidence of sensory integration issues in balance. Other significant findings included abnormal Subjective Visual Vertical (SVV) tests (25.7%) and video head impulse test (vHIT) (13.0%).

**Table I: Sociodemographic characteristics of the study participants (n=268)**

| Sr. No. | Sociodemographic factors | Number (n=268) | Percentage (%) |
|---|---|---|---|
| 1. | Age (years) | | |
| | <30 years | 46 | 17.2 |
| | 30-40 years | 43 | 16.0 |
| | 40-50 years | 80 | 29.9 |
| | 50-60 years | 59 | 22.0 |
| | >60 years | 40 | 14.9 |
| 2. | Sex | | |
| | Male | 113 | 42.2 |
| | Female | 155 | 57.8 |
| 3. | Duration | | |
| | < 1 week | 41 | 15.3 |
| | 1-4 weeks | 116 | 43.3 |
| | 4-12 weeks | 93 | 34.7 |
| | >12 weeks | 18 | 6.7 |
| 4. | Associated symptoms | | |
| | Ear fullness | 11 | 4.1 |
| | Headache | 41 | 15.3 |
| | Tinnitus | 67 | 25.0 |
| | Fluctuated hearing | 18 | 6.7 |
| | Nausea & vomiting | 82 | 30.6 |
| 5. | Past medical history | | |
| | Hypertension | 107 | 40.1 |
| | Diabetes | 46 | 17.2 |
| | Dyslipidemia | 36 | 13.4 |
| | Coronary heart disease | 24 | 9.0 |
| | Stroke/transient ischemic attack | 13 | 4.9 |

**Table II: Description of the etiological factor for the vertigo among study participants (n=268)** [18]

| Sr. No. | Etiology | Number (n=268) | Percentage (%) |
|---|---|---|---|
| 1. | Benign Paroxysmal Positional Vertigo | 110 | 41.0 |
| 2. | Vestibular Peripheral Dysfunction | 43 | 16.0 |
| 3. | Meniere's disease | 11 | 4.1 |
| 4. | Orthostatic dysregulation | 46 | 17.2 |
| 5. | Vestibular migraine | 19 | 7.1 |
| 6. | Gravity Perception Disturbance | 16 | 6.0 |
| 7. | Psychogenic vertigo | 13 | 4.9 |
| 8. | Unknown | 10 | 3.7 |

**Table III: Description of the abnormal findings of the study participants**

| Sr. No. | Examination findings | Number (n=268) | Percentage (%) |
|---|---|---|---|
| 1. | Nystagmus | 75 | 27.9 |
| 2. | Abnormal Caloric-test | 29 | 10.8 |
| 3. | Abnormal video Head Impulse Test | 35 | 13.0 |
| 4. | Abnormal cervical-Vestibular Evoked Myogenic Potential 1 | 23 | 8.5 |
| 5. | Abnormal Subjective Visual Vertical | 69 | 25.7 |
| 6. | Abnormal interictal episodic Magnetic Resonance Imaging | 18 | 6.7 |
| 7. | Abnormal Skew-test | 118 | 44.0 |
| 8. | Hypertension | 73 | 27.2 |

These results are consolidated in Table III, which illustrates the complexity of diagnosing vestibular disorders.

*Clinical Presentation and Diagnosis*

The clinical presentation varied significantly among different etiologies. Patients diagnosed with BPPV had a mean age of 49.5 years and had symptoms for an average of 4.3 weeks. Patients with Vestibular Peripheral Dysfunction (VPD) were younger and had longer symptom durations. Meniere's disease was associated with distinctive symptoms, such as ear fullness (27.3%) and rotatory dizziness (36.4%). Orthostatic dysregulation was observed in younger patients (mean age 39.0 years) with longer symptom durations (8.2 weeks). These detailed analyses provide insight into the specific clinical manifestations related to each etiology, as summarized in Table IV.

*Management Outcomes*

Regarding the management outcomes of patients with vertigo, a substantial majority (91.0%) showed improved recovery following treatment interventions. Full recovery was achieved in a small fraction (7.1%), highlighting the

**Table IV: Description of the study participants according to the etiological factor (n=268)**

| Etiology | Total number of subjects | Mean ± (SD) Age | Mean duration of symptoms (in weeks) | Headache n (%) | Ear fullness n (%) | Evoked Dizziness n (%) | Rotatory dizziness n (%) |
|---|---|---|---|---|---|---|---|
| Benign Paroxysmal Positional Vertigo | 110 | 49.5 ± 13.8 | 4.3 ± 2.2 | 12 (11) | 3 (2.7) | 99 (90) | 10 (9.1) |
| Vestibular Peripheral Dysfunction | 43 | 42.1 ± 23.2 | 6.6 ± 3.8 | 1 (2.3) | 0 (0) | 38 (88.4) | 0 (0) |
| Meniere's disease | 11 | 50.8 ± 18.3 | 2.5 ± 2.0 | 2 (18.2) | 3 (27.3) | 7 (63.6) | 4 (36.4) |
| Orthostatic dysregulation | 46 | 39.0 ± 12.2 | 8.2 ± 5.6 | 13 (28.3) | 1 (2.2) | 41 (89.1) | 0 (0) |
| Vestibular migraine | 19 | 44.6 ± 17.3 | 4.3 ± 5.5 | 8 (42.1) | 0 (0) | 1 (5.3) | 0 (0) |
| Gravity Perception Disturbance | 16 | 51.4 ± 16.7 | 6.4 ± 4.8 | 2 (12.5) | 2 (12.5) | 14 (87.5) | 0 (0) |
| Psychogenic vertigo | 13 | 36.3 ± 12.6 | 7.2 ± 6.7 | 1 (7.6) | 0 (0) | 0 (0) | 0 (0) |
| Unknown | 10 | 48.2 ± 16.6 | 10.2 ± 6.7 | 2 (20) | 2 (20) | 4 (40) | 0 (0) |

**Table V: Outcome of the management done for patients with vertigo (n=268)**

| Sr. No. | Treatment effect | Number (n=268) | Percentage (%) |
|---|---|---|---|
| 1. | Full recovery | 19 | 7.1 |
| 2. | Improved recovery | 244 | 91.0 |
| 3. | Discharged from hospital; without treatment of dizziness | 3 | 1.1 |
| 4. | Deceased | 2 | 0.7 |

effectiveness of treatment strategies employed. A minimal number of in-patients were discharged without specific treatment for dizziness (1.1%), and the mortality rate was low (0.7%), indicating an overall favorable prognosis for most patients when appropriately managed (Table V)

## DISCUSSION

The exploration of vertigo and dizziness in our study, encompassing 268 patients from an ENT department, provides a rich tapestry of data that elucidates the intricate nature of these conditions. By delving deep into demographic characteristics[7-9], etiological factors, examination findings, and treatment outcomes, our study contributes to the broader discourse on these prevalent yet often perplexing conditions. This discussion seeks to contextualize our findings within the existing body of knowledge, emphasizing critical insights and identifying areas for further investigation.

The gender disparity observed in our study, with a higher prevalence of vertigo and dizziness among females (57.8%) than males (42.2%), is consistent with previous research indicating a gendered dimension to these conditions.[12,13,19,20] This finding could be attributed to various biological and hormonal factors that may predispose women to certain types of vestibular disorders more than men. Additionally, the age distribution in our cohort, particularly the prominence of symptoms in the 40-50 years age bracket, raises important considerations regarding the life stage at which these conditions tend to manifest more frequently. This age-related trend might reflect not only the natural aging process and its impact on vestibular function but also the accumulation of risk factors such as cardiovascular diseases, hypertension, or diabetes, which are known to influence vestibular health.[10,11,21,22]

The identification of BPPV as the leading cause of vertigo in our patient population corroborates its established prevalence in the general and clinical settings.[14,23] This reaffirms the importance of BPPV in the differential diagnosis of vertigo, underscoring the need for clinician awareness and proficiency in its diagnosis and management.24 Furthermore, the significance of vestibular peripheral dysfunction and orthostatic dysregulation observed in our study points to the multifactorial nature of vertigo and dizziness, necessitating a comprehensive assessment approach to accurately pinpoint the underlying etiologies.[25] The variance in symptom duration, with a notable segment experiencing symptoms for 1-4 weeks, underscores the complexity of these conditions, highlighting potential delays in seeking treatment or the persistence of symptoms, which could significantly impact patients' quality of life and overall wellbeing.

The role of vestibular function tests, as evidenced by the prevalence of abnormal S-test results and nystagmus among our patients, is pivotal in the diagnostic process for vertigo and dizziness.[26] These findings not only underscore the value of such assessments in elucidating the vestibular contributions to patient symptoms but also highlights the challenges clinicians face in achieving a definitive diagnosis. The heterogeneity in examination findings necessitates a holistic diagnostic strategy, integrating comprehensive patient history, symptomatology, and targeted tests to navigate the diagnostic labyrinth of vertigo and dizziness effectively.[2] The predominance of improved recovery outcomes in our study (91.0%) mirrors the potential of current management strategies to ameliorate symptoms and enhance patient quality of life. This observation is particularly encouraging, as it reinforces the efficacy of tailored treatment plans based on a thorough understanding of the etiology of the condition. However, the variability in recovery trajectories underscores the importance of personalized medical approaches, considering the individual patient's clinical profile, etiological factors, and lifestyle considerations to optimize treatment efficacy.

The diversity in the treatment responses observed in our cohort underscores the critical importance of personalized approaches for managing vertigo and dizziness. This finding

aligns with the evolving paradigm in healthcare towards individualized patient care, which considers the unique aspects of each patient's condition and life circumstances. For instance, the application of vestibular rehabilitation, an evidence-based approach recommended for many vestibular disorders (Hall et al., 2016), could be tailored to the specific needs and capabilities of each patient, enhancing the overall effectiveness of the intervention and helping to develop targeted and effective management strategies, leading to optimal patient care and curbing increased healthcare costs.[15-17,27]

A major strength of our study is its detailed analysis of a sizeable cohort from a specialized clinical setting, offering a nuanced understanding of vertigo and dizziness. However, this study had some limitations. The retrospective design, reliant on medical records, may have introduced biases related to documentation quality and completeness. Additionally, our findings, derived from an ENT department, might not fully encapsulate the broader spectrum of vertigo and dizziness presentations encountered in other clinical settings such as neurology or primary care. Addressing these limitations, future studies could adopt a prospective design that incorporates standardized assessment tools and protocols to ensure uniformity and comprehensiveness in data collection. While comprehensive, our study opens several avenues for future research. One area of particular interest is the exploration of the long-term outcomes in patients with vertigo and dizziness. Studies examining the persistence of symptoms, recurrence rates, and impact of various treatment modalities over time could provide valuable insights into the chronic nature of these conditions and the effectiveness of current management strategies. Furthermore, research on the development and validation of standardized protocols for the diagnosis and treatment of vertigo and dizziness could significantly enhance clinical practice, leading to improved patient outcomes.

The complex interplay of demographic factors, etiological contributors, diagnostic challenges, and treatment outcomes is observed as vertigo which encompasses a wide spectrum of disorders. This interplay may mask the initial presentation of vertigo and can lead to misdiagnosis, as the patient at times may not be in a state to correctly give the precipitating events in chronological order. Attenders who accompany patients may provide version of their understanding of their symptoms at the initial assessment of the patient. It is the clinician's experience and acumen that should be carefully sorted through this complex interplay to properly diagnose and treat the patient.

## CONCLUSION

Our study contributes to the body of knowledge on vertigo and dizziness by highlighting the complex interplay between demographic factors, etiological contributors, diagnostic challenges, and treatment outcomes. This underscores the necessity for a patient-centered, multidisciplinary approach to managing these conditions tailored to the unique needs of each individual. As we advance, it is imperative that we continue to refine our understanding of vertigo and dizziness through rigorous research, ultimately guiding the evolution of clinical practice towards more effective and personalized patient care.

## REFERENCES


1. Walther LE. Current diagnostic procedures for diagnosing vertigo and dizziness. GMS Current Topics in Otorhinolaryngology, Head and Neck Surgery [Internet]. 2017 Dec 18 [cited 2020 Sep 24]; 16. Available from: https://www.ncbi.nlm.nih.gov/pmc/articles/PMC5738933/
2. Strupp M, Brandt T. Diagnosis and treatment of vertigo and dizziness. Dtsch Arztebl Int 2008; 105(10): 173-80.
3. Hackenberg B, O'Brien K, Döge J, Lackner KJ, Beutel ME, Münzel T, Wild PS, Pfeiffer N, Chalabi J, Matthias C, Bahr-Hamm K. Vertigo and its burden of disease-Results from a population-based cohort study. Laryngoscope Investig Otolaryngol 2023; 8(6): 1624-30.
4. Xing Y, Si L, Zhang W, Wang Y, Li K, Yang X. Etiologic distribution of dizziness/vertigo in a neurological outpatient clinic according to the criteria of the international classification of vestibular disorders: a single-center study. J Neurol 2024; 271(5):2446-2457. doi: 10.1007/s00415-023-12166-3. Epub 2024 Jan 17. Erratum in: J Neurol 2024. doi: 10.1007/s00415-024-12495-x. PMID: 38231268; PMCID: PMC11055744.
5. Thompson TL, Amedee R. Vertigo: a review of common peripheral and central vestibular disorders. Ochsner J. 2009 Spring; 9(1): 20-6.
6. Turner B, Eynon-Lewis N. Systematic approach needed to establish cause of vertigo. Practitioner 2010; 254(1732):19-23, 2-3. PMID: 21133189.
7. Agus S, Benecke H, Thum C, Strupp M. Clinical and Demographic Features of Vertigo: Findings from the REVERT Registry. Front Neurol 2013; 4: 48.
8. Baydan M, Avcı ÖS, Yeğin S, Binay K, Hançer G, Öztaş S, Büyükatalay ZÇ, Yılmaz S. Etiological and Demographic Characteristics of Patients with Vestibular Symptoms, Retrospective Analysis. J Ankara Univ Fac Med; 73(3): 270-5.
9. Wassermann A, Finn S, Axer H. Age-Associated Characteristics of Patients With Chronic Dizziness and Vertigo. J Geriatr Psychiatry Neurol 2022; 35(4): 580-5.
10. Prell T, Mendorf S, Axer H. Tolerance to Dizziness Intensity Increases With Age in People With Chronic Dizziness. Front Neurol 2022; 13: 934627.
11. Iwasaki S, Yamasoba T. Dizziness and Imbalance in the Elderly: Age-related Decline in the Vestibular System. Aging Dis 2014; 6(1): 38-47.
12. Ogun OA, Janky KL, Cohn ES, Büki B, Lundberg YW. Gender-based comorbidity in benign paroxysmal positional vertigo. PLoS One 2014; 9(9): e105546.
13. Corazzi V, Ciorba A, Skarżyński PH, Skarżyńska MB, Bianchini C, Stomeo F, Bellini T, Pelucchi S, Hatzopoulos S. Gender differences in audio-vestibular disorders. Int J Immunopathol Pharmacol. 2020 Jan-Dec;34:2058738420929174. doi: 10.1177/2058738420929174. PMID: 32525749; PMCID: PMC7290256.
14. Benecke H, Agus S, Kuessner D, Goodall G, Strupp M. The Burden and Impact of Vertigo: Findings from the REVERT Patient Registry. Front Neurol 2013; 4: 136.
15. Wang X, Strobl R, Holle R, Seidl H, Peters A, Grill E. Vertigo and dizziness cause considerable more health care resource use and costs: results from the KORA FF4 study. J Neurol 2019; 266(9): 2120-8.
16. Kovacs E, Wang X, Grill E. Economic burden of vertigo: a systematic review. Health Econ Rev 2019; 9(1): 37.
17. Stephan AJ, Kovacs E, Phillips A, Schelling J, Ulrich SM, Grill E. Barriers and facilitators for the management of vertigo: a qualitative study with primary care providers. Implement Sci. 2018 Feb 8;13(1):25. doi: 10.1186/s13012-018-0716-y. Erratum in: Implement Sci 2018; 13(1): 82.

18. Bisdorff AR, Staab JP, Newman-Toker DE. Overview of the International Classification of Vestibular Disorders. Neurol Clin. 2015; 33(3): 541-50.
19. Vandenbroeck, Sebastian & Lerut, Bob & Vinck, A.S. (2018). Twenty-two years of Benign Paroxysmal Positional Vertigo at Sint-Jan Hospital Bruges: a retrospective analysis of 3785 patients. B-ENT. 14. 247-50.
20. Rahul, Raveendran & Andrews, Chakramakal & Karuthedath, Sridevi & Vinayakumar, Arayamparambil. (2016). Prevalence, risk factors and clinical presentations of patients with peripheral vertigo: a retrospective study from a tertiary care hospital. International Journal of Advances in Medicine. 106-9.
21. Coronel-Touma GS, Monopoli-Roca C, Almeida-Ayerve CN, Marcos-Alonso S, Gómez de la Torre-Morales D, Serradilla-López J, Cruz-Ruiz SS, Batuecas-Caletrío Á, Sánchez-Gómez H. Influence of Age and Cardiovascular Risk Factors in Vestibular Neuritis: Retrospective Cohort Study. J Clin Med 2023; 12(20): 6544.
22. Anson E, Jeka J. Perspectives on Aging Vestibular Function. Front Neurol. 2016; 6: 269.
23. von Brevern M, Radtke A, Lezius F, Feldmann M, Ziese T, Lempert T, et al. Epidemiology of benign paroxysmal positional vertigo: a population based study. J Neurol Neurosurg Psychiatry 2007; 78(7): 710-5.
24. Palmeri R, Kumar A. Benign Paroxysmal Positional Vertigo. 2022 Dec 26. In: StatPearls [Internet]. Treasure Island (FL): StatPearls Publishing; 2024 Jan–. PMID: 29261987.
25. Post RE, Dickerson LM. Dizziness: a diagnostic approach. Am Fam Physician. 2010 Aug 15;82(4):361-8, 369. PMID: 20704166.
26. Zuniga SA, Adams ME. Efficient Use of Vestibular Testing. Otolaryngol Clin North Am 2021; 54(5): 875-91.
27. Hall CD, Herdman SJ, Whitney SL, Cass SP, Clendaniel RA, Fife TD, Furman JM, Getchius TS, Goebel JA, Shepard NT, Woodhouse SN. Vestibular Rehabilitation for Peripheral Vestibular Hypofunction: An Evidence-Based Clinical Practice Guideline: From The American Physical Therapy Association Neurology Section. J Neurol Phys Ther 2016; 40(2): 124-55.

# Utilizing perfusion index for early identification of circulatory shock in neonates

**Navin Umapathy, MD[1], Varshini Chandrasekar, MD[2], Lal D Nair, Dch[3], Vaanmathi A S, MD[4]**

[1]Postgraduate , Department of Paediatrics, Saveetha Medical College Hospital ,SIMATS, Saveetha University, [2]Postgraduate , Department of Paediatrics, Saveetha Medical College Hospital, SIMATS, Saveetha University, [3]Director, Saveetha CDC, Department of Paediatrics, Saveetha Medical College Hospital, SIMATS, Saveetha University, [4]Associate Professor , Department of Paediatrics, Saveetha Medical College Hospital, SIMATS, Saveetha University

## ABSTRACT

**Introduction: Neonatal circulatory shock poses a significant challenge in intensive care settings and necessitates early recognition and intervention to prevent adverse outcomes. The perfusion index (PI), derived from pulse oximetry signals, is a potential adjunct tool for assessing peripheral perfusion and predicting shock in neonates. This prospective observational study aimed to evaluate the correlation between PI and circulatory shock in neonates with the goal of establishing PI as an objective parameter for early shock identification.**

**Materials and Methods: Study was conducted in the neonatal intensive care unit (NICU) of Saveetha Medical College Hospital, India, in 2023, between January and June. This study enrolled 100 neonates who underwent hemodynamic monitoring over 48-72 hours. Hemodynamic parameters including heart rate, blood pressure, and PI were systematically recorded. Statistical and Receiver operating characteristic curve analyses were used to assess the relationship between PI and shock.**

**Results: Neonates experiencing shock exhibited significantly lower PI values than those without ($P < 0.05$). ROC curve analysis identified a PI threshold of 0.7 for predicting shock, demonstrating a high sensitivity (92.5%) and specificity (94.78%). Additionally, a significant association was observed between PI and serum lactate level ($p < 0.05$), underscoring the utility of PI as a predictor of shock severity.**

**Conclusion: The study suggests that a PI < 0.7 may serve as an indicator of circulatory shock in neonates, offers good sensitivity and specificity. The PI, along with clinical parameters and serum lactate levels, is a valuable tool for early shock identification in neonatal intensive care. Further research, including multicenter studies, are warranted to validate these findings.**

**KEYWORDS:**
*Perfusion index, neonatal shock, reliable predictor, NICU,peripheral hypoperfusion*

## INTRODUCTION

The peripheral hemodynamics of a newborn baby ultimately determines the amount of oxygen and nutrients that reach its tissues. The rate of oxygen delivery had no effect on oxygen consumption in neonates with adequate perfusion. Infants born with compromised blood flow have oxygen consumption rates linked to tissue microcirculation. Tissue perfusion is only considered "normal" when all three of the following conditions are met: cardiac output, vasomotor tone, and oxygen delivery capacity of the blood. Shock, characterized by an acute breakdown of the circulatory system, is a clinical condition that fails to maintain nutrition and perfusion to tissues.[1] The strength of the pulse can be assessed by a tool, the perfusion index, which indirectly measures the perfusion at the peripheries. A pulse oximeter is commonly used to assess blood oxygen levels. There are two distinct parts of the signal: the arterial, pulsating part, and the non-arterial, non-pulsating part that comes from places like bone and connective tissue.[2] The pulsatile part shifts when the peripheral perfusion changes, leaving the non-pulsatile components unchanged. The ratio, as shown by the pulse oximeter, was varied. Because changes in arterial saturation are more likely to cause interference with red light signals, infrared light is preferred.[3,4]

$$\text{Perfusion index (PI)} = \frac{\text{Pulsatile signals of infrared}}{\text{Non pulsatile signals of infrared}} \times 100$$

PI is commonly reported as a percentage ranging from 0.02% (very weak pulse) to 20% (very strong pulse). To evaluate neonatal shock,clinicians use parameters that are subject to individual interpretation. The PI displayed by a pulse oximeter is an objective parameter that provides an indirect measure of perfusion in the peripheries. To obtain an objective measure of PI, we aimed to study the correlation between PI and BP to predict shock.

## MATERIALS AND METHODS

A prospective observational study was conducted after obtaining approval from our institutional ethical committee, including all neonates with hemodynamic instability admitted to the Level 3 Neonatal Intensive Care Unit (NICU) of Saveetha Medical College Hospital located in Tamil ( India) between January 2023 and June 2023. Informed written consent for the study was obtained from the parents of the neonates. We hypothesized that a lower perfusion index is expected in neonates with shock and should correlate with other shock parameters. This study included neonates with shock, respiratory distress, hypoglycemia,

*This article was accepted: 26 November 2024*
*Corresponding Author: Navin Umapathy*
*Email: navinu02@gmail.com*

**Table I: Haemodynamic parameters noted among babies**

| Haemodynamic parameters | Babies with shock | Babies without shock | p-value |
|---|---|---|---|
| Systolic Bp (in mmHg) | 64.21±7.9 | 68.5±2.4 | 0.03 |
| Diastolic Bp (in mmHg) | 40.21±4.9 | 47.15±3.9 | 0.04 |
| Mean Arterial Pressure(MAP) (in mmHg) | 46.79±5.8 | 49.15±2.54 | 0.05 |
| Heart Rate (bpm) | 152.12±13.67 | 146.14±3.45 | 0.04 |

**Table II: Association between shock and perfusion index**

| Perfusion index(PI) | Shock Present (number of babies) | Shock Absent (number of babies) | p-value |
|---|---|---|---|
| ≤0.7 | 24 | 2 | |
| >0.7 | 3 | 71 | <0.04 |
| Total | 27 | 73 | |

**Table III: Association between PI and serum lactate**

| PI | Serum Lactate (≥5) | Serum Lactate (≤5) | p-value |
|---|---|---|---|
| ≤0.7 | 20 | 7 | |
| >0.7 | 4 | 69 | <0.04 |
| Total | 24 | 76 | |

Majority of babies who had serum lactate more than 5 had a perfusion index less than 0.7. Hence, the association is statistically significant (P<0.05)(Table III).

sepsis, seizures, and perinatal asphyxia. Children with major congenital anomalies and other life-threatening illnesses diagnosed during the antenatal period were excluded.

Neonates in the level 3 NICU requiring hemodynamic monitoring were enrolled in the study after obtaining written consent from their parents. A sample size of 100 was chosen, and the children were recruited using a convenient sampling method. Perfusion parameters were monitored by the principal investigator from the time of enrollment until 48 hours in stable neonates and for 72 hours in sick neonates. 8th hourly monitoring were done for all babies from the time of recruitment until 48 h.

Neonates with shock were monitored for 20 min until perfusion normalized and continued as planned until 72 h. The following parameters were monitored: heart rate, Blood Pressure (BP) including [Systolic Blood Pressure (SBP), Diastolic Blood Pressure (DBP),Mean Arterial Pressure (MAP)], PI using a pulse oximeter, and at least one value for blood lactate levels. The following criteria were set for definition:

Shock/poor perfusion was defined as having a weak and fast pulse (HR > 180/min), Capillary Refill Time (CRT) >3 s, cold extremities, and with or without the following signs in addition: lethargy, not responding to stimulation, and very pale. As per the unit policy, the shock and comorbid conditions were treated.

Monitoring: Heart rate was assessed using stethoscopes in non-agitated babies. Blood pressure was measured in the right upper limb in the supine posture in a quiet environment, and an appropriately sized cuff was used.4 Selection of BP cuff was made based on the criterion that the width of the cuff should be 2/3rd of the arm length. Blood Lactate levels were obtained from arterial blood gas analysis, which is often performed for all babies admitted to the NICU and requires hemodynamic monitoring. PI in the right upper limb was measured using pulse oximetry.

## STATISTICAL ANALYSIS

Data were collected and consolidated using Microsoft Excel software and analyzed using JAMOVI software, version 2.3.28. Frequency analysis was performed for descriptive variables, percentage analysis was used for categorical variables, and mean and standard deviation were used for continuous variables. The correlation between the PI and other shock parameters was calculated using the area under the ROC curve. The cutoff value of PI was set, and values below or above it were used to predict babies in shock/not.

## RESULTS

In this study, 34% of neonates were born with a gestational age below 34 weeks, and 66% had a gestational age above 34 weeks, with a mean gestational age of 35.78 weeks and a standard deviation of 2.23 weeks. Almost 47 babies were delivered via lscs, with 53 delivered via normal delivery. Approximately 28 babies had a birth weight of less than 1.75 kg while the rest had above 1.75 kg of birth weight. Certain neonatal complications were noted in the study population, such as birth ashyxia (12 babies), Respiratory Distress Syndrome (36 babies), apnea (4 babies), Meconium Aspiration Syndrome (MAS)(22 babies), sepsis (14 babies), hyperbilirubinemia (35 babies), 5 babies required ventilator support, 2 babies, intraventricular hemorrhage (IVH) and 4 babies developed Retinopathy of Prematurity (ROP)(Figure I).

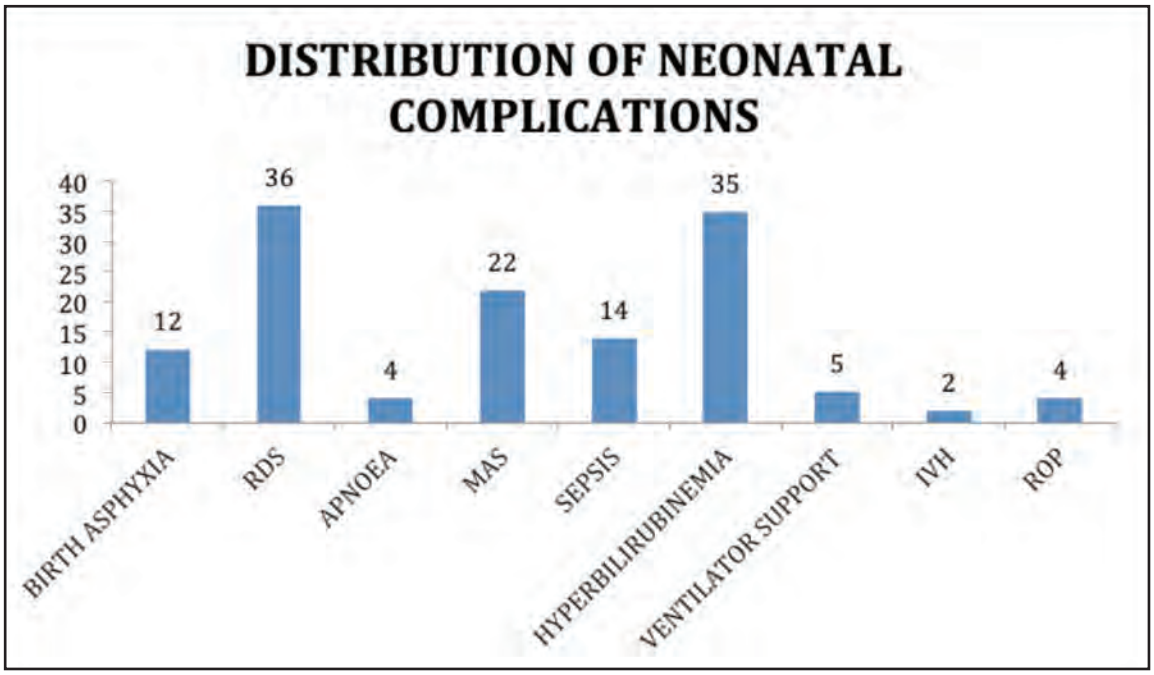


**Fig. 1:** Distribution of neonatal complications among study population

Mean systolic BP of 64.21±7.9 (mmHg) was recorded in babies with shock while 68.5±2.4 (mmHg) was recorded in non shock babies. Mean Diastolic BP of 40.21±4.9 (mmHg) respectively, in babies with shock, whereas non-shock babies had a Mean Diastolic BP of 47.15±3.9 (mmHg). The mean MAP was 46.79±5.8 (mmHg) in babies who had shock, while the rest of the babies had a mean MAP of 49.15±2.54 (mmHg). Mean Heart rate was 152.12±13.67 (Beats per minute) in neonatal shock while non shock babies had a mean heart rate of 146.14±3.45 (Beats per minute). All of the above cardiovascular parameters were statistically significant (Table I).

In our study population of 100 babies, 27 had clinical features of shock, of which 24 babies had a PI less than 0.7. Out of 73 non-shock babies, two had a PI of less than 0.7. This association was statistically significant ($p<0.05$) (Table II) and emphasized that PI can be utilized as a reliable predictor of neonatal shock in the NICU.

Association between neonatal shock and PI has a Sensitivity of 92.5% and a specificity of 94.78% with a positive predictive value of 81.24% and negative predictive value of 96.43%.

## DISCUSSION

Neonatal shock is a diagnosis with many indulging parameters and subjective decisions on management.1 Although babies have more blood volume( ml/kg) than adults, even a small quantity of blood loss will result in neonatal shock. There are numerous reasons for shock, such as sepsis, IVH, poor feeding, cardiac causes, and pneumothorax, and early detection of neonatal shock is the primary factor for early management and recovery.[1] Oscillatory automatic BP measurements are reliable and are routinely used in all NICU. Manual BP cannot be recorded because babies' artery pulsations are not loud enough to be heard with a stethoscope.[2] The relationship between heart rate, blood pressure, and serum lactate levels is substantially less. Increased ICU and hospital mortality are linked to elevated serum lactate levels. Although lactate levels play a crucial role in ICU care, many times, it becomes an oversimplification that equates hyperlactatemia with hypoperfusion.[2] Most of the parameters used for clinical assessment of shock in neonates are subjective,which leads to unnecessary treatment of shock. These clinical factors result in greater interobserver variability. This creates a demand for objective assessment of shock, which can detect hypoperfusion in neonates, resulting in the early identification and management of shock in newborns.

In the ICU, normal serum lactate levels are present in approximately 50% of critically ill septic patients.[4] Uncertainty surrounds the pathophysiology underlying the normal serum lactate levels in some critically ill ICU patients. Even among patients who ranked among the sickest in the highest quartile, serum lactate level was a reliable predictor of mortality. When a patient presents to the emergency department (ED) with septic shock, the initial serum lactate level is independently correlated with mortality. Therefore, measurement of the first serum lactate level may be a reliable indicator of prognosis in patients with septic shock. Perfusion index (PI) is a marker of hypoperfusion. Therefore, a drop in PI indicates activation of the sympathetic system, which is seen on many occasions such as shock,pain, stress,etc.[5,6] We created a receiver operating characteristic (ROC) curve that can detect impending shock by changing the percentage of the perfusion index (PI). Certain factors like pain, stress,

hypothermia can influence the values of PI.[7] In medical literature, only few studies have been done for predicting hypoperfusion using PI. Few studies have used PI to assess the severity of illness and correlate low flow in the superior vena cava (SVC) with PI in neonates.[8,9] Hence, the present study aimed to determine whether the perfusion index can be used to predict shock. Certain parameters such as temperature and gestational age can influence PI.[10]

In the present study, about 66% were above 34 weeks of gestational age and 34% were below 34 weeks of GA, Mean GA was 35.78 and SD was 2.23. Approximately 53% of the patients were male and 47% were female. Nearly 47% had normal deliveries and 53% had LSCS. Approximately 29% had a birth weight less than 1.75 kg. The mean birth weight was 2.02 kg and the standard deviation was 0.85 kg. Certain neonatal complications noted in the study population included birth asphyxia (12 babies), RDS (36 babies), Apnea (4 babies), MAS (22 babies), sepsis (14 babies), hyperbilirubinemia (35 babies), ventilator support (5 babies), IVH (2 babies had IVH and ROP (4 babies developed ROP. Mothers of babies had certain antenatal complications, such as gestational diabetes mellitus(37%), pregnancy-induced hypertension (22%), obesity (4%), Overt Diabetes mellitus (2%), and no other complications.

In a study, a significant positive correlation was detected values of PI (less than 0.44) and low flow rate in superior vena cava in preterm neonates.5 In a study done in the adult population, the values of PI (1.4) detected hypo perfusion in patients with shock.[6]

PI measurements can be affected by artificial factors such as temperature, skin pigmentation, and motion artifacts, which could lead to inaccuracies.[11-13] Another prospective study showed that PI ranging from 0.30 to 10.0, with a median value of 1.4, had skewed distribution and concluded that PI can be used to monitor peripheral perfusion in critically ill patients.[9] Severity of illness using the SNAP score was studied by De Felice et al., in which a value of 0.86 PI detected the severity of sickness in newborn.[14] This study also showed a high sensitivity value. He et al. and Lian et al. found that changes in PI post-resuscitation are predictive of mortality, especially in septic patients.[15-17] The study done in 2020 showed a positive correlation between PI and Cardiac Index during the early treatment phase of septic shock.[18] PI showed moderate ability to detect fluid responsiveness in patients with septic shock on norepinephrine infusion. Increased PI after a 200 mL crystalloid challenge can detect fluid responsiveness with a positive predictive value of 92%.[19]

Similar to the above studies, but with comparatively lower values, the majority of the neonates in the present study population who had shock had a perfusion index less than 0.7. This association was statistically significant ($p<0.05$). The majority of neonates with serum lactate levels > 5 had a perfusion index less than 0.7. This association was also statistically significant ($p<0.05$).

## CONCLUSION

Clinical shock in neonates can be predicted with reasonable accuracy when the perfusion index is below 0.7. A perfusion index below 0.7 exhibits high sensitivity and low false positivity in anticipating clinical shock. The perfusion index, displayed on modern pulse oximeters, could serve as an additional valuable parameter for assessing peripheral perfusion. Furthermore, it correlates with serum lactate levels, aiding the prediction of shock. A more extensive study with a larger sample size may be necessary to gain deeper insights into the perfusion index and its ability to predict impending shocks.

## REFERENCES


1. Wynn JL, Wong HR. Pathophysiology and treatment of septic shock in neonates. Clin Perinatol 2010; 37(2): 439-79.
2. Nuntnarumit P, Yang W, Bada-Ellzey HS. Blood pressure measurements in the newborn. Clin Perinatol 1999; 26(4): 981-96.
3. Pinto Lima A, Beelen P, Bakker J. Use of a peripheral perfusion index derived from the pulse oximetry signal as a noninvasive indicator of perfusion. Crit Care Med 2002; 30: 1210-3.
4. Engle WD. Definition of normal blood pressure range. The elusive target. In: Kleinman CS, Seri I, Polin RA, editors. Hemodynamics and cardiology. Neonatology questions and controversies. 2008: 39-65.
5. Mehandale SG, Rajasekhar P. Perfusion index as a predictor of hypotension following propofol induction - A prospective observational study. Indian J Anaesth 2017; 61(12): 990-5.
6. de Boode WP. Clinical monitoring of systemic hemodynamics in critically ill newborns. Early Hum Dev 2010; 86(3): 137-41.
7. Weindling M, Paize F. Peripheral haemodynamics in newborns: best practice guidelines. Early Hum Dev 2010; 86(3): 159-65.
8. Lee J, Rajadurai VS, Tan KW. Blood pressure standards for very low birthweight infants during the first day of life. Arch Dis Child Fetal Neonatal Ed 1999; 81(3): F168-70.
9. Lima AP, Beelen P, Bakker J. Use of a peripheral perfusion index derived from the pulse oximetry signal as a noninvasive indicator of perfusion. Crit Care Med 2002; 30(6): 1210-3.
10. Gupta S, Donn SM. Assessment of neonatal perfusion. Semin Fetal Neonatal Med 2020; 25(5): 101144.
11. Lima A, van Bommel J, Sikorska K, van Genderen M, Klijn E, Lesaffre E, Ince C, Bakker J. The relation of near-infrared spectroscopy with changes in peripheral circulation in critically ill patients. Crit Care Med 2011; 39(7): 1649-54.
12. Elshal MM, Hasanin AM, Mostafa M, Gamal RM. Plethysmographic Peripheral Perfusion Index: Could It Be a New Vital Sign? Front Med (Lausanne) 2021; 8: 651909.
13. Hasanin A, Mukhtar A, Nassar H. Perfusion indices revisited. J Intensive Care 2017; 5: 24.
14. He H, Long Y, Liu D, Wang X, Zhou X. Clinical classification of tissue perfusion based on the central venous oxygen saturation and the peripheral perfusion index. Crit Care 2015; 19: 330.
15. Rasmy I, Mohamed H, Nabil N, Abdalah S, Hasanin A, Eladawy A, et al. Evaluation of perfusion index as a predictor of vasopressor requirement in patients with severe sepsis. Shock. 2015; 44: 554-9.
16. He HW, Liu DW, Long Y, Wang XT. The peripheral perfusion index and transcutaneous oxygen challenge test are predictive of mortality in septic patients after resuscitation. Crit Care 2013; 17.
17. He HW, Liu WL, Zhou X, Long Y, Liu DW. Effect of mean arterial pressure change by norepinephrine on peripheral perfusion index in septic shock patients after early resuscitation. Chin Med J 2020; 133: 2146-52.
18. Lian H, Wang X, Zhang Q, Zhang H, Liu D. Changes in perfusion can detect changes in the cardiac index in patients with septic shock. J Int Med Res 2020; 48(8): 300060520931675.
19. Hasanin A, Karam N, Mukhtar AM, Habib SF. The ability of pulse oximetry-derived peripheral perfusion index to detect fluid responsiveness in patients with septic shock. J Anesth. 2021; 35: 254-61.

# Quorum quenching nanoparticles against wound pathogens – A scoping review

**Jayasree Anandan, MSc, Rajeshkumar Shanmugam, PhD**

Nanobiomedicine lab, Centre for Global Health Research, Saveetha Medical College and Hospitals, Saveetha Institute of Medical and Technical Sciences, Saveetha University, Chennai, Tamil Nadu, India

**ABSTRACT**

**Introduction: Quorum sensing (QS) enables bacteria to coordinate colony-wide activities, including those associated with infections. Quorum quenching (QQ) inhibits QS and is a promising method for controlling bacterial infections. Several In vitro experiments have been conducted to identify nanoparticles (NPs) as potential quorum quenching inhibitors. This review examines the potential of nanoparticles for quorum quenching, focusing on the QS-regulated pathogenicity of wound pathogens.**

**Materials and Methods: Observational studies were conducted to explore the capacity of nanoparticles to quorum quench wound pathogens.**

**Results: A review of observational studies indicated that nanoparticles exhibit significant quorum-quenching capabilities against wound pathogens. Numerous nanoparticles, including silver, gold, and zinc oxide, have been demonstrated to inhibit QS-regulated activities, thereby reducing bacterial virulence and biofilm formation. These results suggest that nanoparticles could serve as potent agents for mitigating bacterial infections and enhancing wound healing.**

**Conclusion: Nanoparticles show considerable potential as quorum-quenching agents, effectively decreasing bacterial virulence and biofilm formation in wound pathogens. These results indicate promising applications of nanoparticles in managing bacterial infections and improving wound healing.**

**KEYWORDS:**
*Quorum sensing, Quorum quenching, Wound pathogens, Nanoparticles*

## INTRODUCTION

Bacterial cells have the capacity to communicate with one another by producing and detecting extracellular chemicals (autoinducers) that can passively or actively pass through cell membranes, which is called quorum sensing (QS).[1] Consequently, the bacterial population can synchronize the expression of several genes to enable a simultaneous response. When their concentration reaches a particular threshold, autoinducers (AI) engage with transcriptional regulators within bacteria possessing the QS system, resulting in alterations to genetic expression patterns.[2] A greater number of genes were turned on or off when a specific cell density was attained. Furthermore, autoinducers attach to the extracellular segments of histidine kinase membrane receptors, initiating autophosphorylation and eliciting a corresponding cytoplasmic response.[3] Gram-positive and Gram-negative bacteria exhibit distinct QS systems, mainly due to the chemical composition of their autoinducers. L-homoserine lactones (HSLs), which generally, but not exclusively, diffuse passively across the cell membrane, are utilized by gram-negative bacteria, whereas gram-positive organisms predominantly employ autoinducing peptides for transportation.[4] The investigation of quorum sensing inhibitors has emerged as a highly intriguing field in antimicrobial research.[5] Antimicrobial compounds that target the virulence mechanisms in various bacteria by inhibiting quorum sensing have emerged as a new class of drugs. The exploration of QS inhibitors appears as one of the Quorum Quenching (QQ) strategies has been suggested to obstruct quorum sensing. These approaches involve eliminating or breaking down signaling molecules, hindering their production, impeding the formation of signaling molecules and receptor complexes, and thwarting the binding of signal transduction cascades.[6]

Every open wound has bacteria from endogenous or exogenous sources because of the absence of a protective barrier in the skin. The host immune system usually keeps these microorganisms in check or removes them during the initial phases of chronic wound formation. However, if the bacteria adhere to the wound surface and proliferate, they initiate biofilm formation.[7] Once a biofilm is firmly formed, neither the host's immune system nor antimicrobial medications will be effective in eradicating it. The biofilm is considered to be developed and more challenging to remove at this point, and the wound will be infected by the biofilm.[8] In these circumstances, there is a greater chance that a wound will not heal and will develop as an open clinical infection (i.e., symptoms of inflammation or purulence). Therefore, preventing biofilm formation in the early stages is essential to expedite and improve the healing process of chronic wounds.[9]

The utilization of nanotechnology in agriculture, therapeutics, diagnostics, and other fields has gained significant attention owing to recent advancements.[10] Drug resistance has been growing steadily and has challenged the scientific community to develop better antibacterial drugs. Metal nanoparticles (NPs) have been proven to function as powerful antibacterial agents. Antibacterial NPs are thought

*This article was accepted: 03 August 2025*
*Corresponding Author: Rajeshkumar Shanmugam*
*Email: rajeshkumars.smc@saveetha.com*

to have the potential to target multiple biomolecules simultaneously, thereby minimizing the chance of antibiotic resistance and developing drug-resistant strains.[11] Antimicrobial nanoparticles have been linked to several mechanisms, including free metal ion toxicity caused by metals breaking off the nanoparticle surfaces and oxidative damage triggered by reactive oxygen species (ROS) generated on these surfaces.[12] Bacteria show membrane damage as a result of the adsorption and subsequent penetration of nanoparticles into their cells. By changing the cell wall's usual negative charge, NPs adsorption causes depolarization, which increases the permeability of the wall.[13] This review investigates the potential of nanoparticles against quorum sensing in wound pathogens, thereby inhibiting their virulence and biofilm formation.

## MATERIALS AND METHODS

*Protocol and Sources of Information*

This scoping review was conducted in accordance with the Preferred Reporting Items for Systematic Reviews and Meta-Analyses Extension for Scoping Reviews (PRSIMA-ScR). The study material consisted of articles on the quorum-quenching activity of nanoparticles on wound pathogens, published before June 1, 2022. These articles were sourced from PubMed database.

*Eligibility Criteria*

We included primary In vitro studies published in English to evaluate the relationship between the use of nanoparticles and antimicrobial activity against the most prevalent microorganisms associated with wound infections, such as *P. aeruginosa, S. aureus, E. coli, K. pneumonia*, and other pathogens. There were no restrictions on the publication date or study location.

*Data Charting Process*

Both authors (J.A. and R.S.) performed data extraction. They utilized a pre-defined Excel form to gather the following information from each article: study identification details, study type, study objective, quorum sensing ability of wound pathogens, and the effectiveness of various nanoparticles against wound pathogens (In vitro).

*Inclusion and exclusion criteria:*

The inclusion criteria were articles reporting studies that used nanoparticles to act against wound pathogens and provided information about the quorum sensing ability of these pathogens. Meanwhile, the extension criteria consisted of articles that could not be accessed in the full text, were in non-English languages, or were not original research.

## RESULTS

Searches were conducted between June and September 2023, and updated in January 2024. Database searches identified 273 manuscripts from 2001 to 2022. Figure 1 shows a PRISMA flowchart detailing the search and selection processes. After removing eight duplicates, 265 manuscripts were selected for the initial screening. Articles without full-text availability or those falling outside the inclusion criteria (wound pathogens) were analyzed, resulting in the exclusion of 238 articles. Articles were excluded based on their titles and abstract relevance. Ultimately, 23 articles were assessed for eligibility and included in this review, while 4 manuscripts were excluded due to accessibility issues. The frequency of publications has increased recently, reflecting growing interest in the field.

## QUORUM-SENSING WOUND PATHOGENS

Bacterial biofilm on the wound is a thin layer caused by a cluster of bacteria attached to the surface of the wound, which is caused by both gram-negative and gram-positive bacteria, such as Escherichia coli, *Staphylococcus aureus, Pseudomonas aeruginosa, Staphylococcus epidermidis, Enterococcus faecalis, Klebsiella pneumonia* and other pathogens.

Pseudomonas aeruginosa is a notable human disease-causing organism that mostly affects individuals with cystic fibrosis (CF), cancer, and organ transplant recipients. It can also be detected in burns and cutaneous bruises.[14] The three Quorum Sensing circuits in this bacterium are active. One of these circuits is controlled by hormone-sensitive lipase (HSLs) and includes the genes LasR transcriptional activators-lasR and lasI, the genes responsible for producing the autoinducer (N-3-oxo-dodecanopyl)-L-homoserine lactone, which is essential for this circuit's signaling. The second circuit, also regulated by homoserine lactone, comprises the rhlI gene, rhlR gene encoding the transcriptional activator RhlR, and an enzyme responsible for the production of the N-(butanoyl)-L-homoserine lactone autoinducer.[15] The compound 2-heptyl-3-hydroxy-4-quinolone is synthesized by the products of the pqsABCDEH genes and is regulated by the PqsR regulator16. The regulatory hierarchy for all three systems involves LasR positively regulating RhlR, whereas RhlR exerts a negative regulatory influence on PQS.[17]

The significance of QS in human diseases associated with *P. aeruginosa* has been well established. According to numerous investigations, 90 percent of *P. aeruginosa* samples that can cause infections have working HSL systems. In one instance, it has been demonstrated that patients with cystic fibrosis typically have N-(3-oxododecanoyl)-HSL, the major *P. aeruginosa* auto inducer.[18] Polysaccharide alginate, a crucial part of the matrix created by *P. aeruginosa* strains, is a QS-controlled virulence factor that shields biofilms from macrophage destruction.[19]

Gram-positive *Staphylococcus aureus* is a non-motile coccus that produces a yellow pigment and clusters of cells. Numerous illnesses, including bacteremia, endocarditis, sepsis, and infections of the epidermis and various other tissues, are brought on by this bacterium.[20] *S. aureus* aids in infections caused by the synthesis of an extensive array of virulence factors, including enzymes, exotoxins, and adhesins.[21] A significant portion of these virulence factors is regulated by Agr system, which is an accessory gene regulator dependent on quorum sensing.[22]

The RNAII transcript and hld gene consist of genes located within the AGR locus, namely agrA, agrC, agrD, and agrB. The pro-peptide AgrD undergoes conversion into auto

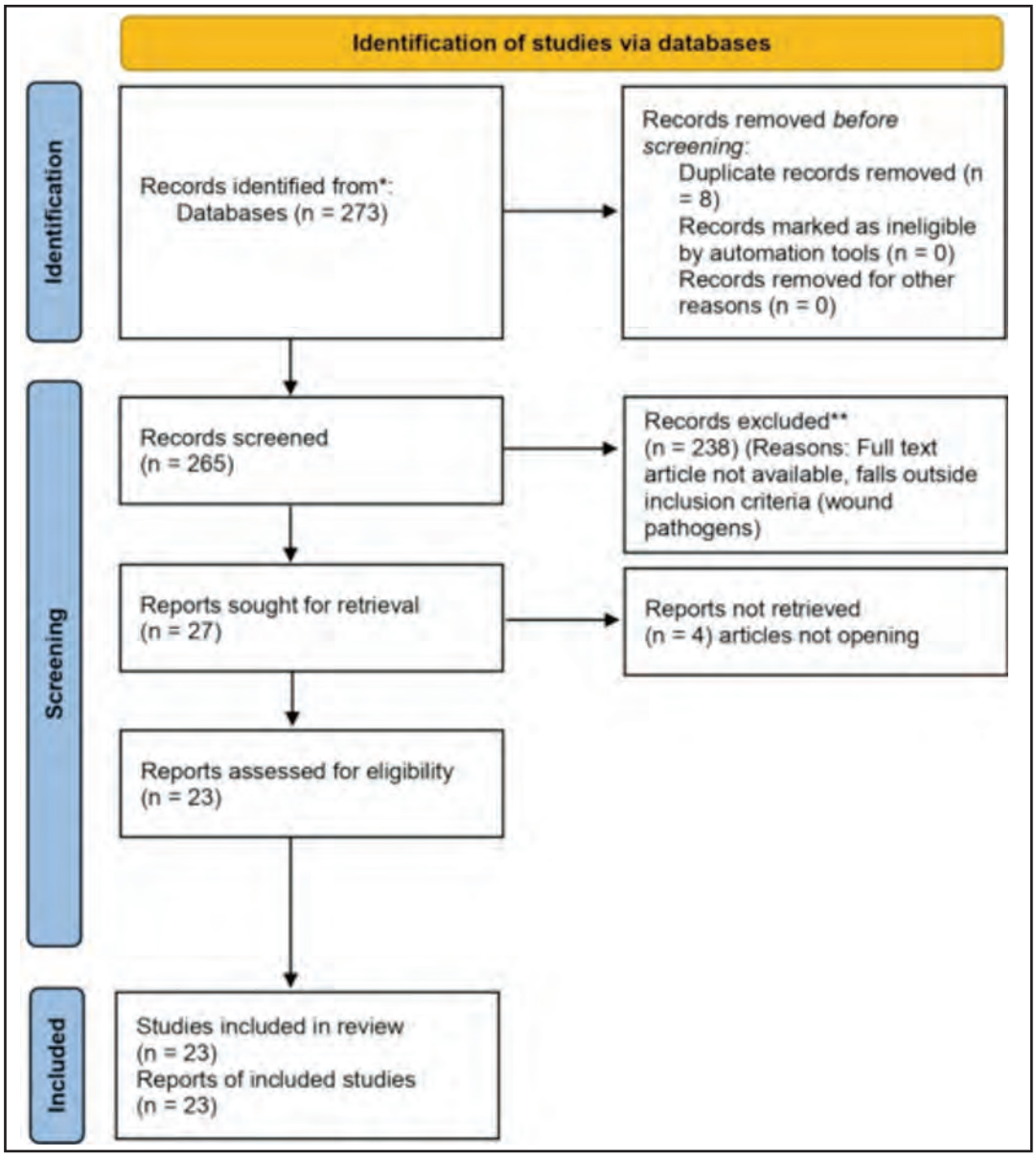


**Fig. 1:** Flow chart for the scoping review process

inducing peptides (AIPs). This conversion occurs through the export and processing of the pheromone AgrD, which is facilitated by AgrB and SpsB peptidase.[23] These peptides vary in length, typically spanning seven to nine amino acids, but they share a common feature: a thiolactone ring located at their C-terminus.[24] The *S. aureus* hld gene of *S. aureus* produces an RNAIII effector molecule that post-transcriptionally controls many virulence factors.[25,26] RNAIII is responsible for regulating biofilm production by *Staphylococcus aureus*. Because of its limited motility, this bacterium forms flatter biofilms than genera that exhibit greater mobility.[27] Teichoic acid-based glycocalyx or slime is incorporated into the *S. aureus* biofilm.[28] In addition to the previously mentioned factors, polysaccharide intercellular antigen (PIA) and extracellular DNA (eDNA) are significant components of biofilms. These substances are produced as a result of extensive cell lysis, facilitated by the holing homolog CidA, and contribute to the formation and stability of biofilms.[29]

*Klebsiella pneumonia* is a gram-negative bacterium known for its ability to induce various infections, including urinary tract infections, pneumonia, wound infections, surgical site infections, meningitis, and intra-abdominal infections. The synthesis of AI-2 (autoinducer-2) in non-motile or sessile *Klebsiella pneumonia* cells appears to function as a regulator of biofilm formation and the production of lipopolysaccharides (LPS) 30. The process of quorum sensing among wound pathogens occurs as depicted in figure 2.

## QUORUM QUENCHING NANOPARTICLES

Nanoparticles can serve as excellent quorum quenchers, offering an excellent solution due to their unique physicochemical properties that allow them to interact with bacterial cells. Specifically, metal and metal oxide nanoparticles (such as silver, zinc oxide, and titanium dioxide) can attach to bacterial cell membranes, causing

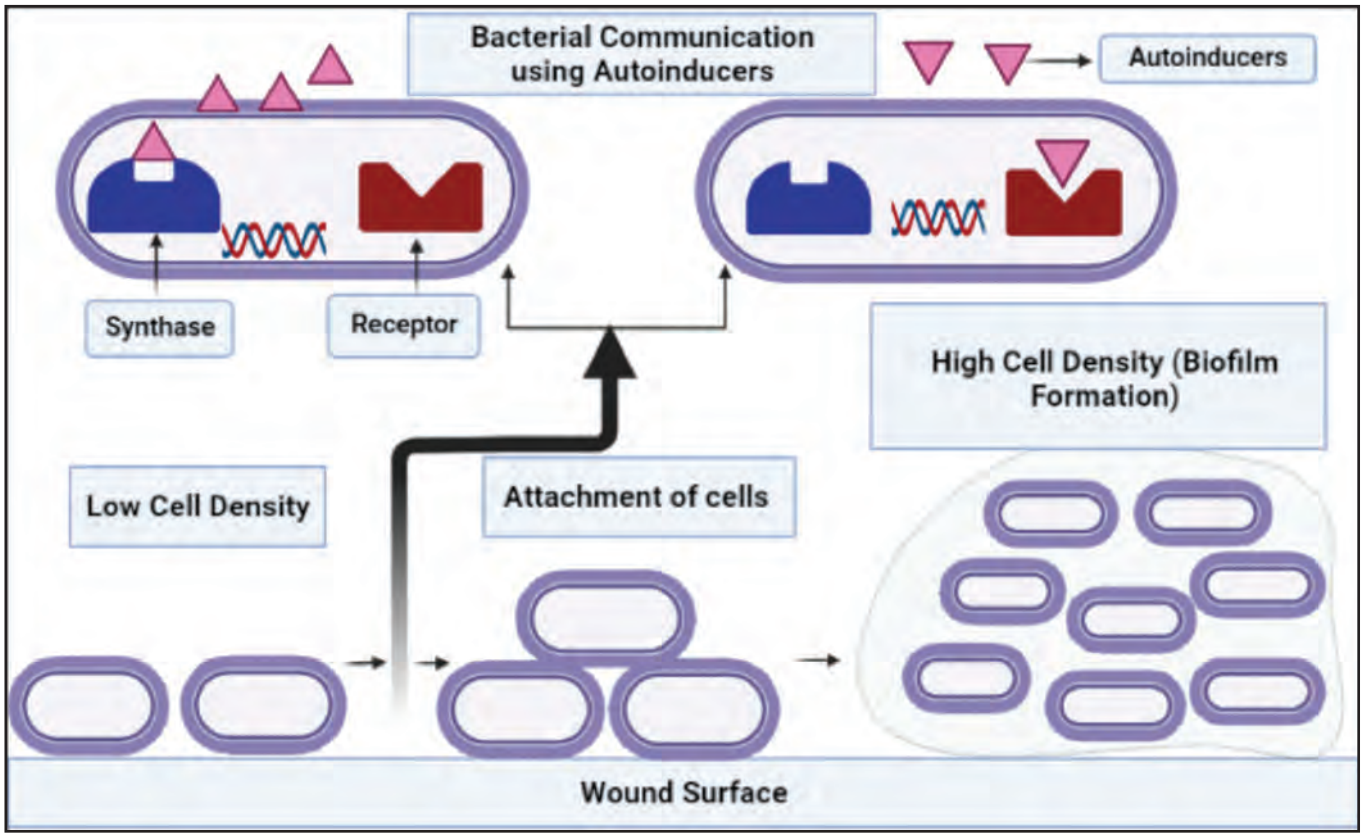


**Fig. 2:** Quorum sensing of wound pathogens

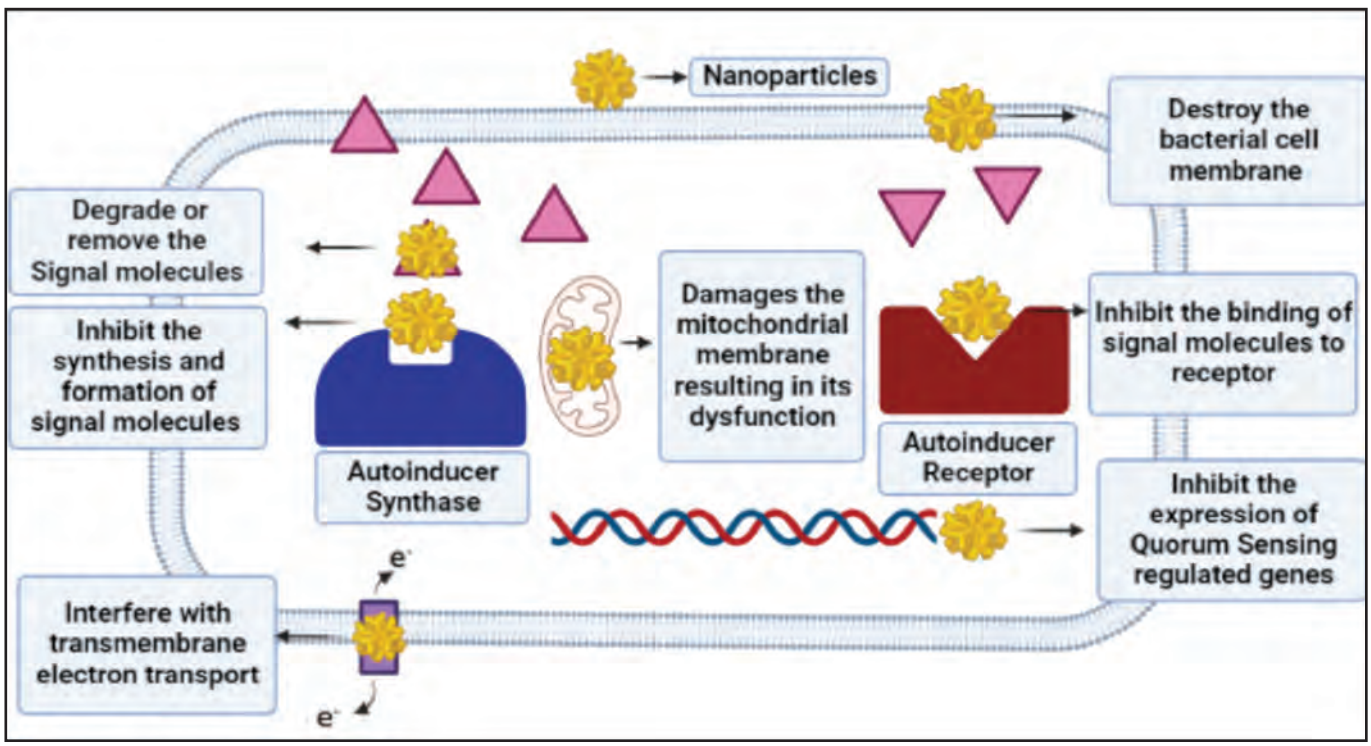


**Fig. 3:** Quorum Quenching Efficacy of Nanoparticles

**Table I: Studies that displays the Quorum quenching ability of different nanoparticles:**

| First author | Publication year | Type of nanoparticles | Outcomes |
|---|---|---|---|
| Jagtap S[31] | 2013 | Silver nanowires | Inhibited the biofilm growth of *P. aeruginosa* |
| Bamal D[32] | 2021 | Silver nanoparticles (AgNPs) | Exhibited bactericidal activity against *Proteus mirabilis, Staphylococcus aureus*, and *Pseudomonas aeruginosa* |
| Kalishwarlal[33] | 2010 | AgNPs | Hindered the first phase of bacterial adherence of *P. aeruginosa* and *Staphylococcus epidermidis* to the colonized surface |
| Martinez-Gutierrez F[34] | 2013 | AgNPs | Destroyed the biofilm produced by *P. aeruginosa* |
| Mohanta YK[35] | 2010 | AgNPs | Effectively lower the initial stages of *P. aeruginosa* biofilm formation by restricting bacterial attachment to the polystyrene surfaces |
| Xu L[36] | 2020 | Startch stabilized AgNPs | Disrupted the biofilms of *P. aeruginosa* and *S. aureus* |
| Masurkar SA[37] | 2012 | Cymbopogan citratus leaf extract AgNPs | Inhibited biofilm formation by *S. aureus* |
| Qais FA[38] | 2018 | AgNPs | Suppressed the gene expression of PAO1 virulence genes of *P. aeruginosa* |
| Lamin A[39] | 2022 | AgNPs | Suppressed the expression of genes - lasA, lasB, phzA1, and rhlA in the planktonic cells of *P. aeruginosa* (PAO1) |
| Shin D[40] | 2019 | AgNPs | Significantly reduced the production of C12-AHL (Acyl homoserine lactones) and C4-AHL |
| Wagh MS[41] | 2013 | Silver nanowires | Effectively suppressed biofilm formed by *P. aeruginosa* |
| Chaudhari[42] | 2015 | PEGlyted silver coated carbon nanotubes | Decreased the expression of virulence genes safC, ychP, sseA, sseG, and even sdiA (a quorum sensing gene) in *S. aureus* |
| Sathyanarayanan MB[45] | 2013 | Gold nanoparticles (AuNPs) | Significantly reduced the biofilms of S. aureus and P. aeruginosa |
| Samanta S[46] | 2017 | Laccaria fraterna mycelium mediated AuNPs | Significantly inhibited *P. aeruginosa* pyocyanin synthesis and QS-regulated biofilm formation |
| García-Lara B[47] | 2015 | Zinc oxide nanoparticles (ZnONPs) | ZnONPs provides several options for combating against *P. aeruginosa* infections that are multi-drug resistant |
| Al-Shabib NA[48] | 2018 | Ochradenus baccatus leaves mediated ZnONPs | Suppressed QS-regulated biofilm formation in *P. aeruginosa, E. coli,* and many other bacteria. |
| Al-Shabib NA[49] | 2016 | Nigella sativa mediated ZnONPs | Down regulated the lasB gene, resulting in a subsequent reduction in the production of AHLs |
| Liao C[50] | 2020 | UV radiation exposed titanium dioxide nanoparticles ($TiO_2$NPs) | Efficiently inhibited the proliferation of methicillin-resistant *S. aureus* |
| Cho KH[51] | 2005 | $TiO_2$NPs | Showed influence on the expression of QS and efflux pump genes in multi-drug resistant *P. aeruginosa* strains |
| Ahmed FY[52] | 2021 | *Aloe barbadensis* mediated $TiO_2$NPs | Reduced the cell viability of *P. aeruginosa* biofilm |
| Rajkumari J[53,54] | 2019 | Chitosan nanoparticles | Blocked the migration of AHLs into the cytoplasm and inhibited AI synthase in *E. coli* |
| Subhaswaraj[55] | 2018 | Cinnamaldehyde-encapsulated chitosan nanoparticles | Inhibited the virulence factors and biofilms in *P. aeruginosa* PAO1 strain. |

structural damage and increased permeability. This attachment leads to the leakage of cellular content and eventual cell death. Additionally, nanoparticles can penetrate biofilms and disrupt their structural integrity, thereby inhibiting quorum sensing and reducing bacterial communication and virulence. Studies on the QQ ability of different nanoparticles are summarized in Table I.

## DISCUSSION

Quorum sensing (QS) plays a crucial role in the pathogenesis and persistence of wound infections caused by various bacterial species. QS-regulated production of factors, such as exopolysaccharides, can inhibit phagocytosis and other immune responses, allowing bacteria to evade destruction by the immune system of the host.[56] The presence of quorum-sensing bacteria in wounds can delay the healing process by maintaining chronic inflammation and tissue damage. Moreover, QS can interfere with the efficacy of conventional antimicrobial treatments by promoting biofilm formation and increasing resistance, necessitating the development of alternative therapeutic strategies to target QS pathways.[57]

Nanoparticles can serve as outstanding quorum quenchers by targeting biofilms formed by wound pathogens and multidrug-resistant bacteria. Nanoparticles can penetrate biofilms and disrupt their structural integrity, which is particularly important because biofilms protect bacteria from

antibiotics and the host immune system, contributing to chronic infections.[58] Additionally, nanoparticles can be incorporated into wound dressings, gels, and ointments for direct application to infected wounds, providing continuous antimicrobial action and promoting faster healing.[59]

Mohanta YK et al. (2010) showed that AgNPs with sizes ranging from 1 to 10 nm, applied at a concentration of 4 g mL-1, effectively lowered the initial stages of *P. aeruginosa* biofilm formation by restricting bacterial attachment to polystyrene surfaces. In addition to reducing cell viability within the biofilm and inducing morphological changes such as cytoplasmic condensation, it was also demonstrated that the production of biofilm matrix components was diminished.[35]

Researchers have been giving a lot of attention to gold nanoparticles (AuNPs) in both fundamental and applied research. AuNPs have extensive applications in biology and diagnostics and function as catalysts for diverse purposes. One of the primary advantages of AuNPs is their simple chemical reduction method of synthesis and comparatively low toxicity compared to other nanomaterials.[43] They exhibit antibacterial activity against several organisms including methicillin-resistant organisms.[44]

Zinc oxide nanoparticles (ZnONPs) diminish the virulence factors of *P. aeruginosa* and biofilm development in animal models, resulting in fewer infections. Nevertheless, research involving clinical or environmental isolates is rare, and they are often conducted using laboratory strains such as PAO1 and PA14. The study conducted by García-Lara B et al. (2015) examined the impact of ZnONPs, known for their potency in quorum and virulence quenching of the PAO1 strain, on six clinical strains from cystic fibrosis patients, a clinical strain from urine that was resistant to furanone C-30, two mutants of PA14 that were gallium-resistant, one mutant that was resistant to PA14 C-30, and four environmental isolates. For most strains, ZnONPs efficiently reduced the formation of elastase, pyocyanin, and biofilms, independent of their origin or resistance to the traditional quorum quencher C-30 or cutting-edge antibacterial gallium. According to research findings, ZnONPs could offer different options for treating *P. aeruginosa* infections that are resistant to treatment because of their potential broad-spectrum quorum quenching activity against relevant strains.[47]

The influence of TiO2NPs on the expression of QS and efflux pump genes in multi-drug-resistant *P. aeruginosa* isolates was also examined. The investigation revealed that TiO2NPs exhibited enhanced antibacterial action against *P. aeruginosa* strains compared with $TiO_2$ powder, resulting in a significant 96% reduction in biofilm production. Additionally, the application of $TiO_2$NPs, either alone or in conjugation with antibiotics, significantly reduced the expression of key efflux pump genes (MexY, MexB, and MexA) and genes regulated by (lasR, lasI, rhll, rhlR, pqsA, and pqsR). This suggests that $TiO_2$NPs can influence the expression of the efflux pump and quorum-sensing genes that regulate biofilm formation, enhancing the therapeutic effectiveness of conventional antibiotics.[51]

Chitosan nanoparticles offer a means to enhance the quorum sensing inhibitory effects of various antimicrobial drugs. Chitosan and its derivatives can be used to encapsulate phytochemicals, thereby increasing their Anti-quorum sensing (Anti-QS) effects. For instance, compared to their free forms, the encapsulation of flavonoids like baicalein and quercetin enhanced their QQ potential against the *E. coli* sensors when compared to their free forms. The quorum quenching mechanism of these flavonoid-loaded nanocapsules involves either blocking the migration of AHLs into the cytoplasm or inhibiting AI synthase. Non-toxic chitosan also demonstrated QQ action in *E. coli* and caused cell aggregation at low doses. Cell aggregation suggests that QS is inhibited by slowing the diffusion of AHLs.[53,54] The quorum quenching capability of the NPs to inhibit QS and destroy bacterial cells is illustrated in figure 3.

## CONCLUSIONS

An efficient alternative approach for treating microbial infections is interference with Quorum Sensing is Quorum Quenching. Nanoparticles exhibiting anti-quorum sensing (anti-QS) properties act as potential antibacterial agents against bacterial infections, especially in the current scenario, where the sustained effectiveness of antibiotics is uncertain. Nanoparticles have emerged as a novel category of antibacterial agents and carriers for drug delivery owing to their exceptional physicochemical properties, diminutive size, and substantial surface area-to-volume ratio. The capacity of nanoparticles to inhibit QS suggests that they have a good chance of successfully treating infections caused by bacterial biofilms. For clinical use, it will be extremely beneficial to fully understand the mechanism underlying QQ action and, consequently, the way in which NPs interfere with bacterial virulence. At present, there is a dearth of information regarding the ecotoxicities and clinical applications of nanoparticles. Before nanoparticles receive approval for widespread clinical use, comprehensive research is imperative to elucidate both their positive and negative impacts.

## ACKNOWLEDGEMENTS

We would like to thank the Saveetha Institute of Medical and Technical Sciences for their support.

## REFERENCES

1. Garg N, Manchanda G, Kumar A. Bacterial quorum sensing: circuits and applications. Antonie Van Leeuwenhoek 2014; 105: 289-305.
2. Zhang W, Li C. Exploiting quorum sensing interfering strategies in gram-negative bacteria for the enhancement of environmental applications. Front. microbiol. 2016; 6: 1535.
3. Ke X, Miller LC, Bassler BL. Determinants governing ligand specificity of the V ibrio harveyi L ux N quorum-sensing receptor. Mol Microbiol 2015; 95(1): 127-42.
4. LaSarre B, Federle MJ. Exploiting quorum sensing to confuse bacterial pathogens. Microbiol Mol Biol Rev 2013; 77(1): 73-111.
5. Nandi S. Recent advances in ligand and structure based screening of potent quorum sensing inhibitors against antibiotic resistance induced bacterial virulence. Recent Pat Biotechnol 2016; 10(2): 195-216.

6. Wolska KI, Grudniak AM, Markowska K. Inhibition of bacterial quorum sensing systems by metal nanoparticles. Metal Nanoparticles in Pharma 2017: 123-38.
7. Percival SL, McCarty SM, Lipsky B. Biofilms and wounds: an overview of the evidence. Adv Wound Care. 2015; 4(7): 373-81.
8. Wolcott RD, Rhoads DD, Bennett ME, Wolcott BM, Gogokhia L, Costerton JW, Dowd SE. Chronic wounds and the medical biofilm paradigm. J Wound Care 2010; 19(2): 45-53.
9. Pg B. Wound microbiology and associated approaches to wound management. Clin Microbiol Rev 2001; 14: 244-69.
10. Valcárcel J, Ortín J. Viral cell biology: Influenza raids the splicing store. Nat Microbiol. 2016 Jun 24;1(7):1-2.
11. Slavin YN, Asnis J, Hńfeli UO, Bach H. Metal nanoparticles: understanding the mechanisms behind antibacterial activity. J Nanobiotechnology 201715: 1-20.
12. Besinis A, De Peralta T, Handy RD. The antibacterial effects of silver, titanium dioxide and silica dioxide nanoparticles compared to the dental disinfectant chlorhexidine on Streptococcus mutans using a suite of bioassays. Nanotoxicology. 2014; 8(1): 1-6.
13. Leung YH, Ng AM, Xu X, Shen Z, Gethings LA, Wong MT, Chan CM, Guo MY, Ng YH, Djurišić AB, Lee PK. Mechanisms of antibacterial activity of MgO: non-ROS mediated toxicity of MgO nanoparticles towards Escherichia coli. Small. 2014; 10(6): 1171-83.
14. Ammons MC, Ward LS, Fisher ST, Wolcott RD, James GA. In vitro susceptibility of established biofilms composed of a clinical wound isolate of Pseudomonas aeruginosa treated with lactoferrin and xylitol. Int J Antimicrob Agents. 2009; 33(3): 230-6.
15. Steindler L, Bertani I, De Sordi L, Schwager S, Eberl L, Venturi V. LasI/R and RhlI/R quorum sensing in a strain of Pseudomonas aeruginosa beneficial to plants. Appl Environ Microbiol. 2009; 75(15): 5131-40.
16. Rather MA, Saha D, Bhuyan S, Jha AN, Mandal M. Quorum quenching: A drug discovery approach against Pseudomonas aeruginosa. Microbiol Res 2022 Aug 23: 127173.
17. Soto-Aceves MP, Cocotl-Yañez M, Servín-González L, Soberón-Chávez G. The Rhl quorum-sensing system is at the top of the regulatory hierarchy under phosphate-limiting conditions in Pseudomonas aeruginosa PAO1. J Bacteriol 2021; 203(5): 10-128.
18. Moradali MF, Ghods S, Rehm BH. Pseudomonas aeruginosa lifestyle: a paradigm for adaptation, survival, and persistence. Front cell infect microbiol 2017; 7: 39.
19. Skariyachan S, Sridhar VS, Packirisamy S, Kumargowda ST, Challapilli SB. Recent perspectives on the molecular basis of biofilm formation by Pseudomonas aeruginosa and approaches for treatment and biofilm dispersal. Folia Microbiol 2018; 63: 413-32.
20. Taj Z, Chattopadhyay I. Staphylococcus aureus Virulence Factors and Biofilm Components: Synthesis, Structure, Function and Inhibitors. InESKAPE Pathogens: Detection, Mechanisms and Treatment Strategies 2024 Mar 30 (pp. 227-270). Singapore: Springer Nature Singapore.
21. Cheung GY, Bae JS, Otto M. Pathogenicity and virulence of Staphylococcus aureus. Virulence. 2021 Dec 31;12(1):547-69.
22. Singh R, Ray P. Quorum sensing-mediated regulation of staphylococcal virulence and antibiotic resistance. Future Microbiol 2014; 9(5): 669-81.
23. Zhao A. Studies of the Biosynthesis, Signaling, and Manipulation of the Staphylococcal Agr Quorum Sensing Circuit (Doctoral dissertation, Princeton University).
24. Lyon GJ, Novick RP. Peptide signaling in Staphylococcus aureus and other Gram-positive bacteria. Peptides 2004; 25(9): 1389-403.
25. Fechter P, Caldelari I, Lioliou E, Romby P. Novel aspects of RNA regulation in Staphylococcus aureus. FEBS Lett 2014; 588(15): 2523-9.
26. Winn M. Expanding the biocatalytic toolkit: utilising biofilms as an adaptable biocatalytic platform and the development of a general, regioselective pyrrole halogenase (Doctoral dissertation, University of East Anglia).
27. Stoodley P, Hall-Stoodley L, Costerton B, DeMeo P, Shirtliff M, Gawalt E, Kathju S. Biofilms, biomaterials, and device-related infections. InHandbook of polymer applications in medicine and medical devices 2013 Jan 1 (pp. 77-101). William Andrew Publishing.
28. Husain Fm, Ahmad I, Asif M, Tahseen Q. Influence of clove oil on certain quorum-sensing-regulated functions. J Biosci 2013; 38(5): 1-0.
29. Wolska KI, Grudniak AM, Markowska K, 2016. Inhibitors of bacterial quorum sensing systems and their role as potential therapeutics. Postepy Mikrobiologii, 55(3): 300-308.
30. Sun S, Zhang H, Lu S, Lai C, Liu H, Zhu H. The metabolic flux regulation of Klebsiella pneumoniae based on quorum sensing system. Sci. Rep 2016; 6(1): 38725.
31. Jagtap S, Priolkar KR. Evaluation of ZnO nanoparticles and study of ZnO–TiO2 composites for lead free humidity sensors. Sensor Actuat B-Chem. 2013; 183: 411-8.
32. Bamal D, Singh A, Chaudhary G, Kumar M, Singh M, Rani N, Mundlia P, Sehrawat AR. Silver nanoparticles biosynthesis, characterization, antimicrobial activities, applications, cytotoxicity and safety issues: An updated review. Nanomaterials 2021; 11(8): 2086.
33. Kalishwaralal K, BarathManiKanth S, Pandian SR, Deepak V, Gurunathan S. Silver nanoparticles impede the biofilm formation by Pseudomonas aeruginosa and Staphylococcus epidermidis. Colloids Surf B Biointerfaces 2010; 79(2): 340-4.
34. Martinez-Gutierrez F, Boegli L, Agostinho A, Sánchez EM, Bach H, Ruiz F, James G. Anti-biofilm activity of silver nanoparticles against different microorganisms. Biofouling. 2013; 29(6): 651-60.
35. Mohanta YK, Biswas K, Jena SK, Hashem A, Abd_Allah EF, Mohanta TK. Anti-biofilm and antibacterial activities of silver nanoparticles synthesized by the reducing activity of phytoconstituents present in the Indian medicinal plants. Front microbiol 2020; 11: 1143.
36. Xu L, Wang YY, Huang J, Chen CY, Wang ZX, Xie H. Silver nanoparticles: Synthesis, medical applications and biosafety. Theranostics 2020; 10(20): 8996.
37. Masurkar SA, Chaudhari PR, Shidore VB, Kamble SP. Effect of biologically synthesised silver nanoparticles on Staphylococcus aureus biofilm quenching and prevention of biofilm formation. IET nanobiotechnol 2012; 6(3): 110-4.
38. Qais FA, Khan MS, Ahmad I. Nanoparticles as quorum sensing inhibitor: Prospects and limitations. Biotechnological applications of quorum sensing inhibitors. 2018: 227-44.
39. Lamin A, Kaksonen AH, Cole IS, Chen XB. Quorum sensing inhibitors applications: A new prospect for mitigation of microbiologically influenced corrosion. Bioelectrochemistry. 2022; 145: 108050.
40. Shin D, Gorgulla C, Boursier ME, Rexrode N, Brown EC, Arthanari H, Blackwell HE, Nagarajan R. N-acyl homoserine lactone analog modulators of the Pseudomonas aeruginosa Rhll quorum sensing signal synthase. ACS Chem. Biol 2019; 14(10): 2305-14.
41. Wagh MS, Patil RH, Thombre DK, Kulkarni MV, Gade WN, Kale BB. Evaluation of anti-quorum sensing activity of silver nanowires. Appl Microbiol Biotechnol 2013; 97: 3593-601.
42. Chaudhari AA, Jasper SL, Dosunmu E, Miller ME, Arnold RD, Singh SR, Pillai S. Novel pegylated silver coated carbon nanotubes kill Salmonella but they are non-toxic to eukaryotic cells. J Nanobiotechnology 2015; 13(1): 1-7.
43. Yeh YC, Creran B, Rotello VM. Gold nanoparticles: preparation, properties, and applications in bionanotechnology. Nanoscale 2012; 4(6): 1871-80.
44. Mobed A, Hasanzadeh M, Seidi F. Anti-bacterial activity of gold nanocomposites as a new nanomaterial weapon to combat photogenic agents: Recent advances and challenges. RSC Adv 2021; 11(55): 34688-98.

45. Sathyanarayanan MB, Balachandranath R, Genji Srinivasulu Y, Kannaiyan SK, Subbiahdoss G. The effect of gold and iron-oxide nanoparticles on biofilm-forming pathogens. Int Sch Res Notices 2013; 2013.
46. Samanta S, Singh BR, Adholeya A. Intracellular synthesis of gold nanoparticles using an ectomycorrhizal strain EM-1083 of Laccaria fraterna and its nanoanti-quorum sensing potential against Pseudomonas aeruginosa. Indian J Microbiol 2017; 57: 448-60.
47. García-Lara B, Saucedo-Mora MÁ, Roldán-Sánchez JA, Pérez-Eretza B, Ramasamy M, Lee J, Coria-Jimenez R, Tapia M, Varela-Guerrero V, García-Contreras R. Inhibition of quorum-sensing-dependent virulence factors and biofilm formation of clinical and environmental Pseudomonas aeruginosa strains by ZnO nanoparticles. Lett Appl Microbiol 2015; 61(3): 299-305.
48. Al-Shabib NA, Husain FM, Hassan I, Khan MS, Ahmed F, Qais FA, Oves M, Rahman M, Khan RA, Khan A, Hussain A. Biofabrication of Zinc Oxide Nanoparticle fromOchradenus baccatusLeaves: Broad-Spectrum Antibiofilm Activity, Protein Binding Studies, and In VivoToxicity and Stress Studies. J Nanomater 2018; 2018: 1-4.
49. Al-Shabib NA, Husain FM, Ahmed F, Khan RA, Ahmad I, Alsharaeh E, Khan MS, Hussain A, Rehman MT, Yusuf M, Hassan I. Biogenic synthesis of Zinc oxide nanostructures from Nigella sativa seed: Prospective role as food packaging material inhibiting broad-spectrum quorum sensing and biofilm. Scientific reports 2016; 6(1): 36761.
50. Liao C, Li Y, Tjong SC. Visible-light active titanium dioxide nanomaterials with bactericidal properties. Nanomaterials. 2020 Jan 9;10(1):124.
51. Ahmed FY, Aly UF, Abd El-Baky RM, Waly NG. Effect of titanium dioxide nanoparticles on the expression of efflux pump and quorum-sensing genes in MDR Pseudomonas aeruginosa isolates. Antibiotics 2021; 10(6): 625.
52. Rajkumari J, Magdalane CM, Siddhardha B, Madhavan J, Ramalingam G, Al-Dhabi NA, Arasu MV, Ghilan AK, Duraipandiayan V, Kaviyarasu K. Synthesis of titanium oxide nanoparticles using Aloe barbadensis mill and evaluation of its antibiofilm potential against Pseudomonas aeruginosa PAO1. J Photochem Photobiol B 2019; 201: 111667.
53. Omwenga EO, Hensel A, Shitandi A, Goycoolea FM. Chitosan nanoencapsulation of flavonoids enhances their quorum sensing and biofilm formation inhibitory activities against an E. coli Top 10 biosensor. Colloids Surf B Biointerfaces 2018; 164: 125-33.
54. Qin X, Engwer C, Desai S, Vila-Sanjurjo C, Goycoolea FM. An investigation of the interactions between an E. coli bacterial quorum sensing biosensor and chitosan-based nanocapsules. Colloids and Surfaces B: Biointerfaces 2017; 149: 358-68.
55. Subhaswaraj P, Barik S, Macha C, Chiranjeevi PV, Siddhardha B. Anti-quorum sensing and anti-biofilm efficacy of cinnamaldehyde encapsulated chitosan nanoparticles against Pseudomonas aeruginosa PAO1. Lwt 2018; 97: 752-9.
56. Castillo-Juárez I, Maeda T, Mandujano-Tinoco EA, Tomás M, Pérez-Eretza B, García-Contreras SJ, Wood TK, García-Contreras R. Role of quorum sensing in bacterial infections. World J Clin Cases 2015; 3(7): 575.
57. Zhao G, Usui ML, Lippman SI, James GA, Stewart PS, Fleckman P, Olerud JE. Biofilms and inflammation in chronic wounds. Adv Wound Care 2013; 2(7): 389-99.
58. Afrasiabi S, Partoazar A. Targeting bacterial biofilm-related genes with nanoparticle-based strategies. Front microbiol 2024; 15: 1387114.
59. Mihai MM, Dima MB, Dima B, Holban AM. Nanomaterials for wound healing and infection control. Materials 2019; 12(13): 2176.

# The rare cases of pneumatic colorectal perforation: A cautionary tale of compressed air misuse

**Muthu Kumar, MS, Balavignesh Durai, MS, Vijayshree Shyamsundar, MS, Manish Babu UG, MS, Sanjana Chiramel, MS**

Saveetha Institute of Medical and Technical Sciences: SIMATS Deemed University, General Surgery, Saveetha Nagar ,, Thandalam, Chennai -Bengaluru Nh48, Chennai, Tamilnadu 602105, India

## ABSTRACT

**Barotrauma is a medical condition caused by sudden pressure changes in the body causing damage to multiple parts of the body. However, it is an infrequent occurrence when it comes to Colo-rectal perforation, wherein the trauma occurs due to the insufflation of compressed air through the anus. Several factors influence the outcome of a patient with colonic perforation due to barotrauma such as the severity of the injury, hemodynamic status of the patient, the patient's general health and well-being, the time taken for active medical/ surgical intervention since the injury, aggressive intravenous antibiotics administration to prevent sepsis, post-operative complications like surgical site infection, post-op ileus, anastomotic leak, etc. Overall, the patient's prognosis largely depends on early diagnosis, effective initial resuscitation, timely surgical intervention, and intensive post-operative care for a favorable outcome. Recently, we came across 2 cases of extensive pneumoperitoneum with Colo-rectal perforation as a result of the forceful insufflation of compressed air through the anus. Prompt medical intervention was necessary to prevent any further complications and they underwent surgical repair of the colorectal perforation.**

## INTRODUCTION

High-pressure air has become prevalent in industrial settings, with blowgun dust cleaners as common pneumatic tools.[1] It is crucial to be mindful of the appropriate use of cleaning agents in factories. Failure to do so can have devastating consequences, putting the lives of employees at risk due to pneumatics. These cleaners produce air pressure ten times higher than the resting anal pressure in adults (0.84 kg/cm$^2$).[2] Compressed air can easily penetrate clothing and cause rapid and forceful inflation of the rectum and colon, which can lead to bursting of the bowel wall due to its high bursting pressure [3], The insufflation of compressed air into the large intestine can result in a perforation of the bowel, which presents with a sudden onset of abdominal pain, distension, and respiratory distress due to tension pneumoperitoneum.[4] Unfortunately, due to its rarity, workers may not be adequately informed about the potential dangers associated with the unintentional or intentional use of compressed air near the anal canal, leading to serious colorectal injuries[5,6] which can be fatal. In this context, we present a case of severe colorectal laceration resulting from compressed air exposure, culminating in pneumoperitoneum, peritonitis, shock, and sepsis.

## CASE REPORT

*Case 1*

An 18-year-old Bihari man residing in Chennai, a daily wage factory worker by occupation was brought to the ER with complaints of severe abdominal pain and abdominal distension for the last 4 hours. He gave an alleged history of trauma caused by forceful insufflation of a compressed air blower by inserting the blower nozzle into the anal canal. On examination, he was found to be tachypneic with a Glasgow coma scale of 13/15. He was hemodynamically unstable with a BP of 80/50mmhg, a pulse rate of 102 beats per minute, and a room air saturation of 88%. Systemic examination revealed a tense distended abdomen; palpable subcutaneous crepitus over the abdomen, chest, and neck; absent bowel sounds; and decreased air entry to the right side of the chest.

The patient was initially resuscitated by securing two large IV bore cannulas and administered intravenous crystalloids, intravenous broad-spectrum antibiotics, oxygen supplementation by facemask, and nasogastric decompression with continuous monitoring of vital parameters. Abdominal radiography and computed tomography confirmed the presence of gross pneumoperitoneum, which was suggestive of colonic perforation. The expected management in this case comprised emergency surgical intervention involving exploratory laparotomy and repair or resection of the bowel followed by intensive post-operative care and monitoring. In this patient, a flank drain was used to decompress the abdominal distension. Emergency laparotomy was performed, and the peritoneal cavity was filled with colonic content and blood. Large irregular perforations, serosal tears, and gangrene were found in the transverse colon, cecum, ascending colon, and proximal half of the sigmoid colon. After thorough peritoneal lavage, the large intestine was mobilized while safeguarding the bilateral ureter and gonadal vessels, subtotal colectomy was performed, and an end ileostomy was performed. The patient required intensive care support including vasopressors and mechanical ventilation. However, the patient's clinical course was complicated by shock and sepsis, culminating in cardiac arrest refractory to adequate resuscitation. Despite aggressive measures, the patient succumbed to the sequelae of a traumatic incident.

*Case 2*

A 22-year-old man presented to the ER with symptoms of acute onset of breathlessness and abdominal discomfort,

*This article was accepted: 12 August 2024*
*Corresponding Author: Muthu Kumar*
*Email: gmkumaran99@gmail.com*

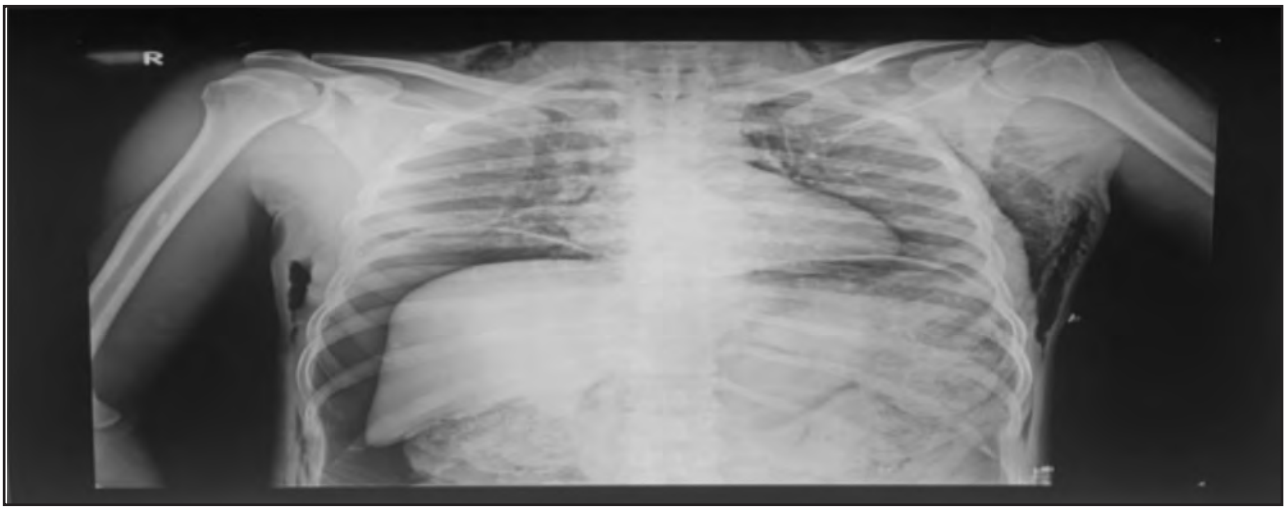


**Fig. 1:** Chest xray showing air under diaphragm indicating and hollow viscus perforation

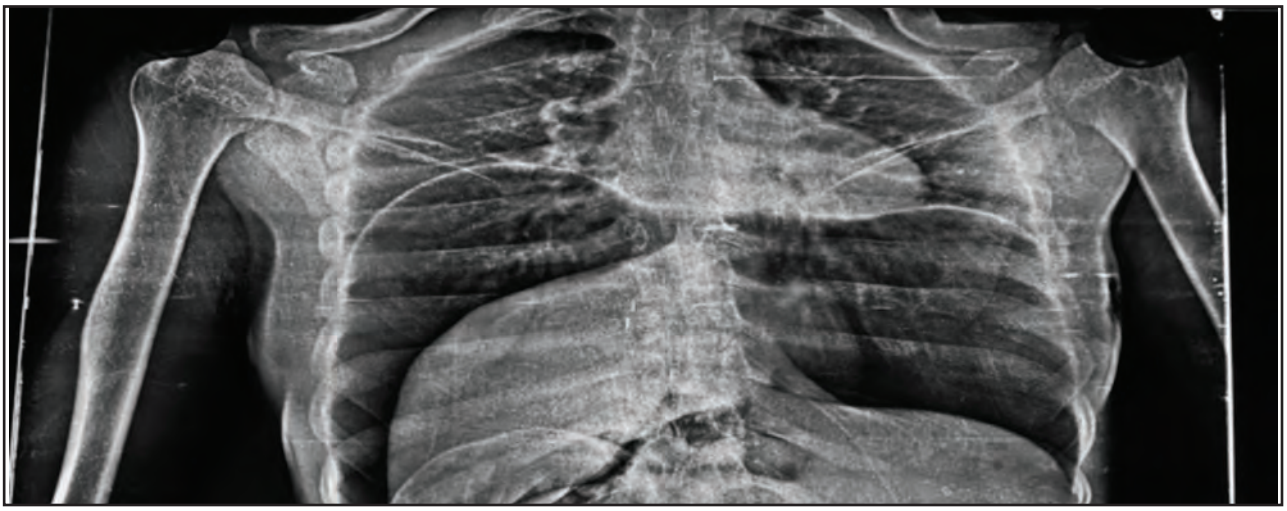

**Fig. 1:** Chest xray showing air under diaphragm indicating and extensive hollow viscus perforation

including pain, abdominal distension, and vomiting for 3 hours. The symptoms started after an incident at his workplace, where his colleagues allegedly insufflated compressed air forcefully into his rectum by using a blow gun. On examination, he had a Glasgow coma scale score of 13/15, bilateral reactive pupils, hemodynamic instability with vitals of 90/50 mmHg, pulse rate of 98 beats per minute, and room air saturation of 84%.

Initial resuscitative measures were performed, and relevant investigations, including abdominal radiography, were performed, which confirmed the presence of pneumoperitoneum. Based on the patient's history, clinical examination, and investigations, a diagnosis of barotrauma causing perforation of the large intestine was made and after aggressive resuscitation, and the patient was promptly taken up for an emergency laparotomy. Intraoperatively, multiple tears were identified in the sigmoid colon along the mesenteric border along with a serosal tear along the tinea coli in the transverse colon. Consequently, resection of the sigmoid colon, closure of the rectal stump, and creation of an end-descending colostomy were performed. The remainder of the large and small bowel and other viscera were normal. The patient recovered following a challenging postoperative course in the intensive care unit. Subsequently, colostomy closure was performed after six weeks.

## DISCUSSION

The most common causes of colon perforation are tumors, diverticulitis, abscess, colitis, foreign body, obstruction, volvulus, iatrogenic, blunt or penetrating abdominal trauma, and colonoscopy-induced barotrauma, with a prevalence of 0.1% to 0.5%.[7,8,9] However, injuries caused by high-pressure air compressors are infrequent and mostly observed among industrial workers.

The cecum is more prone to distention injury due to its larger diameter, as per Laplace's law.[10] While colonoscopy studies suggest that intraluminal pressures greater than 0.109

kg/cm$^2$ (1.547 psi/80 mmHg) are needed for perforation, injuries resulting from high-pressure barotrauma typically occur elsewhere in the colon, notably in the rectosigmoid junction. The anatomical structure of the buttocks and perineum creates an easy passage for compressed air to enter the anal orifice, making the rectosigmoid junction more susceptible to pressure-related barotrauma.[9]

Experimental studies have shown that the human colon can rupture at pressures as low as 120-200 mmHg, with seromuscular rupture occurring even at lower levels. The insult's suddenness causes uneven air distribution and focal perforation. Industrial air compressors, classified by pressure delivery, predominantly employ low- to medium-pressure ranges; however, their use poses significant risks. The resting pressure of the anal sphincter, estimated at 40-80 mmHg, can be easily overcome by forceful airflow from the compressors, resulting in rapid colon inflation.[7,8]

The catastrophic consequences of this phenomenon are highlighted by the fact that a mere 1–2 seconds of pressurized air delivery can cause substantial damage, necessitating urgent management strategies. Rectal injuries beyond the rectosigmoid junction due to pelvic support are rare. The severity of high-pressure barotrauma is determined by several factors, including air pressure, flow velocity, anal resting pressure, and source-to-anal distance.[3] Forceful entry of pressurized air can cause significant damage within seconds, necessitating prompt intervention to prevent serious complications. In this condition, there is a significant amount of pressure in the abdominal area, which can lead to fatal consequences if not promptly treated.

In cases of urgent management, it may be necessary to relieve tension pneumoperitoneum through percutaneous decompression, which involves converting it into open pneumoperitoneum. Depending on the severity of the clinical and radiological signs, the management of pneumatic colon The management of injury can vary from a wait-and-see approach to a formal laparotomy. Careful observation following surgery is crucial because of the potentially delayed presentation of a full-thickness colon perforation.

Management protocols range from expectant observation to surgical intervention with clinical and radiological signs guiding the approach. Prompt recognition and intervention are imperative because the development of tension pneumoperitoneum can lead to fatal hemodynamic and respiratory compromise. Timely conversion of tension pneumoperitoneum to open pneumoperitoneum is crucial, typically achieved through urgent percutaneous decompression methods. A comprehensive understanding of the mechanisms and implications of high-pressure barotrauma is essential for effective management and prevention of potentially life-threatening complications.

## CONCLUSION

In conclusion, a detailed comparison between the two cases highlights the variability in clinical outcomes observed in traumatic colorectal injuries, which is based on the severity of the injury, the time taken to seek medical advice, detailed and reliable history, aggressive resuscitation, and emergency surgical treatment, which can lead to favorable outcomes, as in case 2.

## DECLARATION

No conflict of interest.

## INFORMED CONSENT

Consent for publication of this case report was obtained during writing and after informing the patient.

## REFERENCES

1. Sy ED, Chiu Y-I, Shan Y-S, et al. Pneumatic colon injury following high pressure blow gun dust cleaner spray to the perineum. International Journal of Surgery Case Reports 2015; 6: 218-21.
2. Duthie HL, Watts JM. Contribution of the external anal sphincter to the pressure zone in the anal canal. Gut 1965; 6(1): 64-8.
3. Rosenberg IL. Insufflation Injury of the Bowel. Arch Surg 1972; 105(1): 113.
4. Yin W-B, Hu J-L, Gao Y, et al. Rupture of sigmoid colon caused by compressed air. WJG 2016; 22(10): 3062.
5. Park YJ. Rectal perforation by compressed air. Ann Surg Treat Res 2017; 93(1): 61.
6. Ergin. A Rare Case of Colorectal Injury With Compressed Air. J Med Cases 2013; doi: 10.4021/jmc997w.
7. Jentschura D, Raute M, Winter J, et al. Complications in endoscopy of the lower gastrointestinal tract: Therapy and prognosis. Surg Endosc 1994; 8(6): 672–6.
8. Tulchinsky H. Incidence and management of colonoscopic perforations: 8 years' experience. WJG 2006; 12(26): 4211.
9. Lüning TH, Keemers-Gels ME, Barendregt WB, et al. Colonoscopic perforations: a review of 30,366 patients. Surg Endosc 2007; 21(6): 994-7.
10. Brayko CM, Kozarek RA, Sanowski RA, et al. Diverticular rupture during colonoscopy: Fact or fancy? Digest Dis Sci 1984;29(5): 427-31.

CASE REPORT

# A rare case of pigmented seborrhoeic keratosis of scalp

**Arosish Dash, MBBS**

Department of General Surgery, Saveetha Medical College and Hospital, Saveetha Institute of Medical and Technical Sciences (SIMATS), Saveetha University, Thandalam, Chennai, Tamil Nadu, India

## ABSTRACT

**Seborrheic keratosis (SK) is a prevalent hyperkeratotic dermatological condition characterized by benign proliferation of epidermal keratinocytes, typically occurring in the middle to advanced stages of life. While the trunk is the primary site for lesions, they can also manifest on the extremities, face, and scalp. Although SK is typically benign, there can be morphological overlap with malignant skin lesions, necessitating meticulous differentiation for an accurate diagnosis. This case report describes a 63-year-old male presenting with scalp swelling that was, initially suspected to be malignant. However, histopathological examination revealed pigmented seborrheic keratosis, prompting the need for a comprehensive management approach. Surgical excision with a rotational flap cover was performed successfully, highlighting the importance of precise diagnosis and management in addressing cutaneous lesions. The exact etiology of SK remains elusive, with potential genetic associations implicated in its pathogenesis. Although treatment may not always be necessary, various modalities are available for lesion removal or symptom management, with surgical intervention reserved for cases exhibiting signs of malignancy. Clinicians should be aware of the atypical presentations of SK and, emphasize the need for a multidisciplinary approach involving dermatologists, pathologists, and surgeons for optimal outcomes.**

## INTRODUCTION

Seborrheic keratosis is a prevalent hyperkeratotic condition affecting the epidermis and, typically manifesting in the middle or advanced stages of life. The trunk is the predominant location for lesions; however, they can also be observed on the extremities, face, and scalp[1] Seborrheic keratosis, also known as seborrheic warts or senile warts, typically presents as tiny and fibrous lesions. The occurrence of huge isolated lesions is infrequent. Both males and females are equally impacted, and a majority of patients exhibit numerous lesions that are frequently dispersed in a symmetrical manner.

Although seborrheic keratoses are typically benign tumors characterized by distinct features, there can occasionally be morphological overlap with other malignant skin lesions, highlighting the importance of meticulous differentiation. Recognizing these nuances is vital for accurately distinguishing seborrheic keratoses from both benign and malignant skin tumors. While treatment may not always be imperative owing to its benign nature, a significant proportion of patients still opt for various forms of intervention, underscoring the significance of precise diagnosis and considering patient preferences in the management of these lesions.

The precise etiology of seborrheic keratosis remains unclear. Aging, physical stress, irritation, infection, and host responses have been identified as predisposing variables2. The main risk factor for SK is UV radiation exposure. The otolaryngological literature has not sufficiently clarified the inclusion of seborrheic keratosis as a potential diagnosis for nasal lesions. In this instance, we describe a situation in which a single large, lesion damages the scalp area.

## CASE

A 63-year-old man presented to the outpatient department with a complaint of swelling on his scalp that had persisted for the past year. Given the duration and nature of the swelling, clinical suspicion was inclined towards a potentially malignant lesion, particularly melanoma. To clarify the diagnosis and plan appropriate management, edge-wedge biopsy was promptly performed. Subsequent histopathological examination yielded unexpected results, and the lesion was identified as pigmented seborrheic keratosis, a benign condition. This diagnosis prompted further consideration of the patient's management plan. Although benign, seborrheic keratosis lesions can sometimes exhibit atypical features that raise concerns regarding malignancy. Therefore, a comprehensive approach was adopted to ensure an accurate diagnosis and appropriate management.

In light of the histopathological findings, the decision was made to proceed with excision biopsy along with a rotational flap cover. This surgical intervention aimed not only to address the patient's cosmetic concerns but also to definitively manage the lesion and prevent potential complications or recurrence. The procedure was executed without complications and the patient's postoperative period was uneventful, with careful monitoring revealing healthy wound healing and flap integrity.

Histopathological examination of the excised tissue provided further insights into the nature of the lesion. Seborrheic keratosis, a common benign skin growth, arises from the proliferation of immature keratinocytes. This proliferation leads to the formation of well-demarcated, round or oval, flat-shaped macules on the skin surface. While they are typically slow-growing, these lesions can increase in thickness over time and rarely resolve spontaneously.

*This article was accepted: 07 August 2024*
*Corresponding Author: Rahul Raj Chennam Lakshmi Kumar*
*Email: rahul808@gmail.com*

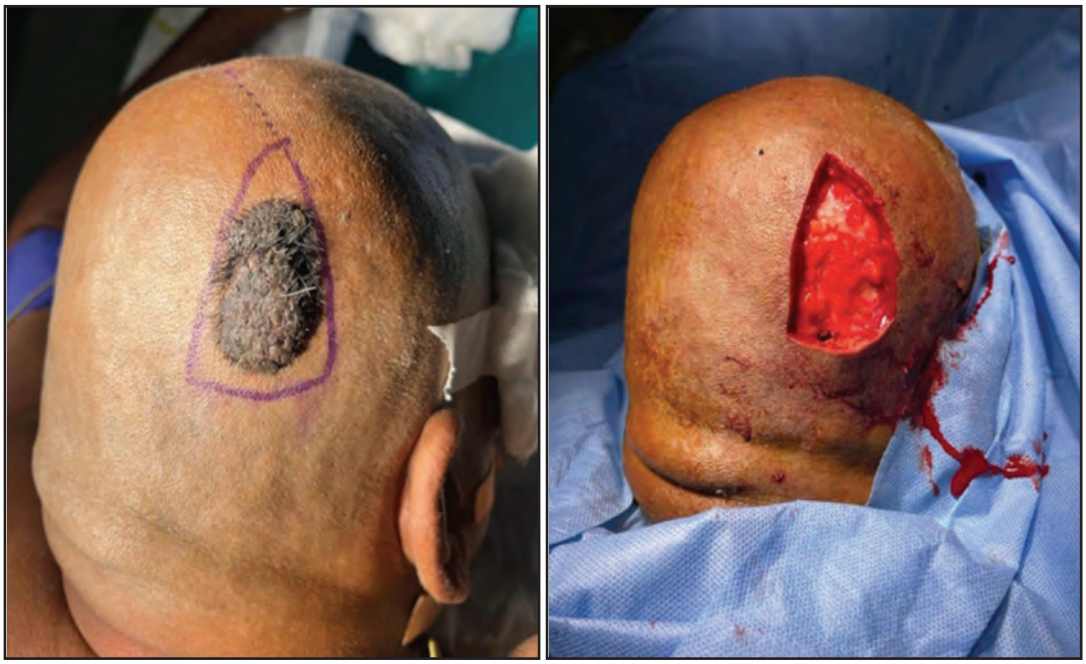

**Fig. 1:** Intra operative before excision and post excision

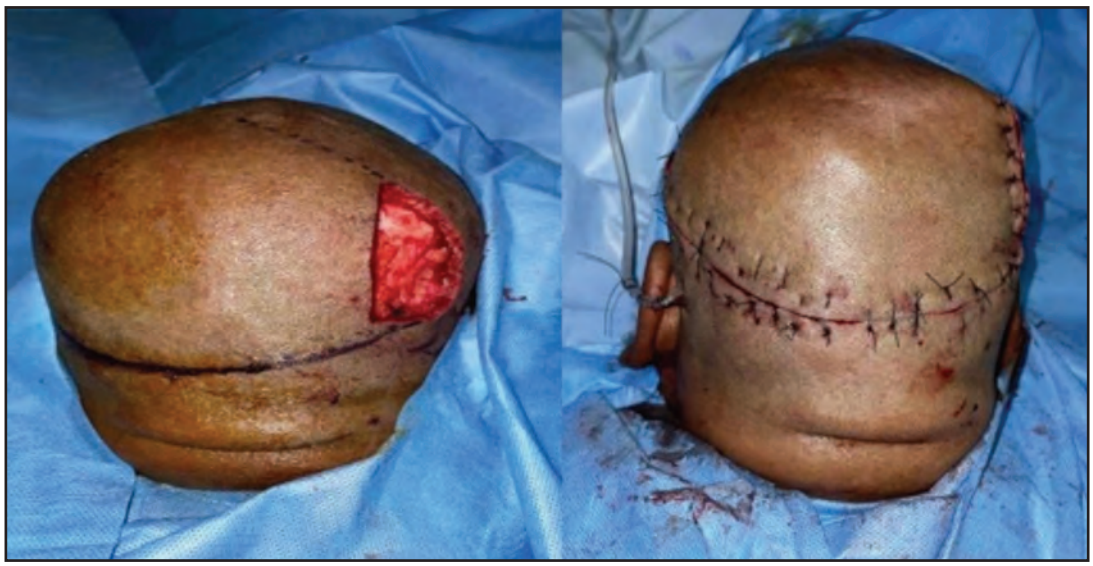

**Fig. 2:** Intra operative rotational flap cover

However, the exact pathogenesis of seborrheic keratosis remains incompletely understood. However, emerging evidence suggests a genetic predisposition, with mutations in the fibroblast growth factor receptor-3 (FGFR3) and PIK3CA oncogenes implicated in its development. Specifically, activating mutations in FGFR3 are common in sporadic cases of seborrheic keratosis, driving the proliferation of keratinocytes and contributing to tumor growth. Moreover, various subtypes of seborrheic keratosis exist, each exhibiting distinct histopathological features including hyperkeratosis, acanthosis, pseudocysts, hyperpigmentation, inflammation, and dyskeratosis.

Histopathological examination of the excised lesion revealed characteristic features consistent with those of seborrheic keratosis. Microscopic evaluation revealed epidermal hyperkeratosis, acanthosis, and pseudohorny cysts with cytoplasmic pigmentation. Additionally, sparse lymphocytic infiltration was observed in the underlying dermis, suggesting a mild inflammatory response to the lesion.

Despite its benign nature, seborrheic keratosis occasionally presents with atypical features that mimic malignant lesions, warranting careful clinical evaluation and histopathological confirmation. Given the high prevalence of seborrheic keratosis, distinguishing between benign and malignant

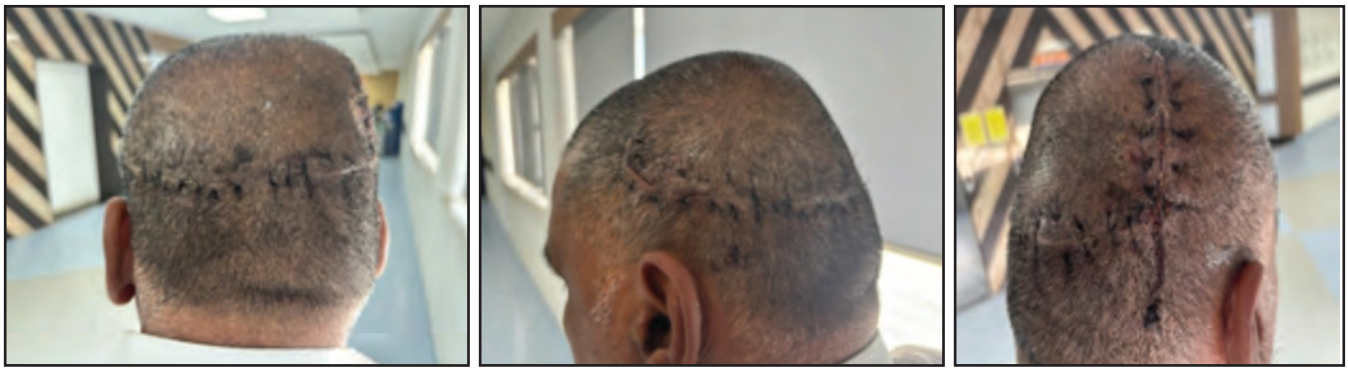

**Fig. 3:** Post operative scar quality

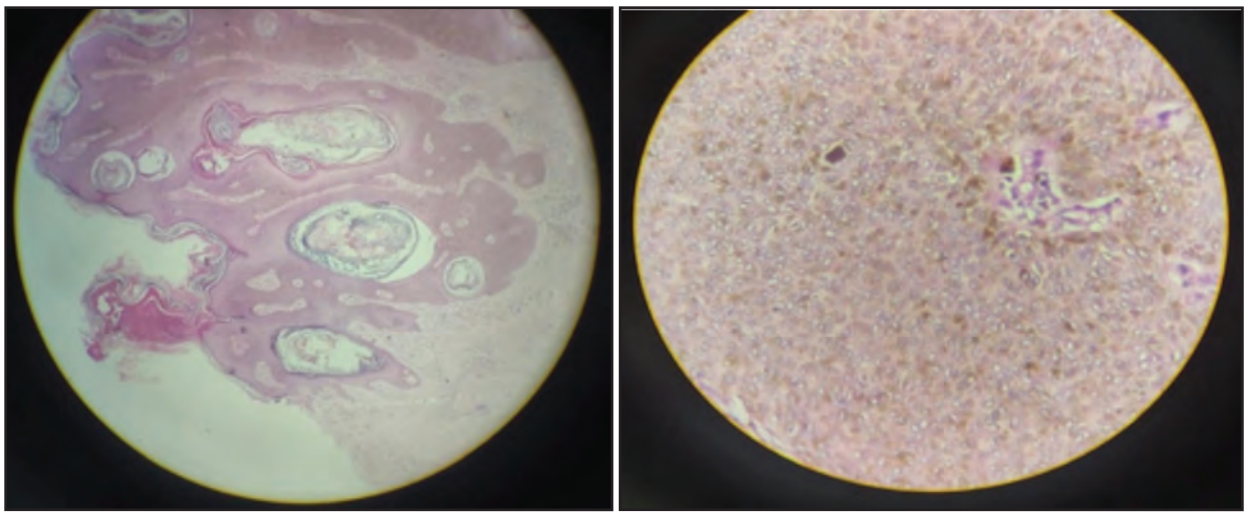

**Fig. 4:** Histopathology examination images. The above HPE section shows skin with acanthosis, papillomatosis with horn cysts ( both true and pseudo cysts), and many keratinocytes showing pigmentation. Granulomas or atypia were noted. Impression suggestive of pigmented seborrhoeic keratosis

lesions is crucial for guiding appropriate management decisions. Biopsy remains the gold standard for definitive diagnosis, particularly for lesions with suspicious clinical features or an inadequate response to conservative management.

The present case emphasizes the importance of a comprehensive approach for the diagnosis and management of cutaneous lesions. Although benign in nature, seborrheic keratosis can pose diagnostic challenges, necessitating careful clinical evaluation and histopathological confirmation. Through meticulous assessment and appropriate intervention, clinicians can ensure optimal outcomes in patients presenting with cutaneous lesions.

## DISCUSSION

Seborrheic keratoses are lesions characterized by their flat, verrucous, polypoid, or pedunculated nature. These lesions typically have a size range of 0.5 cm to 1 cm and exhibit a range of colors, spanning from tan-brown to black. Most of the lesions did not show any symptoms and had clearly defined borders.

Seborrheic keratosis is characterized by uncontrolled growth of immature keratinocytes, leading to the formation of distinct, round or oval, flat-shaped lesions. Usually characterized by gradual growth, these lesions have the tendency to thicken over time and seldom resolve on their own. The aforementioned ailment arises from the non-malignant proliferation of epidermal keratinocytes, wherein a potential hereditary factor is believed to play a role in the formation of multiple lesions. However, the precise mechanism of familial inheritance remains unclear. Although there is still limited understanding of its exact etiology, there are probable associations between fibroblast growth factor receptor 3 (FGFR3) and PIK3CA oncogenes. Mutations in FGFR3, a receptor for tyrosine kinase, are frequently observed in sporadic seborrheic keratosis, and are believed to be responsible for the proliferation of these non-malignant neoplasms. Seborrheic keratosis consists of different subtypes including, acanthotic, hyperkeratotic, clonal, adenoid, irritable, and melanoacanthoma. Pathological lesions sometimes show characteristics of multiple subtypes. The aforementioned intricacy highlights the necessity for thorough evaluation and precise identification in the management of these lesions.

The Leser-Trélat sign refers to the abrupt occurrence of seborrheic keratoses or an escalation in the quantity of lesions, which can potentially be linked to an underlying internal cancer, typically adenocarcinoma affecting the stomach, colon, or breast[3]. Acrochordon, verruca vulgaris, follicular adnexal tumors, melanocytic tumors, and squamous or basal cell carcinoma are among the clinical differential diagnoses that should be considered. Hence, performing a histopathological investigation is crucial to verify the clinical observations. Seborrheic keratosis may need to be removed due to cosmetic preferences, to address symptoms such as itching, bleeding, and inflammation, or to confirm clinical findings. Available treatment modalities include cryosurgery, electrodesiccation, shave excision, carbon dioxide laser vaporization, and surgical removal. Topical corticosteroids can be employed to alleviate symptoms of inflamed lesions[4,5]. Surgical interventions should be limited to cases in which lesions exhibit indications of malignancy. To the best of our knowledge, there have been fewer earlier reports of seborrheic keratosis occurring on the scalp. Medical professionals should be aware of the atypical positioning of lesions. No literature suggests that seborrheic keratosis of the scalp can undergo malignant transformation. It is a primarily benign condition.[6] Our patient had no risk of malignant transformation. The various treatment options available for SK include cryotherapy, electrodessication, curettage, ablative laser treatment, shave biopsy and topical agents.[7] While there is great interest from both patients and providers in a topical non-invasive treatment for SK, no effective topical therapeutic agent has been developed, and this remains an area of unmet need.[8] No adjuvant therapy is required for seborrheic keratosis has been warranted. However, there is no available literature to justify this.

The above HPE section shows skin with acanthosis, papillomatosis with horn cysts ( both true and pseudo cysts), and many keratinocytes showing pigmentation. Granulomas or atypia were noted. Impression suggestive of pigmented seborrhoeic keratosis.

## CONCLUSION

In conclusion, seborrheickeratosis represents a common dermatological condition characterized by the benign proliferation of epidermal keratinocytes, resulting in well-defined, often pigmented lesions. Histopathological examination is essential for accurate diagnosis. In our patient, we performed excision and biopsy with a rotational flap cover. Postoperatively, the patient recovered well without any complications, and the postoperative scar was good. The postoperative histopathology report was the same as the pre-operative report, thereby confirming it a case of pigmented seborrheic keratosis of the scalp.

## REFERENCES

1. King R, Page RN, Googe PB. Desmoplastic seborrheic keratosis. Am J Dermatopathol 2003; 25: 210-4.
2. Anderson PJ, Zuk JA, Rao GS, Berry RB. Squamous cell carcinoma arising within seborrheic keratosis. Plast Reconstr Surg 1998; 102: 453-5.
3. Kyrmizakis DE, Vrentzos EE, Papadakis CE, Chroniaris NE, Bizakis JG, Amanakis ZE. Seborrheic keratosis of the auricle: report of an unusual case. Ear Nose Throat J 2002; 81: 107-9.
4. Thomas I, Kihiczak NI, Rothenberg J, Ahmed S, Schwartz RA. Melanoma within the seborrheic keratosis. Dermatol Surg 2004; 30(4 Pt 1): 559-61.
5. Lambert PR, Fechner RE, Hatcher CP. Seborrheic keratosis of the ear canal. Otolaryngol Head Neck Surg 1987; 96:198-201.
6. Barthelmann S, Butsch F, Lang BM, Stege H, Großmann B, Schepler H, Grabbe S. Seborrheic keratosis. J Dtsch Dermatol Ges. 2023; 21(3): 265-277. [PubMed]
7. Greco MJ, Bhutta BS. Seborrheic Keratosis. [Updated 2024 May 6]. In: StatPearls [Internet]. Treasure Island (FL): StatPearls Publishing; 2024 Jan-.
8. Jackson JM, Alexis A, Berman B, Berson DS, Taylor S, Weiss JS. Current Understanding of Seborrheic Keratosis: Prevalence, Etiology, Clinical Presentation, Diagnosis, and Management. J Drugs Dermatol. 2015; 14(10): 1119-25.

# Acknowledgement
# Supplement 1 Issue 2025

**The Editorial Board of The Medical Journal of Malaysia gratefully acknowledge the following individuals for reviewing the papers submitted for publication:**

1. Dr Aina Mariana
2. Prof Andee Dzulkarnaen Zakaria
3. Dr Chellakannu A
4. Dr Faathir Baihaqi Ghifary
5. Dr Mohd Nazri Ali
6. Dr Padmalochana K
7. Dr Rebwar A Hasan
8. Prof Dr Shatriah Ismail
9. Dr Sujatha J
10. Prof Dr Victor Hoe Chee Wai